# Reactive oxygen and nitrogen species production in cardiomyoblasts during hypoxia and reoxygenation

**RAJITHA THUSHARA KOLAMUNNE**

Doctor of Philosophy

**ASTON UNIVERSITY**

April 2010

Aston University

# Reactive oxygen and nitrogen species production in cardiomyoblasts during hypoxia and reoxygenation

Rajitha Thushara Kolamunne

Doctor of Philosophy

April 2010

## SUMMARY

Hypoxia is a stress condition in which tissues are deprived of an adequate $O_2$ supply; this may trigger cell death with pathological consequences in cardiovascular or neurodegenerative disease. Reperfusion is the restoration of an oxygenated blood supply to hypoxic tissue and can cause more cell injury. The kinetics and consequences of reactive oxygen and nitrogen species (ROS/RNS) production in cardiomyoblasts are poorly understood. The present study describes the systematic characterization of the kinetics of ROS/RNS production and their roles in cell survival and associated protection during hypoxia and hypoxia/reperfusion. H9C2 cells showed a significant loss of viability under 2% $O_2$ for 30min hypoxia and cell death; associated with an increase in protein oxidation. After 4h, apoptosis induction under 2% $O_2$ and 10% $O_2$ was dependent on the production of mitochondrial superoxide ($O_2^{-\bullet}$) and nitric oxide ($^{\bullet}NO$), partly from nitric oxide synthase (NOS). Both apoptotic and necrotic cell death during 2% $O_2$ for 4h could be rescued by the mitochondrial complex I inhibitor; rotenone and NOS inhibitor; L-NAME. Both L-NAME and the NOX (NADPH oxidase) inhibitor; apocynin reduced apoptosis under 10% $O_2$ for 4h hypoxia. The mitochondrial uncoupler; FCCP significantly reduced cell death via a $O_2^{-\bullet}$ dependent mechanism during 2% $O_2$, 30min hypoxia. During hypoxia (2% $O_2$, 4h)/ reperfusion (21% $O_2$, 2h), metabolic activity was significantly reduced with increased production of $O_2^{-\bullet}$ and $^{\bullet}NO$, during hypoxia but, partially restored during reperfusion. $O_2^{-\bullet}$ generation during hypoxia/reperfusion was mitochondrial and NOX- dependent, whereas $^{\bullet}NO$ generation depended on both NOS and non-enzymatic sources. Inhibition of NOS worsened metabolic activity during reperfusion, but did not effect this during sustained hypoxia. Nrf2 activation during 2% $O_2$, a sustained hypoxia and reperfusion was $O_2^{-\bullet}/^{\bullet}NO$ dependent. Inhibition of NF-κB activation aggravated metabolic activity during 2% $O_2$, 4h hypoxia. In conclusion, mitochondrial $O_2^{-\bullet}$, but, not ATP depletion is the major cause of apoptotic and necrotic cell death in cardiomyoblasts under 2% $O_2$, 4h hypoxia, whereas apoptotic cell death under 10% $O_2$, 4h, is due to NOS-dependent $^{\bullet}NO$. The management of ROS/RNS rather than ATP is required for improved survival during hypoxia. $O_2^{-\bullet}$ production from mitochondria and NOS is cardiotoxic during hypoxia/reperfusion. NF-κB activation during hypoxia and NOS activation during reperfusion is cardiomyoblast protective.

**Keywords; mitochondria; superoxide; nitric oxide; NOS; protein oxidation; NOX, NF-κB; Nrf2; reperfusion; H9C2 cells**

**To**

**my loving wife and parents,**

**whose sacrifice and love has made it possible to complete this thesis**

**Acknowledgements**

I would like to express my sincere thanks to my supervisor Professor Helen Griffiths for offering me this PhD position and giving me tremendous support, advice and encouragement throughout the project. Special thanks to my associate supervisor Dr David Poyner for his advice and kind support throughout the period. I'm very grateful to Dr Ann Vernallis for providing me with restriction enzymes, plasmids-DNA (NF-κB and β-galactosidase) for her advice and kind support in bioinformatics and molecular biology techniques. Thanks also to Professor Peter Lambert for providing me with hypoxic chambers and his constant help with fluorescence microscopy. They all are very supportive, whose personal investment was instrumental in getting this project off the ground. I would like to thank Dr Melissa Grant for providing me with plasmid DNA (NQO1 and TKRL), staining protocol. Thanks also to Dr Mark Prince (School of Engineering and Applied sciences) provided me technical support for confocal microscopy. Many thanks for Michele Clare for doing protein carbonyl assay as instructed.

Alan Richardson**,** Chris Bache**,** Roy McKenzie, Kamaljit McKenzie, Sue Turner, Paul Fundak and Steve Wells deserve thanks for their patient help in various ways. Thanks also to David Aveston and Paul Hughes (Chemical Engineering and Applied Chemistry) for their logistic support in gas delivery throughout the project. I would like to thank Chris, Dan, Irundika, Khujesta and Rachel for all good times in the Lab and all those support me outside the lab, especially Dr Eric Adams, Dr Steve Russell, Dr Eric Hill, Dr Nagamani Bora, Dr Richard Darby and Dr Xiaolin Li. Thanks to James Barwell, Dr David Nagel and Dr Matthew Conner for their help in gene cloning. Finally, heartfelt thanks are due to my parents and wife. I'm grateful to financial support from Aston University via an International Overseas Bursary.

## ABBEVIATIONS

| | |
|---|---|
| AAD | Aminoactinomycin D |
| ADP | Adenosine diphosphate |
| AIF | apoptosis-inducing factor |
| Ang II | Angiotensin II |
| ANOVA | Analysis of variance |
| Apaf-1 | Apoptotic protease activating factor 1 |
| ARC | Apoptosis repressor caspases |
| ARE | Antioxidant responsive element |
| ATP | Adenosine triphosphate |
| BCA | Bicinchoninic acid |
| BSA | Bovine serum albumin |
| cAMP | Cyclic adenosine monophosphate |
| CAT | Catalase |
| CCCP | Carbonyl cyanide 3-chlorophenylhydrazone |
| cGMP | Cyclic guanosine monophosphate |
| CoQ | Coenzyme Q |
| COX-2 | Cyclooxygenase II |
| CVD | Cardiovascular diseases |
| DAF | Diaminofluorescein |
| DAFDA | Diaminofluorescein diacetate |
| DCF | Dichlorofluorescein |
| DHE | Dihydroethidium |
| DHR | Dihydrorhodamine |
| DMEM | Dulbecco's modified Eagle's medium |
| DMF | Dimethylformamide |
| DMSO | Dimethylsulfoxide |
| DNA | Deoxyribonucleic acid |
| DNase | Deoxyribonuclease |
| DNP | Dinitrophenol |
| DNPH | Dinitrophenylhydrazine |
| DPI | Diphenylene iodonium |
| EGTA | Ethylene glycol tetra acetic acid |
| ELISA | Enzyme linked immunosorbent assay |
| eNOS | Endothelial nitric oxide synthase |
| EPR | Electron paramagnetic resonance |
| ESP | Electron spin polarization |
| ETS | Electron transport system |
| $FADH_2$ | Flavin adenine dinucleotide |
| FBS | Fetal bovine serum |
| FCCP | Carbonyl cyanide *p*- trifluoromethoxy-phenylhydrazone**,** |
| FITC | Fluorescein isothiocyanate |
| FMN | Flavin mononucleotide |
| GCL | Glutamate cysteine ligase |

| | |
|---|---|
| GFP | Green fluorescent protein |
| GPX | Glutathione peroxidase |
| GRD | Glutathione reductase |
| GSH | Glutathione, reduced form |
| GST | Glutathione transferase |
| $H_2$DCFDA | 2, 7-dichlorofluorescein diacetate |
| HEPES | 4- (2-hydroxyethyl) -1-piperazine ethanesulfonic acid |
| Hif-1α | Hypoxia inducible factor -1α |
| HO-1 | Heme oxygenase-1 |
| HOCl | Hypochlorous acid |
| HPLC | High performance liquid chromatography |
| HRP | Horseradish peroxidase |
| HSP | Heat shock protein |
| ICAD | Inhibitor of caspase-3-activated DNase |
| ICAM | Intercellular adhesion molecule |
| IL-1 | Interleukin-1 |
| iNOS | Inducible nitric oxide synthase |
| KEAP1 | Kelch-like ECH-associated protein 1 |
| KO | Knockout |
| LB | Luria Bertani |
| L-NAME | $N^G$-nitro-L-arginine methylester |
| L-NMMA | $N^G$-monomethyl-L-arginine acetate |
| LPS | Lipopolysaccharide |
| MAP kinase | Mitogen-activated protein kinases |
| Mn-SOD | Mn superoxide dismutate |
| MnTBAP | Mn(III)tetrakis(4-Benzoic acid)porphyrin chloride |
| MPTP | Mitochondrial permeability transition pores |
| MTS | [3-(4,5-dimethylthiazol-2-yl)-5-(3carboxymethoxyphenyl)-2-(4-sulfophenyl)-2H-tetrazolium |
| MTT | 3- (4, 5-dimethylthiazol-2-yl) -2, 5-diphenyltetrazolium |
| NAD | Nicotinamide adenine dinucleotide |
| FAD | Flavin adenine dinucleotide |
| NADH | Nicotinamide adenine dinucleotide hydrogenase |
| NADPH | Nicotinamide adenine dinucleotide phosphate |
| NF-κB | Nuclear factor κB |
| nNOS | Neuronal nitric oxide synthase |
| $^{\bullet}NO$ | Nitric oxide |
| NOS | Nitric oxide synthase |
| NOX | NADPH oxidases |
| NQO1 | NAD(P)H dehydrogenase quinone 1 |
| Nrf2 | Nuclear factor E2-related factor 2 |
| $O_2^{\bullet-}$ | Superoxide |
| $O_2NOCO_2^-$ | Nitrosoperoxycarbonate |
| OD | Optical density |
| $OH^{\bullet}$ | Hydroxyl radical |

| | |
|---|---|
| $OH\text{-}E^+$ | 2-hydroxyethidium |
| $ONOO^-$ | Peroxynitrite |
| PBS | Phosphate buffered saline |
| PCR | Polymerase chain reaction |
| PDGF | Platelet derived growth factor |
| PI | Propidium iodide |
| PI3K | Phosphatidylinositol 3-kinase |
| PKC | Protein kinase C |
| $pO_2$ | Partial oxygen pressure |
| PRX | Peroxiredoxin |
| PVDF | Polyvinylidene fluoride |
| RC-DC | Reducing agent compatible and detergent compatible |
| RNase | Ribonuclease |
| RNS | Reactive nitrogen species |
| ROS | Reactive oxygen species |
| SDH | Succinate dehydrogenase |
| SDS | Sodium dodecyl sulphate |
| PAGE | Polyacrylamide gel electrophoresis |
| SOD | Superoxide dismutase |
| TBE | Tris borate EDTA |
| TCA | Tricarboxylic acid |
| TE | Tris EDTA |
| TNF-α | Tumor necrosis factor -α |
| Trx | Thioredoxin |
| TrxR | Thioredoxin reductase. |
| VCAM-1 | Vascular cell adhesion molecule-1 |
| VDAC | Voltage-dependent anion channel |
| VSMCs | Vascular smooth muscle cells |
| WT | Wild type |
| X-gal | 5-bromo-4-chloro-3-indolyl-b-D-galactopyranoside |
| XIAP | X-linked Inhibitor of Apoptosis Protein |
| XTT | Sodium 3´-[1-(phenylaminocarbonyl) - 3, 4-tetrazolium]-bis (4-methoxy-6-nitro) benzene sulfonic acid hydrate |

**CONTENTS** **PAGE**

## LIST OF TABLES



## LIST OF FIGURES

# CHAPTER 1

# INTRODUCTION

## 1.1 What are free radicals?

A free radical is an atom or molecule which is stable and exists with one or more unpaired electrons in its molecular orbital such as superoxide anion ($O_2^{\bullet-}$), hydroxyl ($HO^{\bullet}$) and nitric oxide ($^{\bullet}NO$). If an orbital in the outer shell of a molecule lose an electron from a pair, the molecule becomes a radical, which is unstable and therefore highly reactive (Mason, 1995)**.** Free radicals often react with another molecule(s) to be stabilized (Shackelford et al., 2000). Partially reduced $O_2$ metabolites are known as "reactive oxygen species" (ROS) due to their higher reactivity over molecular $O_2$. In other terms, reactive oxygen species may be identified as any chemical species containing one or more unpaired electrons potentially capable of independent existence.

The main reactive oxygen species include superoxide ($O_2^{\bullet-}$), hydroxyl radical ($OH^{\bullet}$) and $H_2O_2$, which is a non-radical. $O_2^{\bullet-}$ can be dismutated (by cytosolic or mitochondrial superoxide dismutase; SOD) to hydrogen peroxide ($H_2O_2$) which is a biologically active and stable molecule (**Figure 1.1**). $H_2O_2$ is non-polar and often diffuses into the cytosol of cells through membranes (Henderson and Chappell, 1993). Myeloperoxidase which is the most abundant enzyme in neutrophils, catalyses the conversion of $H_2O_2$ and $Cl^-$ to hypochlorous acid (HOCl) (Kettle et al., 1993) (**Figure 1.1**). This potent oxidant can cause considerable tissue damage in many inflammatory diseases as reported by Kettle et al., (1993).

A newly formed radical may react with another species to become stable by donating the unpaired electrons, or may react with a free radical scavenger (i.e. primary antioxidant or chain breaking species), to become unreactive (Nordberg and Arner, 2001). Free radicals are known to damage cells and tissues through reactivity with another molecule. In this way, radical species are reported to perturb cellular antioxidant defence systems, damaging biological molecules including protein, carbohydrates, lipids and nucleic acids (Tahara et al., 2009). Free radical generation is a consequence of many metabolic reactions in living systems that may generate low levels of radicals. There are number of enzymes, which employ radicals for synthesis of specific enzyme products; cyclooxygenase, tyrosine hydroxylase, nitric oxide synthase, lipooxygenase and ribonucleoside reductase (Thomas, 2000).

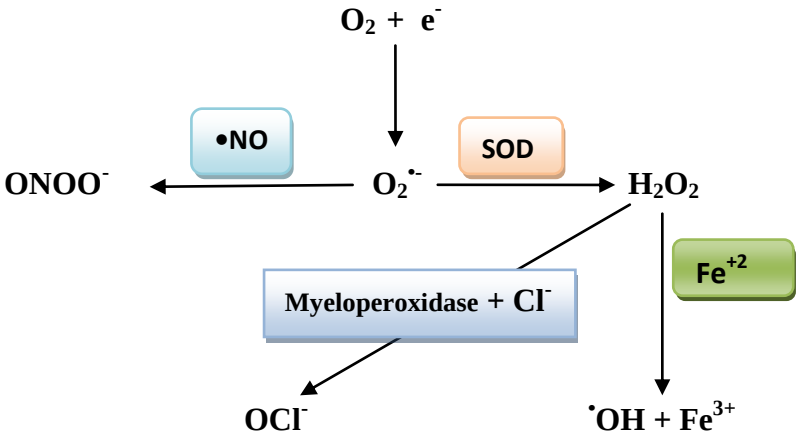


**Figure 1.1 Schematic ROS generation from oxygen ($O_2$), adapted from Hool (2005).** Superoxide ($O_2^{\bullet-}$) is generated directly from the reduction of oxygen and then dismutated to hydrogen peroxide ($H_2O_2$) in the presence of superoxide dismutase (SOD). Reactions with chloride ion ($Cl^-$), nitric oxide ($^{\bullet}NO$) and iron ($Fe^{2+}$) are as indicated.

Reactive nitrogen species (RNS) include $^{\bullet}NO$ and their related species such as peroxynitrite anion ($ONOO^-$) **(Figure 1.1).** $O_2^{\bullet-}$ undergoes a diffusion-controlled reaction with $^{\bullet}NO$ to produce $ONOO^-$ (Beckman and Koppenol, 1996). Peroxynitrite is relatively long-lived, stable molecule, which has an ability to reach critical targets of cells, as it is membrane permeable (Glebska and Koppenol, 2003). Each of these reactive oxygen and nitrogen species are reported to impair cellular homeostasis through alterations in cellular thiols, protein, lipid, and nucleic acid structure and function with resultant disruption of cell signalling cascades (Patel et al., 1999).

This can be explained by potent oxidising capacity of ROS/RNS which lead to oxidation, nitrosation or nitration of amino acids/residues (Griffiths, 2005). To minimize potential damage to macromolecules and cellular environment, cells express antioxidant enzymes including superoxide dismutase to reduce $O_2^{\bullet-}$ to $H_2O_2$, catalase and glutathione peroxidase which reduce $H_2O_2$ to $H_2O$ (Thannickal and Fanburg, 2000). Glutathione peroxidase uses the low MW thiol glutathione as a reducing agent in this reaction. Oxidative stress is defined as an imbalance between oxidant production and antioxidant capacity.

Oxidative stress has been implicated in many pathological injuries within the cardiovascular system including atherosclerosis, hypertension, hypoxia, and ischaemic reperfusion.

## 1.2 Sources of ROS/RNS production

Superoxide is the intermediate precursor of reactive oxygen species in most oxygenated biological systems. It is formed when molecular oxygen acquires an additional electron (Wardman, 2007). Having two unpaired electrons in antibonding orbital with parallel spins makes ground state $O_2$ able to accept one electron at a time. Superoxide anion is potent damaging molecule probably indirectly, and is less reactive than $^{\bullet}OH$. Therefore, $O_2^{-\bullet}$ can diffuse longer distance until it encounters critical molecular targets, whereas $^{\bullet}OH$ reacts indiscriminately and expendably within a smaller radius from the site of generation (Benov et al., 1998).

### 1.2.1 Superoxide production from mitochondria

The mitochondrion is believed to be a major superoxide producer in many cells. The principle function of the mitochondrion is to harness the free energy release from electron transport from complex I and III and IV by coupling the transport of protons out of the mitochondrial matrix to the intermembrane space with the production of ATP according to the chemiosmotic theory.

The transfer of protons from the matrix to the intermembrane space may create an electrochemical gradient, which maintains mitochondrial membrane potentials ($\Psi_{mt}$) across the inner membrane. The proton gradient or electrochemical gradient is used to generate a chemiosmotic potential (between the mitochondrial matrix and intermembrane space) or proton motive force which is critically important to ATP production. This electrochemical gradient plays a major role in converting the energy derived from redox reactions of electron transport to the potential energy stored in ATP.

Complex IV harnesses the energy from the electrochemical gradient to make ATP energy from ADP + Pi at ATP synthase. The ATP synthase is made up of two subunits; $F_0$ and $F_1$. $F_0$ creates the channel for proton movement across the membrane where $F_1$ harvests the free energy derived from proton movement down the electrochemical gradient (from the intermembrane space to the matrix during aerobic respiration) by catalyzing the ATP production **(Figure 1.2 and 1.3).**


**Figure 1.2 Mitochondrial electron transport system (ETS), taken from Moncada and Erusalimsky (2002).**

During mitochondrial respiration, the kinetic and thermodynamic factors underlying the interaction of potential one-electron donors with $O_2$ and that control mitochondrial ROS production depend on the standard reduction potentials and pH value of the mitochondrial matrix. The standard reduction potential for the transfer of an electron to $O_2$ to form $O_2^{\bullet-}$ is −160 mV at pH 7, for 1M $O_2$ under standard conditions. This standard reduction potential is stable across most biological pH values including mitochondria (Murphy, 2009). In mitochondria, it has been reported that electron transport complexes I and III (**Figure 1.2**) are important sources of mitochondrial ROS (Murphy, 2009). However, mitochondria produce less ROS at higher respiration rates, including enhanced oxidative phosphorylation or in the presence of uncouplers and under oxidative stress due to certain pathological conditions.

$O_2^{\bullet-}$ release from complex I occurs via forward electron transfer, electron release from NADH (reduced nicotinamide adenine dinucleotide) and reverse electron transfer from succinate. Additionally, mitochondrial enzymes, particularly flavoenzymes including α-ketoglutarate dehydrogenase and glycerol phosphate dehydrogenase, are involved in the production of $O_2^{\bullet-}$. (See Tahara et al. (2009) for review**) (Figure 1.3).**


**Figure 1.3 Mitochondrial electron transport system showing $O_2^{-\bullet}$ generation by substrate metabolism, electron leakage sites, and effects of respiratory chain inhibitors and uncouplers. Taken and adapted from Tahara et al. (2009).** The sites of action of the complex I inhibitor, rotenone; the complex III inhibitors, myxothiazol and antimycin A; the complex V inhibitor, oligomycin and the uncoupler, FCCP are shown.

Mitochondrial complex I is a major site of superoxide production from NADH in the respiratory chain. The FMN (Flavin mononucleotide) cofactor accepts electrons from NADH and passes them through a chain of seven Fe-S (iron–sulphur) locations to the CoQ (Co-enzyme Q) reduction site, with another Fe-S centre close to the FMN with any reverse transfer of electrons to CoQ. Mitochondrial complex II is known to be a second funnelling site of electrons into ETS.

In complex II, electrons from succinate enter the ETS via $FADH_2$. Then, electrons are transferred to CoQ and carried through the rest of electron transport chain. Complex III has for a long time been regarded as a source of $O_2^{\bullet-}$ within mitochondria (Chandel et al., 1998; Chandel et al., 2000). Mitochondrial complex III fluxes the electrons from the CoQ pool to cytochrome *c* which is a bridge between complex III and complex IV. Mitochondrial cytochrome *c* consists of three haem and Fe-S locations, and those interact transiently with CoQ during electron transfer (Iwata et al., 1998). It has been reported that generation of $O_2^{\bullet-}$ is increased when complex III is inhibited by antimycin where $O_2^{\bullet-}$ is derived from the reaction of $O_2$ with an ubisemiquinone radical bound to the Qo site. This $O_2^{\bullet-}$ is released from complex III to the mitochondrial matrix and intermembrane space as shown in **Figure 1. 3.** $O_2^{\bullet-}$ is unable to penetrate mitochondrial lipid membranes although it may be transferred through anion channels and therefore it may be trapped in a compartment where it is produced, including inside the mitochondrial matrix (Murphy, 2009).

During normal metabolic respiration, mitochondria can produce superoxide, especially in the electron rich aerobic environment in the vicinity of the inner mitochondrial membrane within the ETS. Mitochondria can reduce nearly 1-3% of the $O_2$ consumed in aerobic respiration (Boveris and Chance, 1973, Boveris et al., 1972) by transferring a one single free electron to molecular oxygen at the level of NADH CoQ reductase (Complex I). Subsequently CoQ cytochrome C reductase (Complex III) donates a single electron to $O_2$ for $O_2^{\bullet-}$ production (Turrens, 1997).

### 1.2.2 Nitric oxide and peroxynitrite generation from mitochondria

Nitric oxide ($^{\bullet}NO$) is a reactive and transient radical molecule that can diffuse across the cell membrane. It is known that common $^{\bullet}NO$ is generated from guanido nitrogen of L-arginine by at least three distinct isoforms of nitric oxide synthase in the cells (Pacher et al., 2007). It appears that $^{\bullet}NO$ can damage biological molecules after forming $ONOO^-$ with $O_2^{\bullet-}$. Peroxynitrite is a strong biological oxidant and nitrating species formed from the near-diffusion-limited reaction of the free radicals, nitric oxide and superoxide anion (Beckman and Koppenol, 1996).

$^{\bullet}$NO at nanomolar level can interact with the mitochondrial ETS by causing rapid and selective reversible inhibition of cytochrome oxidase. $^{\bullet}$NO related species or RNS in mitochondria including $ONOO^-$, $NO_2$, $N_2O_3$ and S-nitrosothiols (from $^{\bullet}$NO and thiol reaction) cause slow, non-selective, weak, but irreversible or slowly reversible inhibition of many mitochondrial components including proteins, lipids and mt-DNA. Moreover, the inhibition observed in most cells in response to $^{\bullet}$NO or expression of inducible nitric oxide synthase (iNOS or NOS2) appears to be largely competitive with $O_2$ (Brown and Borutaite, 2007) **(Figure 1.4).**


**Figure 1.4 Interactions between $^{\bullet}$NO, reactive nitrogen species, reactive oxygen species and the mitochondrial respiratory chain, taken from Brown and Borutaite (2007).** The oxidation of $^{\bullet}$NO with oxygen in the inner membrane of mitochondria produces $NO_2$ and $N_2O_3$, and further $^{\bullet}$NO can react with thiols (RSH) to produce S-nitrosothiols (RSNO). $^{\bullet}$NO and RNS inhibit respiratory complexes I, III and IV. $O_2^{\bullet-}$ reacts with $^{\bullet}$NO to form $ONOO^-$, which further inhibits the ETS, aconitase and the Mn-SOD. A lightning bolt illustrates the sites of RNS mediated inhibition (Brown and Borutaite, 2007).

### 1.2.3 Superoxide production from NADPH oxidase

In phagocytes and certain non-phagocytic cells in the colon, kidney, brain and vascular smooth muscle cells (VSMCs), cell membrane bound NADPH (nicotinamide adenine dinucleotide phosphate) oxidase functions as the major ROS generating centre (Cheng et al., 2004). The enzyme complex is comprised of several subunits, including cytochrome b558 and two membrane bound subunits (the small subunit p22phox bound to the catalytic subunit gp91phox (Nox 2) and cytosolic units, Rac1 in non-phagocytic cells and Rac2 in phagocytes as well as, p47 phox and p67phox which are recruited to the membrane bound Nox/p22phox complex upon activation.

Rac1 and Rac2 belong to the low molecular weight G protein Rac family. Some studies suggest that NADPH oxidase activity may decrease during hypoxia with a reduction in ROS production (Mohazzab and Wolin, 1994; Paky et al., 1993). In atherosclerotic inflammatory sites, recruitment of neutrophils and over-production of ROS, mainly by NADPH oxidase, leads to lipid oxidation. Protein expression studies suggest that p47phox expression is predominant in neutrophils compared to non-phagocytes such as smooth muscle cells/fibroblasts, offering further insight into putative ROS generation in vascular inflammatory sites. Some reports suggest ROS generation may also be increased due to mechanical forces and agonist-stimulation by certain hormones such as Angiotensin II (Griendling et al., 2000). Mechanical forces that induce ROS generation in endothelial cells through NAD(P)H include cyclic stretch and laminar, oscillatory shear stress (Griendling et al., 2000).

Angiotensin II is a major peptide hormone in the renin-angiotensin-aldosterone system. It is reported that Angiotensin II plays a pivotal role in signalling in the cardiovascular system by generating ROS through NADPH oxidase (Yoshimoto et al., 2004). The NAD(P)H/NADH oxidase in VSMCs, endothelial cells and adventitial fibroblasts has been shown to elicit an increase in intracellular superoxide production after AngII treatment.

It has been reported that PDGF (platelet derived growth factor), TNF-α, thrombin and lactosylceramide stimulate NAD(P)H oxidase dependent $O_2^{\bullet-}$ production in smooth muscle cells (Griendling et al., 2000). ROS generated by NADPH in VSMCs is required for cell differentiation, proliferation, migration, secretion of inflammatory cytokines and apoptosis (Clempus and Griendling, 2006).

### 1.2.4 Other sources of ROS/RNS

In addition to mitochondria and the NADPH oxidase complex, there are number of other cellular sources of radical species. They include nitric oxide synthase (NOS), xanthine oxidase, peroxisome and endoplasmic reticulum. Other minor level $O_2^{\bullet-}$ producers in the cytosol include enzymes of the arachadonic acid cascade that may produce ROS during lipid metabolism. Some cytochrome P-450 isozymes are also reported to generate $O_2^{\bullet-}$. Autooxidation of ascorbic acid, low molecular weight thiols, adrenalin and flavin coenzyme can also produce ROS under various conditions. ROS/RNS producers are tabulated (**Table 1.1)** along with any cellular defence mechanism. In addition to the above sources of endogenous free radical production, there other ways of free radical production via exogenous agents; cigarette smoking, air pollution and toxic radical generation from drug metabolism including nitrofurantoin and penicillamine (Mason, 1995).

## 1.3. ROS/RNS as signalling molecules

ROS and RNS can act as signalling molecules in various cell types, mediating and/or modifying physiological events related to gene transcription and transduction after receptor ligand binding. In vascular homeostasis and pathogenesis, ROS/RNS play a pivotal role in downstream and upstream intracellular cell signalling. Downstream signalling cascades operate by second messengers such as $Ca^{2+}$, cAMP, phospholipid metabolites and phosphorylation cascades. These pathways subsequently lead to activation of transcription factors that govern specific gene expression patterns.


**Table 1.1 The sources of ROS/RNS production and associated antioxidant defence, adapted from Nordberg & Arner (2001).** SOD - superoxide dismutase, GPX - glutathione peroxidase, CAT - catalase, PRX - peroxidase, GRD - glutathione reductase, Trx –thioredoxin and TrxR - thioredoxin reductase and NOS – nitric oxide synthase.

However, there are important implications of ROS/RNS in intracellular cell signalling and regulation, including cytoprotection and antioxidant defence during hypoxia/reperfusion. $O_2^{\bullet-}$ and $H_2O_2$ are considered the most important ROS signalling molecules (Griendling et al., 2000). The ROS/RNS molecules in signalling are structurally diverse and include $^{\bullet}NO$, $O_2^{\bullet-}$, $H_2O_2$ and peroxynitrite (Griendling et al., 2000; Harrison et al., 2003).

Intracellular signalling pathways are implicated in cell death during hypoxia and/or following reoxygenation, although the mode of cell death; apoptosis or necrosis may vary among different cell types. $ONOO^-$ has been identified as a mediator of cytotoxicity due to its variable reactivity with cellular thiols, proteins and DNA (Patel et al., 1999). $ONOO^-$ or $^{\bullet}NO$ is also important as a cell-signalling molecule, in addition to its pathological roles. For instance, low concentrations of $^{\bullet}NO$ are formed by endothelial nitric oxide synthase (eNOS) in vascular endothelial cells and function as a mediator of vasodilatation (Thannickal and Fanburg, 2000). $^{\bullet}NO$ inhibits proliferation and migration of smooth muscle cells, platelet aggregation and adhesion of leukocytes to the endothelium (Tarpey and Fridovich, 2001).

ROS generation from mitochondria has been implicated in vasodilatation of cerebral artery and vasoconstriction in pulmonary arteries (Schumacker, 2003; Beardsley et al., 2005). However, particular ROS species have not been investigated. $O_2^{\bullet-}$ and superoxide dismutase exhibit many modulatory effects in $^{\bullet}NO$ dependent cell signalling and endothelial dependent-relaxation in vascular systems (Tarpey and Fridovich, 2001). Generation of $O_2^{\bullet-}$ and $H_2O_2$ mediates proinflammatory events by regulating the transcription and expression of vascular cell adhesion molecule-1 and monocyte chemotactic protein-1 (Tsao et al., 1996; Marumo et al., 1997).

### 1.4 Free radicals as damaging molecules

Oxidative stress can be induced by variety of environmental factors including oxygen deprivation (hypoxia and anoxia), UV stress and herbicide metabolism (Kobayashi et al., 2003; Štajner et al., 2003; Renzing et al., 1996; Flores-Sanchez and Verpoorte, 2008). The cellular components susceptible to damage by free radicals are lipids (peroxidation of unsaturated fatty acids in membranes), proteins (nitration, oxidation and denaturation), carbohydrates and nucleic acids. However, the outcome of oxidative stress mainly depends on organs/tissue, species, endogenous antioxidant content and defence signalling pathways. It is postulated that overproduction of radicals may overcome the cellular antioxidant defence, and free radical mediated damage may persist in pathological conditions including ageing, chronic inflammation and ischaemia/reperfusion.

#### 1.4.1 DNA damage

Oxidative damage to DNA is associated with many pathological conditions such as ischaemia/reperfusion, carcinogenesis, mutagenesis and ageing. One of most reactive free radicals, hydroxyl radical ($^{\bullet}OH$) causes damage to DNA. The presence of oxidized DNA is known as a marker for ROS-mediated DNA damage (Halliwell, 1999; Nakano et al., 2003). The guanine base is more sensitive to oxidation, thereby, it is considered as a reasonable biomarker for oxidative injury (Kehrer, 2000).


**Figure 1.5 The mechanism of formation of guanine products from ˙OH addition to the C8 position of guanine, adapted from Dizdaroglu et al. (2002).**

Mechanisms of damage involve abstractions and addition reactions by free radicals leading to carbon (C)-centered sugar radicals and ˙OH- or H-adduct radicals of heterocyclic bases, which may be further fragmented after additional reactions with free radicals. The modification of DNA takes place by the ˙OH which attacks the deoxyribose moiety leading to the release of free bases from DNA and generates strand breaks. Other changes occur in bases, with the resultant cross linking as a result in additions and abstractions (Dizdaroglu et al., 2002). The formation of guanine products from the C8-OH adduct, which is formed by attack of ˙OH to the C8-position of guanine, is a common alteration in the DNA molecule **(Figure 1.5).** It is important to note the presence of oxidized purines or pyrimidines at low levels and at critical sites may cause functional problems (Kehrer, 2000). There are nearly 200,000 base lesions formed per day after oxidation with endogenous ROS generation. Adversely, DNA damage may lead to impaired hydrogen bonding, fidelity of DNA and/or RNA polymerase and conformational changes to the DNA template during DNA synthesis (Kehrer, 2000). The presence of 8-hydroxyguanine is a marker of oxidative stress in nuclear and mitochondrial DNA (nDNA and mtDNA).

It has been reported that oxidative damage is significant in mitochondrial DNA, especially, since the absence of bound histones and deficiency in repair mechanism renders mtDNA susceptible compared to whole nDNA (Zastawny et al., 1998). Moreover, Bristow and Hill, (2008) reported the genomic instability of DNA repair mechanisms in tumor cells in respect to transcription and translational proteins during acute and chronic, severe hypoxia. Oxidative mtDNA damage is associated with induction of nuclear phosphorylation and the dysfunction of mitochondria in ischaemic heart disease (Ferrari, 1996).

### 1.4.2 Lipid Damage

Oxidation of lipids refers to the loss of hydrogen from lipids in cells that may result in cell damage. Lipids include polyunsaturated fatty acid (PUFA) that may contain multiple double bonds in between which lie methylene $–CH_2-$ groups containing reactive hydrogen. The reaction proceeds by a free radical chain reaction which consists of initiation, propagation and termination. Disruption of PUFA in the phospholipid bilayer may result in functional and structural impairment leading to irreversible cell damage. The reaction may be initiated by ROS, such as $^{\bullet}OH$ whereby a fatty acid radical and $H_2O$ are produced by the abstraction of a hydrogen atom from a double bond in a polyunsaturated carbon chain **(Figure 1.6)**. The resultant fatty acid radical is unstable and readily reacts with diradical $O_2$ to form a peroxyl radical.

The peroxyl radical is highly reactive and can abstract another hydrogen atom from neighbouring fatty acid molecule, yielding another radical species and lipid hydroperoxide, thereby establishing the propagation step of the chain reaction. The lipid hydroperoxide formed is unstable and can decompose to various species including malondialdehyde, or it can be reduced to the more stable alcohol form. The lipid bilayer itself may also become more permeable thereby disrupting ion homeostasis (Young and McEneny, 2001). In addition, some of the oxidized fatty acid species that are formed such as the isoprostanes or the hydroperoxides can regulate the apoptosis (Kehrer, 2000). Other lipids may also undergo significant oxidation, particularly cholesterol, resulting in several hydroxycholesterol products (Griffiths et al., 2002).


**Figure 1.6 Schematic representation of ROS induced lipid damage in polyunsaturated fatty acid, taken from Young and McEneny, (2001).**

### 1.4.3 Protein damage

Protein damage can occur as a result of oxidation or nitration of amino acids within a polypeptide chain due to the interaction with ROS and RNS. Accumulation of these oxidized or nitrated proteins may have deleterious effects including disruption of ion channel transport, inactivation of enzymes and ultimately lead to necrosis and apoptosis in vitro (Obrosova, 2006; Davidson et al., 2001; Ischiropoulos and Beckman, 2003).

Oxidation and nitration of proteins has been identified from *in vivo* tissue isolated from several chronic conditions such as inflammation and ageing. Protein oxidation may also be a radical chain reaction where initiation takes place when $^{\bullet}OH$ radical (Reaction *a* and *b*) abstracts a hydrogen atom of an amino acid residue, thereby, forming a carbon-centered radical (Reaction *c*) **(Figure 1.8).**

Then C-centered radical reacts rapidly with $O_2$ to form an alkylperoxyl radical (Reaction *d*) which is an intermediate in generation of alkylperoxide and formation of alkoxyl radical (Reaction *h*). The alkoxyl radical is converted to a hydroxyl protein derivative (reaction *j*). Alkyl, alkylperoxyl, and alkoxyl radical intermediates in this pathway may undergo side reactions with neighbouring amino acid residues in the same or a different polypeptide chain to produce to a another carbon-centered radical **(Figure 1.7 and 1.8)** (Berlett and Stadtman, 1997).


**Figure 1.7 ROS mediated oxidation of protein - C centred radicals, taken from Berlett and Stadtman, (1997).**

Interestingly, in the absence of oxygen under conditions of hypoxia or anoxia or when tissues become ischaemic, when Reaction *d* in **figure. 1.8** is prevented; the carbon-centered radical may react with another carbon-centered radical to form a protein-protein cross-linked derivative (Berlett and Stadtman, 1997).

Direct oxidation of amino acids including lysine, arginine, proline, and threonine residues may yield carbonyl derivatives on side chains. Alternatively, carbonyl groups may be introduced into proteins by reactions with aldehydes (4 hydroxy-2-nonenal, malondialdehyde) produced during lipid peroxidation (**Figure 1.6**) (Berlett and Stadtman, 1997; England et al., 2003). The formation of protein carbonyls has been used as a marker of ROS-mediated protein oxidation, and determination of carbonyl may reflect the degree of oxidative stress (England et al., 2003; Berlett and Stadtman, 1997).


**Figure 1.8 ROS mediated oxidation of protein-protein cross linking and peptide bond cleavage, taken and adapted from Berlett and Stadtman (1997).**

The nitration of proteins is a marker of $ONOO^-$generation. Tyrosine and tryptophan residues are selective targets of $ONOO^-$ - dependent nitration, but, methionine and cysteine residues are particularly vulnerable to oxidation by $ONOO^-$. Nitration of aromatic residues and oxidation of thiol containing residues depend on the availability of $CO_2$ and $ONOO^-$ reacts rapidly with $CO_2$ to form $O=NOOCO_2^-$ or $O_2NOCO_2^-$ derivatives which may direct the modifications to nitrate aromatic compound in the protein chain (Berlett and Stadtman, 1997).

## 1.5 Physiology and pathophysiology of hypoxia and hypoxia/reperfusion injury

Hypoxia is a stress condition in which tissues are deprived of adequate oxygen supply whereas ischaemia is a condition in which the blood flow (oxygen and glucose) is restricted to a tissue and results in anoxia. The effect of hypoxia and ischaemia may not be identical, but they are difficult to separate clinically (Peters et al., 2000). Hypoxia and subsequently ischaemia is an important cause of reversible or irreversible tissue injury, but it depends on severity and duration of the insult. The German pathologist Rudolf Virchow in 1858 first defined and described ischaemia in the heart, as an imbalance between myocardial oxygen supply and demand due to a decrease of blood flow as a result of narrowing of the coronary artery (Liem et al., 2007). Coronary heart disease is one of the leading causes of death and disability in the world. Epidemiological data indicate that its morbidity and mortality rates will exceed those of cancer and infectious disease in the near future (Murray and Lopez, 1997). Hypoxia could arise due to narrowing of a blood vessel due to fatty deposits (atherosclerosis) and restricted blood supply to neighbouring tissue or cells. If this process takes place in the coronary artery, the condition is known coronary ischaemia and leads to coronary heart disease **(Figure 1.9)**. It is therefore essential to restore coronary flow to the ischaemic myocardium by interventions such as angioplasty, thrombolytic treatment or coronary bypass surgery (Jennings and Reimer, 1991).

Cardiac hypoxia as a result of ischaemia mainly results in irreversible cell damage, which may further progress to contractile failure, ventricular remodelling and arrhythmias. Reperfusion is the restoration of oxygenated blood supply to hypoxic or ischaemic tissues. Reperfusion injury refers to irreversible damage to a tissue caused when blood supply carrying oxygen returns to the tissue after a period of ischaemia or hypoxia. The absence of $O_2$ alone or $O_2$ and nutrients for a period from blood result in a condition in which inflammation and oxidative stress is typical in many organs including heart, brain, liver, kidney and intestine. The energy demand for these tissues depends on limited mitochondrial respiration and possibly glycolysis alone (de Groot and Rauen, 2007). In general, the susceptibility of cells or tissues to hypoxia or ischaemia reperfusion injury is a major clinical challenge after an infarct and after successful organ transplantation.


**Figure 1.9 Coronary heart disease and myocardial infarction** (www.focalcool.com).

Inflammation during hypoxia/reperfusion includes both the cellular and humoral responses. Many metabolic changes are induced in hypoxia or ischaemia/reperfusion injury. Coronary occlusion in the heart or microvascular occlusion in other tissue may result in complete deprivation of the $O_2$ supply (anoxia) which triggers loss of the mitochondrial ATP supply, accumulation of lactic acid, overload of intracellular $Ca^{2+}$, osmotic swelling due to loss of $Na^{+}$ homeostasis, mitochondrial permeability transition and disruption of membrane potential and finally, cell death via necrosis (de Groot and Rauen, 2007) **(Figure 1.10 and 1.11).**

During reperfusion injury in a tissue, release of ROS/RNS by macrophages, endothelial cells, neutrophils, lymphocytes, platelets, parenchyma cells and leukocytes add to the existing damage to the endothelium, thrombus formation, cytotoxic enzyme release, increased vascular permeability and increased cytokine release. These effects contribute induced tissue injury through effects on signal transduction pathways mediated by ROS and/or $Ca^{2+}$ leading to activation of enzymes or mediators involved in cell death and dysfunction (de Groot and Rauen, 2007; Björk et al., 1982; Mueller et al., 1997; Weiss, 1989). The progression of cell death in ischaemia under anoxia is shown schematically in **figure 1.11.**

Deleterious effects may persist for a period of time, weeks or months. This depression of cardiac function (myocardial stunning) of the ischaemic-reperfused heart is common in patients after coronary bypass surgery or in patients with a heart transplant (de Groot and Rauen, 2007).


**Figure 1.10 Paradoxical effects of reperfusion in the ischaemic heart. Reperfusion contributes to further tissue damage, taken from Dhalla and Duhamel (2007).**

Irreversible or reversible cell death or infarction size induced by an acute coronary occlusion mainly depends on severity and duration of ischaemia. Several treatments restore blood flow (reperfusion therapy) in patients with acute myocardial infarction; but clinical reperfusion therapy such as thrombolysis is not effective in supporting survival of ischaemic cells. Cardiac cell death is mainly associated with restoration of blood supply; reperfusion. Recent development of current methods for improving the efficacy of thrombolysis and percutaneous coronary interventions during revascularization or cardioprotection therapy have improved survival, but many effects of these therapies remain unresolved.

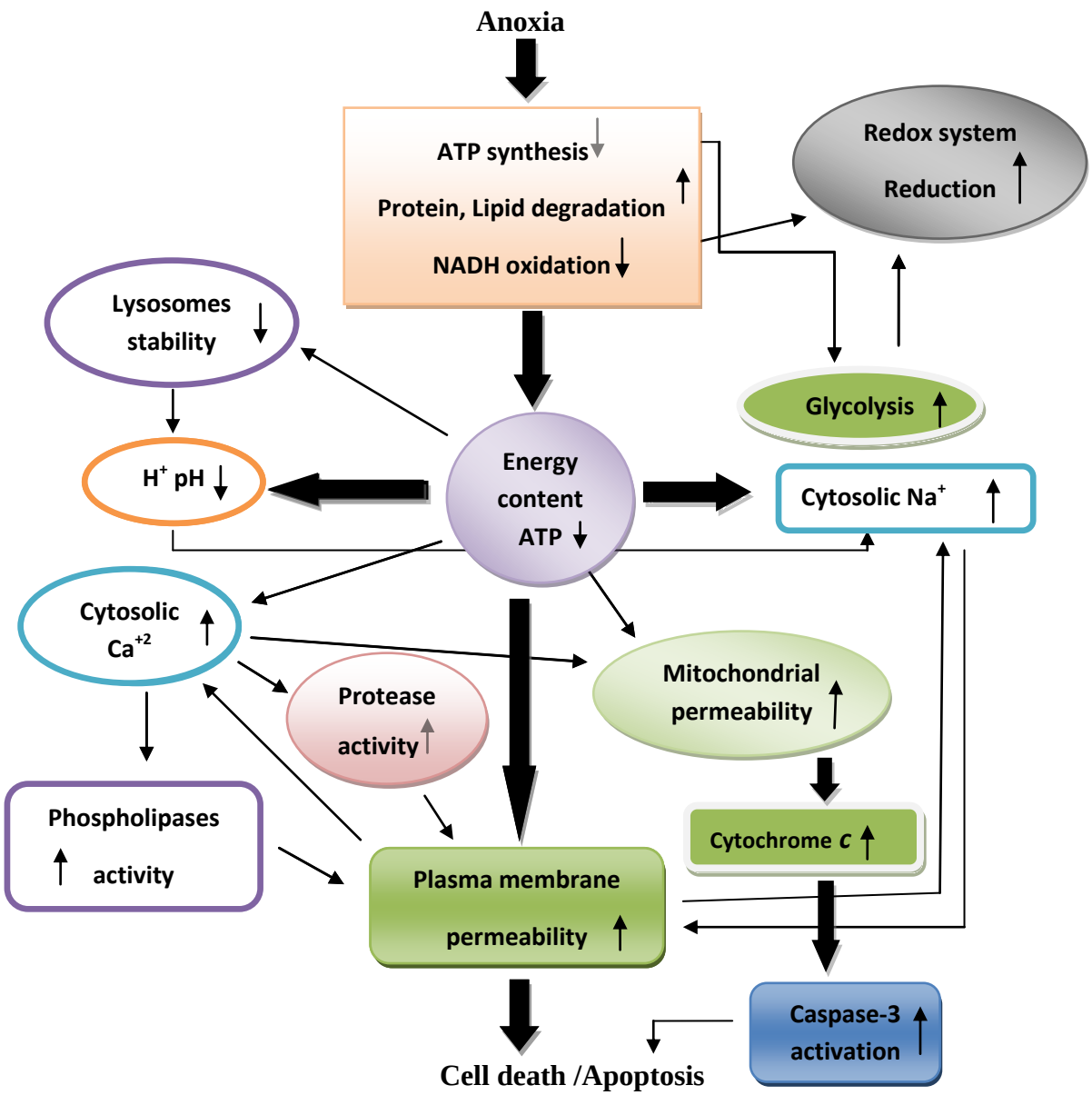


**Figure 1.11 Schematic presentation of progression to cell death in ischaemic tissue under anoxia, adapted from de Groot and Rauen (2007) and Crompton (1999). ↑- increase or ↓- decrease.**

### 1.6 ROS/RNS signalling in cardiovascular disease

Signalling mechanisms of ROS/RNS are of particular relevance to cardiovascular diseases (CVD); myocardial infarction, ischaemia/reperfusion, atherosclerosis and hypertension, and have been studied recently in vascular cells. During atherosclerosis, activation of the enzymes in both

infiltrating macrophages and vascular cells generate high levels of ROS/RNS, thereby changing the oxidation status of thiols on signalling proteins (Harrison et al., 2003; Taniyama and Griendling, 2003; Levonen et al., 2001). The ROS/RNS involved in redox signalling pathways can be generated from the NADPH oxidases and NOS or mitochondria as a major ROS generation site. Mainly, mitochondrial ROS formation is associated with the cell signalling that controls proliferation (Li et al., 1997), hypoxia, necrosis and apoptosis (Chandel and Budinger, 2007; Bonavita et al., 2003; Kim et al., 2003). The redox cell signalling pathways that are activated are balanced between those that protect endothelial and vascular smooth muscle cells with those that initiate cell death through apoptosis (Sauer et al., 2001; Schafer et al., 2003).

A major challenge at the present time is to understand how the localized production of ROS/RNS contributes to the atherosclerotic lesion formation and how it makes a plaque (Patel et al., 2000). Therefore, particular attention is being made to associated mechanisms through which cells generate and detect ROS/RNS and their metabolic products, particularly oxidized lipids or proteins produced by enzymatic and non-enzymatic mechanisms (Li and Jackson, 2002). There is increased interest in how ROS/RNS contribute to cellular protection in addition to deleterious effects as a number of therapeutic interventions based on reactive species which have not demonstrated clinical benefits in treating vascular diseases. Strikingly, use of low molecular weight antioxidants and inhibitors of cyclo-oxygenase pathway has not been successful (Taniyama and Griendling, 2003). It was assumed these agents would have therapeutic benefits as some ROS/RNS and oxidized lipids have potentially beneficial effects as signal transduction molecules in cytoprotection (Taniyama and Griendling, 2003). Therefore, it is important to examine sources of free radical generators; mitochondria, NADPH oxidase and NOS in vascular systems in the pathophysiology of cardiovascular disease.

Interestingly, lipid oxidation products are implicated in the progression of atherosclerosis which is the underlying cause of myocardial infarction and strokes. The mitochondrion is a site of redox signalling which is mediated by oxidized lipid products (Zmijewski et al., 2005).
In general, vascular pathologies are multifactorial, but it is known that mitochondrial dysfunction can contribute to the pathophysiology of vascular diseases; ischaemia, hypoxia and reperfusion.

It is not only the dysfunction of mitochondrial energy production, but also mitochondria-dependent redox signalling pathway that contribute to cell survival and/or injury (Zmijewski et al., 2005).

### 1.7 Cell death during hypoxia, anoxia, or hypoxia/reperfusion

Cell death during hypoxia was thought to be by necrosis based on various ultrastructural findings in hypoxic cells (Jennings et al., 1975). However, recent biochemical investigations have demonstrated the feasibility of hypoxia-induced apoptosis (Muschel et al., 1995). McCully et al. (2004) reported that both necrosis and apoptosis contribute to myocardial infarct size during ischaemia/reperfusion. Therefore, cell death in cardiomyocytes is induced by two mechanisms; necrosis and apoptosis, which are different morphologically (Watkins et al., 1995).

#### 1.7.1 Necrosis

Necrosis has been reported as a passive degenerative process induced by direct toxic and physical injuries (Shimizu et al., 1996) in addition to cellular stress conditions. Cellular necrosis is associated with chronic, severe hypoxia or anoxia condition due to absence of $O_2$, which may have impaired ATP production. However, cellular endogenous factors such as intrinsic adaptive mechanisms, hypoxic tolerance and tissue type may determine the degree of necrotic cell death. Characteristically, necrotic cells swell, accumulate intracellular water, chromatin clumps, DNA degenerates, large cytosolic vacuoles are seen, ATP is depleted, mitochondria swell, and the cells lyse with intracellular contents spilled into the extracellular space **(Figure 1.12).** This results in activation of inflammatory reactions with recruitment of macrophages (Shimizu et al., 1996; Naoi et al., 2000; McCully et al., 2004). Necrosis can occur during trauma, and thrombosis, with depletion of high energy stores, and disruption of the cellular membrane involving fluid and electrolyte alterations, the loss of potassium and magnesium ions, and accumulation of sodium, chloride, hydrogen, and calcium (McCully et al., 2004).

### 1.7.2 Apoptosis

Apoptosis is a conserved process of cell suicide that plays an integral role in embryonic development, tissue homeostasis and tissue remodelling. Deregulation of apoptosis may result in excess cell death, and is implicated in pathogenesis of human disease. It is now evident that apoptosis plays a key role in the pathogenesis of a variety of cardiovascular diseases including myocardial infarction, ischaemia/reperfusion heart failure and stroke (Crow et al., 2004).


**Figure 1.12 The sequence of ultra structural changes in apoptosis and necrosis, taken from Cruchten and Broeck. (2002).**

Cardiomyocytes may undergo apoptosis in response to hypoxia and reperfusion. Acidosis, serum or glucose deprivation, metabolic inhibition and other stimuli such as stretch, tumour necrosis factor and *Fas* ligand also trigger cardiomyocyte apoptosis (McCully et al., 2004; Adrain and Martin, 2001; Bromme and Holtz, 1996; Clerk et al., 2003; Crow et al., 2004). Apoptosis is an ATP-dependent mechanism of cell death, which is known as programmed cell death whereby damaged cells are cleared out in controlled manner without provoking inflammation. Apoptosis is characterized by the generation of fragmented nuclei with highly condensed chromatin and

fragmented DNA, plasma membrane blebbing, externalization of phosphatidylserine and cell shrinkage due to reduction in cytoplasm or protrusion of cytoplasm and organelles and then formation of membrane-bound apoptotic bodies (Crow et al., 2004; Shimizu et al., 1996; Cruchten and Broeck, 2002). These membrane-bound apoptotic bodies containing cytosol and processed organelles are formed and then removed by recruited macrophages via phagocytosis (Cruchten and Broeck, 2002) **(Figure 1.12).** Clinically, apoptosis has been observed in samples collected from patients after myocardial infarction and end-stage heart failure (Olivetti et al., 1996; Narula et al., 1996) and also, in animal models of ischaemia/reperfusion injury (Levrand et al., 2006; Cruchten and Broeck, 2002; McCully et al., 2004).

Two major pathways of apoptosis exist; the extrinsic, death receptor-mediated pathway and the intrinsic pathway. The intrinsic pathway triggers a mitochondrial mediated pathway involving cytochrome *c* release. The immediate effect of apoptosis via the intrinsic pathway is the activation of procaspases and dysfunction of the mitochondria. Therefore, apoptosis follows via specialized machinery; the central component of this machinery is a proteolytic system involving a family of proteases called caspases. These enzymes are involved in a cascade that is triggered in a response to proapoptotic signals and culminates in cleavage of structural proteins and DNA resulting in disassembly of the cell (Thornberry and Lazebnik, 1998, Nicholson et al., 1995). In apoptosis, procaspase activation is regulated by members of the Bcl-2 and inhibitor of apoptosis (IAP) protein families. Both intracellular and extra cellular signals mainly act by regulating the levels or activity of members of the Bcl-2 and IAP families (Alberts et al., 2008; Galonek and Hardwick, 2006;Kim et al., 2006).

The Bcl-2 family of proteins; pro-apoptotic factors regulate the activation of procaspases, but, some other proteins of the same family such as Bcl-2 or BcL-$X_L$; anti-apoptotic factors inhibit apoptosis at least by inhibiting release of cytochrome *c* from mitochondria (Alberts et al., 2008; Kim et al, 2006; Galonek and Hardwick, 2006). The Bcl-2 family anti-apoptotic factors include Bcl-2, Bcl-xL, Bcl-w/Bcl2L2, Mcl-1, Bcl2A1/Bfl-1, NR-13, Boo/Diva/Bcl2-L-10 and Bcl-B as

reported. The first group of pro-apototic factors include Bik/Nbk, Blk, Hrk/DP5, BNIP3, Bcl2L11/BimL/Bod, Bad, Bid, PMAIP1/Noxa, PUMA/Bbc3 and Bmf (Willis and Adams, 2005; Kim et al., 2006; Galonek and Hardwick, 2006; Huang and Strasser, 2000; Adams and Cory, 2001; Borner, 2003). All members listed above holds only a specific BH3 domain unlike other members in Bcl-2 family (Huang and Strasser, 2000**)**. The second group of pro-apoptotic factors includes Bax like pro-apoptotic factors including Bax, Bak, Bok/Mtd, Bcl-xs (Kim et al., 2006; Galonek and Hardwick, 2006; Huang and Strasser, 2000). PUMA and Noxa are both BH3-only proteins which are known as other pro-apoptotic factors which can activate p53-mediated apoptosis (Willis and Adams, 2005; Yu and Zhang,2008; Vousden, 2005). BH3 only members and their ability to interact with other pro-survival family members to permit bax/Bak to form mitochondrial pores. The proapototic factors, like Bad, function by binding to and inactivating the anti-apoptotic factors, whereas Bax and Bak, trigger the release of cytochrome *c* from mitochondria (Jiang and Wang, 2004; Galonek and Hardwick, 2006) and Bid in Bcl-2 family can promote the activation of both Bax and Bak (Willis and Adams, 2005;Jiang and Wang, 2004; Kim et al, 2006). If the genes encoding Bax and Bak are not activated or expressed, cells can resist to apoptotic stimuli (Kim et al., 2006; Galonek and Hardwick, 2006; Huang and Strasser, 2000).

IAP (i.e. X-linked inhibitor of apoptosis, XIAP) are known to inhibit apoptosis either by binding to procaspases, like 9 and/or 3 to prevent their activation or binding to active caspases, like caspae-9 (Verhagen et al., 2001;Crow et al., 2004). When Bax and Bak stimulate the release of cytochrome *c*, it can activate Apaf-1 and at the same time, the other protein released by mitochondria can block the activity of IAPs (Verhagen et al., 2001;Crow et al., 2004, Kim et al., 2006; Galonek and Hardwick, 2006). Caspases are a subclass of cysteine proteases that cleave substrate after aspartic acid residue which are crucial to the activation of execution of apoptosis (Thornberry and Lazebnik, 1998). Caspases are constitutively expressed and synthesized as inactive zymogens referred commonly as procaspases, containing an N-terminal prodomain and a C-terminal catalytic domain consisting of ~17-24kDa (p20) and ~10-12kDa (p10) subdomain.

Caspases are classed according to their function, as either upstream (initiator) caspases; caspases 2, 8, 9, 10 and 12 or downstream (effectors, executioner) caspases; 3, 6 and 7 (Nicholson et al., 1995; Crow et al., 2004) **(Figure 1.13).** Induction of cell death largely depends on the interactions between different modulators, typically activation of apoptosis in cardiac myocytes is multiple stressor-dependent. In cardiovascular disease multiple stressors include cytokines, increased oxidative stress, and DNA damage. Upstream procaspases are activated by dimerization and autolysis and inactive downstream procaspases activated by proteolytic cleavage mediated by initiator caspases. Procaspase-3 has a major role in apoptosis, when it is cleaved, in turn; it activates other executioner caspases and leads to the subsequent characteristic features of apoptosis (Thornberry and Lazebnik, 1998; Nicholson et al., 1995) **(Figure 1.13).**

### 1.8 Hypoxia induced apoptosis of cardiomyocytes

Despite the convincing evidence that apoptosis occurs following hypoxia, the molecular mechanism and signalling pathway(s) activated by hypoxic stimuli and resulting in cardiac cell apoptosis are enigmatic to date. Ischaemia/reperfusion mediated cardiomyocyte apoptosis is regulated by several redox- sensitive transcription factors and genes including NF-κB and AP-1 respectively (Maulik et al., 2000; Sun and Oberley, 1996). Satriano and Schlondorff. (1994) reported the activation of NF-κB by $O_2^{-\bullet}$ in mouse glomerular mesangial cells in response to tumour necrosis factor-alpha, whereas Pignatti and Stefanelli (2003) reported the modulation of NF-κB activity with NOS-dependent $^{\bullet}NO$ in cardiomyocytes. In contrast, Levrand et al. (2005) reported the inhibition of NF-κB activation by $ONOO^-$ during ischaemia/reperfusion in cardiomyocytes. However, the role, duration of production and specific type of ROS/RNS to activate NF-κB and modulation of apoptosis during hypoxia/reperfusion remains unknown. In accord with previous reports, prolonged hypoxia of 24-72h was needed to induce significant apoptosis in primary cultures of neonatal rat cardiac myocytes (Yaoita et al., 1998). Hypoxia alone is reported to be a very weak apoptotic stimulus in H9C2 cardiomyoblasts, however serum withdrawal can significantly enhance the proapoptotic actions (Bonavita et al., 2003). Unlike other cells, cardiomyocytes have an intrinsic pathway to protect themselves from severe hypoxia.

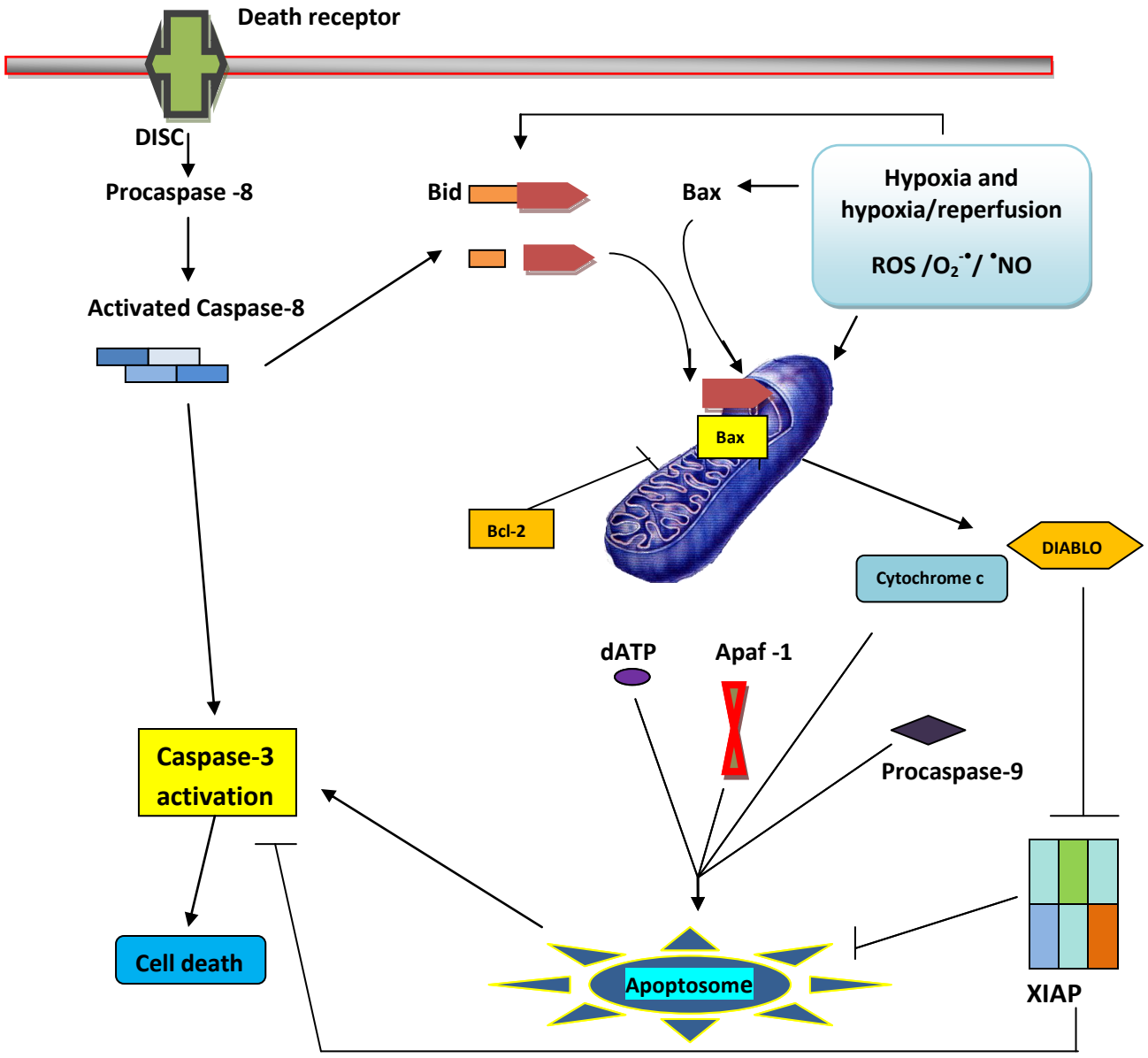


**Figure 1.13 Central apoptotic pathway, adapted from Crow et al. (2004) and Kim et al. (2006).** In the extrinsic pathway, death receptor activation stimulates procaspase-8 activation. Then, activated caspase-8 cleaves downstream procaspase-3, which triggers proteolytic digestion of the cell. In the intrinsic pathway, intracellular and extracellular death stimuli carry signals to mitochondria through Bax and Bid, which translocate to outer membrane and then stimulate release of apoptogens; cytochrome *c* , Smac and DIABLO. Bcl-2 and Bcl-$x_L$ are anti-apoptotic factors. In the cytoplasm, cytochrome *c* + dATP+Apaf-1 and procaspase-9 form apoptosome. Then, activated procaspase-9 induces proteolytic cleavage of procaspase-3. XIAP can inhibit activation of procaspase-9, active caspase-9 and 3. Activated caspase-8 cleaves Bid and then the, C-terminus of cleaved Bid translocates and inserts into the outer membrane of mitochondria, thereby activating Bax and Bak and release of cytochrome c.

It has been suggested the presence of high levels of endogenous apoptosis inhibitors such as apoptosis repressor caspases (ARC) that interact selectively with the death domain of the Fas (CD95/Apo-1) death receptor and upstream initiator caspases 2 and 8, respectively support cell survival (Bonavita et al., 2003). Furthermore, other survival factors for cardiomyocytes include interleukin-6, cardiotrophin 1 and insulin-like growth factor 1 and have been shown to be protective by inhibiting cardiomyocyte apoptosis pathways (Bonavita et al., 2003). An absence of glucose in neonatal rat cardiac myocytes during hypoxia-induced significant apoptosis as reported by cytochrome *c* release and DNA fragmentation (Malhotra and Brosius, 1999). However, the mechanism by which enhanced glycolysis protects against hypoxia-induced apoptosis is unknown.

### 1.9 ROS/RNS generation in cardiovascular system

Mitochondria and NAD(P)H enzymatic complexes are considered the main centres of ROS generation in the cardiovascular system (Abramov et al., 2007). Other sources of ROS generation can become significant in non-physiological conditions including superoxide generation from xanthine oxidase in hypoxic tissues (Abramov et al., 2007). NADPH oxidase has been proposed as the major superoxide producer in the vascular system (based on the use of inhibitors of flavoproteins such as diphenyleneiodonium (DPI)) compared to xanthine oxidase, NOS, cytochrome P-450 reductase and oxidoreductases of the mitochondrial respiratory chain and ubiquinone oxidoreductase (Balcerczyk et al., 2005). It has been reported that NOS-dependent and independent $^{\bullet}$NO production occurs in the cardiovascular system and in rat heart (Raat et al., 2009; Brown and Borutaite, 2007; Zweier et al., 1999; Strijdom et al., 2009).

Many investigators have demonstrated that there is a NOS-dependent increase in $^{\bullet}$NO production in the myocardium during early ischaemia (Strijdom et al., 2009). However, these studies do not clearly specify the cellular sources of $^{\bullet}$NO production and/or which NOS isoforms are responsible for $^{\bullet}$NO generation under pathological conditions (Strijdom et al., 2009; Brown and Borutaite, 2007).

Several studies have shown that increased expression of eNOS and iNOS generates $^{\bullet}$NO during ischaemia, but their regulation and activation are not well understood during hypoxia (Raat et al., 2009). Recently, studies have shown that activation occurs of cellular nitrite sources to generate $^{\bullet}$NO during ischaemia and also in reperfusion as a cytoprotective measure, but their mechanism and contribution are not well described (Raat et al., 2009). Peroxynitrite is involved in myocardial cytotoxicity by direct oxidation of lipids, proteins, and DNA (Pesse et al., 2005; Pacher et al., 2005), the activation of metalloproteinases (Wang et al., 2002) and nitrotyrosine formation. Moreover, $ONOO^-$ generation associates with myocardial oxidative stress, which may contribute to myocardial apoptosis (Kumar and Jugdutt, 2003). $ONOO^-$ acts as a potent signalling molecule in cardiomyocytes by activating all members of the MAP kinase family (Pesse et al., 2005), and inhibiting the activation of nuclear factor kappa B (Levrand et al., 2005).

### 1.10 Mitochondria in hypoxia/reperfusion

The mitochondrion is the energy producer for cell survival, but is involved in the cell death during hypoxia/reperfusion. Mitochondrial death during hypoxia/reperfusion is associated with mitochondrial permeability transition pore (MPTP) opening during both necrosis and apoptosis (Crompton, 1999). MPTP opening results in depolarization of membrane potential ($\Delta\psi m$) which may in turn reduce the proton motive force to harness energy from ATP synthase at mitochondrial complex IV. Instead, ATP depletion occurs as cells attempt to maintain lost membrane potential in an adaptive process. However, sustained opening of MPTP results in release of cytochrome *c* and activation of the apoptogenic molecules, Smac/DIABLO and APAF-1 within the intermembrane space (Honda et al., 2005). This may result in the induction of cell death via by cleaving procaspase-9 during apoptosis. It has been reported that generation of ROS/RNS plays a critical role in determining the opening of MPTP (Zhao, 2004).

Sustained opening of MPTP may result in matrix swelling due to diffusion of water and ultimately rupture of the outer membrane. It is believed that intracellular $Ca^{2+}$ overload in the mitochondria plays a role in mitochondrial swelling and rupture of outer membrane and $Ca^{2+}$ buffering mediated hypoxia/reperfusion induced-cell death is widely established (Lemasters et al., 2009).

Moreover, MPTP opening is pH-sensitive, but its relative sensitivity is unknown under hypoxia/reperfusion conditions (Crompton, 1999; Crow et al., 2004). Typically, MPTP opening can be activated by overexpression of proapoptotic factors such as Bcl-2 family members; Bax, Bak, Bad, Noxa, Puma, and Bid (Kim et al., 2003; Crompton, 1999; Honda et al., 2005). MPTP opening during hypoxia may be further sustained during reperfusion; however, this depends on the interplay between matrix $Ca^{2+}$ level, ROS, intracellular $Mg^{2+}$ and pH (Crompton, 1999; Zhao, 2004). As a cardiac protective mechanism, particularly during preconditioning, cells may adapt by; (1) opening of $Mg^{2+}$ and ATP dependent mt-KATP channels leading to depolarization, and decreasing the electrochemical gradient for $Ca^{2+}$ during reperfusion; (2) opening of mt-KATP channels to promote matrix swelling that can help to maintain membrane integrity where it can run efficient electron transport; (3) opening of mt-KATP that may reduce ROS production, thereby, preventing MPTP opening (Crompton, 1999; Honda et al., 2005; Penna et al., 2009). mt-KATP channel function during preconditioning is under investigation as an approach to improve therapeutic interventions against reperfusion injury.

### 1.11 ROS/RNS generation during hypoxia/reperfusion

During normoxia, $O_2^{\bullet-}$ anion radicals are produced by the mitochondrial electron transport system at NADH coenzyme Q reductase (complex I); and ubiquinol–cytochrome c reductase (complex III). During ischaemia, reduction of iron-sulphur and ubiquinone components occurs with an inhibition of complex I which may trigger the decline in superoxide dismutase activity and result in the mitochondrial superoxide burst (Murphy, 2009). In the myocardium, it is believed that the mitochondrion is the main source of ROS from the respiratory chain (Becker et al., 1999). The ETS often generates a large flux of electrons which may be potentially capable of reducing $O_2$ (Becker et al., 1999). After exposure to hypoxia, probably redox components of the respiratory chain impair complexes I and III in their reduced state, causing more superoxide or ROS formation possibly via ubisemiquinone radical intermediates (Becker, 2004a). Experiments with the electron transfer inhibitors amytal and myxathiazol demonstrated complex III as a major site of ROS production during ischaemia (Becker et al., 1999).

Recent studies show that NADH dehydrogenase in complex I is inactivated partially during hypoxia-reperfusion due to accumulation of $O_2^{\bullet-}$ and ROS which may cause loss of the Fe-S clusters in the complex. Moreover, complex II may also produce ROS during hypoxia, by switching its catalytic activity from SDH to fumarate reductase activity at reduced oxygen tension (Murphy, 2009). There is no clear evidence of ROS generation from complex IV, except for its role as a cellular oxygen sensor with the function of cytochrome *c* oxidase (Palacios-Callender et al., 2007). During normoxic respiration, antioxidant enzymes such as Mn superoxide dismutase (Mn-SOD) in mitochondrial matrix and Cu/Zn superoxide dismutase (Cu/Zn-SOD) in the mitochondrial intermembrane space and cytosol swiftly dismutate excess $O_2^{\bullet-}$ produced within the matrix, intermembrane space and outer membrane to $H_2O_2$ (Murphy, 2009; Okado-Matsumoto and Fridovich, 2001). The resultant $H_2O_2$ is then degraded to $O_2$ and $H_2O$ by cytosolic or mitochondrial catalase, glutathione peroxidase (Thannickal and Fanburg, 2000) and peroxiredoxin (Vivancos et al., 2005). The contribution of ROS in promoting ischaemic damage has been demonstrated by the reduced damage observed in reperfused heart of transgenic mice overexpressing Mn-SOD (Chen et al., 1998). GSH peroxidase-catalysed removal of $H_2O_2$ reduces GSH concentration and can result in a redox change in the mitochondria and cytosol.

Overproduction of ROS during a prolonged hypoxic insult can further disrupt mitochondrial homeostasis by irreversibly oxidising proteins such as cytochrome oxidase (Murphy, 2009), DNA and lipids. In contrast, a lower level of ROS generation is required to induce cardioprotective mechanisms that preserve mitochondrial integrity and the myocardium during episodes of hypoxia or ischaemia. Within the hypoxic heart, mitochondria are likely to be the main source of ROS in muscle cells (Vassilopoulos and Papazafiri, 2005; Turrens, 1997; Suleiman et al., 2001). Other sources such as the NADPH oxidase complex in vascular cells (Souza et al., 2002) or xanthine oxidase in endothelial cells, pulmonary cells and neuronal cells can generate $O_2^{\bullet-}$ (Pearlstein et al., 2002; Abramov et al., 2007; Becker et al., 1999; Becker, 2004a). Moreover, NOS isoforms also can produce $O_2^{\bullet-}$ and $H_2O_2$ when L-arginine substrate is limited in supply (Pou et al., 1999).

However, the relative contribution of aforementioned sources for $O_2^{\bullet-}$ production during hypoxia alone in cardiomyocytes has not been clearly established.

### 1.12 NOS in hypoxia/reperfusion

Nitric oxide ($^{\bullet}$NO) can be generated in many cells or tissue types including myocardium in the heart and have profound effects on cardiac function. $^{\bullet}$NO is principally generated by $^{\bullet}$NO synthases (NOS), which catalyze the conversion of L-arginine to $^{\bullet}$NO and L-citrulline, however, there are non-enzymatic sources including endogenous nitrite stores, generating $^{\bullet}$NO or their related species during ischaemia/reperfusion. nNOS and eNOS are constitutively expressed and their activation is calcium/calmodulin-dependent. However, iNOS is expressed only under stimulated conditions such as microbial or immunological stimuli, and there is no relation to intracellular calcium level (Kanno et al., 2000).

There is considerable interest in mitochondrial NOS as previously reported by Zenebe et al. (2007). Even in the presence of mtNOS, the contribution of mitochondria to $^{\bullet}$NO production might not be important under *in vivo* ischaemia/reperfusion. Some authors have reported that the main site of $^{\bullet}$NO synthesis is non-mitochondrial, probably by nitrosyl-heme complexes as those are formed in ischaemic hearts (Tiravanti et al., 2004). Several authors have documented the beneficial effects of administration $^{\bullet}$NO donors attenuating ischaemic injury (Pabla and Curtis, 1995; Wainwright and Martorana, 1993; Kanno et al., 2000; Strijdom et al., 2009). Moreover, pharmacological inhibition of NOS and transgenic iNOS or eNOS knockout (KO) mice show more severe hypoxic injury in the heart (Kanno et al., 2000).

In further support of a protective role of $^{\bullet}$NO, eNOS-KO mice attenuates cardiac recovery after ischaemia/reperfusion, but overexpression of eNOS accelerates functional recovery of the heart. Moreover, pharmacological inhibition of NOS attenuates the developed pressure after ischaemia/reperfusion in mice and guinea pig hearts; to NOS-dependent $^{\bullet}$NO formation is cardiacprotective and can attenuate myocardial stunning in mice and guinea pigs (Schulz et al., 2004).

However, the protective efficacy of NOS-dependent •NO is species dependent, as NOS isoforms expression is species dependent (Pabla and Curtis, 1996). In rats, both low and high •NO concentration are ineffective in activating cardiac protection while intermediate concentrations are protective (Schulz et al., 2004). eNOS-KO mice have an increased infarct size after ischaemia reperfusion, suggesting the importance of eNOS activity during ischaemia/reperfusion (Schulz et al., 2004). Moreover, addition of a •NO donor at the time reperfusion or just before reperfusion had beneficial effects, such as a decrease in irreversible injury and reduced neutrophil adhesion to the endothelium (Sato et al., 1995).

### 1.13 Quantification of ROS and RNS during hypoxia-reperfusion using fluorescent probes

There are number of direct and indirect methods available to detect ROS/RNS at an intracellular level; but facile detection of ROS is still problematic. The use of reliable and precise methods to assess ROS/RNS production is crucial. Fluorescent probes are widely used for *in vitro* determination of ROS and RNS. Fluorescent probes are fluorophores that may be designed to localize within a specific region of a biological tissue and to respond to a specific signal such as amount of ROS and RNS. ROS/RNS cause oxidation or nitration of the fluorescent probe which is initially in a chemically reduced state and an associated increase in fluorescence. Therefore, the proportion of fluorescence is correlated to the amount of intracellular ROS/RNS. The reduced dyes are known to be colourless and non-fluorescent; once oxidized, the dyes are highly coloured and fluorescent. It is important to understand the chemical properties of the probe, particularly their chemical reactivity towards ROS/RNS.

Most dyes have variable sensitivity, but some have specificity for a particular reactive species. However, in complex biological research, physical properties also play an important role, therefore understanding the physical properties such as solubility in the culture medium, biodistribution, absorption spectra, fluorescent emission spectra and fluorescent lifetime is important (Wardman et al., 2007).

In hypoxia-reperfusion experiments, the ideal properties of fluorescent ROS/RNS sensor would include (a) being cell membrane permeant and exhibiting stochiometric binding to intracellular ROS (b) having no cellular toxicity (c) undergoing efficient oxidation to a fluorescent product by ROS (d) showing intracellular sequestration of the fluorescent oxidised form (Kudin et al., 2005) (e) having mono-specificity for a particular species and (f) stability within the intracellular environment. The following section explains the particular fluorescent probes that can be employed in ROS/RNS-related research.

### 1.14 The construction of new reporter systems for ROS/RNS detection

There is increasing evidence suggesting that mitochondrial dysfunction, mitochondrial-based $O_2^{\bullet-}$ generation and other ROS/RNS are implicated in the pathophysiology of cardiovascular disease, aging, cancer, neurodegenerative disease, inflammatory disorders, diabetes, and diabetic complications (Mukhopadhyay et al., 2007). Chemiluminescence and fluorescence-based assays have been widely available to measure cell-derived superoxide.

Detecting $O_2^{\bullet-}$ using fluorescent probes provides benefits of analysis by fluorescence microscopy, flow cytometry, a fluorescence microplate reader, and a cell sorter. However, selectivity, simplicity, reactivity and availability are important factors. The novel fluoroprobe; MitoSOX Red (MitoSOX) has been used for selective detection of $O_2^{\bullet-}$ (Mukhopadhyay et al., 2007), but only in mitochondria, not as a global $O_2^{\bullet-}$ indicator. Other new approaches are dependent on the effects of $O_2^{\bullet-}$ and other radical species on gene expression systems. Some organism such as *E.coli* have various gene expression systems sensitive to ROS/RNS. Those systems have been utilized to construct reporter systems to monitor environmental stress factors (Belkin et al., 1996), and also to monitor $O_2^{\bullet-}$ and other radical species generation in *in vivo* animal models (Koo et al., 2003;Kim et al., 2005; Niazi et al., 2007). If the promoter region of $O_2^{\bullet-}$- sensitive gene segment is fused to *a Renilla reniformis* luciferase gene as a reporter, that system can be used as a quantitative indicator to assess intracellular $O_2^{\bullet-}$ production.

This type of system may have number advantages including accurate quantification of superoxide produced, exclusion of $O_2^{\bullet-}$ related species which may have evolved from secondary oxidations, detailed information about the redox state of the cell or tissue and possible *in vivo* detector of $O_2^{\bullet-}$ production in animal models. A reporter gene system has been described for the individual detection of $H_2O_2$ and singlet oxygen generation in *Chlamydomonas reinhardtii*, a plant model organism. This system employs various HSP70A promoter segments fused to *a Renilla reniformis* luciferase gene as a reporter (Shao et al., 2007).

Other reporter systems have been reported that use SOXRS of *E. coli* and green fluorescent protein (GFP) of *Aequorea victora* where GFP showed an increased fluorescence in the presence of $O_2^{\bullet-}$ (Shibuya et al., 2004). It is clear now, there is a raised possibility of using those reporter gene plasmid constructs to quantify $O_2^{\bullet-}$ generation *in vivo* and in vitro animal models under hypoxia or hypoxia/reperfusion.

### 1.15 The validity of the fluorescent probe for $^{\bullet}$NO determination compared to EPR

There are three widely used major methods available for detection of $^{\bullet}$NO; such as chemiluminescence, electron spin resonance (ESR) /Electron Paramagnetic Resonance (EPR) and fluorometric methods including selective fluorescent probes. There are several advantages and disadvantages in all methods. However, direct $^{\bullet}$NO measurements are difficult due to low concentrations and short half-life, therefore, EPR spin trapping has been reported as one of best methods for quantification of $^{\bullet}$NO (Kleschyov et al., 2007). ESR or EPR based techniques show higher sensitivity and selectivity for radical species or paramagnetic species in variety of application methods (Archer, 1993, Tsuchiya et al., 1996, Berliner et al., 2001).

EPR is a tool that determines the resonant absorption of microwave radiation by paramagnetic systems in the presence of an applied magnetic field (Kleschyov et al., 2007). EPR can be used as a direct or non-direct in *vivo* and *in vitro* methods to analyse endogenous or exogenous $^{\bullet}$NO production in intact tissues or isolated organ or small animals (Kuppusamy and Zweier, 2004).

Despite above advantage of EPR tools, they are limited by expensive instrumentation, sample preparation, and complicated and intensive operation under laboratory conditions, where fluorescent probes are an easier and rapid method for $^{\bullet}NO$ detection in cell culture systems. Moreover, with the development of fluorometry techniques, there are new small molecule probes which are available that can discriminate between $ONOO^-$ and nitroxyl radicals in culture systems when determining $^{\bullet}NO$ generation, with increasing development of biocompatible probes for use in animals and tissues (Kleschyov et al., 2007; McQuade and Lippard, 2010).

## 1.16 Cardiac protection during hypoxia/reperfusion

### 1.16.1 Defence mechanisms in biological systems

*In vivo* and *in vitro* biological systems have natural defence mechanisms against ROS/RNS to prevent damage if they are overproduced. Natural defence mechanisms consists of endogenous antioxidant enzymes; superoxide dismutase, glutathione peroxidase, catalase and thioredoxin reductase and non-enzymatic antioxidants; coenzyme Q, thioredoxins, glutathione, endogenous nitric oxide, and antioxidant vitamins (Elsässer et al., 2001; Downey and Cohen, 2006). $^{\bullet}NO$ itself has been reported as a protective molecule during hypoxia in several reports (Beckman and Koppenol, 1996; Bereesewicz et al., 1995). The addition of exogenous antioxidants, radical traps and low molecular weight ROS scavengers can also overcome deleterious effects of excessive generation of ROS/RNS. The presence of excess ROS/RNS can in turn trigger activation of a number of redox-sensitive transcription factors such as NF-κB and Nrf2 that in turn promote the expression of antioxidant enzymes such as MnSOD and GCS respectively (Penna et al., 2009; Maulik et al., 2000; Thimmulappa et al., 2002).

In addition to ROS/RNS mediated cytoprotection during hypoxia/reperfusion via NF-κB and Nrf2, hypoxia inducible factor (HIF)-1α activation plays an essential role in triggering protection against cellular injury and metabolic alterations from the consequences of oxygen deprivation during hypoxia.

According to recent reports, HIF 1α activation confers protection against ischaemia–reperfusion (I/R) injury, provided that HIF 1α activation has been induced before the onset of lethal ischaemia (Loor and Schumacker, 2008). The term "cardiac protection" defines an activation of protective mechanism during hypoxia to adapt cells for survival. Numerous reports describe cardiac preconditioning under mild hypoxic conditions that protects against later severe hypoxia. But low concentrations of ROS/ RNS play a vital role in modulating signalling mechanisms of cardioprotection.

### 1.16.2 Preconditioning in the heart with hypoxia and hypoxia/reperfusion

Reperfusion after ischaemia may restore function to the myocardium, but paradoxically, also results in additional damage to the tissue. The proliferative ability of cardiomyocytes is limited; therefore, loss of cardiomyocytes cannot be compensated for and a strategy of controlling cell death is required to attenuate the heart damage induced by reperfusion. Cardiac protection during ischaemia has been unsuccessful with therapeutic interventions to date, which have attempted to minimize infarct size or subsequent reperfusion damage. Preconditioning makes tissue more resistant for subsequent episodes of ischaemia or reperfusion insult (Murry et al., 1986). There are two types of preconditioning; first window protection (classical preconditioning) and second window protection. The classical preconditioning occurs after first 5min of reperfusion and it extends until 3h whereas the second window of protection occurs between 12-72h later (Yellon and Downey, 2003; Ardehali, 2006; Balakumar et al., 2009).

The mechanisms of these two processes are not clear; however, first window protection is associated with posttranslational modifications of proteins whereas the second window of protection depends on cardiac protective agents available intracellularly. Cardiac preconditioning is associated with complex redox signalling mechanisms in rat heart (Penna et al., 2009). It has been reported that redox activity of endogenous and exogenous ROS/RNS generated at low concentrations during transient ischaemia may trigger protective mechanisms (Costa et al., 2005). Mitochondrial ROS/RNS mediate first window protection, with $O_2^{\bullet-}$, $^{\bullet}NO$ and $H_2O_2$ reported as the major molecules in the cascade.

Moreover, scavenging of hydroxyl radical and $ONOO^-$ have shown their involvement in preconditioning (Kevin et al., 2003; Becker, 2004b; Becker et al., 1999). Other sources of $O_2^{\bullet-}$ production are also important in preconditioning; NADPH oxidase plays a pivotal role in ischaemic preconditioning, as NADPH oxidase KO-mice cannot be preconditioned (Bell et al., 2005). It has been reported that ROS mediates PKC and, thereby to induce associated effects of cardiac protection with MPTP, mitochondrial $_K$ATP channels and BAX/BAD (Penna et al., 2009).

In ischaemic heart and also during reperfusion period, $^{\bullet}$NO production takes place and is involved with preconditioning via the mitochondrial $_K$ ATP channels (Penna et al., 2009). Moreover, inclusion of exogenous $^{\bullet}$NO by $^{\bullet}$NO donors and endogenous $^{\bullet}$NO have shown to produce cardiac protection during ischaemia/reperfusion in various tissues including myocardium. It is believed that endogenous $^{\bullet}$NO is involved in cardiac preconditioning during ischaemia/reperfusion through several mechanisms including reducing platelet aggregation, neutrophil activity and adhesion in a cGMP-dependent manner in *in vivo* models (Penna et al., 2009).

### 1.16.3 Post conditioning in the heart with reperfusion

Post conditioning is defined as intermittent interruption of coronary flow in the very early phase of a reperfusion, to activate cardiac protection. Cardiac effects of postconditioning depend critically on the duration of index and severity of ischaemia at the early phase of reperfusion. Moreover, it has been shown recently that redox signalling is paramount at the time of myocardial reperfusion (i.e. after period of hypoxia or ischaemia), to mediate the cardioprotection elicited by ischaemic preconditioning (Dave et al., 2008; Liu et al., 2008). Post conditioning is associated with multiple mechanisms including reduction of apoptosis, necrosis, endothelial dysfunction so as to, minimise endothelial/leukocyte interactions, and to reduce inflammation. The contribution of $^{\bullet}$NO in cardioprotection has been shown by administering of L-NAME, 5min before the beginning of reperfusion in rabbit heart; this exacerbates the reperfusion injury (Xi-Ming et al., 2004). The significant role of nitrite in ischaemia/reperfusion injury has recently been suggested.

It is argued that whether $^{\bullet}NO$ (from either enzymatic or non-enzymatic sources during reperfusion) or $ONOO^-$ (produced after reaction with $O_2^{-\bullet}$ and $^{\bullet}NO$) mediate the cardiacprotection during ischaemia/reperfusion (Penna et al., 2006). However, the mechanism of the involvement of $ONOO^-$ in the cardiac protection and post conditioning remains unclear (Dawn and Bolli, 2002; Yellon and Downey, 2003; Pagliaro, 2003).

In summary, the mechanism of postconditioning includes occupation of adenosine receptors, activation of NOS and non enzymatic processes to produce $^{\bullet}NO$, opening of mitochondrial $K_{ATP}$ channels and blockage of MPTP under acidosis and production of ROS, thereby producing $ONOO^-$ and triggering the activation of PKC and MAPKs. However, ROS/RNS may be protective in the pre-hypoxic phase and/or play roles in redox signalling during cardiac protection, but they can act deleteriously in the post-ischaemic phase causing reperfusion injury. Therefore future investigations are warranted.

### 1.17 Cellular defence mechanism-signalling via NF-κB and Nrf2 activation

There are only a few transcription factors, including NF-κB and NE-E2-related factors (Nrf2; Nrf1, Nrf2 and Nrf3 and Nrf2-associated factor INrf2), known to be activated by ROS and/or electrophiles generated during oxidative stress or chemical exposure of cells respectively. The activation mechanism of Nrf2 is different from the NF-κB pathway (Jaiswal, 2004).

#### 1.17.1 Nrf2 activation and ARE

As a protective pathway against ROS/RNS under oxidative stress conditions, higher organisms have developed elaborate defence mechanism comprising phase II detoxification enzymes and antioxidant proteins. These antioxidant proteins include NAD(P)H: quinone oxidoreductase 1(NQO1) a flavoprotein, glutathione, S-transferase (GST), heme oxygenase 1 (HO-1), superoxide dismutase (SOD1), NOS and glutamate cysteine ligase (GCL). All these genes contain specific nucleotide sequence in their gene promoter; the antioxidant response element (ARE) which can drive gene transcription. The consensus sequence of ARE is 5′-TA/CANNA/GTGAC/TNNNGCA/G-3′ (Wasserman and Fahl, 1997).

The antioxidant responsive element (ARE) is a *cis*-acting regulatory element or enhancer sequence, which is the promoter gene sequence of phase II detoxification enzymes and the aforementioned antioxidant proteins. Under unstimulated conditions, Nrf2 is sequestered in the cytoplasm by Keap1. Activation signals include protein kinase pathways (MAPK, PI3K and PKC) and ROS or electrophiles that can dissociate the Nrf2-Keap1 complex which may result in nuclear translocation of Nrf2 with small Maf proteins, thereby causing the transcriptional activation of downstream target genes; NQO1,GST,GCL,SOD1 and HO-1 (Heiss et al., 2009; Lee and Johnson, 2004 ) **(Figure 1.14).** The cytoplasmic Keap1 protein acts as a repressor of Nrf2-mediated ARE activity (Heiss et al., 2009).

Among antioxidant proteins, NQO1 plays an important role in detoxification of metabolic reduction of redox cycling quinones (Sally et al., 2007; Nioi et al., 2003; Nguyen et al., 2009; Heiss et al., 2009) and evidence from gene-knockout models has shown the pivotal role of NQO1 in the cytoprotective responses invoked by electrophilic stress (Nioi et al., 2003). Moreover, activation of ARE promoter and NQO1 gene up-regulation occurs during ischaemia-reperfusion (Leonard et al., 2006). In the activation of NQO1 protein, Maf protein must be bound to NQO1-ARE independent of Nrf2 (Itoh et al., 1997), unlike other antioxidant genes.

### 1.17.2 NF-κB activation

NF-κB (nuclear factor κB) is a redox-sensitive transcription factor which plays a pivotal role in the regulation of immune, apoptotic, cell proliferation, survival and inflammatory responses. NF-κB is ubiquitously expressed and can be activated by variety of stimuli including cytokines, endotoxin and oxidative stress. NF-κB activation regulates expression of various genes, thereby, co-ordinating cellular homeostasis with the control of balance between cell survival and cell death (Kukreja, 2002). At rest, NF-κB is sequestered in the cytoplasm by IkB and then can be activated upon multiple steps of phosphorylation through a protein kinase cascade of activation signals (Adrienn et al., 2003; Beinke and Ley, 2004). Under stimulated conditions, IkB immediately undergoes phosphorylation and ubiquitination and result in release of sequestered NF-*κ*B **(Figure 1.15)**.


**Figure 1.14 ARE-driven gene expression by Nrf2, taken from Lee and Johnson (2004 ).**

Then, NF-*κ*B translocates into the nucleus and binds with the promoter region of genes where it can promote transcription of specific, regulated genes including inducible nitric oxide synthase (iNOS), cyclooxygenase II (COX-2), Mn-superoxide dismutase (MnSOD), anti-apoptotic agents such as Bcl-2, inhibitor of apoptosis activation factors (IAFs), A1, and cytokines, tumour necrosis factor (TNFα), HO-1, interleukins; IL-1 and IL-6, cell adhesion molecules; ICAM, VCAM, selectins, FAS ligand and other transcription factors such as p53 (Kukreja, 2002, Adrienn et al., 2003). NF-κB/DNA binding activity associates in ischaemia/reperfusion and preconditioning under oxidative stress due to its redox sensitivity.

Activation of NF-κB may reflect an early pathway to promote gene transcription for cardiac protection during preconditioning. Ischaemic preconditioning induces NF-κB DNA binding activity after coronary occlusion in rabbit hearts (Kukreja, 2002). In the presence of NOS inhibitors, NF-κB DNA binding was blocked, where $ONOO^-$ and $^{\bullet}OH$ are responsible for activation of NF-κB under ischaemic conditions.

Adding to this, Takano et al. (1998) reported NF-κB dependent gene transcription of iNOS and synthesis of $^{\bullet}NO$ in heart during delayed preconditioning. NF-κB activation is involved in hypoxia/reperfusion injury, particularly in the vascular endothelium in where NF-κB activation promotes neutrophil adhesion. Early studies showed that NF-κB nuclear binding increased in microvascular endothelial cells during reperfusion but not during hypoxia (Kupatt et al., 1997). However, it is possible to induce cardiac dysfunction through overexpression of myocardial cytokines if NF-κB is activated for a long time during ischaemia/reperfusion (Kukreja, 2002). Therefore, NF-κB is a key regulator of the balance between cell death and survival**.**


**Figure 1.15 Generic pathway of NF-κB activation, taken from Beinke and Ley (2004).**

### 1.18 What remains unknown in hypoxia and hypoxia/reperfusion?

In the present study, there are still unanswered questions related ROS/RNS generation and their associated detrimental effects and beneficial effects during hypoxia and hypoxia/reperfusion. Previously, there has even been a dispute about whether hypoxia increases or decreases the production of ROS from mitochondria (Duranteau et al., 1998; Toescu, 2004; Waypa and Schumacker, 2005; Lesnefsky et al., 2004; Murphy, 2009).

However, the effects of severity and duration of hypoxia for particular cells or tissues that induces ROS/RNS generation, detrimental effects or induces cellular antioxidant defence mechanism against hypoxia insult remains unknown. The development of therapeutic interventions requires clearer understanding of pathways for treating ischaemia/reperfusion.

### 1.19 Hypothesis and aims

#### 1.19.1 Hypothesis

An increase in ROS/RNS generation leads to myocardial cell death during hypoxia or hypoxia/reperfusion, which is dependent on the severity and duration of ROS/RNS production. Inhibition of specific sites of ROS/RNS generation prevents hypoxia and hypoxia/reperfusion-induced cell death. Hypoxia and hypoxia/reperfusion-induced superoxide and/or nitric oxide increase the activity of redox sensitive transcription factors that can influence cell survival.

### 1.19.2 Aims

1. To optimise analytical conditions for using fluorescent probes in order to achieve optimum oxidation with intracellular ROS/RNS *in vitro.*

2. To develop and determine the stability of the hypoxic system.

3. To characterise the kinetics and sources of ROS/RNS production during mild (10% $O_2$) and severe hypoxia (2% $O_2$) under acute (30min) and chronic time periods ($\geq$ 1h).

4. To investigate the amount of cell death and effects on metabolic activity during mild and severe hypoxia at different time points.

5. To investigate the mode of cell death (necrosis or apoptosis) during mild and severe hypoxia under acute and chronic conditions.

6. To investigate whether pharmacological inhibition of ROS/RNS generating enzymes or antioxidant treatments can afford protection against hypoxia-induced cell death and hypoxia/reperfusion-induced changes in metabolic activity.

7. To develop appropriate reporter assays in order to investigate whether activation of transcription factors NF-κB and Nrf2 mediates the cellular defence against hypoxia or hypoxia/reperfusion.

8. To investigate whether ROS/RNS activate Nrf2 and/or NF-κB during hypoxia and any role for NF-κB in cell death or survival using pharmacological inhibitors of NF-κB transcription.

# CHAPTER 2

# MATERIALS AND METHODS

## 2.1 Preface

This chapter describes the different methods employed in this thesis to collect accurate data for the investigation of the experimental hypotheses. It includes standard experimental methods, modified methods and in-house developed novel techniques. Due to limitations of some published methods, they were modified and optimised accordingly for application to a particular experimental model or time point.

Standard methods include cell culture, Winkler assay for dissolved oxygen measurements, sodium dodecyl sulphate polyacrylamide gel electrophoresis (SDS-PAGE), western blot, protein quantification assays, MTT cell viability assay, protein carbonyl ELISA, plasmid DNA transfection, Maxiprep of plasmid DNA extraction, plasmid DNA sequencing, analysis of plasmid DNA by restriction digestion and agarose gel electrophoresis. In house-developed techniques and modifications of protocols are described separately under each experiment. Those include induction of hypoxia/reperfusion and validation of the hypoxic chamber, time of addition of drug and/or probe solutions under hypoxic/reperfusion conditions, optimisation of various fluorescent probe conditions to quantify ROS/RNS during hypoxia/reperfusion, necrotic and apoptotic cell death analysis. The western blot analysis for procaspase-3 cleavage and a Dual Glo luciferase reporter assay for co-transfection studies were also modified.

## 2.2 Materials

The solvents were purchased from Fisher Scientific (Loughborough, UK) unless otherwise specified. H9C2 (1-2) myoblasts (CRL-1446) were obtained from LGC Ltd (Middlesex, UK). DMEM (12-614F), foetal bovine serum (FBS), trypsin-EDTA (0.53mM) solution (17161E), penicillin (100U/ml)-streptomycin (100µg/ml) mixture (17-603E), L-glutamine (17-605E) were obtained from Cambrex Bioscience, Wokingham Ltd (Berkshire, UK). Cell culture plates, culture flasks and petri dishes were obtained from Corning Ltd, UK. Trypan Blue Solution (0.4%) was purchased from Sigma (UK).

All gases and premixed special gases were from BOC Ltd (Guildford, UK). Eppendorfs and universals were obtained from Appleton Woods Ltd. Specific reagents, chemical products and instruments are as stated in the method.

## 2.3 Methods

### 2.3.1 Cell culture

In hypoxia-reperfusion injury research, in vivo models or primary cardiomyocytes are routinely used. The embryonic heart-derived rat myoblasts were used throughout the project as they are similar to cardiomyocytes biochemically and offer a reproducible model for the study of myocardial hypoxia/reperfusion. Specifically routine cell culture and handling was possible for long term studies. Cells were passaged at 70-80% confluence to prevent them differentiating to myotubes at higher confluency as previously described (Kimes and Brandt, 1976). Experiments were performed with cells between passage numbers 14 – 20.

### 2.3.1.2 Routine cell culture

ATCC H9C2 (1-2) rat-myoblasts were cultured in Dulbecco's modified Eagle's medium (DMEM) and supplemented with heat inactivated 10% fetal bovine serum (FBS), 4mM L-glutamine and 1% penicillin/streptomycin according to the supplier's instructions. This is referred to as complete culture medium. Cells were grown in cell culture - treated T75cm$^2$ flasks at 37 °C in a humidified atmosphere of 5% $CO_2$ and 95% air.

### 2.3.1.3 Passage of H9C2 cells

At 70-80% confluence, cells were trypsinised (0.125% (w/v) trypsin, 0.02% (w/v) EDTA and 0.02% (w/v) glucose) in 5ml of 0.15M phosphate buffer saline (PBS)) for 1-3 minutes. Complete culture medium was added to each flask and mixed with the trypsinised cells to inactivate trypsin. Cells were centrifuged at 400g for 5minutes at room temperature in a 50ml-centrifuge tube. The supernatant was removed and the pellet manually agitated and resuspended into 8ml of culture medium. Following the cell counts by trypan blue exclusion, cells were subcultured into T75/T150 flasks at 1:2 to 1:4 ratios. Media was replaced routinely every 2 days.

### 2.3.2 Trypan blue exclusion test for cell viability

In order to obtain accurate results and reproducible data from an experiment system, it is important to maintain the same cell number between experiments. Therefore, a haemocytometer was used to count cells. The viable cell density was determined as the number of trypan blue excluding cells in a haemocytometer. The advantage of the trypan blue exclusion test is it is simple, rapid and able to provide results comparable to other dyes such as Erythrosin B or Nigrasin. The chromopore of trypan blue is negatively charged and does not enter the cell unless the membrane is damaged (Thomadaki et al., 2007). Therefore, all the cells which actively exclude the dye were considered as viable. Dead cells stain a blue colour.

#### 2.3.2.1 Method

When the cells were at 70-80% confluence, the monolayer was washed three times with PBS and trypsinised by addition of 5ml of trypsin EDTA for 2-3 minutes at 37ºC. Cells in suspension were harvested and resuspended in 8ml of complete medium. Trypan blue (15µl) was added to an equal volume of cell suspension and mixed by gentle agitation.

Then the mixture (30µl) was transferred to both chambers of a haemocytometer (Weber Scientific International, Teddington, UK). Total live cells were counted in the 1mm centre square as viewed under the microscope (Magnification10x; Olympus, Japan). The count was repeated twice. The volume of each square of the haemocytometer with a cover slip in place represents a total volume of $0.1mm^3$. The viable cells actively excluded the dye whereas dead cells absorbed the dye and were visible as blue in colour.

The viable cell density was determined as follows:

**Cell density (per ml) = average count per square x dilution factor x $10^4$**

### 2.3.3 Hypobaric and normobaric oxygen chamber for cell culture

As described in the general introduction, there are various methods available to model hypoxia, however, in this thesis; a cost effective and reproducible system was preferred. To determine consistent hypoxia conditions in the chamber, the system was optimised and then validated routinely.

#### 2.3.3.1 Chamber design and optimisation

A hypoxic or normoxic environment was established inside a special metal (wall thickness 4mm, length 25cm, area of the cylinder $125cm^2$) chamber (McIntosh and Fildes, USA) using premixed gases (2% $O_2$+98% $N_2$, 10% $O_2$+90% $N_2$ and 21% $O_2$ +79% $N_2$; BOC, UK).

Two metal chambers were mounted inside a commercially available incubator (BioRad, UK) at 37°C. The chambers have airtight lids which are fitted with gas inlet and outlet ports. A screw was fitted to each gas inlet and outlet ports to control the gas flow and perfusion into the chamber **(Figure 2.1).** The medium was replaced and reagents were added by opening the door at the front of the main incubator.

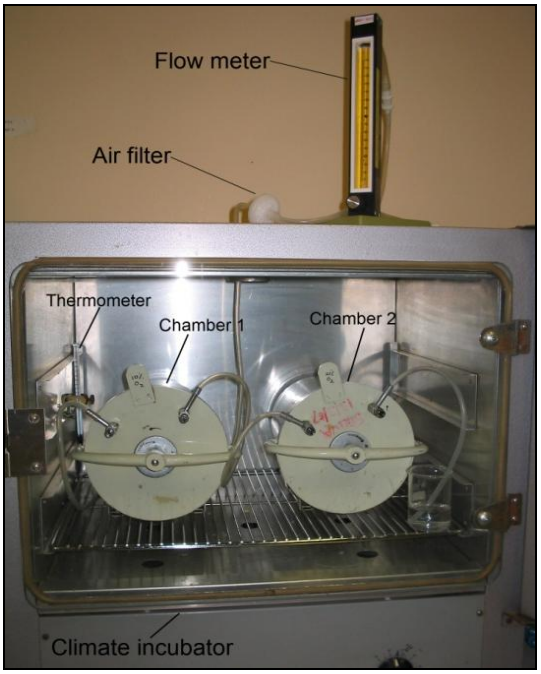


**Figure 2.1 Complete hypoxia chamber**
Complete hypoxia chamber set up in a climate incubator at 37ºC.

A thermometer was set up inside the incubator to allow monitoring of the internal temperature. The chambers and apparatus were maintained at 37ºC during hypoxia or normoxia. To create humidified conditions in the chamber, a small water tray was placed at the bottom of each chamber and the cell culture plate holder was constructed top of it **(Figure 2.2A).** The gas inlet was externally fixed with gas tubing (4mm diameter, BOC, UK) which was connected to the appropriate hypoxic (2% or 10% oxygen + balanced nitrogen) or normoxic (21% oxygen + 79% nitrogen) gas cylinder.

The main gas flow into the chamber was controlled by a flow meter (BOC, UK). It was connected between the chamber and premixed gas cylinder. Premixed gas was allowed to flow through a sterile filter (0.2µM, Millipore, UK) after passing the flow meter. Through the inlet, premixed gas at 25ml/min flow rate was allowed to enter the airspace (3L) of the chamber **(Figure 2.2A and 2.2B).** Gas exited through the outlet at same flow rate and prevented the pressure build-up or backflow of air.

**(A)**

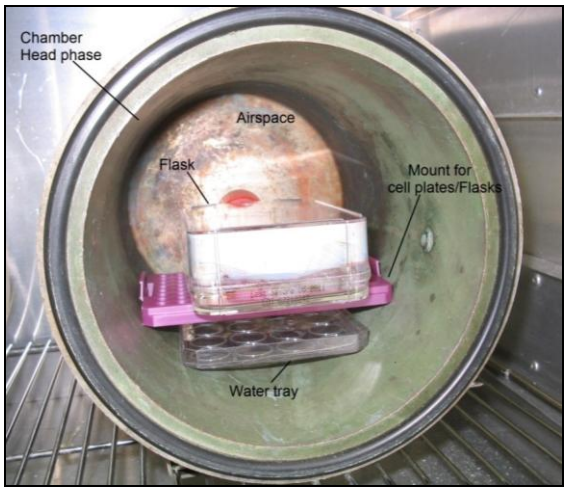


**(B)**

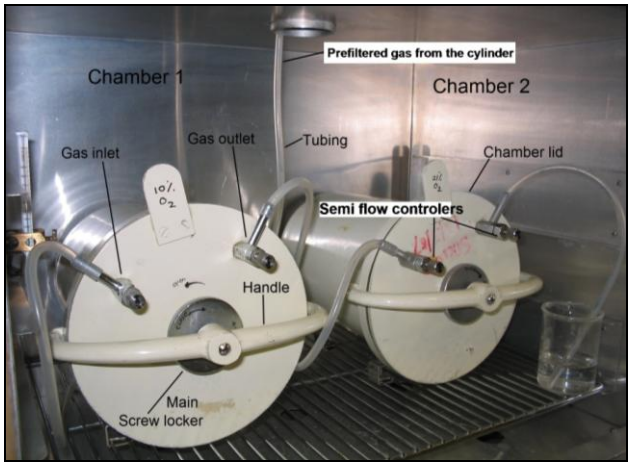


**Figure 2.2 Hypoxic gas chamber**
(A) Inside chamber view, (B) View of full incubator system.

### 2.3.3.2 Hypoxic/normoxic medium preparation

Cells were maintained in preincubated hypoxic or normoxic Dulbecco's modified Eagle's medium (Phenol red-free DMEM) which was supplemented with 25mM HEPES (4- (2-hydroxyethyl) -1-piperazine ethanesulfonic acid), 1% penicillin/streptomycin. Prior to hypoxia or normoxia experiments, the medium was preincubated for 24h in hypoxia (2% $O_2$ + 98% $N_2$ or 10% $O_2$ + 90% $N_2$) and for control experiments in normoxia (21% $O_2$ + 79% $N_2$) (BOC, UK). To assess the stability of pH value throughout the hypoxia or normoxia, a sample of each preincubated medium was measured for pH using the pH probe (Appleton Wood, UK).

### 2.3.4 Winkler Test for dissolved oxygen in the medium

To measure oxygen tension, there are wide range of oxygen electrodes or probes available in the market, however, they require larger volumes than available in culture medium (1ml) in a well, therefore, the Winkler assay was routinely employed to measure dissolved oxygen concentration in culture medium as previously described (Grant and Griffiths, 2007; Helm et al., 2009) .

### 2.3.4.1 Method

The Winkler test was used to determine the level of dissolved oxygen in culture medium under hypoxia or normoxia. This method was adapted from Winkler, 1888. After pre-equilibrating the medium at 37°C in various oxygen tensions (2%, 10%, 21% $O_2$) for 24h, the dissolved oxygen level in each sample (1ml) from the flasks (75$cm^2$) was measured by addition of manganese II sulphate (40 µl, 48%, w/v). The mixture was swirled gently to minimise the risk of incorporation of air into the sample. Then potassium iodide (80 µl, 15% w/v, dissolved in 70%, w/v, potassium hydroxide) was added to yield a pinkish-brown manganese hydroxide precipitate. Sulphuric acid (120 µl, 50% w/v) was added to dissolve the precipitate and the sample was allowed to stand for 2min. Starch solution (400µl, 0.1% w/v) was added, turning the solution blue due to formation of iodine–starch complex.

Sodium thiosulphate (0.31% w/v) was titrated into this solution, with swirling, until the solution turned colourless. The dissolved oxygen level is proportional to the volume of sodium thiosulphate titrated. The addition of 1 ml sodium thiosulphate is equivalent to 10 mg dissolved oxygen/l. To verify that the dissolved oxygen level at different oxygen tensions did not change over the experimental period, the test was repeated again after 30min, 1h and 4h of hypoxia / normoxia. The partial oxygen pressure inside the medium ($pO_2$) was calculated using dissolved oxygen concentrations in the following formula (**Figure 2.3**); the dissolved oxygen concentration in medium at 1atm under ambient conditions is considered as 6.00mg/L as previously described by Grant and Griffiths (2007).


**Figure 2.3 Formula for partial gas pressure calculations**
(Mortimer, 1956; www. wateronthewеb.org).

### 2.3.5 Modification of cell culture plate lid

The standard culture plate lids were modified before experimentation. The plate lid of each cell microtiter plate (24 and 96 well) was perforated with 2mm diameter holes using a heated (red-hot) needle (2mm width x 4cm length). The holes were pierced in the centre of each culture well.

The holes in each plate lid were externally sealed by gas-impermeable adhesive strips (Appleton Wood, UK). Each hole can be opened by lifting the adhesive strip for addition of redox sensitive dyes or inhibitors/drugs. This technique was adapted to prevent the incorporation of external air into the culture medium when plates were removed from the chamber for manipulation (**Figure 2.4).**

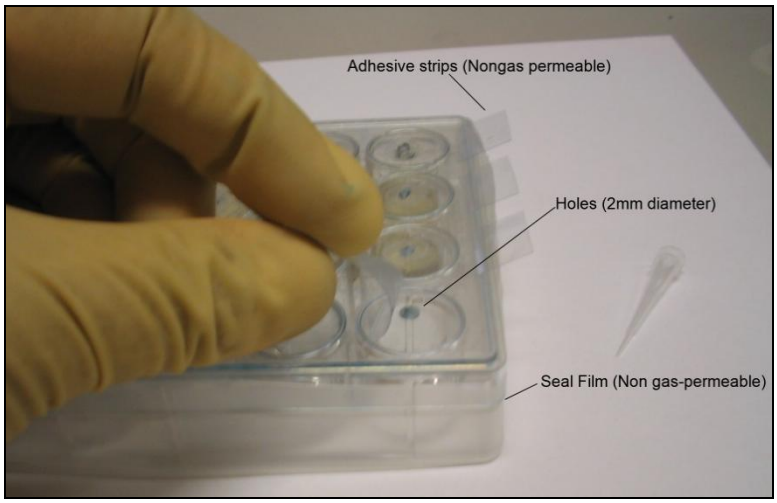


**Figure 2.4 Modification of culture plate lid**
Culture plates were modified with holes for probe additions.

### 2.3.6 Determination of cell viability

There are several methods available to determine cell viability. Most available methods are based either on metabolic activity or cell membrane integrity of viable cells. In general, metabolic activity is measured in terms of metabolically active mitochondrial reductases and their oxidation with tetrazolium salts which is cleaved into a coloured formazan product (e.g. MTT, MTS, XTT and WST-1 colorimetric assays). This method can therefore be used to measure cytotoxicity, proliferation or activation of cells or tissues. As previously explained the mitochondrion is strongly implicated in hypoxia-induced redox changes through the electron transport system. Therefore, the MTT (3- (4, 5-dimethylthiazol-2-yl) -2, 5-diphenyltetrazolium)

assay was used to assess cell viability in terms of metabolically active mitochondria after exposure to hypoxia. The MTT assay is technically convenient, no washing steps are required and it is easy to apply in most experimental designs. The main advantages of the MTT assay are rapidity and precision, and the lack of any radioisotope use. The ATP levels of cells are also analyzed to estimate the cellular energy capacity and thus viability. Therefore, CellTiter-Glo luminescent assay (Promega, UK) was employed to assess cellular ATP levels during hypoxia. The CellTiter-Glo® Luminescent Cell Viability Assay is a homogeneous method to determine the quantitation of the ATP present in metabolically active cells. In principle, mono-oxygenation of luciferin is catalyzed by luciferase in the presence of $Mg^{2+}$, ATP and molecular oxygen **(Figure 2.5).** Therefore, the generation of a luminescent signal is directly proportional to the amount of ATP present in metabolically active cells. The Cell-Titer-Glo luminescent assay is easy to use directly in experiments model as cell washing, removal of medium or multiple pipetting steps are not required.


**Figure 2.5 The luciferase reaction.** Mono-oxygenation of luciferin is catalyzed by luciferase in the presence of $Mg^{2+,}$ ATP and molecular oxygen, taken from www.promega.com.

### 2.3.6.1 MTT assay

Cardiomyoblast viability was determined using an MTT (3-[4, 5-dimethylthiazol-2-yl] - 2, 5 diphenyltetrazolium) assay based on the reduction of 3-[4, 5-dimethylthiazol-2-yl] - 2, 5 diphenyltetrazolium bromide by mitochondrial reductases [succinate dehydrogenase] in viable cells to insoluble violet formazan crystals, which are solubilised by the addition of a detergent solution.

Then, the colour can be quantified by a spectrophotometer (van de Loosdrecht et al., 1994). Cells were seeded at a density of 3 x $10^4$ cells/well (1ml) in DMEM in 24 well flat-bottomed microtiter plates. Cells were grown at 37 °C in a humidified atmosphere of 5% $CO_2$ and 95% air until they reached to 80-90% confluence. One hour prior to the completion of each hypoxic and/or normoxic period, MTT solution (100µl of 5mg/ml in 0.01M PBS) was added to all wells.

After completing hypoxia or normoxia, lysis buffer (100µl, 20% w/v SDS in 50% DMF, $dH_2O$ (50%), pH 4.7 adjusted with 2.5% of glacial acetic acid) was added to each well and incubated for a further 16 hours at 37°C in a humidified atmosphere of 5% $CO_2$ and 95% air. After promptly agitating the content of each well, 250µl of the content of each well was transferred to a well in 96 well microtiter plate. The formation of formazan was assessed by measuring the optical density (OD) at 570nm in the microplate reader (Denley, UK). Cell viability was calculated by comparing results to normoxic cells which were considered as 100% viable. The MTT assay was employed to measure hypoxia (2% and 10% $O_2$ + balanced $N_2$) - induced reduction in cell viability vs normoxia for 30min,1h, 4h and 24h and hypoxia/reperfusion studies. To measure the mitochondrial metabolic activity during hypoxia/reperfusion, MTT was added for 2h reperfusion period immediately after hypoxia (30min or 4h).

### 2.3.6.2 Measurements of ATP

Cells were seeded at a density of 3x$10^4$ cells/well (24-well plate) and when cells reached 80% confluence, media was replaced with DMEM/HEPES under different oxygen tensions as previously explained. Five minutes prior to completion of hypoxia for 4h, plates were sealed and centrifuged at 1300rpm for 5min at room temperature. This step was important to avoid loss of any dead or partially dead cells floating in the media. Then, 900µl of media was removed from each well and loaded with 100µl of Cell Titer Glo reagent according to manufacturer's instructions (1:1 ratio for medium to Cell Titer Glo reagent) (Promega, UK).

Wells in the absence of cells were also loaded with same volume of Cell Titer Glo reagent for background luminescent measurements. The content of each plate was gently mixed to induce lysis and then incubated for another 10min to stabilize the luminescent signals. Finally, luminescence was recorded at room temperature in Spectramax GEMINI EM plate reader at emission: 542nm.

### 2.3.7 Measurements of ROS/RNS generation

ROS/RNS generation was measured using four different fluorescent probes, dihydroethidium (DHE), 2, 7-dichlorodihydrofluorescein diacetate ($DCFH_2$-DA), dihydrorhodamine (DHR), and 4, 5-diaminofluorescein diacetate (DAF-2-DA) according to their specificity for particular ROS/RNS.

#### 2.3.7.1 Fluorescent probes and preparation

##### 2.3.7.1.1 Dihydrodroethidium (DHE)

Dihydroethidium is widely used as $O_2^{\bullet-}$ detector in tissues and the assay system was recently reviewed (Fernandes et al., 2007; Zhao et al., 2005). This probe has unique specificity towards $O_2^{\bullet-}$ radical over other radicals in the intracellular environment and oxidation results in a specific spectrum that can be measured by a fluorescence detector. Chemically and enzymatically generated $O_2^{\bullet-}$ can react with DHE to form a fluorescent product that differs from ethidium ($E^-$), which is a di-electron oxidised product of DHE (Zhao et al., 2005). In contrast, other ROS and RNS such as $H_2O_2$, $^{\bullet}OH$, $ONOO^-$, and $OCl^-$ failed to oxidise DHE to the same product. Moreover, Zhao et al. (2005) showed that the reaction of DHE with $O_2^{\bullet-}$ and its resultant DNA complex produce a different fluorescent spectrum. Zhao et al. (2003) demonstrated that $O_2^{\bullet-}$ can oxidise with DHE to form 2-OH-$DE^+$ as a specific product according their HPLC method **(Figure 2.6)**.

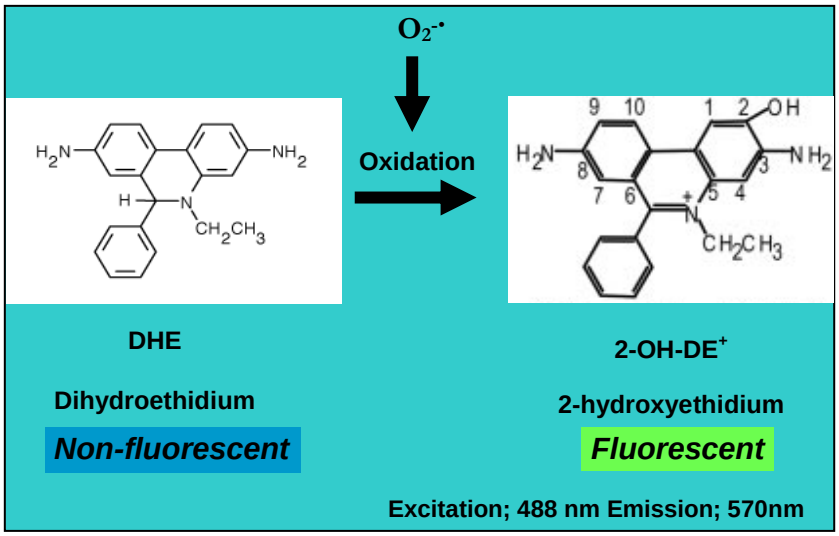


**Figure 2.6 Oxidation of DHE in the presence of $O_2^{\bullet-}$, adapted from Zhao et al. (2005); Wardman et al. (2007).** (+) indicate the inclusion of catalyst or peroxides. Blue colour indicates the non-oxidised compound of dye whereas yellow colour indicate the oxidised product of dye.

Further studies suggest the formation of E+ in the presence of $O_2^{\bullet-}$; but, this mechanism is not known (Zhao et al., 2003). In contrast to above explanations, DHE can be oxidized by oxidants other than $O_2^{\bullet-}$, such as $H_2O_2$ in the presence of redox-active metal ion, peroxynitrite and cytochrome *c*; but these oxidants do not produce 2-OH-$E^+$ (Zhao et al., 2005) and possibly result in products with different fluorescent spectra as well.

DHE is a photosensitive reduced non-fluorescent compound. The photochemically oxidised form has a positive charge, so it cannot diffuse into cells. Therefore, DHE is suitable marker for intracellular $O_2^{\bullet-}$ generation using specific wavelengths for detection that measure 2-OH-$DE^+$. DHE is freely permeable into cells and rapidly oxidized to fluorescent ethidium in the presence of superoxide. Free unoxidised DHE emits blue fluorescence, however, it emits red fluorescence when the oxidised ethidium intercalates into cellular DNA. A stock solution (1mg/ml) of DHE was prepared in absolute ethanol. Before being stored at -20°C, the stock solution was purged in nitrogen to avoid air oxidation. Aliquots of 4mM working solutions were made in ethanol and purged in nitrogen again before storage at -20°C.

#### 2.3.7.1.2 2, 7- dichlorofluorescein diacetate ($DCFH_2$-DA)

$DCFH_2$-DA is the most common probe in *in vitro* biological research. The oxidation of the probe is described below (**Figure 2.7**). $DCFH_2$-DA has a very low reactivity toward superoxide radicals and hydrogen peroxide. However, in the presence of a catalyst, reaction of $H_2O_2$ can be achieved in the cytosol. Recent reports suggest that $DCFH_2$-DA fluorescence is much more likely due to cytosolic redox change as it cannot get into mitochondria (Abramov et al., 2007). $DCFH_2$-DA can exhibit subject background fluorescence due to metal impurities in culture media. $DCFH_{2\text{-}DA}$ can also be oxidised by peroxyradicals in the presence of catalyst and can be directly oxidized by $ONOO^-$ without the catalyst **(Figure 2.7).**

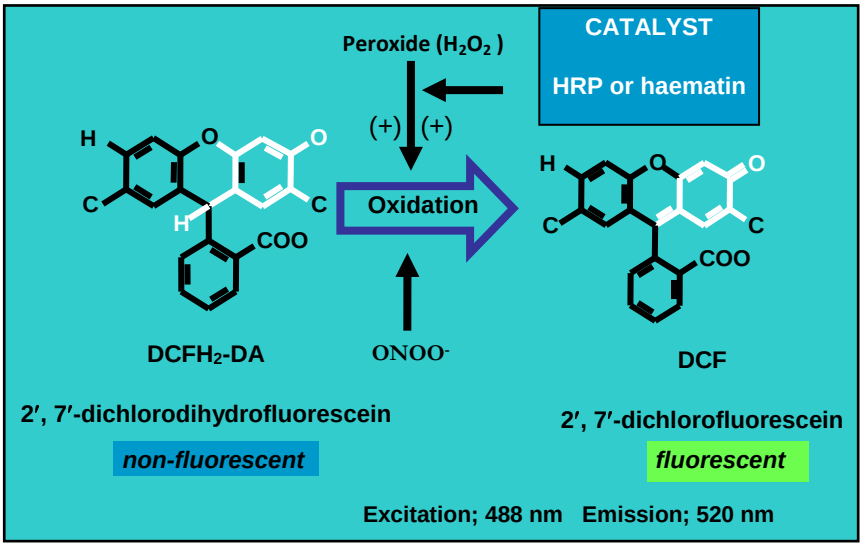


**Figure: 2.7 Oxidation of $DCFH_2$-DA in the presence of $H_2O_2$ and $ONOO^-$.** (+) indicate the inclusion of catalyst or peroxides. Blue colour indicates the non-oxidised compound of dye whereas yellow colour indicate the oxidised product of dye (Wardman et al., 2007; Tarpey et al., 2004).

$DCFH_2$-DA is oxidised in the presence of intracellular reactive oxygen species such as $H_2O_2$, peroxy radicals and peroxynitrite (Royall and Ischiropoulos, 1993a). $DCFH_2$-DA is used to assess cytosolic based ROS/RNS.

A stock solution (1mg/ml) of $DCFH_2$-DA was prepared in dimethylsulfoxide (DMSO) and stored at -20°C after purging with nitrogen. Aliquots of 4mM working solutions were made in DMSO and stored at -20°C. Aliquots were purged in nitrogen in the dark to avoid air oxidation.

#### 2.3.7.1.3 Dihydrorhodamine 123 (DHR)

Dihydrorhodamine (DHR) is cell–membrane permeant, mitochondrially retained-fluorescent (Tarpey et al., 2004) and lipophilic (Crow, 1997), uncharged (Royall and Ischiropoulos, 1993a) probe that is often used to detect ROS and RNS in cells via oxidation to the respective fluorescent product. The oxidised fluorescence can be easily determined or typically monitored in a continuous assay system using a fluorometer at emission fluorescence; 525nm following excitation; 488nm (Henderson and Chappell, 1993). It has been widely used as a stain for mitochondria (Royall and Ischiropoulos, 1993) and possesses the aforementioned properties with intracellular fluorescence stability up to 1h. However, it is not mono-specific. DHR has an ability to enter mitochondria and be oxidised to fluorescent rhodamine in the presence of ROS/RNS (Frantseva et al., 2001; Henderson and Chappell, 1993). The oxidised rhodamine partitions over time to mitochondria due to their large inside-negative transmembrane potentials (Emaus et al., 1986).

DHR is not oxidised by superoxide or $H_2O_2$ alone requiring a cofactor such as heme containing peroxidase (HRP) or cellular peroxidases (Hempel et al, 1999; Henderson and Chapell et al., 1999) but can react directly with $ONOO^-$ (Henderson and Chappell, 1993) **(Figure 2.8).** Therefore the quantitative estimation of intracellular $H_2O_2$ is questionable as it is mediated through secondary reactions. However, qualitative conclusions may be made. Several other cell derived oxidants such as $ONOO^-$, but not $^{\bullet}NO$ or $OCl^-$ can directly oxidise DHR. The spectrum of oxidised rhodamine is the same, regardless of the oxidizing agent (Tarpey and Fridovich, 2001).

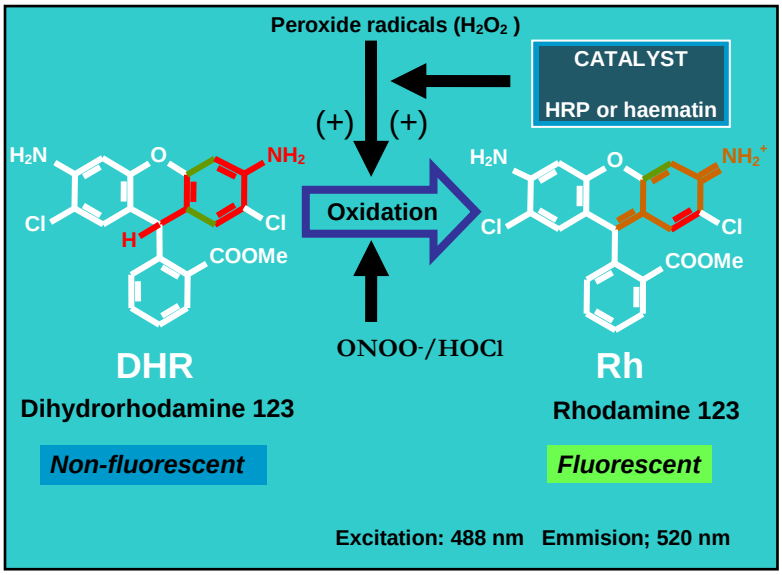


**Figure 2.8 The oxidation of DHR in the presence of $H_2O_2$ and $ONOO^-$, adapted from Wardman et al. (2007) and Royall and Ischiropoulos et al. (1993).** (+) indicate the inclusion of catalyst or peroxides. Blue colour indicates the non-oxidised compound of dye whereas yellow colour indicate the oxidised product of dye.

DHR is a cell-membrane permeant, mitochondrially retained-fluorescent and lipophilic dye; the uncharged (Kooy et al., 1994) probe is also used to detect ROS/RNS such as $H_2O_2$, HOCl and peroxynitrite in cells and after oxidation is converted to a highly fluorescent form of rhodamine (Royall and Ischiropoulos, 1993a)**.** However, it is used to assess mitochondrial based ROS/RNS. A stock solution (1mg/ml) of DHR was prepared in DMSO in the dark and stored in -20°C after purging with nitrogen. Aliquots of 4mM working solutions were prepared in DMSO and stored in -20°C. Aliquots were purged in nitrogen to avoid air oxidation.

#### 2.3.7.1.4 4, 5 - Diaminofluorescein diacetate (DAF-2-DA)

The quantification of $^{\bullet}NO$ generation during hypoxia/reperfusion either by mitochondrial NOS or by constitutive cytosolic isoforms is challenging due to low levels of accumulation at early stages.

The ideal method for •NO detection in hypoxia-reperfusion should be able to detect low levels of intracellular •NO and with minimum autoxidation in a cellular system (Kojima et al. 1998) reported NO-specific oxidation of DAF-2-DA. DAF-2-DA is a non-fluorescent cell permeable reagent that can measure intracellular •NO and nitric oxide synthase (NOS) activity in tissues and assay systems. When the probe enters into the cytosol, diacetate groups on the DAF-2-DA reagent are hydrolyzed by cytoplasmic esterases and released DAF-2 is sequestered inside the cell. •NO oxidises the non-fluorescent dye (DAF-2) to a triazole fluorescent derivative (DAF-2T) in the presence of $O_2$ which can be maximally detected at ex: 491nm and em: 513nm **(Figure 2.9).** A 4mM solution of DAF-2-DA was prepared in 0.01M NaOH solution and purged with nitrogen to avoid air oxidation. Aliquots of 4mM working solutions were stored in the dark at room temperature.


**Figure 2.9 The oxidation of DAF-2-DA in the presence of •NO, adapted from** Kojima et al. (1998); Wardman et al. (2007). (+) indicate the inclusion of catalyst or peroxides. Blue colour indicates the non-oxidised compound of dye whereas yellow colour indicate the oxidised product of dye.

### 2.3.8 Optimisation of incubation time points for fluorescent probes

H9C2 rat myoblasts were seeded at $3x10^4$cells/well (1ml) in 24 well plates and cultured for 48h in DMEM, 10% FBS, 4mM L-glutamine and 1% penicillin / streptomycin at 37°C in 5% $CO_2$ humidified atmosphere. Then, cells were briefly washed three times with PBS and loaded with DMEM (25mM HEPES, 1% penicillin, 1% streptomycin, phenol red free), preincubated for 24h at 21% oxygen + 79% $N_2$. For time-dependent measurements of probe oxidation (15min, 20min, 45min and 1h), cells were treated with fluorescent probes at time t=0 and incubated further for 15min, 30min, 45min and 1h. The media in the wells was replaced with fresh preincubated DMEM (at 21% $O_2$ for 24h). At t=60min, the fluorescence was measured at 37˚C in preheated Spectramax GEMINI EM fluorescence plate reader at particular excitation and emission wavelengths **(Table: 2.1).**

| Fluorescent probe | Excitation | Emission | Cut off filter |
|---|---|---|---|
| DHE [1,2,4] | 488nm | 570nm | 560nm |
| DCFDA [4,5,6] | 488nm | 520nm | 515nm |
| DHR [4,5,6] | 488nm | 520nm | 515nm |
| DAF-2-DA[3,5] | 491nm | 513nm | 495nm |

**Table 2.1 Excitation, and emission maxima of fluorescent probes.**
([1]Zhou et al., 2002; [2]Zhou et al., 2005; [3]Kojima et al., 1998; [4]Royall and Ischiropoulos, 1993a; [5]Tarpey and Fridovich, 2001; [6]Tarpey et al., 2004).

### 2.3.9 Using the hypoxia chamber to induce and measure ROS/RNS

H9C2 rat myoblasts were seeded at $3x10^4$cells/well (1ml) in 24 well plates and cultured for 48h in DMEM, 10% FBS, 4mM L-glutamine and 1% penicillin / streptomycin at 37°C in 5% $CO_2$ humidified atmosphere. Then, cells at 80% confluence were washed three times with PBS solution and loaded with preincubated DMEM (phenol red-free, 25mM HEPES, 10% FBS, 1% penicillin / streptomycin, pH 7.4).

In the experimental cells, severe hypoxia ( 2% $O_2$ ) was induced by removing any existing media and replacing it with DMEM, preincubated for 24h at 2% oxygen + 98% nitrogen whereas mild hypoxia (10% $O_2$) was induced by removing any existing media and replacing it with DMEM, preincubated for 24h at 10% oxygen + 90% nitrogen. Control cells were exposed to normoxia by adding DMEM preincubated for 24h at 21% oxygen +79% nitrogen. Before cells were loaded with preincubated medium at specific oxygen tensions, the dissolved oxygen level was measured using the Winkler test to verify the extent of hypoxia or normoxia in the medium. The pH value of each preincubated medium was also determined to ensure physiological homeostasis (pH 7.4).

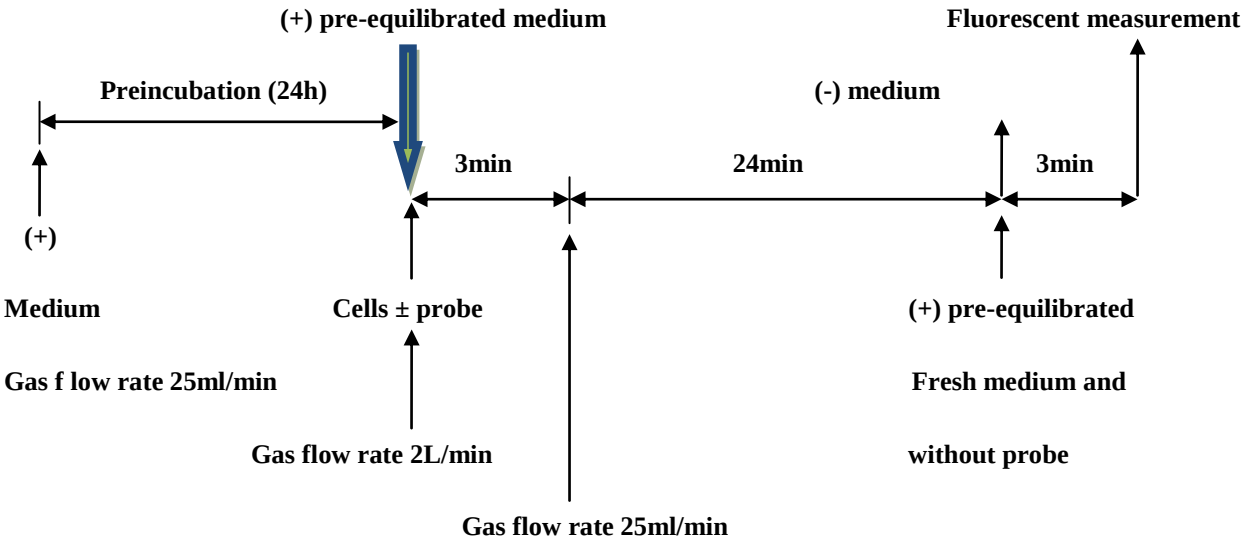


**Figure 2.10 Schematic diagram showing experimental design for fluorescent measurements; acute hypoxia (30min).**

After loading hypoxic medium, the plate was briefly flushed with premixed, sterile-filtered gas of specific $O_2$ tension before it was covered with a lid. Plates were then transferred into a pre-equilibrated hypoxic/normoxic chamber. To flush out any entrapped air inside the chamber, the airspace was perfused with premixed gas at a higher flow rate (2000ml/min) for 5min. During this procedure, the chamber's gas outlet was fully unscrewed to prevent the build up of pressure. This technique was applied for all experimental treatments and controls. All four ROS/RNS-sensitive probes were studied in a single culture plate for each experiment and control.

#### 2.3.9.1 ROS/RNS generation measured during hypoxia for 30min, 1h and 4h

H9C2 rat myoblasts were seeded at $3x10^4$cells/well (1ml) in 24 well plates and cultured for 48h in DMEM, 10% FBS, 4mM L-glutamine and 1% penicillin / streptomycin at 37ºC in 5% $CO_2$ humidified atmosphere. Then, cells were washed three times with PBS and replaced with DMEM (1ml/well) which was preincubated at 2% or 10% $O_2$ + balanced with nitrogen for 24h. Control cells were treated with DMEM preincubated at 21% $O_2$ + balanced with $N_2$. Then, the plate surface was briefly flushed with the gas at the appropriate $O_2$ tension and immediately placed in the chamber shown in **figure 2.1** at specific $O_2$ tension. The fluorescent probes (5µl, 4mM DHE or 2mM DAF-2-DA) were immediately added into wells through the holes in the lid by lifting the adhesive strips and gently mixed. Then, the plate was placed inside pre-equilibrated (hypoxia/normoxia) chamber and the plate sealant strip (Appletonwood, UK) was removed. The chamber was flushed with premixed gas at a higher flow rate (2000ml/min) for 3min. Then, the flow rate was immediately reduced to 25ml/min.

The plate was taken out and medium was replaced gently with DMEM (preincubated at specific $O_2$ tension) at t=27min before completing the 30min hypoxia. This step minimised the fluorescence due to spontaneous oxidation of the probe in the medium. At t=30min, fluorescence in each well was read in a preheated (37ºC) Spectramax fluorescence plate reader (Molecular Devices, USA) at specific excitation and emission wavelengths shown in **table 2.1**.

To measure the ROS/RNS generation in 30min normoxia (control), the same procedure was followed using premixed normoxic gas (21% oxygen balanced with nitrogen) (**Figure 2.10**). For 1h or 4h experiments, the procedure of cell exposure and equilibration at specific oxygen tension was repeated as described previously except that probes were added at t=30min for 1h experiment and t=3h 15min for 4h experiment, and then extracellular dye removed at 3min before the completion of the hypoxic period and replaced with fresh medium.

#### 2.3.9.2 Measurement of ROS/RNS generation during hypoxia/reperfusion

For 2h reperfusion studies after hypoxia for 4h, plates were sealed and taken out at t=3h and 57min and centrifuged at 1000rpm for 3min to avoid any loss of hypoxia induced dead cells. Then, existing medium was gently removed and replaced with pre-equilibrated reoxygenated medium (21% $O_2$ for 24h). Then, at 45min before measurement (5h 15min) fluorescent probe (5µl of DHE or DAF-2-DA) was added into wells through the holes in the plate lid without incorporating air as previously explained. Immediately after that, the plate was returned to the pre-equilibrated normoxic chamber whilst removing the sealer gently.

The chamber was again flushed with premixed normoxic gas at a higher flow rate (2000ml/min) for 3min and immediately decreased to 25ml/min. Reoxygenation was allowed for 2h. After 1h and 57min of reoxygenation, or at t= 5h and 57 min of total experiment duration, cell culture plates were taken out and the medium replaced with preincubated normoxic medium and the fluorescence was read at 37ºC, in a preheated fluorescence reader. For 30min hypoxia and 1h reperfusion studies, the same procedure was employed with media replacement after hypoxia and again at 3 min prior to termination of the experiment. After each experiment of hypoxia-reoxygenation, cell number was estimated by protein quantification. After fluorescent measurements, cell plates were centrifuged at 400g for 5min and then supernatant was carefully discarded without dislodging the pellet. Then, cells were lysed using 2% Triton and used for protein quantification by BCA assay.

Fluorescence in each well was calculated in arbitrary fluorescent units per 1mg of total protein in order to minimise the effect of cell density on fluorescence after hypoxia and reoxygenation.

### 2.3.10 Live imaging of $O_2^{-\bullet}$ or $^{\bullet}NO$ generating cells under confocal microscopy

Superoxide production by H9C2 cells during hypoxia was assayed using DHE (Molecular Probes, UK), a red fluorescent probe for *in vivo* superoxide detection, and imaged with a Carl Zeiss LSM 700 confocal microscope (Germany). At t=0min and t=3h15min for 30min and 4h experiments respectively, 20µM DHE was added to cells cultured in microscopic chambers and previously exposed to control (21% $O_2$), mild (10% $O_2$) and severe (2% $O_2$) hypoxia for 30min and 4h in the hypobaric chamber at 37 ºC. Hypoxic conditions were maintained at the time of imaging, by keeping chambers sealed from ambient air.

The 488nm argon laser line was used to excite DHE, which was measured by fluorescence emission using a band pass filter from 570-590nm (Zhao et al, 2005). Same procedure was applied for intracellular $^{\bullet}NO$ detection during hypoxia using DAF-2-DA fluorescent probe (Excitation: 480-490nm and emission: 510-520nm). Illumination intensity was set up at a minimum (0.1-0.2% of laser output) to avoid photooxidation and the pinhole set to give the optical beam at 2nm. Each experiment was undertaken using by at least 3 independent chamber wells.

### 2.3.11 Inhibitor effects on ROS/RNS generation and cell death

Inhibitors/antioxidants were used to assess ROS generation in H9C2 cardiomyoblasts during hypoxia/reoxygenation and the effects on cell viability. Inhibitors used were rotenone ($C_{23}H_{22}O_6$), FCCP (carbonyl cyanide *p*-(trifluoromethoxy)-phenylhydrazone)**,** apocynin (4'-hydroxy-3'-methoxy-acetophenone), allopurinoland L-NAME($N^G$-nitro-L-arginine methylester).

#### 2.3.11.1 Rotenone

Rotenone is a potent mitochondrial complex I inhibitor which specifically inhibits the NADH dehydrogenase. Rotenone at higher concentrations is also widely utilised as an insecticide or pesticide in the agriculture industry. It is a naturally occurring compound extracted from the root of *Derris sp*. A stock solution of rotenone (4mM) was prepared in DMSO and stored in the dark at room temperature (Dawson et al., 1986).

#### 2.3.11.2 Apocynin

Apocynin is a selective, potent inhibitor of phagocyte NADPH oxidase, preventing production of superoxide by blocking the migration of p47 phox to membrane which is required for formation of a functional NADPH complex (Touyz, 2008; Stolk et al., 1994b). However, apocynin is widely considered as a more specific NADPH oxidase inhibitor than DPI, a potent flavoprotein inhibitor or a non-specific inhibitor for NADPH oxidase, but commonly used as a NOX inhibitor (Bedard and Krause, 2007). Apocynin is a naturally occurring botanical compound which isolated from *Picrorhiza kurroa* (Stolk et al., 1994a). A stock solution of apocynin (4mM) was prepared dissolving in DMSO and stored at room temperature in dark.

#### 2.3.11.3 FCCP

FCCP, a potent uncoupler of oxidative phosphorylation, was selected for these studies because it has been used extensively to induce uncoupling of mitochondrial oxidative phosphorylation in many cell types, including cardiac myocytes (Hool and Arthur, 2002). It is a hydrophobic weak acid and it can readily diffuse across the mitochondrial membrane. The mode of action of FCCP in the inner mitochondrial membrane is unknown. The stock solution of FCCP (4mM) was prepared in DMSO and stored at 4˚C in the dark. The 200µM diluted aliquots (100µl) were employed as working solutions in experiments.

### 2.3.11.4 L-NAME

L-NAME is known as potent NO synthase inhibitor. Its function is not selective between different types of $^{\bullet}$NO synthases. A stock solution (40mM) of L-NAME was prepared freshly in Milli Q (MQ) water and used each day.

### 2.3.12 Cell treatment with inhibitors

Cells at $3x10^4$/well (1ml) were seeded into 24 well plates and allowed to grow to 80% confluence over 2-3 days under standard conditions (section: 2.3.1.2). Hypoxia was induced for varying times (30min-4h) by replacing medium with fresh medium which had been pre-incubated for 24h at 2%, 10% or 21% oxygen and then transferring cells to hypoxic chambers flushed with gas (5ml/min) of the same oxygen tension (section: 2.3.9.1).

In order to determine the generation and effects of specific ROS/RNS, before initiation of hypoxia for 30min or 4h duration and before initiation of reperfusion for 2h after 4h hypoxia, cells were treated with an appropriate inhibitor; 20µM rotenone, 20µM apocynin, 1µM FCCP and 200µM L-NAME at t=-2min before induction of hypoxia or hypoxia/reperfusion and inhibitors remained throughout the hypoxic/normoxic/reperfusion period. Control cells received an equal volume of vehicle and were exposed to hypoxia or normoxia for 30min and 4h as appropriate.

### 2.3.13 Nuclear morphology of necrotic and apoptotic cell death

Nuclear morphological changes were assessed in H9C2 cells after exposure to hypoxia using the fluorescent nuclear binding dye Hoechst 33342 (Calbiochem,UK) which binds to the minor groove and stains DNA blue after entering into damaged or viable H9C2 cells. Therefore, Hoechst 33342 stains the condensed chromatin of apoptotic cells more brightly than the chromatin in normal viable cells.

PI or 7-AAD can be used to discriminate late apoptotic or necrotic cells which have lost membrane integrity from early apoptotic cells which still have intact membranes by dye exclusion. Therefore, propidium iodide (Sigma-Aldrich, UK) was used and it binds and stains DNA red only in necrotic and late apoptotic cell where PI cannot enter into cells with preserved membrane integrity. Necrotic cells have round nuclei with red fluorescence, whereas round nuclei of viable cells are stained only with Hoechst 33342 blue fluorescence (Shimizu et al., 1996) (**Table 2.2**).

| **Conditions** | **PI staining** | **Hoescht 33342 staining** |
|---|---|---|
| Viable | Nuclei not stained | Round nuclei |
| Necrosis | Round nuclei stained | Round nuclei |
| Early apoptosis | Nuclei not stained | Fragmented nuclei |
| Late apoptosis (secondary necrosis) | Fragmented nuclei stained | Fragmented nuclei |

**Table 2.2 Mode of cell death defined by fluorescence staining (Shimizu et al., 1996).**

### 2.3.13.1 Method of staining apoptotic or necrotic cells

Immediately after hypoxia or control treatments (30min and 4h) in the presence or absence of ROS scavengers/inhibitors, cells grown on cover slips were washed with PBS and treated with PI + Hoechst (10ng/ml, 20min). After 3x washing cells with PBS, they were then fixed in 4% paraformaldehyde. Following further 2x washing with PBS, nuclear/DNA morphology was visualised under a ZEISS (Carl Zeiss, Germany) fluorescence microscope according to manufacturer's instructions**.**

Late apoptotic cells were detected by chromatin condensation and nuclear fragmentation (positive PI) but not early apoptotic cells (negative PI), whereas necrotic cells were detected as intact round nuclei (positive PI) (Levrand et al., 2006; Shimizu et al., 1996) (**Table 2.2**).

### 2.3.14 Quantification of necrotic cells

Quantitative necrotic cell death was measured as a ratio of PI to Hoechst staining considering the uptake of PI into necrotic dead cell DNA and Hoechst 33342 (Calbiochem, UK) uptakes into DNA of dead cells and viable cells. Cells were grown in 24-well culture plates until 80-95% confluency. Then cells were washed with 3x PBS and exposed to different hypoxia conditions and time periods. After hypoxia exposure, culture medium and cells were removed and centrifuged to make a pellet at 400g for 3min at room temperature. Then cells were suspended in 10µg/ml PI for 20min at 4ºC and after 3xPBS washing, exposed to 10µg/ml Hoechst 33342 for 20min at 4ºC. Finally, cells were suspended in PBS and dual-fluorescence was measured by excitation at 535nm/emission at 617nm for PI and excitation at 346nm/emission at 460nm for Hoechst 33342.

### 2.3.15 Protein carbonyl ELISA

Protein carbonyl formation during hypoxia is an indicative measure of protein oxidation induced by hypoxia. The quantity of protein carbonyls can be determined by derivatising with dinitrophenylhydrazine (DNPH) and quantifying bound DNP using a colorimetric or immunological method. The ELISA method is more sensitive and discriminatory than colorimetric methods and also can be used with microgram quantities of protein lysate.

The quantity of protein carbonyls in each protein sample is determined by comparing its absorbance with that of a known reduced/oxidized BSA standard curve.Proteins are non-specifically adsorbed to the plate wells. Proteins are then derivatised with DNPH. During the washing step, unconjugated DNPH is washed away.

Then adsorbed proteins are probed with anti-DNP primary antibody followed by HRP-conjugated secondary antibody. Proteins for the standard curve are prepared by oxidising serum albumin samples with and calibrating their carbonyl content by the colorimetric method (Carty et al., 2000).

### 2.3.15.1 Method

H9C2 cells were grown at 95% confluence were washed with 3xPBS and loaded with pre equilibrated medium at 2% $O_2$, 10% $O_2$ and 21% $O_2$. Then, culture flasks were exposed to hypoxia or normoxia for 30min and 4h. After each experiment, cells were incubated with protease cocktail inhibitor for 30min at -20ºC prior to lysis in Laemmli buffer. Both carbonyl standards and experimental samples were diluted in 50mM sodium carbonate buffer (1.59 g/L $Na_2CO_3$, 2.93 g/L $NaHCO_3$ and pH 9.2).

Samples (50µl/well) were plated in 96 well plates (Maxisorb, NUNC) and incubated for 1h at 37 ºC. Then, wells were washed 3x washing buffer (Tween-20 0.05% v/v in PBS) and with 1mM DNPH (2, 4- dinitrophenylhydrazine, 2M HCl) except blank wells and incubated for 1h at room temperature in the dark. After that, wells were washed and incubated with blocking agent (Tween-20 1% v/v in PBS) overnight at 4 ºC. The following day, sample wells were washed and incubated with anti-DNP primary antibody (1:2000 in Tween-20 1% v/v in PBS) for 2h at 37 ºC. Samples well were then washed gently and incubated with HRP conjugated-secondary antibody (1:5000 in Tween-20 1% v/v in PBS) for 1h. To remove excess secondary antibodies, wells were washed gently and loaded with substrate (50µl/well) solution (0.15M sodium citrate phosphate, pH5, 2g/L O-Phenylenediamine**,** 4.4mM $H_2O_2$). Following incubation (15min) at room temperature in the dark, the colour development reaction was terminated by adding 2M $H_2SO_4$. Absorbances were finally recorded at 490nm in the microplate reader (Biotek EL800). Total protein carbonyl content (nmol/mg) in each sample was quantified against the known concentration of standards.

### 2.3.16 Evaluation of apoptosis on the base of cleavage of procaspase-3

There are several methods available to determine caspase-3 activation during apoptosis. Initially, a fluorimetric caspase-3 assay was performed to quantify active caspase-3, but results were poor compared to control samples due to low caspase-3 activity under experimental conditions (data not shown). However, detection of the cleavage of procaspase-3 was more sensitive to determine induction of apoptosis under the conditions used. Therefore, to investigate apoptotic cell death during hypoxia, western blot analysis was performed to visualise the cleavage of procaspase-3.

#### 2.3.16.1 Method

After each period of hypoxia in the presence or absence of inhibitors, cells were trypsinised. After 3 x PBS washes, cells were treated with protease inhibitor cocktail (1µl/mg of total protein) (P8340, Sigma, UK) for 30min at -20ºC. Then cells were lysed in 2x Laemmli sample buffer (5% SDS) and aliquots (100µl) of lysates stored in -20 ºC for subsequent analysis. Proteins (20µg) were resolved by 15% Tricine-SDS-PAGE and transferred to polyvinylidene fluoride (PVDF) membrane (GE Healthcare, Buckinghamshire, UK) in transfer buffer with an ice-pack at 115V, 240mA for 2h prior to blocking overnight at 4 ºC with 5% non-fat dried milk powder in Tris-buffered saline containing 0.1% Tween 20 (0.1% TTBS, pH 7.5). The membrane was incubated overnight at 4 ºC with an appropriate dilution of anti-procaspase-3 (33kDa for complete fragment; Millipore) and anti-cleaved caspase-3 (17- to 19-kDa fragments) (Cell Signalling, UK) primary antibodies (1:1000).

The following day, membranes were washed with 25ml of washing buffer 0.1% TTBS for 8 x 15min at room temperature. Blots were then incubated for 1h with a 1:20,000 dilution of the appropriate horseradish peroxidase-conjugated secondary antibody (Cell Signalling, UK) at room temperature and followed by 8 x 15min washes with 0.1% TTBS at room temperature. The immunoblot signal was visualized by incubating PVDF membranes using enhanced chemiluminescence (GE Healthcare, Buckinghamshire, UK) mixed solution according manufacturer's instructions and then exposed to X-ray film (GE Healthcare, Buckinghamshire, UK) for 45 seconds in a dark room.

The film was developed and fixed gently using developer and fixer solutions (Kodak Chemicals, Japan). Finally, films were washed with copious amounts of water for 3min and air dried.

### 2.3.17 Quantification of total protein content in cell lysate

#### 2.3.17.1 RC-DC assay

The RC-DC (Bio Rad, USA) protein assay was used to quantify total protein content of samples after cells are lysed into Laemmli buffer. The RC-DC assay is a colorimetric assay which is compatible with complex mixtures such as Laemmli buffer which contain both reducing agents and detergents. Also this assay is sensitive for wide range (0.2-1.5mg/ml) of protein concentrations. This assay is based on a modification of Lowry method of protein estimation. Peptide bonds in protein sample initially form complexes with $Cu^{2+}$ ions and then reduce to $Cu^{1+}$ ions under alkaline conditions. Then this $Cu^{1+}$ ion reacts with tyrosine, tryptophan and cysteine amino groups in the presence of Folin reagent to produce an unstable product. This unstable product is then reduced to tungsten blue and detected at 630nm using spectrophotometer (Lowry et al., 1951).

##### 2.3.17.1.1 Method

H9C2 cardiomyoblasts were seeded at a density of 3 $x10^4$ cells/well and cultured at 37°C in a 5% $CO_2$ humidified atmosphere in DMEM supplemented with 10% FBS and 1% penicillin/streptomycin mixtures. At 80-90% confluence, hypoxia was induced for varying times (30min-4h) in the presence or absence of inhibitors by replacing medium with fresh medium which had been pre-incubated for 24h at 2%, 10% or 21% oxygen and then transferring cells to hypoxic chambers flushed with gas (5ml/min) of the same oxygen tension. After the hypoxic period was completed, cell metabolism was inhibited by incubation on ice for 20min and cells were washed twice in ice cold 0.15M PBS. Cells were harvested by scraping. 1ml of boiled 2 x Laemmli buffer (63mM Tris HCl, 4mM $Na_2P_2O_7$, 5mM EDTA, 41% Glycerol v/v, 2% SDS w/v, 0.007% bromophenol blue, pH 6.8) and 100µl of protease inhibitor cocktail (P8340, Sigma, UK)

was added to minimize proteolysis. Genomic DNA was sheared using a 21G needle. The total protein extracts were transferred into a microfuge tube. Some aliquots were taken for protein estimation, others were diluted in 2 x Laemmli buffer and stored at -20°C for western blot analysis. Protein samples (5µl of 2 and 1 fold dilutions) and BSA standards (0, 0.2, 0.4, 0.6, 0.8, 1.0, 1.2, 1.4 and 1.5 mg/ml in Laemlli buffer) were pipetted into clean, dry microfuge tubes in triplicate and 25µl of RC reagent I was added. Samples were vortexed and incubated for 1min at room temperature.

Then, 25µl of RC reagent II was added and samples were vortexed and centrifuged at 15,000xg for 5min. The supernatant was discarded by inverting the tubes on clean, absorbent tissue paper until the liquid was completely drained. Then, 25µl of reagent A' (1:50 v/v, DC reagent S to DC reagent A) was added to each microfuge tube and samples vortexed and incubated for 5min at room temperature or until the precipitate was completely dissolved. After vortexing the samples again, each tube was added with 200µl of RC reagent B and vortexed immediately. After 15min incubation of samples, the content of each tube (200µl) was transferred to 96 well plates and the absorbance detected at 630nm. Protein concentrations were determined by comparison to the standard curve.

#### 2.3.17.2 Bicinchoninic acid (BCA) protein assay

The BCA protein assay was employed to quantify total protein content of samples when cells are lysed in culture medium or PBS with 2% Triton. The BCA assay was also adapted from the Lowry method (1951) and is based on reduction of $Cu^{2+}$ to $Cu^{1+}$ by proteins under alkaline conditions. Then, colorimetric detection of $Cu^{1+}$ is achieved with bicinchoninic (BCA) acid. When the assay is performed, initially, $Cu^{2+}$ chelates with proteins in alkaline sodium potassium tartate solution to produce a light blue complex with $Cu^{1+}$. Second, BCA reacts with the $Cu^{1+}$ and produces an intense purple-coloured product. Two molecules of BCA react with one molecule of $Cu^{1+}$. The coloured BCA/copper complexes are water-soluble and show a sharp linear absorbance at 562 nm that is directly proportional to protein concentration in samples.

The reaction that leads to BCA/copper colour formation strongly depends on the four different amino acid residues; cysteine or cystine, tyrosine, and tryptophan in the protein. Whenever required, the BCA assay was used to estimate protein concentrations in the samples as it is highly sensitive colorimetric technique.

#### 2.3.17.2.1 Method

Protein samples (10µl) and bovine serum albumin (BSA) standards (0, 2, 4, 6, 8 and 10 µl of BSA diluted with 10, 8, 6, 4, 0 µl of deionised water) were aliquotted into independent wells in triplicate. Then, to each well was added 200µl copper sulphate-bicinchoninic acid mix solution (1:50 v/v) and the plate was incubated for 30min at 37°C. The absorbances were read at 570nm and protein concentrations were determined by comparison to the standard curve.

### 2.3.18 Cloning of Bacterial Plasmids

#### 2.3.18.1 Preparation of Luria Bertani (LB) agar plates and LB broth for selection of Clones in *E. coli*

LB agar solution (15g/L) was prepared by dissolving 10g of tryptone, 5g of yeast extract, 5g of NaCl, (Sigma, UK) in 1000ml of deionised $H_2O$ and then transferring the content into a flask which contains 15g of LB agar. The solution was autoclaved for 30min at 121°C. Petri dishes (15mm) were labelled for each of the three different bacterial plasmids DNA; pGL 3 [*3enh/conA/luc*]; pGL 3 [*nqo*1*/luc*] and pGL4.74 [*hRluc*/TK] (Promega, UK); pGL 3 [*3enh/conA/luc*] and pGL 3 [*nqo*1*/luc*]. Plasmid pGL 3 [*3enh/conA/*luc] was kindly donated by Dr Ann Vernallis (Aston University, UK) and plasmids; pGL4.74 [*hRluc*/TK] and pGL 3 [*nqo*1*/luc*] were kindly donated by Dr Melissa Grant (University of Birmingham, UK) (plasmid maps are shown in Appendix). After autoclaving, LB agar solution was cooled down to 45°C and was supplemented with the sterile ampicillin sodium salt (Sigma, UK) solution (100µg/ml).
Agar plates were prepared by pouring LB agar solution (25ml) into Petri dishes under aseptic sterile conditions and any air bubbles were burst if necessary by flaming with a Bunsen burner. Plates were allowed to cool and solidify.

When plates were completely hardened, they were inverted and stored at 4°C until needed. LB broth solution (25g/L) was prepared by mixing 15g of LB agar in 600ml of deionised $H_2O$ in a sterile Erlenmeyer flask and autoclaved for 30min. After autoclaving and cooling to 45°C, LB agar solution was supplemented with the sterile ampicillin sodium salt (Sigma, UK) solution (100µg/ml). LB broth solution was stored sterile at 4-8°C.

#### 2.3.18.2 Transformation of *E. coli* (DH5α) with recombinant plasmids: pGL 3 [*3enh/conA/*luc], pGL 3 [*nqo1/*luc] and pGL4.74 [*hRluc*/TK]

Polypropylene culture tubes were chilled on ice, one per single transformation. Frozen DH5α *E. coli* competent cells (Invitrogen, UK) were removed from -70°C and placed on ice for 5min. After gently mixing the thawed competent cells by flicking, competent cells (50µl) were transferred to each chilled tube and dilutions of cells prepared at 1:10 and 1:100 ratio in LB agar solution supplemented with ampicillin. Three transformation reactions; undiluted, 1:10 and 1:100 were conducted for each plasmid.

Then, 2µl of plasmid DNA was added to each tube and flicked quickly several times. Immediately, tubes were equilibrated on ice for 10min. A heat block (Thermo Scientific, UK) was set up at 42°C. The cells were heat shocked for 45sec at 42°C exactly and immediately placed on ice for 2min. Each tube of transformed cells was diluted with cold sterile LB broth (950 µl) and incubated for 1h at 37°C with shaking (9g). After the incubation period, the contents of each tube were transferred into a microfuge tube and centrifuged at 5000g for 3min. Cells were plated with undiluted cells, 1:10 and 1:100 diluted cells on independent ampicillin treated LB agar plates. Then, plates were inverted and incubated at 37°C for 14-16 hours. Throughout the protocol, sterile aseptic conditions were employed to avoid any contamination.

### 2.3.18.3 Starting culture for DNA preparation by Maxiprep

In order to prepare a starter culture for Maxiprep DNA extraction, a single colony of *E. coli* (DH5α) was carefully selected from a freshly grown (14-16h) selective culture using a sterile pipette tip. The LB broth medium (5ml, 100µg/ml ampicillin) was inoculated with one selected bacterial colony and incubated overnight with shaking (~16g) at 37°C. The following day, bacterial suspensions (1.5ml) were transferred to sterile 1.5ml eppendorf tubes and centrifuged at 13,000xg for 5min to harvest the bacteria. After discarding the supernatant, the bacterial cell pellet was resuspended in fresh LB broth (1ml). For Maxipreps, a large flask of LB broth (400ml, 100µg/ml ampicillin) was inoculated with LB broth (1ml) containing bacterial cells and incubated overnight with shaking at 37°C.

### 2.3.18.4 Maxiprep of bacterial plasmid DNA

Large scale purification of plasmid DNA was performed by using a Marligen Maxiprep Kit (Marligen, USA) according to the manufacturer's instructions. The column was equilibrated by adding 30ml of equilibration buffer and solution to the column and it was allowed to run through by gravity flow. Meanwhile, bacterial cells from 400ml of an overnight culture were harvested by centrifugation at 4480g for 10min at room temperature. The cell pellets were resuspended in cell suspension buffer (10ml) containing RNase A until the cell pellet was homogeneous. Cell suspension was added to cell lysis buffer (10ml) and mixed gently by inverting the capped tube five times and incubating at room temperature for exactly 5min.

To the mixture, neutralization buffer was added (10ml) and mixed immediately by inverting until the solution was homogeneous. The mixture was centrifuged at 15,000g at room temperature for 10min. Then, the equilibrated column was loaded with supernatant and the eluent/buffer in the column was allowed to drain by gravity. The column was washed with wash buffer (60ml). In all steps, column flowthrough was discarded. DNA was eluted by adding 15ml of elution buffer to the column and flowthrough was collected into clean polypropylene tubes. Isopropanol 10.5ml was added to the evaluate and mixed, then, centrifuged at 15,000g at 4°C for 30min.

Supernatant was discarded and the plasmid DNA pellet was washed with 5ml of 70% ethanol and again centrifuged at 15,000g at 4°C for 5min. The ethanol wash was carefully pipetted off and the precipitate was air dried for 10-15min.

Finally, the precipitated DNA was dissolved in 500µl of TE buffer and transferred into fresh tubes. All purified plasmid DNA solutions were aliquoted (10µl) and stored at -80ºC.

### 2.3.18.5 Determination of Plasmid DNA concentrations and purity

Total plasmid DNA concentration and the purity of each sample was determined using a NanoDrop™ 8000 Spectrophotometer (Thermo Scientific, UK) according manufacturer's instructions. The upper and lower measurement pedestals were cleaned first with 70% ethanol and then by Milli Q water on lint free wipe (Kimwipes, UK). The instrument was initialized using 2µl of deionised water and "Nucleic acid application module" was selected. The instrument was blanked using 2µl of TE buffer. Then, each plasmid DNA sample (2µl) was pipette onto the lower measurement pedestal. The sampling arm was closed and OD reading was initiated automatically at A260nm and A280nm.

When the measurement was complete, both the upper and lower pedestals were wiped clean using lint free wipes before pipetting the second sample. This step prevents the sample carryover in successive measurements for samples varying by more than 1000 fold in concentration. The readings of samples at A260nm were accepted as DNA concentrations and the ratio of A260/A280 was used to assess the purity**.** A ratio of ~1.8 was accepted as pure sample of DNA.

### 2.3.18.6 Restriction analysis of purified plasmid DNA

To reassess the presence of sequences (promoter, enhancer and reporter gene) of DNA inserts in purified plasmids, restriction analysis was performed using single enzyme digestions according to manufacturer's instructions.

Plasmid DNA maps were referred to identify particular restriction sites in all three different purified plasmids (Plasmid maps in appendix**)**. Following restriction-digestion, fragments were separated on 1% agarose gel as described below.

### 2.3.18.6.1 Restriction endonuclease digestion of purified plasmid DNA

Plasmid DNA (1µg-1.5µg) was mixed with 2µl of 10X reaction buffer, 1µl of appropriate restriction endonuclease (Fermentas, USA) and the volume made up to 20µl with deionized $H_2O$. The digests were incubated in a water bath set to 37°C for 4h. Genomic DNA was digested as above except that digests were incubated at 37°C overnight to allow for complete digestion of genomic DNA. Finally, restriction enzymes were heat-inactivated at 80ºC in 20min according to manufacturer's instructions.

### 2.3.18.6.2 Agarose gel electrophoresis of digested plasmid DNA fragments

1 % agarose gel was prepared by boiling an appropriate mass of agarose powder in Tris-borate EDTA buffer (89mM Tris; pH 7.6, 89mM boric acid and 2mM EDTA) (TBE) buffer until dissolved and 0.5µg/ml ethidium bromide (Fisher Scientific) was added. Then, agarose solution was gently poured into a horizontal mini-gel tank (10cm x 15cm) (Bio Rad, USA) and gel was allowed to set at room temperature for 10min with 12 well comb.

DNA samples (volumes ranged from 2-50µl) were mixed with one-sixth volume of loading buffer (12% glycerol v/v, 60mM $Na_2EDTA$, 0.6% SDS w/v, 0.003% bromophenol blue w/v, 0.003% xylene cyanol w/v) and loaded onto the gel. Standard DNA ladder (New England Bio labs, UK) was run adjacent to DNA samples. They comprised of 1Kbp or 100bp DNA fragments and were diluted in loading buffer as before. Electrophoresis was carried out in 1X TBE at 150V, 250mA for 1h. Gels were visualized using UV light on a transilluminator and images were captured by Polaroid camera (Kodak, Japan) (**Figure 2.11).**

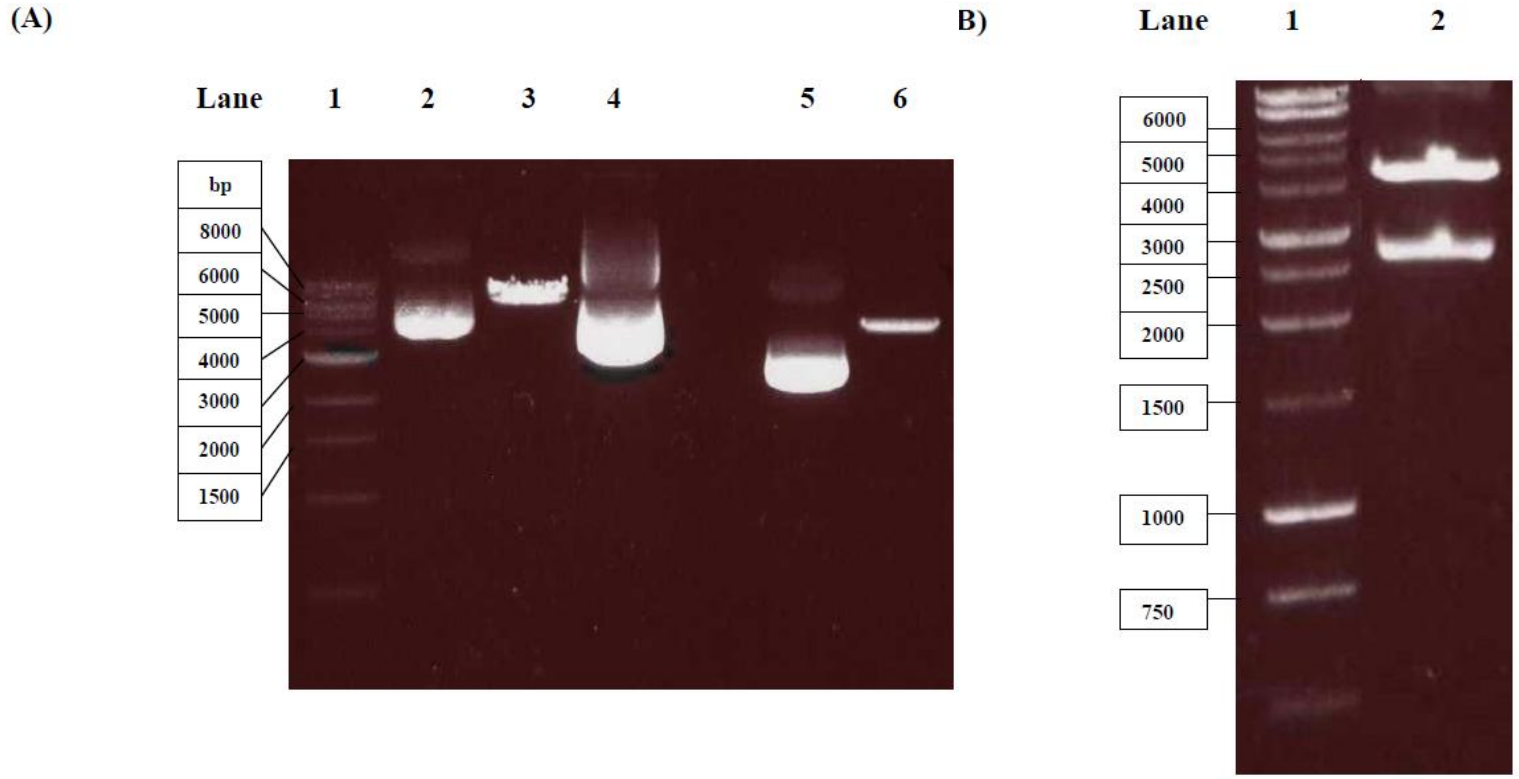


**Figure 2.11 Restriction digestion and agarose gel electrophoresis of plasmid DNA.** Plasmid DNA vectors were digested with HIND III or Bam HI and electrophoretic migration was analysed in 1% agarose gel containing, 0.5µg/ml ethidium bromide. Following electrophoresis, the DNA fragments were visualised using UV light and photographed. The sizes of restriction digests were determined by comparing to a DNA ladder (Lane 1 in A and B). HIND III cleaves plasmid DNA; pGL 3 [*3enh/conA*/luc] and pGL4.74 [*hRluc*/TK] at a single restriction site, yielding linear DNA. Bam HI plasmid cleaves pGL 3 [*nqo*1/luc] plasmid DNA at two restriction sites, yielding two linear DNA fragments. The linear DNA fragments ( Lane 3 (A); pGL 3 [*3enh/conA*/luc] + HIND III, lane 6 (A); pGL4.74 [*hRluc*/TK] + HIND III and lane 2 (B); pGL 3 [*nqo*1/luc] + Bam HI migrate towards the positive electrode slowly, whereas super-coiled uncut-plasmid DNA migrates faster (Lane 2 (A); pGL 3 [*3enh/conA*/luc], lane 4 (A); pGL 3 [*nqo*1/luc] and lane 5 (A) pGL4.74 [*hRluc*/TK]).

### 2.3.19 Primer designing

Primer sequences were designed using "Invitrogen Oligo design" on line software (Invitrogen, UK) referring to recommended sequences for pGL 3 (GL primer 2) and pGL 4 (RV primer 3) basic plasmids (Promega, UK) and the primer sequence for pGL 3 [nqo1/luc] designed according to the 5'-upstream region of NQO1 ( genomic walking) as described by Nio1 *et al.* (2003). All primers were synthesized by Invitrogen, UK and stored frozen as 100µM in 1xTE (10mM Tris base, 1mM EDTA, pH 8.0) buffer at -20°C until use. Annealing conditions were computed using the Wallace formula (Tm= [4(G+C) +2(A+T)] -5°C (Suggs et al., 1981) according to the recommended temperature range of Functional Genomic Labs, University of Birmingham, UK **(Table 2.3)**.

### 2.3.20 Sequencing of plasmid DNA

In order to reassess further the presence of DNA consensus sequences; promoter region, enhancer and reporter in purified plasmid DNA samples. DNA sequence analysis was performed using 250ng of purified plasmid DNA in an ABI3730 DNA analyser (Applied Biosystems, USA) at the Functional Genomic Labs, University of Birmingham, UK. The DNA Reaction mixture was prepared as follows for each purified plasmid DNA sample **(Table: 2.4)**.

| Plasmid DNA Types | Primer sequence (5' to 3') | Annealing temperature (Tm) | % GC | Molecular Weight |
|---|---|---|---|---|
| **pGL3 [*nqo*1/luc]** | CGCCTCGAGGCCCTC TGAATACTTTCAACAA | 59°C | 51 | 9401.2 |
| **pGL3 [*3enh/coA*/luc]** | CTTTATGTTTTTGGCG TCTTCCA | 47°C | 39 | 6978.6 |
| **pGL4.74 [*hRluc*/TK]** | GACGATAGTCATGCC CCGCG | 53°C | 53 | 6104.0 |

**Table 2.3 DNA sequencing specific primer.** Single primers were designed as described in methods and were based on sequence information of plasmid manufacture and Genbank (NCBI, USA).

| Reagent | Quantity | | |
|---|---|---|---|
| | **pGL 3 [*nqo*1/luc]** (1188.2ng/µl) | **pGL 3 [*3enh/conA*/luc]** (1693.7ng/µl) | **pGL4.74 [*hRluc*/TK]** (663.9ng/µl) |
| **Plasmid DNA** | 2.10µl (250ng) | 1.47µl (250ng) | 3.76µl (250ng) |
| **Primer** | 3.2µl | 3.2µl | 3.2µl |
| **Deionised water** | 4.7µl | 5.33µl | 3.04µl |
| **Total Volume** | **10µl** | **10µl** | **10µl** |

**Table 2.4 Composition of plasmid DNA reaction mixture.** The reaction mixture for each purified plasmid was prepared according to the Functional Genomic Lab's instructions.

Samples were loaded onto a 96 well plate and run in the automated process of ABI3730 DNA analyser. Big Dye terminator V3.1 (10µl) (Applied Biosystem) was added into each sample (10µl) by the ABI3730 analyser robot and the labelling reaction, PCR cycle sequencing cycles (Sanger sequencing method (Ramp at 96ºC for 10cycles/Ramp at 50ºC for 5cycles/Ramp at 60ºC for 240cycles and repeat further 24 and then total x 25 cycles) and purification of samples was performed Qiagen DyeEx plates (Qiagen, USA) according to size-exclusion principle to remove unincorporated dye and reagents from samples initially. Finally samples were analysed on the capillary sequencer ABI 3730 to produce the plasmid DNA sequence. The sequence of purified plasmids is shown in the appendix.

### 2.3.21 Transient transfection of plasmid DNA into H9C2 myoblasts

#### 2.3.21.1 Optimisation of plasmid DNA transfection with Lipofectamine 2000 (Lipofection)

One day before transfection, H9C2 myoblasts were seeded at 1.5 x $10^5$ cells/well in 1ml of culture medium (DMEM, 10% FBS and 4mM L-glutamine) without antibiotics in 24 well plates and the cells were incubated at 37°C in a humidified atmosphere of 5% $CO_2$ and 95% air. After 24h, H9C2 cells at 90% confluence were transfected with pGL 3 [*nqo*1/luc] plasmid for determination of Nrf2 activation or pGL 3 [*3enh/conA/*luc] for NF-κB activation and control plasmid pGL4.74 [*hRluc*/TK] for thymidine kinase using Lipofectamine 2000 (Invitrogen, UK). The manufacturer's standard protocol was modified in some steps to achieve optimum transfection efficiency.

Initially, the total DNA to Lipofectamine 2000 ratio for each transfection was optimised using total DNA to Lipofectamine 2000 ratios of 1:2, 1:3 and 1:4 according manufacturer's instructions. The total amount of DNA was held constant with varying amount of lipofectamine. Similarly, control plasmid DNA to experimental plasmid DNA ratio was optimised using 1:9, 1:10 and 1:11 ratios as previously described elsewhere.

The amount of control plasmid DNA; pGL4.74 [*hRluc*/TK] was held constant with varying amounts of experimental plasmids; pGL 3 [*nqo*1/luc] or pGL 3 [*3enh/conA/*luc]. For each transfection, DNA/Lipofectamine complexes were prepared as follows. Each sample was diluted and gently mixed in 50µl of Opti-MEM I reduced serum medium (Invitrogen, UK) in 1.5ml polypropylene tubes.

Then, an appropriate amount of Lipofectamine 2000 was diluted and gently mixed with 50µl of Opti-MEM I reduced serum medium and incubated for 25min (Dalby et al., 2004). After the 25min incubation, the diluted DNA samples (1:10) were combined with diluted Lipofectamine 2000 (Total volume=100ul) and incubated for 25min at room temperature to achieve the optimal complex formation as previously reported (Dalby et al., 2004). Meanwhile, cells were washed with PBS and Opti-MEM I reduced-serum medium and the medium in each well was replaced with 400µl of fresh Opti-MEM I reduced-serum medium. After a 25min incubation period, 100µl of DNA and Lipofectamine 2000 complex was added to each well containing cells with 400µl of medium and then the contents in each well were gently mixed by rocking the plate back and forth. Cells were incubated for a 24h period at 37°C in a humidified atmosphere of 5% $CO_2$ and 95% air. After the first 6h of transfection, wells were loaded with 500µl of culture medium containing 20% FBS and 8mM L-Glutamine to all transfected and non-transfected cells.

Non-transfected cells served as controls for background luminescent measurements in luciferase assay. To test for transgene expression, cells were gently washed 2xPBS and loaded with phenol red-free medium (1ml/well) containing 2µM LPS and incubated for 4h period. It has been reported that LPS can induce NF-κB (Tsao et al., 1996) and Nrf2 (Rushworth et al., 2008) activation. Therefore, 10ng/ml LPS treatment was employed to activate these transcription factors as a positive control in luciferase assay.

### 2.3.21.2 Luciferase reporter gene assay

To measure the luciferase reporter activity in transfected cells after exposure to hypoxia, a Dual Glo luciferase assay (Promega, UK) was performed according to an in-house modified protocol. Before conducting the luciferase reporter assay, plates were centrifuged at 300g for 3min to avoid loss of dying cells due to exposure to hypoxia or LPS treatment. Then, medium in each well was completely discarded and loaded with 100µl of serum and phenol red-free DMEM. To measure the *Firefly* luciferase activity, each transfected or non-transfected cell treatment was incubated with 100µl Dual Glo luciferase reagent and mixed gently to induce cell lysis on a rocker for 2min. Then, plates were incubated for another 8min at room temperature and *Firefly* luminescence was measured in a Spectramax luminometer (Molecular Devices, USA) at emission: 542nm and at room temperature.

To measure the *Renila* luciferase activity for control gene expression and transfection efficiency, both transfected and non-transfected cells were incubated with 100µl of Dual Glo Stop and Go reagent and gently mixed for 2min on a rocker. After 6min incubation at room temperature, the *Renilla* luminescence was measured in a luminometer at room temperature, in the same order as the firefly luminescence measurement. In order to obtain optimal and consistent results avoiding inconsistencies with transfection efficiency, the ratio of luminescence of experimental reporter to control reporter was calculated as follows according manufacturer's instructions.

Ratio of control firefly luminescence/Renilla luminescence=X

Ratio of Experimental well firefly luminescence/Renilla luminescence=Y

Relative ratios; control = X/X=1 and experimental well=X/Y

### 2.3.22 Visualisation of transfection efficiency using cytochemical staining of β-galactosidase

The transfection efficiency was determined using cytochemical staining of β-galactosidase expression. One day before lipofection, H9C2 cells at 90% confluence were seeded on 60-mm tissue culture dishes at a density of $1.5x10^5$ cells/dish and loaded with 5ml of culture medium (phenol-red free DMEM, 10% FBS, 4mM L-glutamine) without antibiotics and incubated for 24h at 37°C in a humidified atmosphere of 5% $CO_2$ and 95% air. Then, β-galactosidase plasmid DNA Lipofectamine 2000 complexes were prepared at 1:4 ratio in 0.5 ml Opti-MEM I reduced serum medium as previously described (Section 2.3.21.1). The β-galactosidase plasmid DNA was kindly donated by Dr Ann Vernallis (Aston University, UK).

After 24h, the cell culture dish was washed with 2x PBS and 1x Opti-MEM I reduced serum medium and loaded with 2ml Opti-MEM I reduced serum medium and return to 37°C humidified incubator with of 5% $CO_2$ and 95% air. Once the DNA/Lipofectamine 2000 complexes were ready, β-galactosidase plasmid DNA/Lipofectamine solutions were added evenly to culture dishes as appropriate and incubated for another 24-48h at 37°C in a humidified atmosphere of 5% $CO_2$ and 95% air. After 6h of transfection, each dish was loaded with 2.5ml of culture medium containing 20% FBS and 8mM L-Glutamine and re-incubated for 48h.

Cells were then washed with 2x PBS at room temperature and loaded with 5ml of cell fixative solution (2% v/v formaldehyde, 0.2% v/v glutaraldehyde, 1x PBS). After 2min, cells were washed with 1x PBS and loaded with 5ml of histochemical staining solution (5mM $Fe_3Fe[CN]_6$, 5mM $Fe_4Fe[CN]_6$, 2mM $MgCl_2$, 1x PBS, 1mg/ml X-gal (5-bromo-4-chloro-3-indolyl-β-galactoside) and incubated for 24h at 37°C. Finally, cells were washed gently with 4x PBS and covered with 1ml of PBS to examine under a light microscope. The transfection efficiency was estimated by counting the relative numbers of stained and unstained cells. Mean transfection efficiency ~30% was estimated from three independent studies **(Figure 2.12A and 2.12B).**

**(A)**

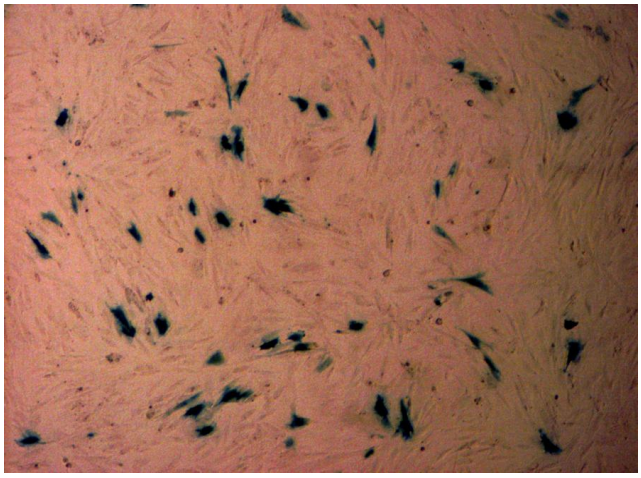

**(B)**

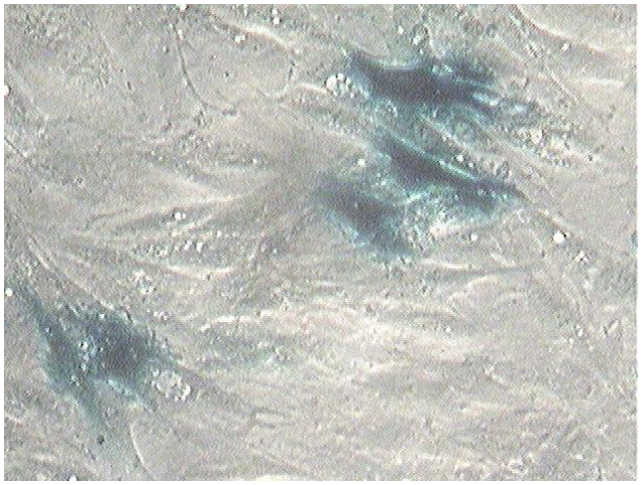

**Figure 2.12 β-Galactosidase expression in H9C2 cells after 48h.** H9C2 cell transfected with plasmid DNA harbouring β-Galactosidase. Cell monolayers were histochemically stained with X-gal. (A) Transfected cells at 20x magnification (B) Transfected cells at 40x magnification.

### 2.3.23 Statistical Analysis

Results are presented as sample mean ± SEM. Statistical analysis was performed using Graphpad Prism TM software and tested by one-way ANOVA (nonparametric) using Tukey's post-hoc test. All results are means of three independent experiments. P< (0.05)* was considered as significantly different from controls and P< (0.05) was considered as significantly different from treatments.

# CHAPTER 3

# OPTIMISATION OF CONDITIONS FOR USE OF FLUORESCENT PROBES TO DETECT ROS/RNS

## 3.1 Preface

This chapter describes the optimisation of conditions for use of various fluorescent probes in measuring intracellular ROS/RNS during hypoxia and hypoxia/reperfusion, and the validation and optimisation of the hypobaric chamber. Initial studies determined the optimum incubation time for detecting probe oxidation with ROS/RNS during normoxia, in respect of their fluorescent intensity and kinetics of formation. Subsequent experiments were conducted to verify whether the hypoxic system can render cells hypoxic without affecting the pH in culture medium over the period of hypoxia. The optimised protocol of fluorescence dye applications was used to measure intracellular ROS/RNS generation in *in vitro* cell culture system.

## 3.2 Introduction

### 3.2.1 Fluorescent probes

The production of ROS/RNS is associated with deleterious changes to biomolecules and/or changes in biochemical functions in cells (sections 4.2 and 5.2). ROS/RNS generation during hypoxia alone or hypoxia/reperfusion has been established in neuronal cells from the use of free radical scavengers (Abramov et al., 2007). Their detection by a validated probe is critically important to understand their associated role in cardiac cell toxicity during hypoxia ± reperfusion. It is hard to characterise ROS/RNS due to their short half-lives, the action of *in vivo* antioxidant defence and their high reactivity with a variety of substrates (Gomes et al., 2005; Tarpey et al., 2004; Tarpey and Fridovich, 2001).

The use of probes *in situ* is an excellent approach to measure ROS/RNS due to their potential for sensitivity, simplicity in application and high resolution of images under the microscope. The development of reliable techniques for detecting ROS/RNS is vitally important to understand deleterious effects of hypoxia or hypoxia/reperfusion.

The number of readily available direct and indirect methods may under- or over-estimate the level of ROS/RNS at an intracellular level as high background fluorescence may be due to probe leakage from the cell system; photoxidation of probe, their non-specific oxidation by other catalytic/redox cycling chemicals and therefore an increase in noise (Gomes et al., 2005).

Recent reports have shown leakage of DCF fluorescent probes from skeletal muscle fibres and their extracellular photooxidation that increases background fluorescence (McArdle et al., 2005). However, Murrant et al. (1999) have suggested the ways of minimising background fluorescence and photo oxidation in experimental systems. Previously published work has described the use of probes over variable periods during hypoxia or ischaemia to assess ROS/RNS generation (Duranteau et al., 1998; Chandel et al., 2000; Chandel and Schumacker, 1999).

The presence of probe over longer time points may lead to increased autooxidation, time-dependent decay of fluorescence and saturation/insufficient amount of probe for oxidation thereby this approach may not indicate an accurate estimation of ROS/RNS produced over period. Therefore, it is important to determine optimum oxidation time point(s) as measured by fluorescence spectrometry which gives minimum background noise with high signals. This chapter describes the quantitative optimisation of fluorescent probe oxidation conditions to minimise photo/autooxidation and fluorescent decay.

It has been reported that mitochondria generate $O_2^{-\bullet}$ as a by-product of oxidative phosphorylation. Approximately 1–3% of mitochondrial $O_2$ consumed may produce $O_2^{-\bullet}$ by interaction with "leaked" electrons at mitochondrial complex I, II and III (Hool and Arthur, 2002; Guzy et al., 2005; Chandel et al., 2000). $O_2^{-\bullet}$ is the primary ROS produced and can undergo further reactions to produce subsequent radical species. Therefore, a panel of probes has been selected for optimisation that has specificity for ROS/RNS and sources e.g. mitochondrial and non mitochondrial based-ROS/RNS.

### 3.2.2 Hypobaric oxygen chamber

Hypoxic chambers are widely used to achieve a hypoxic environment in *in vitro* or *in vivo* experiments. In such systems, reduced $O_2$ tensions are perfused with continuous flow. Alternatively, hypoxic-mimic agents such as Co or Ni can be used to mimic cellular hypoxic events chemically (Chachami et al., 2004; Chandel et al., 1998). However, those studies are difficult due to metal toxicity induced cell death (Wang et al., 2000). Cell cultures can be made hypoxic by bubbling nitrogen gas through the medium; the gas should be sterile to avoid contamination (Killilea et al., 2000). Sample manipulations are also difficult during hypoxia; when cells are removed from hypoxia to normoxia, reoxygenation can cause additional stress and metabolic changes in the cells, leading to complications in the interpretation of results.

In kinetic studies of ROS generation during hypoxia, addition of fluorescent probes or inhibitors into cell culture plates or taking sample for dissolved gas analysis is a challenge in wet laboratory practice whilst maintaining stable hypoxic conditions inside the chamber without incorporation of ambient air into experimental samples. The maintenance of stable pH conditions in the culture medium during both hypoxia or normoxia and also stable dissolved $O_2$ level are critical. It is difficult to achieve this without monitoring the changes by advanced instruments such as oxygen sensors and micro pH electrodes. Therefore, a closed environmental system with continuous perfusion of gas mixtures such as Sykes-Moor chambers or Billups-Rothenbergs advanced chambers are often preferred. In the methods section of this thesis, the invention of a simple and economical gas flow system is described to initiate hypobaric hypoxia in cell cultures while allowing simultaneous addition of experimental reagents without incorporation of ambient air.

## 3.3 Results

### 3.3.1 Optimisation of fluorescent probes

To investigate the optimum incubation time to detect oxidation of each fluorescent probe with reactivity of intracellular ROS/RNS generated during inhibition of mitochondrial respiration (as might be expected during hypoxia), fluorescence was measured for various periods: 15min, 30min, 45min and 60min after loading the probe into cells in the presence or absence of mitochondrial complex I inhibitor; rotenone (40µM) as described in section: 2.3.8.

#### 3.3.1.1 Superoxide detection by DHE

H9C2 cells at 70-80% confluence were briefly washed with PBS and loaded with phenol red-free DMEM prior to addition of 20µM DHE in the presence or absence of mitochondrial complex I inhibitor; rotenone (40µM). Cells were incubated in the dark and fluorescence was determined after 15min, 30min, 45min and 60min under normoxia.

In order to minimise background fluorescence, existing culture medium was replaced gently with fresh medium 3min before the fluorescence measurements at optimal wavelengths for detection of 2-hydroxy ethidium (excitation at 488nm and emission at 570nm) as previously reported (Zhao et al., 2005; Zhao et al., 2003).

As illustrated in **figure 3.1,** DHE fluorescence increased time-dependently and maximum oxidation was achieved at t=60min. There was a trend for lower DHE fluorescence after 30min in the presence of rotenone, but this was not significant compared to untreated cells. Therefore, incubation time; 45min was selected as an optimum oxidation period of DHE due to the stability of the oxidised products.

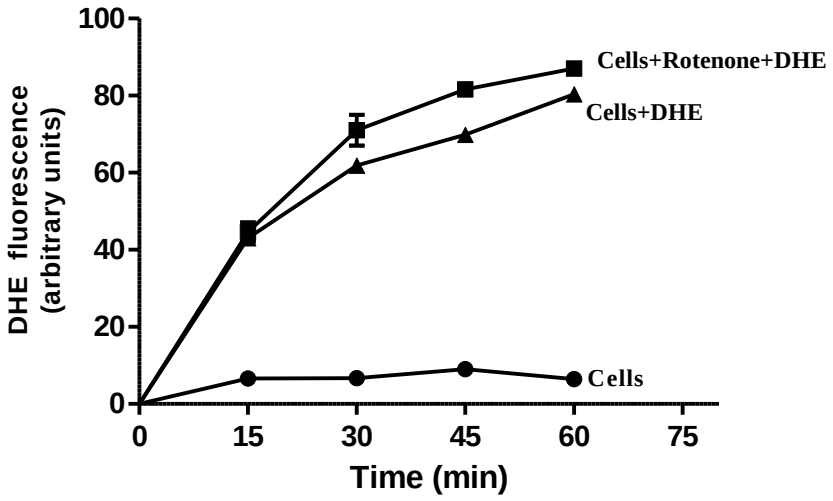


**Figure 3.1 DHE oxidation at different incubation times.** H9C2 cells were seeded at $3x10^4$/well and grown until 70-80% confluence at 37ºC in 5% $CO_2$ in humidified atmospheric conditions. Then cells were washed with PBS and loaded with phenol red-free DMEM. In the presence or absence of 40µM rotenone, the fluorescence was measured after 60min, 45min, 30min and 15min incubations with 20µM DHE in dark in a preheated (37°C) GEMNI fluorescence reader at Excitation: 488nm, Emission: 570nm, cut off filter: 560nm. Data represents the mean±SEM fluorescence of three independent experiments conducted in triplicates.

### 3.3.1.2 Kinetics of $DCFH_2$-DA and DHR123 oxidation

The optimum oxidation periods of $DCFH_2$-DA and DHR123 were assessed in respect to cytosolic and mitochondrial ROS/RNS respectively. H9C2 cells at 70-80% confluence were briefly washed with PBS and loaded with phenol red-free DMEM. To show the sensitivity of DHR123 towards peroxide radicals; 20µM $H_2O_2$ + horse radish peroxidase (HRP) solution was employed as a positive control. Peroxynitrite solution (60µM) was also employed to demonstrate the sensitivity of $DCFH_2$-DA for peroxynitrite anion radical. Cells were treated with 20µM $DCFH_2$-DA or 20µM DHR123 in the absence or presence of 40µM rotenone and incubated for 15min, 30min, 45min, and 60min. Then, fluorescence was measured after replacing the existing medium with fresh phenol red-free DMEM at 3min before the completion of incubation period. Both $DCFH_2$-DA and DHR123 showed time-dependent increases in fluorescence with rotenone treatment. In the presence of rotenone, both probes achieved optimum oxidation at t=45min **(Figure 3.2 A and 3.2B).**

In the positive control, $DCFH_2$-DA showed sensitivity for $ONOO^-$ with increase in fluorescence by 780±83% compared to controls (100±9%). DHR123 showed sensitivity for $H_2O_2$ with increase in fluorescence by 541±44% compared to controls (100±9%) in the presence of HRP only, confirming the requirement of the cofactor; HRP to reduce $H_2O_2$ (Hempel et al., 1999; Henderson and Chappell, 1993; Kooy et al., 1994; Royall and Ischiropoulos, 1993a).

### 3.3.1.3 Optimisation of conditions for the nitric oxide detector; DAF-2-DA

H9C2 cells were cultured in DMEM, 10% FBS under basal conditions. At 70-80% confluence, cells were briefly washed with PBS and loaded with phenol red-free DMEM. To determine the optimum oxidation period of DAF-2-DA, fluorescence was measured in the presence or absence of 40µM rotenone after incubating cells with 10µM DAF-2-DA for 60min, 45min, 30min, and 15min.

**(A)**

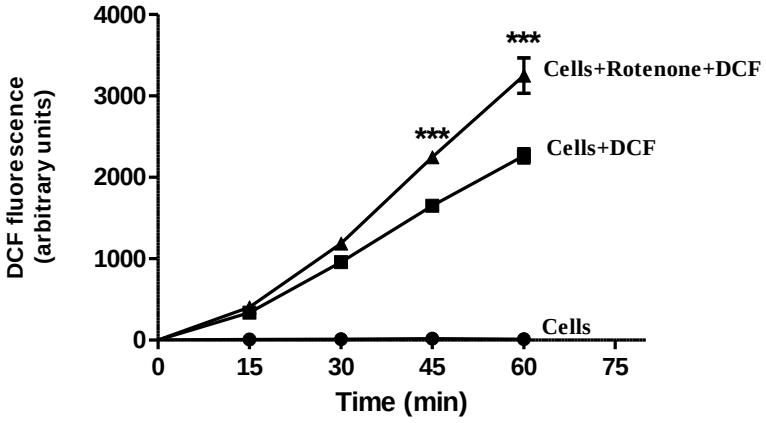


**(B)**

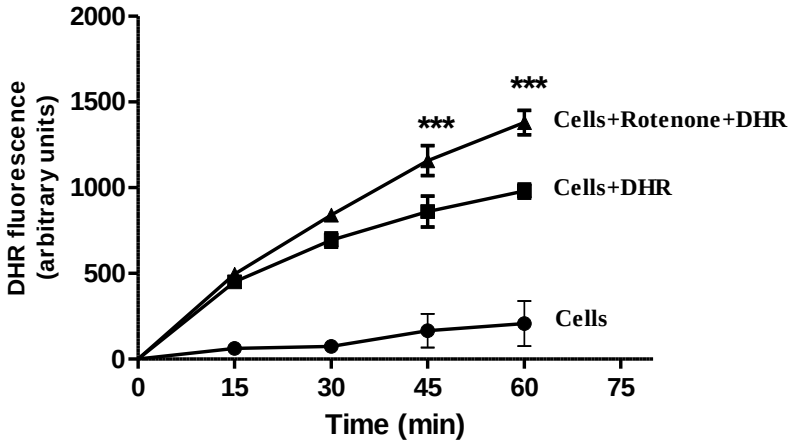


**Figure 3.2 Optimisation of conditions for (A) $DCFH_2$-DA and (B) DHR123 oxidation at different incubation times.** H9C2 cells were seeded at $3x10^4$/well and grown until 70-80% confluence at 37ºC in 5% $CO_2$ in humidified atmospheric conditions. Then, cells were washed with PBS, loaded with phenol red-free DMEM, and experimental cells were treated with 40µM rotenone. The fluorescence was measured after 60min, 45min, 30min and 15min incubations with 20µM $DCFH_2$-DA (A) or 20µM DHR123 (B) at 37ºC in a preheated GEMNI fluorescence reader at Excitation: 488nm, Emission: 520nm, cut off filter: 515nm. Data represents the mean±SEM fluorescence of three independent experiments conducted in triplicates. *** represent $P < 0.0001$, cells+DCF or DHR vs. cells+Rotenone+DCF or DHR (one-way ANOVA), Tukey's post-hoc test.

To minimise the background fluorescence, existing culture medium was replaced with fresh DMEM and plates were read after 3min before the completion of incubation period. A solution of 100µM spermine nonoate was employed as positive control to determine the DAF-2-DA

sensitivity for •NO. The DAF fluorescence was increased by 210±18% compared to control cells (100±8%) in the presence of spermine nonoate (100mM); •NO donor. As illustrated in **figure 3.3**, DAF-2-DA oxidation showed a time-dependent increase in fluorescence from t=0 min to 45min, but was not further increased at t=60min.

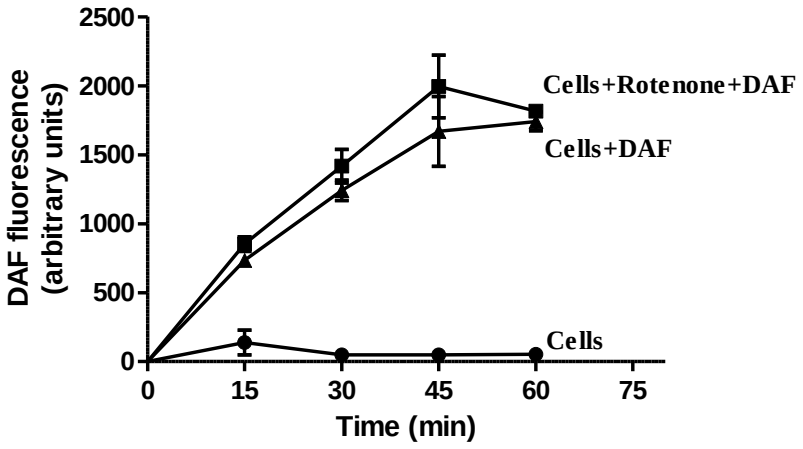


**Figure 3.3 DAF-2-DA oxidation at different incubation periods.** H9C2 cells were seeded at 3 x$10^4$/well and grown until 70-80% confluence at 37ºC in 5% $CO_2$ in humidified atmospheric conditions. Then, cells were washed with PBS and loaded with phenol red-free DMEM and experimental cells were treated with 40µM rotenone. The fluorescence was measured after 60min, 45min, 30min and 15min incubations with 20µM DAF-2-DA at 37ºC in a preheated GEMNI fluorescence reader at Excitation: 491nm, Emission: 513nm, cut off filter: 495nm. Data represents the mean±SEM fluorescence of three independent experiments conducted in triplicates.

### 3.3.2 Validation and optimisation of hypoxia chamber

Initial studies were performed to determine the stability of the hypoxic system i.e. whether it can maintain a stable hypoxic or normoxic environment. Therefore, dissolved $O_2$ level was determined after pre-equilibrating the medium (HEPES-buffered, phenol red-free) for 18h at 2% $O_2$ + 98 % $N_2$ and/or 10% $O_2$ + 90 % $N_2$ using premixed gas in the chamber. Control medium was preequilibrated at 21% $O_2$ + 79% $N_2$. Following equilibration, the dissolved $O_2$ level was routinely measured using the Winkler assay as previously described (Winkler, 1888; Grant & Griffiths, 2007) (Section 2.3.4.2).

After 18h, the dissolved $O_2$ concentration in the medium was 0.23±0.04mg/L ($pO_2$; 14.5 mmHg**)** at 2% $O_2$ + 98% $N_2$ which was a 26-fold decrease compared to $O_2$ concentration in the medium equilibrated under normoxia. The equilibration at 10% $O_2$ + 90% $N_2$ resulted in a 2-fold decrease in $O_2$ concentration compared to normoxic medium. The dissolved $O_2$ concentration in the medium at 10% $O_2$ was 2.78±0.77mg/L ($pO_2$; 72.4 mmHg**)**. The dissolved $O_2$ concentration in control medium (normoxia at 21% $O_2$) was measured as 5.93±0.23mg/L ($pO_2$; 152.2 mmHg**)** (**Figure 3.4**). As shown in **figure 3.4**, the dissolved $O_2$ level in the medium depleted dose-dependently with decreasing $O_2$ tension.

To assess the stability of pH value, pH was measured before and after hypoxia. The pH of the medium was stable during both normoxic (pH 7.4 ± 0.30) and hypoxic exposures (severe hypoxia; pH 7.5 ± 0.21 and mild hypoxia; pH 7.5 ± 0.23) up to 24h period. The results suggest that this system could render cells hypoxia by depleting dissolved $O_2$ concentration in the medium. This hypobaric chamber was adapted in subsequent experiments to induce hypoxia or normoxia.

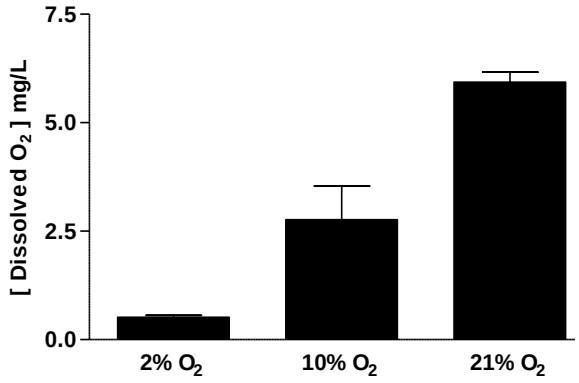


**Figure 3.4 The effect of hypobaric hypoxia on dissolved $O_2$ level in the medium.** HEPES buffered, phenol red-free DMEM were preequilibrated for 24h at different $O_2$ tensions; 2% $O_2$ + 98% $N_2$, 10% $O_2$ + 90% $N_2$ and 21% $O_2$ + 79% $N_2$ in the chamber. The dissolved $O_2$ level in the medium (1ml) was then measured by the Winkler assay. Data represents the mean±S.E.M of three independent experiments conducted in triplicate.

## 3.4 Discussion

### 3.4.1 Optimisation of fluorescent probes

Fluorescent probes are important for *in vivo* and *in vitro* biological research as they can provide unique spatial and temporal information about ROS/RNS molecules. The quantitative oxidation of a non-fluorescent probe to a fluorescent product reflects the amount of ROS/RNS oxidized intracellularly as previously explained (Tarpey and Fridovich, 2001; Tarpey et al., 2004). Therefore, the intensity of fluorescence is proportional to the amount of ROS/RNS generated in the cell (Gomes et al., 2005). However, this may reflect an over estimate of ROS/RNS produced intracellularly as probes can undergo autooxidation outside the cell (McArdle et al., 2005; Murrant et al., 1999). To minimise contribution of artefactual oxidation, experiments were conducted in the dark and old culture medium was always replaced with fresh medium to minimise background fluorescence prior to analysis (Murrant et al., 1999).

The methodology outlined in this thesis has avoided monitoring time-dependent kinetics of fluorescence as oxidised fluorescent products are susceptible to further excitation by the light intensity in the instrument (McArdle et al., 2005) and this results in poor fluorescent signal to noise ratio (Fennell and Baker, 2005). Therefore, the current protocol has been developed so that it uses a single exposure to light (under optimal excitation conditions) after completing the incubation periods; 15min, 30min, 45min and 60min at high signals to minimum fluorescent noise. Killilea et al. (2000) reported the influence of pH on the oxidation of fluorescent probe in the culture medium, therefore, HEPES-treated medium was employed to maintain a stable pH over incubation periods (Killilea et al., 2000).

According to other investigators**,** background fluorescence may reflect metal impurities in the medium (Wardman, 2007). The impurities in medium represents trace ions or catalyst, which can catalyse probe oxidation via Fenton reaction (Wardman, 2007). Principally, the mitochondrion is the major ROS/RNS generation site in many tissues and particular in muscle cells in respiration during normoxia (Jackson et al., 2002; Chandel et al., 1998 and 1997).

To evaluate the contribution of the mitochondrial electron transport system to produce ROS/RNS during normoxia, cells were treated with the mitochondrial complex I inhibitor; rotenone before adding the fluorescent detector probe. This method was adapted from Chandel et al. (1998). The pre-treatment of cells with rotenone mimics the hypoxic response under normoxia (Chandel et al., 1998). The optimal incubation time for a particular probe was assessed by considering stability of fluorescence and retention time of oxidised products in the cell before fluorescence decay in the presence or absence of rotenone.

The fluorescence probes that were examined showed an optimal oxidation either at 45min or 30min and subsequent experiments were applied accordingly. Zha et al. (2005) and (2003) suggested that DHE can only react with cellular $O_2^{-\bullet}$ forming 2-hydroxyethidium (2-OH-$E^+$), which has a distinct fluorescence spectrum of excitation at 490nm and emission at 570nm. Therefore, DHE fluorescence measurements were conducted according Zhao et al. (2005) and (2003). Dose response studies of DHE suggest that it does not react with singlet oxygen, hydroxyl radical, $H_2O_2$, $^{\bullet}NO$ and peroxynitrite (Fennell and Baker, 2005). There are other non-superoxide-dependent ways of oxidizing DHE into $E^+$ which is distinct from the fluorescence spectrum of 2-OH-$E^+$ and intercalates into nucleic acids (Zhao et al., 2005; Zhao et al., 2003). This study suggests that the decrease in DHE fluorescence after rotenone pre-treatment is an indication of decreased production of $O_2^{-\bullet}$ from mitochondrial complex I. It may be due to blockage of formation of ubisemiquinone by rotenone under normoxia (Duranteau et al., 1998). The decrease in DHE fluorescence after rotenone pre-treatment during normoxia is consistent with some, but not all previous reports (Chandel et al., 1998; Chandel and Schumacker, 1999).

It has been reported that $O_2^{-\bullet}$ and DHE reacts at a 1:1 molar ratio (Fennell and Baker, 2005). The total cellular fluorescence of DHE after incubation with cells for 45min may indicate not only $O_2^{-\bullet}$ production from the mitochondria, but also from other sources such as NADPH oxidase, xanthine oxidase and NOS system (Pagano et al., 1998; Souza et al., 2002; Pou et al., 1999).

DCF fluorescence at 45 min in normoxia assesses the cytosolic basal ROS and RNS production, whereas the fluorescence of DHR123 at 45min reports mitochondrial basal ROS/RNS production during normoxia. $DCFH_2$-DA and DHR123 showed their relative sensitivity for positive controls; $ONOO^-$ and $H_2O_2$ + HRP respectively and suggest the generation of those radicals during basal normoxic respiration. The increase in both DHR123 and $DCFH_2$-DA fluorescence in rotenone-treated cells suggests that overproduction of ROS/RNS is due to electron leak from mitochondria. The DCF fluorescence reflects the generation of $ONOO^-$ and probably, peroxy radicals via Fenton-type reaction in the presence of peroxidase enzymes in cytosol or/and readily available HOCl (Killilea et al., 2000; Hempel et al., 1999). In contrast, the increase in DHR123 fluorescence supports a change in mitochondrial redox state and/or increased production of ROS/RNS of mitochondrial origin.

It has been reported that rotenone increases the mitochondrial ROS generation by blocking complex I. When complex I is inhibited with rotenone, electrons may leak into the matrix and may be reduced chemically to form ROS/RNS resulting in the increase in DHR123 fluorescence (Chandel et al., 1998). $^{\bullet}NO$ generation during normoxia was demonstrated by using the DAF-2-DA probe under basal conditions.

The sensitivity of this probe for $^{\bullet}NO$ was confirmed by its reactivity towards the positive control; spermine nonoate, confirming previous reports (Gomes et al., 2005; Tarpey et al., 2004; Kojima et al., 1998). Total DAF fluorescence represents the cellular $^{\bullet}NO$ production during normal physiological conditions by mitochondria or/and cytosolic reactions (Kojima et al., 1998; Strijdom et al., 2006; Nakatsubo et al., 1998). The cell membrane and mitochondrial membrane are permeable to DAF-2-DA, and the probe can only be reactive with $^{\bullet}NO$ after it is hydrolysed to a reactive form; DAF-2, by intracellular esterases (Nakatsubo et al., 1998; Kojima et al., 1998). Extracellular probe cannot be oxidized by $^{\bullet}NO$, however it may subject to background fluorescence due to autooxidation of the probe.

Previous studies have adopted the variable incubation periods including 30min, 2h and 6h of fluorescent probes in cell systems (Abramov et al., 2007; Chandel et al., 1998), but the present system indicates the oxidation of fluorescent probe at its optimum level, precluding non-specific and autooxidation.

Fluorescent probes are often employed in fluorescence microscopy to monitor time dependent increase in fluorescence in specific cells or subcellular organelles with respect to ROS/RNS. Recently, it has been reported that laser exposure in fluorescence microscopy can induce photo-toxicity or affect quantitative fluorescent assessments due to photooxidation as previously reported by Abramov et al. (2007) and McArdle et al. (2005). Therefore, the quantification of ROS/RNS by microscopy may need reliable methods under low light excitation. Supporting this suggestion, in the present method, replacement of old medium with fresh medium has avoided detection of any leftover photoxidised/autoxidised dye in the extracellular medium, resulting in minimum background fluorescence.

Most investigators have omitted the method of minimising background fluorescence; instead they have followed continuous monitoring and kinetics of fluorescence (Abramov et al., 2007; Chandel et al., 1998; Chandel and Schumacker, 1999; Duranteau et al., 1998). In the present study, levels of fluorescence are not directly proportional between dyes, though; the stoichiometry of the reaction may be the same. This is evident with greater increase in fluorescence of some dyes more than another dye that has been exposed to same ROS/RNS. Cells respond to different probes in various ways and probes can leak by passive diffusion or rapidly by active efflux. The doses of probes employed in this thesis have been used by previous investigators (Becker et al., 1999; Zhao et al., 2003; Strijdom et al., 2006; Henderson and Chappell, 1993; Crow, 1997) and were found to be non-toxic.

This study has confirmed the generation of various ROS/RNS including $O_2^{-\bullet}$ and $^{\bullet}NO$ under normal physiological state as consistent with previous authors (Coral and Michael, 2001; Kudin et al., 2005; Ramachandran et al., 2002; Robinson et al., 2006).

The optimum incubation periods for each probe with H9C2 cells have been applied to the study of the time-dependent increase in ROS/RNS generation during hypoxia and hypoxia-reperfusion. The present study was aimed to adapt and optimise the use of probes to detect and quantify radicals in interest; $O_2^{-\bullet}$ or $^{\bullet}NO$ production in subsequent experiments during hypoxia and reperfusion in H9C2 cardiomyoblasts.

### 3.4.2 Hypoxic chamber

Hypoxic chambers should provide a continuous flow of a perfusing gas mixture in order to achieve a stable hypoxic environment (Killilea et al., 2000). The chamber developed in this study is highly versatile, cost-effective and simple to use. The gas exposure system can be used with different compositions of mixed gases (e.g. hyperoxia, anoxia and tobacco smoke) in addition to the gas mixtures used in this thesis. This system allows a convenient approach of simulating a variety of environmental conditions. The suitability of the gas exposure chamber was demonstrated by determining the different dissolved $O_2$ levels in hypoxic or normoxic culture medium during mild (10% $O_2$) and severe (2% $O_2$) hypoxia.

The main advantages of this hypoxic chamber are; (a) minimal gas consumption compared to larger glove box or hypoxic incubators; (b) maximum culture space for 2-4 tissue culture plates or two T75 cell culture flasks in a single chamber; (c) fast recovery time and easy manual operation for conducting an experiment; (d) easy disassembly for cleaning; (e) an ability to resist high gas flow rates. The present study has determined the dissolved $O_2$ concentration in hypoxic or normoxic-culture medium using the Winkler assay which has been modified to minimise incorporation of air.

Further validation studies proved the maintenance of a stable pH range (7.5±0.21) as measured by pH electrode (Appleton Woods, UK) under hypoxic or normoxic incubation periods; 30min and 4h. Therefore, these data confirm that changes in fluorescence were not affected by pH gradients established during hypoxia or normoxia and they are due to different $O_2$ tensions established in culture medium. Since the completion of these studies, more advanced and accurate methods to monitor dissolved $O_2$ and pH at the same time have become available such as the hydrogel micro array system, and such systems could have advantage for future studies to provide real time measurements (Lee et al., 2008). In summary, the present study describes a system that could permit convenient evaluation of ROS/RNS under a variety of environmental conditions using premixed gases, including hypoxia and reperfusion, in H9C2 cardiomyoblasts without a substantial investment of resources compared with other commercial chambers.

# CHAPTER 4

# HYPOXIA-INDUCED ROS/RNS GENERATION

## 4.1 Preface

This chapter examines ROS/RNS generation from cardiomyoblasts during hypoxia compared to basal ROS production. The hypoxia-induced ROS generation depends on the amount of $O_2^{-\bullet}$ produced from various sources. Therefore, global $O_2^{-\bullet}$ generation was assessed by DHE fluorescent probe and visualised in live cells under confocal microscopy. The selective oxidation of DHE probe and basal $O_2^{-\bullet}$ level were determined in the presence of superoxide dismutase mimetic; MnTBAP. During chronic, severe hypoxia, the contribution of mitochondria, NADPH oxidase complex, xanthine oxidase and NOS isoforms as $O_2^{-\bullet}$ producers were assessed in the presence of inhibitors and uncouplers.

## 4.2 Introduction

### 4.2.1 The production of $O_2^{-\bullet}$ during hypoxia

$O_2^{\bullet-}$ generation during hypoxia alone and hypoxia-reperfusion or ischaemia-reperfusion have been widely studied, however, associated mechanisms of toxicity or survival in cardiac cells have not been clearly established. The $O_2^{-\bullet}$ is an important precursor signalling molecule which can dismutate to $H_2O_2$ in the presence of SOD or spontaneously at a slower rate at physiological pH or reacts with $^{\bullet}NO$ to produce $ONOO^-$. Both $ONOO^-$ and $H_2O_2$ are signal transduction molecules and play a vital role in the maintenance of vascular homeostasis and pathogenesis. According to Griendling et al. (2000), $O_2^{-\bullet}$ and $H_2O_2$ are the most important signalling molecules in the cardiovascular system. However, the large scale accumulation of $O_2^{-\bullet}$ during hypoxia can have deleterious effects, leading to irreversible cardiac damage. Hypoxia can enhance $O_2^{\bullet-}$ generation in muscle cells, especially cardiac myocytes (Vanden Hoek et al., 1997; Becker et al., 1999). An increase in ROS generation from cardiomyocytes during ischaemia appears to be paradoxical as the molecular $O_2$ needed to be reduced is in low abundance and this can reduce ATP production. It is evident that ischaemia alone can trigger cardiac cell injury without reperfusion as described in previous reports (Vanden Hoek et al., 1997), but can also afford benefit, if the ischaemic period is short, i.e. ischaemic preconditioning. Therefore, understanding the role of $O_2^{\bullet-}$ production during severe hypoxia is vitally important and may have clinical implications for design of interventions that improve cell survival during and after ischaemia (Becker et al., 1999).

The antioxidants 2-mercaptopropionyl glycine and 1.10-phenanthroline added to culture medium during the ischaemia in cardiomyocytes attenuated oxidant generation, increased cell viability, and improved return of contraction after ischaemia or reperfusion (Vanden Hoek et al., 1997). Abramov et al. (2007) described an increase in ROS generation under the condition of reversed electron flow with less available $O_2$ that depends on mitochondrial membrane potential differences ($\Delta\Psi_m$). The electron flux through the ETS, coupled to proton pumps from the matrix normally maintains the mitochondrial membrane potentials (Murphy, 2009).

Therefore, an inhibition of electron transport system should decrease the proton pumps, resulting in depolarization of the mitochondrial inner membrane. During hypoxia, NADH in complex I becomes increasingly reduced, driving electrons to $O_2$, and leading to loss of $\Delta\Psi_m$ (Levraut et al., 2003). Mitochondrial uncouplers can decrease membrane potentials and reduce $O_2^{\bullet-}$ production as a protective measure.

To support this hypothesis, partial mitochondrial uncoupling with a low dose of FCCP (Carbonyl cyanide 4 - (trifluoromethoxy) phenylhydrazone) significantly improved post-ischaemic recovery of rat hearts via a ROS-dependent pathway (Brennan et al., 2006b; Brennan et al., 2006a). Within the hypoxic heart, mitochondria are likely to be the main source of ROS in muscle cells (Vassilopoulos and Papazafiri, 2005; Turrens, 1997; Suleiman et al., 2001). Other sources such as the NADPH oxidase complex in vascular cells (Souza et al., 2002) or xanthine oxidase in endothelial cells, pulmonary cells and neuronal cells can generate $O_2^{\bullet-}$ (Pearlstein et al., 2002; Abramov et al., 2007; Becker et al., 1999; Becker, 2004a). Moreover, NOS isoforms also can produce $O_2^{\bullet-}$ and $H_2O_2$ when L-arginine substrate is limited in supply (Pou et al., 1999). However, the relative contribution of aforementioned sources for $O_2^{\bullet-}$ production during hypoxia alone in cardiomyocytes has not been clearly established.

### 4.2.2 The production of RNS during hypoxia

Nitric oxide ($^{\bullet}NO$) is a unique biological messenger molecule with various effects in cells and cellular organelles such as mitochondria, including maintenance of mitochondrial integrity and defence during hypoxia. It has been reported that formation of $ONOO^-$ in the presence of $^{\bullet}NO$ and $O_2^{-\bullet}$, can activate protein kinase C (PKC), down regulate $K_{ATP}$ channels and induce release of cytochrome *c* from mitochondrial complex IV, thereby inducing caspase-3 activation. During hypoxia, $^{\bullet}NO$ generation is dependent on the degree of activity of NOS isoforms present in cytosol and mitochondria. Three isoforms of NOS are present in most cell types; the constitutive endothelial (eNOS) and neuronal (nNOS) isoforms, and the inducible (iNOS) isoform (Beckman and Koppenol, 1996; Pou et al., 1999; Porasuphatana et al., 2003).

Zanella et al. (2002) reported the presence of the three isoforms of mtNOS ( eNOS, nNOS and iNOS) in mitochondria of H9C2 rat myoblasts. It has been reported that mitochondrial NOS are constitutively expressed and they can be functionally up-regulated when cells are exposed to hypoxia (Lacza et al., 2001; Lacza et al., 2006). During hypoxia, an increase in [$Ca^{2+}$] in the cytoplasm or mitochondria can activate eNOS to produce $^{\bullet}$NO (Lacaza et al., 2001). Therefore, the increase in $^{\bullet}$NO production is likely to be associated with eNOS activation in both cytosol and mitochondria. During normoxia, a low level of NOS activity was suggested to be a constitutive feature in mitochondria (Lacza et al., 2001). However, the expression of NOS isoforms in mitochondria is still under debate (Lacza et al., 2006).

The baseline $^{\bullet}$NO production in cardiac microvascular endothelial cells is eNOS-dependent and endothelial cells produce more $^{\bullet}$NO than ventricular cardiomyocytes during normoxic respiration, demonstrating that eNOS activity is different between cardiac microvascular endothelial cells and ventricular cardiomyocytes (Strijdom et al., 2006). In contrast, Strijdom et al. (2006) demonstrated iNOS induction occurs in ventricular cardiomyocytes to produce $^{\bullet}$NO, but not in microvascular endothelial cells during hypoxia. Hypoxia pre-exposure increases iNOS mRNA expression in myocardial cells and protects against subsequent damage from a second prolonged hypoxia. Lacaza et al. (2006) have suggested that rat heart mitochondria produce RNS via the respiratory chain rather than through an arginine-dependent mtNOS.

This supports earlier findings of Zweier et al. (1999) who reported the generation of $^{\bullet}$NO from a non-enzymatic pathway. Overall, the impact of $^{\bullet}$NO accumulation during hypoxia is not yet clearly established. Therefore, the effect of $^{\bullet}$NO on cell viability after exposure to hypoxia has been investigated using specific and non-specific NOS inhibitors and other metabolic inhibitors alone and with the RNS-sensitive fluorescent probe, DAF-2-DA.

## 4.3 Results

### 4.3.1 Chronic, severe hypoxia significantly increased $O_2^{-\bullet}$ production in H9C2 cardiomyoblasts.

H9C2 cells were cultured in DMEM, 10% FBS under basal conditions and at 70-80% confluence, cells were washed briefly with PBS and loaded with $O_2$ preequilibrated (2% $O_2$, 10% $O_2$ and 21% $O_2$ in independent experiments), HEPES buffered, phenol red-free DMEM.

To determine $O_2^{-\bullet}$ generation during 30min and 4h under severe (2% $O_2$ + 98% $N_2$) and mild hypoxic (10%$O_2$ + 90% $N_2$) conditions, cells were treated with 20µM DHE and incubated in the hypoxic chamber as described in methods (Sections : 2.3.9.1).

DHE oxidation was determined at different times (30min or 4h) and $O_2$ tension (2%, 10% and 21% $O_2$) to characterise $O_2^{-\bullet}$ production during hypoxia. As illustrated in **figure 4.1A**, there was no significant increase in $O_2^{-\bullet}$ production during acute, severe or mild hypoxia compared to normoxia. However, the increase in DHE oxidation (123.47±5.84% of normoxia control, $P<0.001$, 4h) during chronic, severe hypoxia compared to normoxia (100±3.66%; 4h) or mild hypoxia suggests a significant increase in $O_2^{-\bullet}$ production during chronic, severe hypoxia (see **Table 4.1** for summary of results).

To find out the specificity of DHE fluorescence for $O_2^{-\bullet}$ detection during hypoxia, cells were treated with 50µM MnTBAP prior to adding 20µM DHE. As shown in **figure 4.1B**, MnTBAP significantly reduced DHE fluorescence in hypoxia and normoxia cultured cells. The fluorescence of DHE in cells treated with MnTBAP was not different between hypoxia and normoxia indicating the selective oxidation of DHE probe with $O_2^{-\bullet}$ during hypoxia. MnTBAP treatment significantly reduced the DHE fluorescence in normoxic controls indicating a basal level of $O_2^{-\bullet}$ production under normoxia.

**(A)**

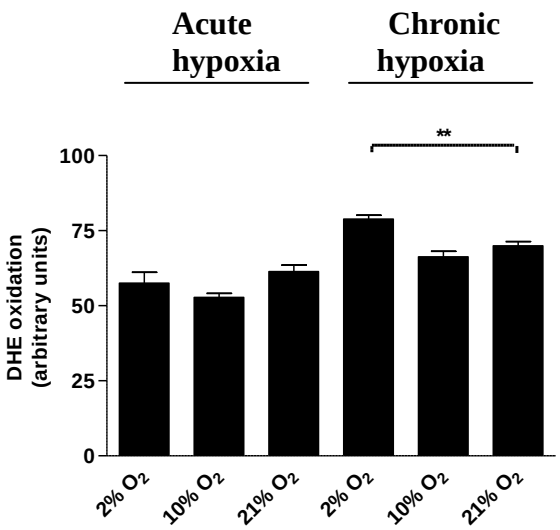


**(B)**

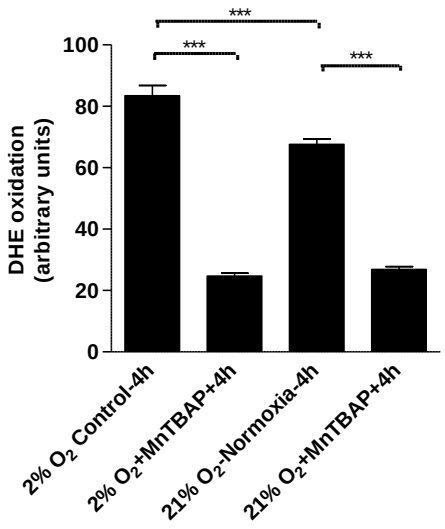


**Figure 4.1 $O_2^{-\bullet}$ production during mild and severe hypoxia for 30min and 4h.** Cells were cultured for 48h in culture medium and were loaded with $O_2$ equilibrated HEPES buffered-phenol red-free DMEM (2% or 10% or 21% $O_2$) after 3 x PBS washes. Experimental cells were exposed to hypoxia after treating cells with 20µM DHE, 45min prior to completion of 4h hypoxia and adding probe at t=0 for 30min hypoxia studies (A). Controls were maintained at normoxia (21% $O_2$). Negative control cells were treated with 50µM MnTBAP 45min prior to complete 4h hypoxia or normoxia (B). After replacing the culture medium, fluorescence was measured at 37°C in Spectramax GEMINI EM fluorescence reader at Excitation: 488nm, Emission: 570nm and cut off filter: 560nm. Data represent the mean±SEM fluorescence of three independent experiments conducted in triplicates. ** represent $P < 0.001$ and *** represent P <0.0001 (one-way ANOVA), Tukey's post-hoc test.

#### 4.3.1.2 Live cell imaging of $O_2^{-\bullet}$ generation during acute and chronic, severe hypoxia

In order to confirm that $O_2^{-\bullet}$ production is intracellular, real-time imaging of cardiomyocytes was undertaken under varying degrees of hypoxia and time (Section: 2.3.10). As visualized in **figure 4.2B**, confocal microscopy images show stronger signals of DHE fluorescence during chronic, severe hypoxia compared to chronic, mild hypoxia and normoxia (**Figure 4.2D & 4.2F**). The intensity of DHE fluorescence signals was weaker in confocal images obtained during acute, severe or mild hypoxia compared to normoxia (**Figure 4.2A, 4.2C and 4.2E**) and is consistent with quantitative fluorescent measurements **(Figure 4.1A).**

#### 4.3.1.3 Effects of respiratory chain inhibition, uncoupling and inhibition of NADPH oxidase complex during mild and severe hypoxia

To identify whether mitochondrial $O_2^{-\bullet}$ is generated during hypoxia, the effects of H9C2 incubation with mitochondrial complex I inhibitor; rotenone and the respiratory chain uncoupler; FCCP during chronic, severe hypoxia were investigated. Cardiacmyoblasts are reported to generate $O_2^{-\bullet}$ via NOX and to investigate any possible contribution of the NOX-dependent respiratory burst to $O_2^{-\bullet}$ generation during chronic, severe hypoxia, the inhibitor apocynin was included. Then fluorescence was measured after adding 20µM DHE in the presence of inhibitors during hypoxia as previously explained in section 2.3.12.

In the presence of FCCP, DHE oxidation was increased significantly during acute, severe hypoxia and acute, mild hypoxia compared to untreated cells **(Figure 4.3A and 4.3B)**. However, in the presence of rotenone, DHE fluorescence was significantly increased during acute, severe hypoxia (30min; 2% $O_2$), but not acute, mild hypoxia **(Figure 4.3A and 4.3B)**. The presence of either rotenone or FCCP reduced DHE oxidation significantly (~10% decrease) due to chronic, severe hypoxia (**Figure 4.3D**), suggesting the involvement of mitochondrial complex I in $O_2^{-\bullet}$ production during severe hypoxia. However, only rotenone, but not FCCP or apocynin was able to attenuate DHE fluorescence significantly during chronic, mild hypoxia **(Figure 4.3E)**.

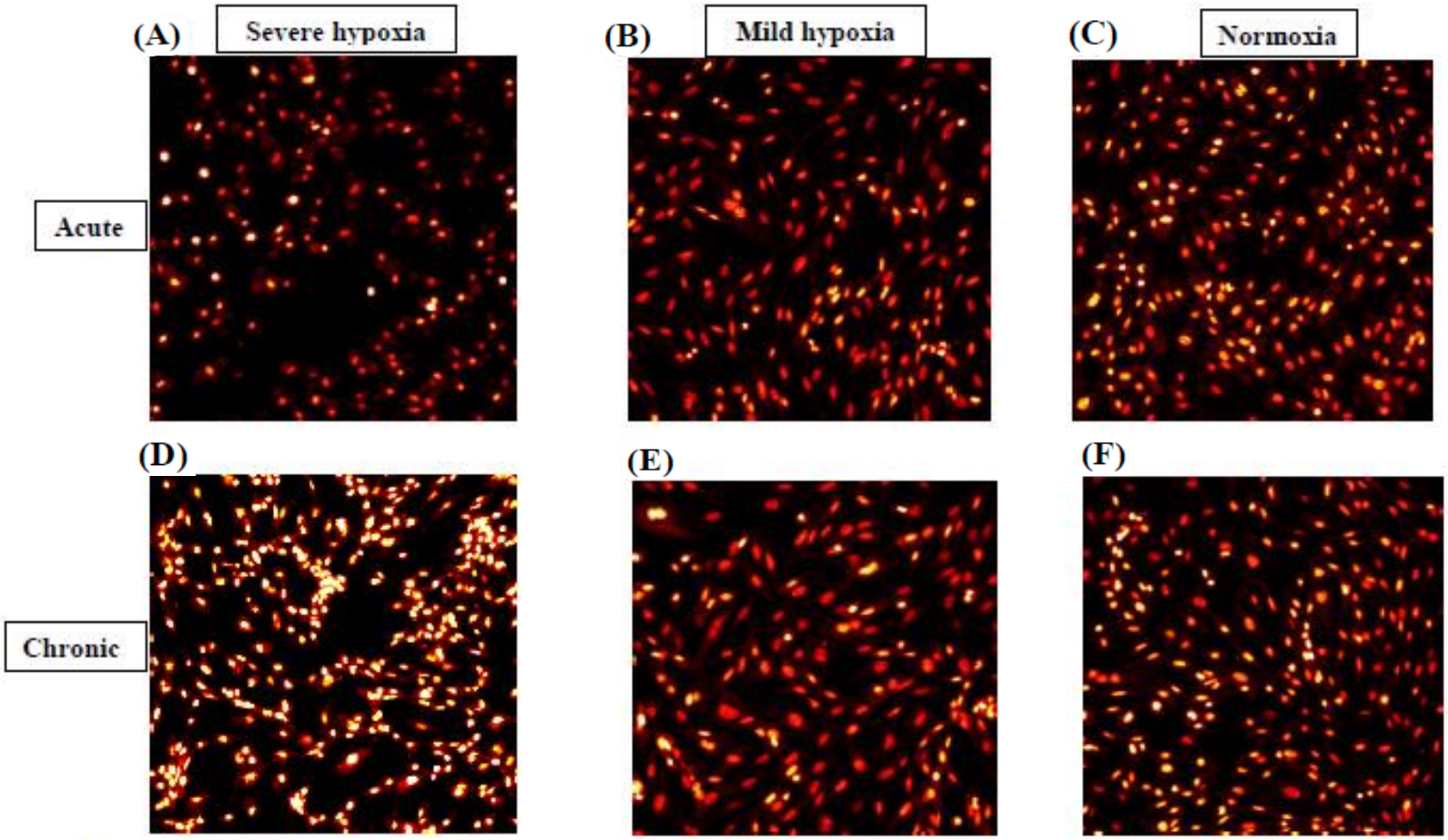


**Figure 4.2 Live fluorescence images showing $O_2^{\cdot-}$ generation during acute (30min) and chronic (4h).** Cells were cultured in microscopic chambers for 48h in culture medium and then loaded with $O_2$ equilibrated HEPES buffered-phenol red-free DMEM (2% or 10% or 21% $O_2$) after 3 x PBS washes. The experimental cells were exposed to hypoxia (2% $O_2$ and 10% $O_2$) whereas controls at normoxia (21% $O_2$). Cells were treated with 20μM DHE, 45min prior to completion of 4h hypoxia and probe was added at t=0 for 30min hypoxia studies. After completing hypoxic incubations, sealed chambers were mounted on the platform of the confocal microscope and cell images were taken by setting up the fluorescence excitation at 488nm and emission at 570nm. Acute and chronic hypoxia at 2% $O_2$ (A), 10% $O_2$ (B) and 21% $O_2$ (C) images were shown as magnification 20x. The images were shown as glow scale in which bright glow yellow indicates the oxidised form of DHE.

The mitochondrial uncoupler, FCCP, the inhibitor of the respiratory chain (rotenone) and apocynin had no effect on DHE oxidation under normoxic conditions after 4h of treatment **(Figure 4.3F**) (see **Table 4.1** for summary of results).

### 4.3.2 Chronic, mild and severe hypoxia significantly increased $^{\bullet}$NO production

H9C2 cells were cultured in DMEM, 10% FBS under basal conditions and at 70-80% confluence, cells were washed briefly with PBS and loaded with $O_2$ preequilibrated (2% $O_2$ and 10% $O_2$), HEPES buffered, phenol red-free DMEM. To determine $^{\bullet}$NO generation during 30min and 4h under severe (2% $O_2$ + 98% $N_2$) and mild hypoxic (10% $O_2$ + 90% $N_2$) conditions, cells were treated with 10µM DAF-2-DA at t=0min and incubated for 30min for acute hypoxia (severe and mild) and 4h for chronic hypoxia (severe and mild) in the chamber (See section: 2.3.91).

The same procedure was applied to normoxic controls at 21% $O_2$ + 79% $N_2$**.** Before measurement of the fluorescence, the old culture medium was replaced with $O_2$-preequilibrated DMEM at t=27min for acute hypoxic cultures and t=3h and 57min for chronic hypoxic cultures. Then, fluorescence was measured at t=30min (for acute hypoxia) and t=4h (for chronic hypoxia)**.**

As illustrated in **figure 4.4**, there was no significant increase in $^{\bullet}$NO production during acute, mild or severe hypoxia compared to normoxia. However, the DAF fluorescence was significantly increased during chronic, mild, (132.12±25.64% vs. 100% control, P<0.0001) and severe hypoxia (183.75±27.33% vs. 100% control, P<0.0001), compared to normoxia (see **Table 4.1** for summary of results).

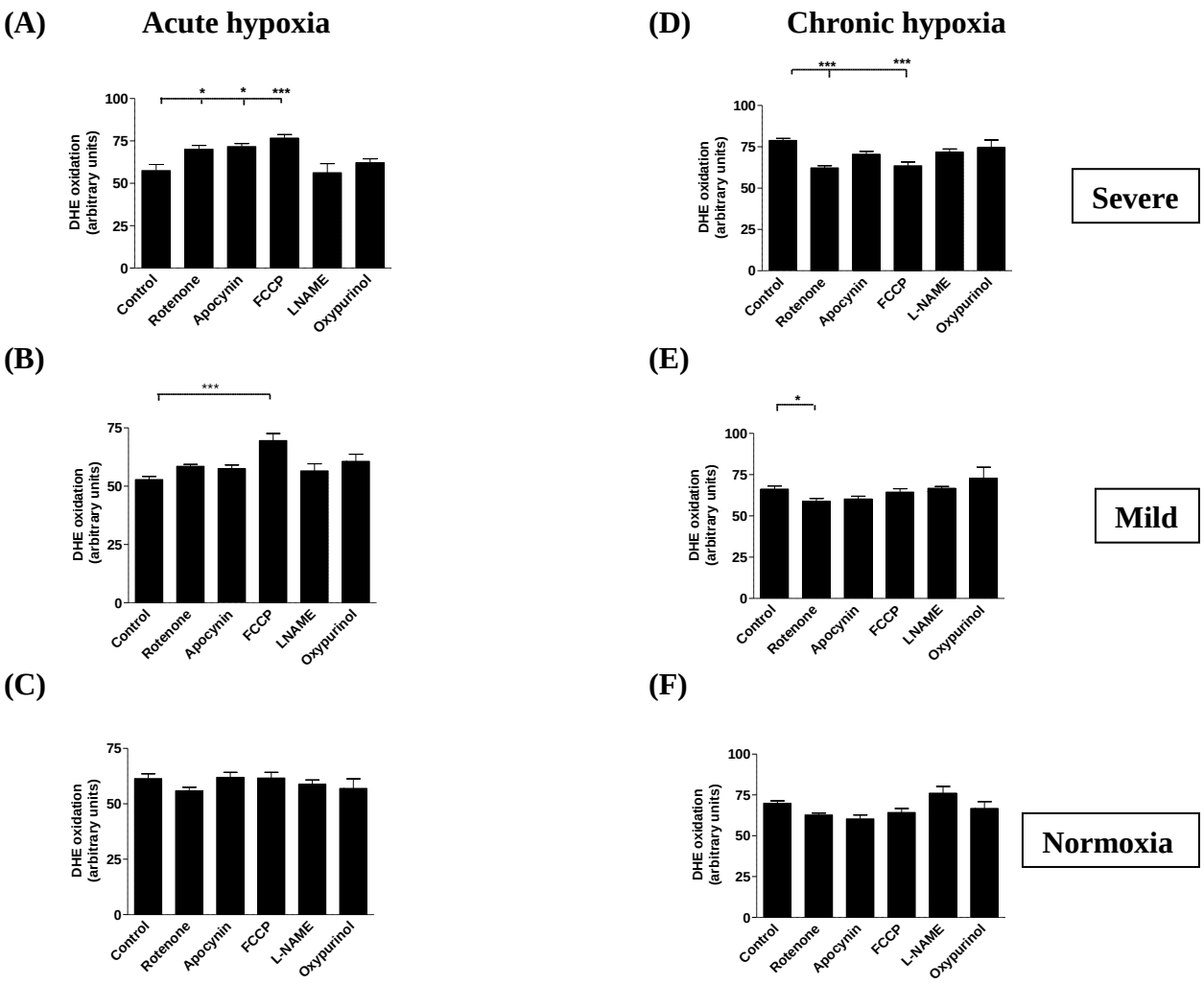


**Figure 4.3 Effects of mitochondrial uncouplers and inhibitors of the respiratory chain and respiratory burst on $O_2^{-\bullet}$ generation during chronic hypoxia in cardiomyoblasts.** H9C2 cells (3 x $10^4$/well) were cultured to 80% confluence, were washed three times with PBS and loaded with oxygen equilibrated HEPES buffered-phenol red-free DMEM (2%, 10% or 2% $O_2$). Cells were treated with and without 20µM rotenone, 100 µM apocynin, 1µM FCCP, 100µM L-NAME, 20µM Oxypurinol or vehicle control at t= -2min. DHE (20µM) was added at t= 0min for acute hypoxia; 2% $O_2$ (A),10% $O_2$ (B) and 21% $O_2$ (C), whereas for chronic, severe hypoxia; 2% $O_2$ (A),10% $O_2$ (B) and 21% $O_2$ (C), DHE (20µM) was added at t=3h 15min. At 30min or 4h, fluorescence was measured at 37°C using a microplate reader determining fluorescence at Excitation: 488nm, Emission: 570nm, cut off filter: 560nm and data are expressed in arbitrary units. Data represent the mean ± SEM fluorescence of three independent experiments conducted in triplicates. * represents $P < 0.05$, *** for $P<0.0001$ (one-way ANOVA), Tukey's post-hoc test.

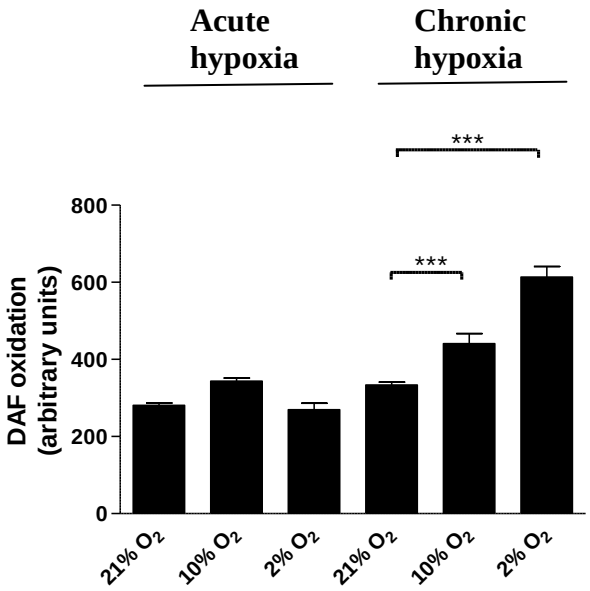


**Figure 4.4 $^{\bullet}$NO production during mild and severe hypoxia for acute (30min) and chronic (4h).** Cells were cultured for 48h in culture medium and were loaded with $O_2$ equilibrated HEPES buffered-phenol red-free DMEM (2% or 10% or 21% $O_2$) after 3 x PBS washes. Then, experimental cells were exposed to hypoxia whereas controls were maintained at normoxia (21% $O_2$). Cells were treated with 10µM DAF-2-DA, 45min prior to completion of 4h hypoxia and probe was added at t= 0 for 30min hypoxia studies. After replacing the culture medium, fluorescence was measured at 37°C in Spectramax GEMINI EM fluorescence reader at Excitation: 491nm, Emission: 513nm. Data represent the mean±SEM fluorescence of three independent experiments conducted in triplicates. *** represent hypoxia vs. controls represent $P < 0.0001$ (one-way ANOVA), Tukey's post-hoc test.

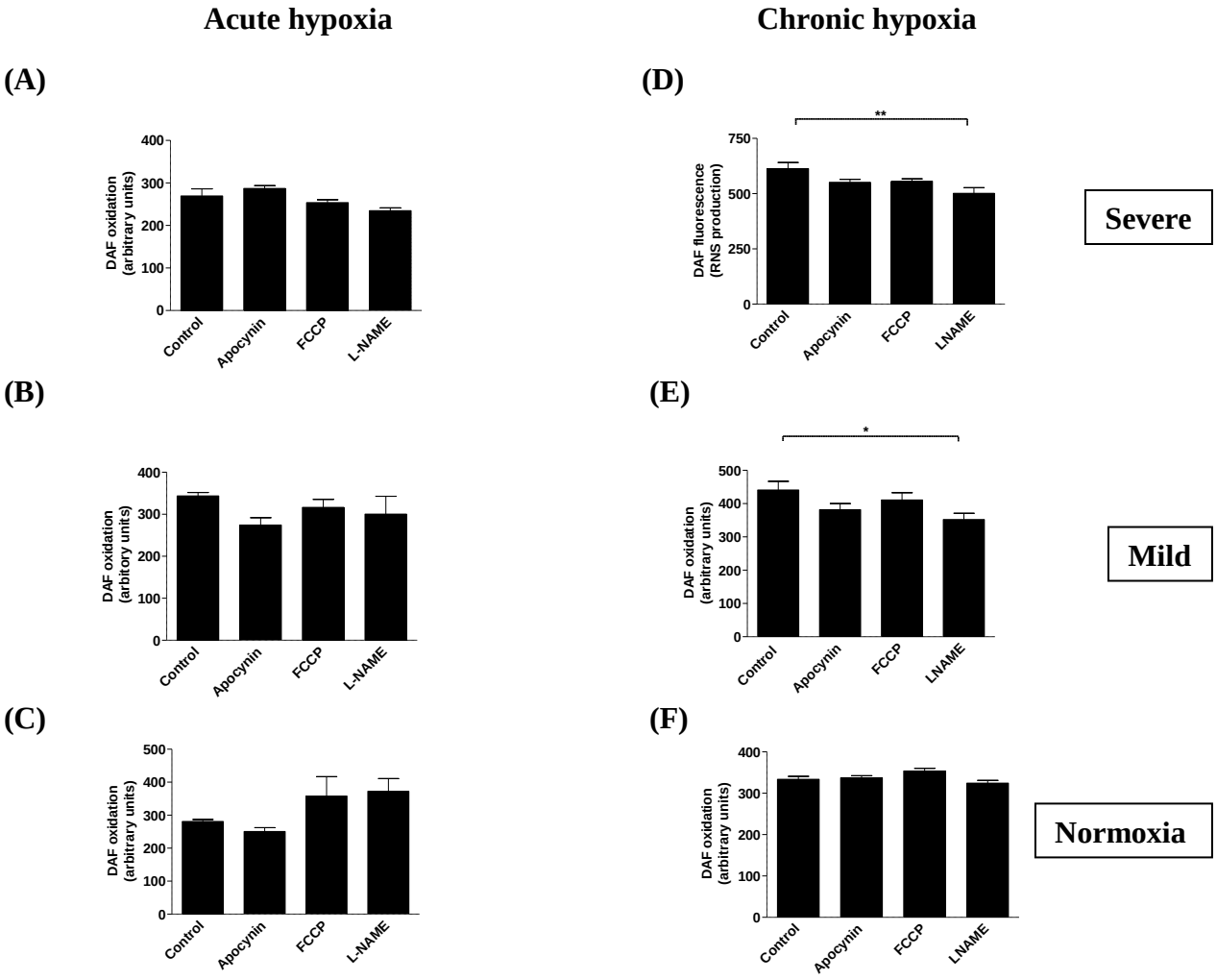


**Figure 4.5 Effects of mitochondrial uncouplers and inhibitors of the respiratory chain on $^{\bullet}$NO generation during severe hypoxia in cardiomyoblasts.** H9C2 cells (3 x $10^4$/well) were cultured to 80% confluence, were washed three times with PBS and loaded with $O_2$ equilibrated HEPES buffered-phenol red-free DMEM. Cells were treated with or without 20µM rotenone, 1µM FCCP, 100 µM L-NAME, or vehicle control at t= -2min for all time points and DAF-2-DA (10µM) was added at t=0 min for 30min hypoxia; 21% (A) 10% (B) or 2% $O_2$ (C) whereas dye was added at t= 3h.15min for 4h hypoxia; 21% (D), 10% (E) or 2% (F) $O_2$. At 30min and 4h, fluorescence was measured at 37°C using a microplate reader determining fluorescence at Excitation: 491nm, Emission: 513nm, cut off filter; 495nm and data are expressed in arbitrary units. Data represent the mean ± SEM fluorescence of three independent experiments conducted in triplicates. * represents $P < 0.05$ and ** represent $P<0.001$ (one-way ANOVA), Tukey's post-hoc test.

### 4.3.2.1 The effect of respiratory uncoupler, L-NAME and inhibition of NADPH oxidase complex on $^{\bullet}NO$ production during mild or severe hypoxia

To identify whether NOS-dependent $^{\bullet}NO$ generation occurs during hypoxia, the effect of H9C2 incubation with the non-selective NOS inhibitor; L-NAME on DAF-2-DA oxidation, was examined during acute and chronic hypoxia (Section 2.3.12). Cardiac myoblasts are reported to generate $O_2^{-\bullet}$ and $^{\bullet}NO$, therefore may form $ONOO^-$ after reaction with $O_2^{-\bullet}$ and $^{\bullet}NO$ at 1: 1 ratio (Jiao et al., 2009). Therefore, the contribution of $O_2^{-\bullet}$ production from NADPH oxidase to modulate DAF fluorescence was investigated during hypoxia, by inhibiting NADPH oxidase complex with 100µM apocynin.

Similarly, the contribution of mitochondrial based $O_2^{-\bullet}$ to form DAF fluorescence during hypoxia was assessed by uncoupling respiratory chain with 1µM FCCP. In the presence of L-NAME, FCCP or apocynin, DAF-2-DA oxidation was not changed significantly during acute, severe or mild hypoxia or normoxia compared to untreated cells (**Figure 4.5A, 4.5B and 4.5C**). However, in the presence of L-NAME, DAF-2-DA oxidation was significantly reduced during chronic, mild hypoxia (79.9±1.8%, $P<0.0001$) and chronic, severe hypoxia (81.8%±2.5%, $P<0.0001$) compared to untreated cells of control, but not with FCCP or apocynin treatment (**Figure 4.5D, E and F**) (see **Table 4.1** for summary of results).

### 4.3.2.2 Live cell imaging of $^{\bullet}NO$ generation during acute and chronic, severe hypoxia

In order to confirm that DAF-2 oxidation is intracellular, real time imaging of cardiomyoblasts was undertaken under chronic, severe hypoxia and normoxia as described in section 2.3.10. As visualised in **figure 4.6A**, confocal microscopy images show stronger signals of DAF fluorescence during chronic, severe hypoxia compared to normoxia (**Figure 4.6B**). Moreover, single cell imaging with DAF showed a concentrated fluorescence at the centre of the cell as visualised in **figure 4.6C**.

**(A)**

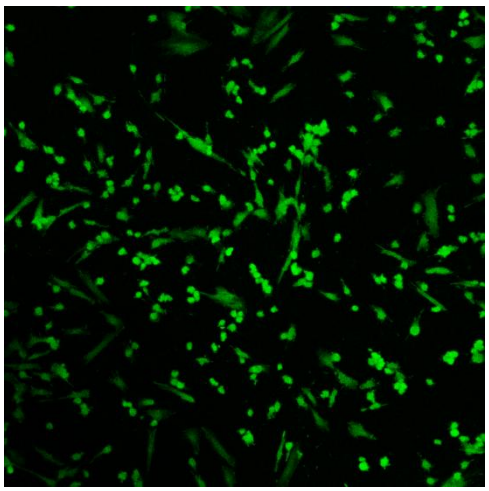

**(B)**

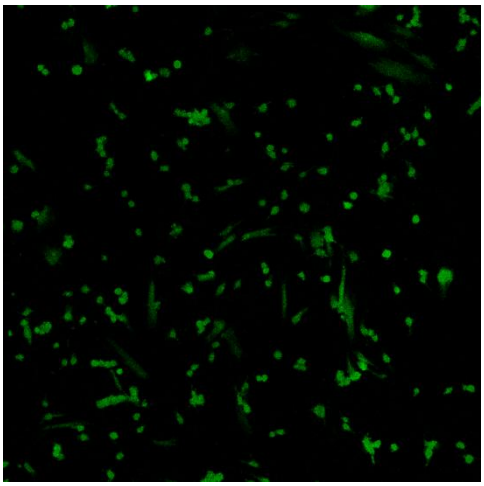

**(C)**

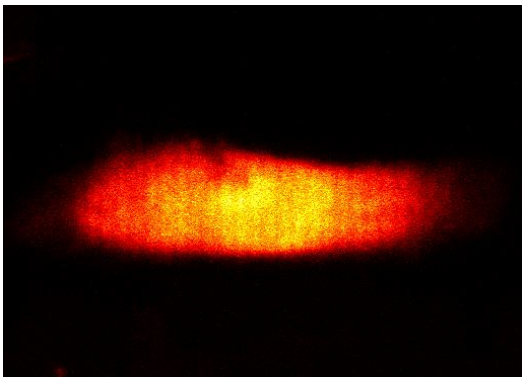

**Figure 4.6 Live fluorescence images showing $^{\bullet}$NO generation during chronic, severe hypoxia vs. normoxia.** Cells were cultured in slide chambers for 48h in culture medium and then loaded with $O_2$ equilibrated HEPES buffered-phenol red-free DMEM (2% or 21% $O_2$) after 3 x PBS washes. The experimental cells were exposed to chronic, severe hypoxia (2% $O_2$) whereas controls were maintained at normoxia (21% $O_2$). Cells were treated with 10µM DAF-2-DA, 45min prior to completion of 4h hypoxia. After completing hypoxic incubations, sealed chambers were mounted on the platform of the confocal microscope and cell images were taken at the fluorescence excitation at 480-490nm and emission at 510-520nm. (A) Chronic, severe hypoxia at 2% $O_2$, magnification 20x (B) normoxia at 21% $O_2$, magnification 10x and (C) DAF fluorescence from a single cell (Colour palette - glow yellow for DAF fluorescence).

## 4.4 Discussion

### 4.4.1 Superoxide generation during hypoxia

In summary, the present study demonstrates that mitochondria are the main site of $O_2^{-\bullet}$ generation in hypoxic cardiomyocytes. Other potential sources of ROS generation sites such as NADPH oxidase, NOS isoforms and xanthine oxidase do not contribute to global $O_2^{-\bullet}$ production during both acute and severe hypoxia. In the current cellular model, the respiratory chain can function optimal at 10% $O_2$ compared to hyperoxic stress-induced cells at 21% $O_2$. Severe hypoxic stress (2% $O_2$) in cardiomyocytes causes $O_2^{-\bullet}$ production (see **Figure 4.7** and **Table 4.1**).

The physiology of cells exposed to low levels of $O_2$ (1-3% $O_2$ hypoxia) is different from that of cells exposed to 0% $O_2$ (anoxia) and 21% $O_2$ (normoxia) (Chandel et al., 2005). ROS are important signalling molecules for adaptive response in cardiomyocytes as previously documented (Duranteau et al., 1998). Increased levels of ROS production during hypoxia, but not anoxia stabilise the transcription factor, HIF-1α (Chandel et al., 1998; Chandel and Schumacker, 1999). To confirm the production of $O_2^{-\bullet}$ in H9C2 cells during 2% $O_2$ hypoxia in the present model system, this study describes the systematic, time and dose-dependent kinetics of $O_2^{-\bullet}$ generation as DHE oxidation during hypoxia in rat cardiomyoblasts. The cell culture system established in this study mimics a physiological ischaemic period through pre-incubation of media (in the absence of FBS and L-glutamine) for 18h under reduced partial $O_2$ pressure and results in 14.5 mmHg in media under 2% $O_2$.

This work confirms that hypoxia causes significant changes in $O_2^{-\bullet}$ generation from mitochondria in cardiomyoblasts during severe, chronic hypoxia as measured by DHE oxidation. In the presence of the superoxide dismutate mimetic, MnTBAP $O_2^{-\bullet}$ production was significantly decreased which suggests the selective oxidation of DHE by $O_2^{-\bullet}$ **(Figure 4.1B)**. However, it is not clear why endogenous SOD in cardiomyoblasts does not completely scavenge $O_2^{-\bullet}$ to dismutate it to $H_2O_2$ during normoxia.

This may indicate either that; (1) endogenous SOD is removed from the site of ROS production but DHE is available; and/or (2) that cells can tolerate lower $O_2^{-\bullet}$ production due to respiratory chain leakage without upregulation of SOD at the given level. Other investigators have suggested that an increase in $O_2^{-\bullet}$ during hypoxia is associated with loss of membrane potentials ($\Delta\Psi_m$) in mitochondria and results in the further leak of electrons to reduce $O_2$ (Abramov et al., 2007; Millar et al., 2007). However, the data obtained in cardiomyocytes reported here suggests only limited generation of $O_2^{-\bullet}$ during acute, severe hypoxia and agrees with previous authors, possibly reflecting the sudden drop of $O_2$ supply at early time points (Vanden Hoek et al., 1997). This could be due to loss of $\Delta\Psi_m$ and accumulation of $O_2^{-\bullet}$ in the mitochondrial compartments that makes DHE less oxidized during early time points (Hool et al., 2005) as further observed in confocal images (**Figure 4.2A**) of acute hypoxia. Moreover, during hypoxia, a decrease in $O_2$ availability may reduce the rate of electron flow through the system, resulting in a slower rate of $O_2^{-\bullet}$ production, even than the normoxic cells.

Waypa and Schumacker, (2005) observed a decrease in $O_2^{-\bullet}$ generation during severe hypoxia in pulmonary vasoconstriction and suggested this was due to the availability of $O_2$ substrate in the medium. However, in Waypa and Schumacker's, system of *in vivo* pulmonary vasoconstriction, partial $O_2$ pressure ($pO_2$) is less than 60mmHg in arteries (Longmore et al., 2001) where the system tested here is much more hypoxic with $pO_2$ at 14.5mmHg. Hool et al. (2005) reported a 40% significant decrease in DHE fluorescence in ventricular cardiomyocytes during hypoxia at $pO_2$ of 15mmHg compared to normoxia (100%, 30min). This is very similar, except Hool et al. (2005) used HEPES treated-hypoxic buffer system where the present system used HEPES treated-DMEM medium. Other sources of ROS generation such as NADPH oxidase, xanthine oxidase and NOS isoforms have been reported in the intact heart (Porasuphatana et al., 2003; Souza et al., 2002; Li and Jackson, 2002). Xanthine oxidase (XO) is active in neurones (Abramov et al., 2007) and endothelial cells during ischaemia or hypoxia respectively and produces ROS, but the importance of this enzyme in cardiomyocytes, is unclear, and some workers have reported absence of xanthine oxidase in chick cardiomyocytes (Becker et al., 1999).

Preliminary studies with oxypurinol, an XO inhibitor did not reduce hypoxia induced DHE oxidation (data not shown) and this suggests that XO is unlikely to generate ROS. Generation of $O_2^{-\bullet}$ from NADPH oxidase complex has been reported (Touyz, 2008; Ushio-Fukai et al., 2002). However, the present study with apocynin did not cause a significant reduction in DHE oxidation in cardiomyoblasts, implying a lack of NADPH oxidase-dependent $O_2^{-\bullet}$ production during chronic, severe or mild hypoxia (**Figures 4.5D, 4.5E** and **Table 4.1**).

Nevertheless, such sources may contribute to produce $O_2^{-\bullet}$ during reperfusion period (Abramov et al., 2007; Dodd-O and Pearse, 2000; Becker et al., 1999; Elisabetta et al., 2008). Three distinct isoforms of NOS (eNOS, iNOS and nNOS) are reported in rat myoblasts (Zanella et al., 2002). The inhibition of NOS isoforms with L-NAME did not reduce DHE oxidation as a measure of $O_2^{-\bullet}$ production, suggesting that NOS isoforms are not participating in $O_2^{-\bullet}$ production during hypoxia. The effect of FCCP on the ETS is not clear; however, it is assumed that the hydrophobicity of FCCP may allow diffusion into the mitochondrial matrix where disassociation of protons into the matrix would dissipate the proton gradient and would result in the collapse of $\Delta\Psi_m$.

Rotenone inhibits the NADH dehydrogenase enzyme present in mitochondrial complex I, resulting in a decrease in NADH reduction which leads to loss of membrane potential in the absence of electron flux through ETS. An increase in mitochondrial $O_2^{-\bullet}$ generation during acute, severe hypoxia is associated with the collapse of mitochondrial membrane potentials in the presence of FCCP or blockage of NADH oxidation at complex I in the presence of rotenone. Though, the similar effects could occur in normoxia, those effects may have led to a change in the oxidation state (NADH: $NAD^+$ ratio) during acute, severe hypoxia and resulted in increase of $O_2^{-\bullet}$ production (Abramov et al., 2007; Millar et al., 2007; Tahara et al., 2009). Moreover, uncoupling of mitochondria during acute, severe hypoxia allows the reducing equivalents that have been accumulated through the compromised respiratory chain to be discharged via electron leakage. Collectively, this enables the dissipation of reducing equivalents more readily (Abramov et al., 2007) (**Figure 4.7**).

Increased DHE fluorescence in the presence of apocynin indicates the activation of NOX complex via an unknown mechanism as H9C2 cardiomyoblasts are non-phagocytic cells as reported (Vejrazka et al., 2005; Touyz, 2008). Chronic, severe hypoxia caused a significant increase in $O_2^{-\bullet}$ confirming many other reports (Li and Jackson, 2002; Vanden Hoek et al., 1998; Abramov et al., 2007), but this was not observed in chronic, mild hypoxia.

When the cells were exposed to severe hypoxia, electron flow may be reversed through the ETS whilst the membranes are being depolarised under limiting $O_2$ supply facilitating electron loss through complex I. When the mitochondrion is at rest during normoxic respiration, $\Delta\Psi_m$ provides the driving force for ATP synthesis and is generated by electron flow through the ETS from NADH or $FADH_2$ (**Figure 4.7**). The mitochondrial membrane potential depends on the protons being pumped into mitochondrial intermembrane space. This is dissipated by the protons flowing back to couple with the membrane bound ATP synthase (complex V) along with pH gradients between intermembrane space and matrix. Therefore, the membrane potential reflects the balance between the rate of electron transport and the rate of ATP synthesis by the mitochondrion. Therefore, a loss of membrane potential in chronic, severe hypoxia would reduced the oxidation of NADH in complex I and $FADH_2$ in complex II and result accumulation of more reducing equivalents. To support this hypothesis, Abramov et al. (2007) explained the reverse flow of electrons through the mitochondrial ETS with the accumulation of reducing equivalents during ischaemia. Reverse flow of electron in mitochondrial electron transport system may indicate as an adaptive response to recover mitochondrial membrane potentials during severe hypoxia.

However, during low $O_2$ tension, reverse electron flow may have led to greater electron leak to produce $O_2^{-\bullet}$ within the mitochondrial matrix, offering an explanation for the data in current study. Moreover, mitochondrial ROS generation depends on the ratio of $NADH/NAD^+$. Therefore, accumulation of more reducing equivalents, especially, more NADH may result in an increase in the $NADH/NAD^+$ ratio. In support of this hypothesis, other investigators reported the significant increase in NADH concentrations in cells under severe hypoxia may create a more reductive environment in the mitochondria (Schumacker et al., 1993; Murphy, 2009).

The increase in NADH concentration is suggested to be an enzymatic adaptation when cells are exposed to prolonged hypoxia for 1-2h (Chandel et al., 1995). Therefore, accumulation of reduced intermediates in the mitochondrial electron transport system (ETS) would potentially support the leaking of electrons for $O_2^{-\bullet}$ generation. The major site of $O_2^{-\bullet}$ generation during severe hypoxia is the mitochondrion according to the current study.

Mitochondrial complex I inhibition (rotenone) significantly attenuated DHE oxidation, indicating mitochondrial electron transport significantly contributes to $O_2^{-\bullet}$ production during chronic, severe hypoxia (**Figure 4.7**). An increase in $O_2^{-\bullet}$ in the presence of complex I inhibitor during acute, severe hypoxia may reflect the rapid leak of electrons to produce $O_2^{-\bullet}$, though there is no apparent increase in $O_2^{-\bullet}$ production in control cells under acute, severe hypoxia. During chronic, severe hypoxia, loss of voltage potentials of cytochrome oxidase should increase the reduction state of mitochondrial electron carriers upstream of cytochrome oxidase including the ubisemiquinone site of complex III. Therefore, this may increase the lifetime of reduced electron carriers (i.e: ubisemiquinone) and thereby, would increase the generation of $O_2^{-\bullet}$ via univalent electron transfer to $O_2$ in the mitochondria (Chandel and Schumacker, 2000; Chandel et al., 2000). The mitochondrial complex I inhibition is upstream to the ubisemiquinone site; suggesting that complex I is the chief site where the ETS is blocked during hypoxia, causing significant increase in $O_2^{-\bullet}$ production. This is consistent with previous authors who carried out studies with site-specific inhibitors (Duranteau et al., 1998; Chandel et al., 1998; Chandel et al., 2000).

It is difficult to understand how mitochondria can alter its redox state due to changes in extracellular $O_2$ tensions. "Peri-mitochondrial" $pO_2$ can be much lower than the extracellular $O_2$ tension due to the difference in $O_2$ concentration gradient between the plasma membrane and mitochondrial membrane (Chandel et al., 2000). The H9C2 cultured cells used in this investigation have been maintained and adapted to 21% $O_2$ during routine culture over many passages (cells were used between 14-18 passages for this study) and are therefore expected to have adapted to living under high $O_2$ tension.

This may have some impact on the levels of antioxidant enzymes (i.e.; Mn-SOD and GSH) present and therefore the cells ability to withstand ROS. Cells studied under 10% $O_2$ do not exhibit any significant change in $O_2^{-\bullet}$ production compared to 21% $O_2$ (**Figures 4.2B, 4.2E and 4.1A**), suggesting the optimal level of respiration at 10% $O_2$.

The presence of MnTBAP significantly decreased DHE oxidation as a measure of $O_2^{-\bullet}$ production during normoxia. Interestingly, MnTBAP treatment did not take DHE fluorescence to zero, suggesting autofluorescence was elicited under the conditions employed at 2% and 21%$O_2$. Co-incubation of cells with FCCP during acute, mild hypoxia (10%; 30min) did increase the steady state level of $O_2^{-\bullet}$ as seen with cells exposed to acute, severe hypoxia. This may reflect the fact that the respiratory chain is optimal at 10% $O_2$ and disruption of a highly efficient metabolic process has catastrophic effects on the cells by increasing $O_2^{-\bullet}$. Since the completion of these studies, highly selective and mitochondrial specific probes are available for detecting $O_2^{-\bullet}$ in the cells or solution based systems and could have an advantage for future studies to provide real time measurements in mitochondrial-specific $O_2^{-\bullet}$ generation. The characterisation of mitochondrial $O_2^{-\bullet}$ production using fluorescence microscopy has clear advantages over cell-based system with inhibitors such as they are less time consuming with exquisite precision and minimal impact on cell viability and function (Mukhopadhyay et al., 2007).

### 4.4.2 $^{\bullet}$NO generation during hypoxia

In summary, the significant increase in DAF fluorescence during chronic normoxia indicates $^{\bullet}$NO production partly dependent on NOS, but also probably from non-enzymatic sources (**Figure 4.7**).

It has been widely accepted that hypoxia can trigger $^{\bullet}$NO generation intracellularly in various cell lines and *in vivo* models. $^{\bullet}$NO has been implicated as a signalling molecule which may modulate cardiomyocyte death during ischaemia/reperfusion with the dysfunction of mitochondrial respiration (Beckman and Koppenol, 1996; Brown, 1999; Borutaite and Brown, 2005).

Moreover, •NO has been associated with the protection against ischaemic cell death (Rakhit et al., 2000). Therefore, the majority of reports suggest that •NO may play a role between cell death and survival, that may be dependent on level of •NO production and duration of exposure.

The present study outlines how the duration and severity of hypoxia contributes to generation of •NO. Many authors have reported an increase in •NO production during hypoxia or ischaemia for 30min and 3h in various cell lines, including cardiac myocytes (Zweier et al., 1995; Strijdom et al., 2006). The present data did not indicate the significant production of •NO during acute, mild or severe hypoxia. Intracellular •NO is produced by NOS isoforms through oxidation of L-arginine to L-citrulline in the presence of available $O_2$ and by non-enzymatic sources (Zweier et al., 1999). Two moles of $O_2$ and 1.5mol of NADPH are required to produce one mole of •NO (Lepore, 2000; Von Bohlen und Halbach, 2003). Both, chronic, mild and severe hypoxia significantly increased •NO production as shown by an increase in DAF fluorescence. However, in the presence of L-NAME, the decrease in DAF fluorescence (~20%) during chronic, mild and severe hypoxia suggests that •NO generation is at least partly NOS-dependent via the L-arginine pathway.

Supporting this evidence, Strijdom et al. (2006) showed a significant decrease in •NO production during hypoxia for 3h, when cardiac microvessel endothelial cells and ventricular cardiomyocytes rat were pre-treated with L-NAME. In contrast, there are reports that suggest the generation of •NO from non-enzymatic sources such as nitrites in rat hearts during ischaemia (Zweier et al., 1999) using EPR spectroscopy, to measure •NO generation from rat hearts perfused with ischaemic bicarbonate buffer solution. Therefore, it is presumed that non-enzymatic sources such as cellular nitrite stores or ETS are available or activated during hypoxia to generate •NO/RNS and their contribution is greater than NOS-dependent •NO generation. In support of this hypothesis, arbitrary value ~300 for •NO during normoxia (4h) indicates the oxidation of DAF with •NO generated from cellular nitrite stores under unstimulated conditions.

Lacza et al. (2001) and Zenebe et al. (2007) reported an increased activity of mtNOS to produce $^{\bullet}$NO during hypoxia or hypoxia/reperfusion. Lacza, et al. (2001) demonstrated increased expression of eNOS in rats exposed to chronic hypoxia, whereas Zenebe et al. (2007) reported increased mtNOS activity to generate $^{\bullet}$NO when cardiomyocytes were exposed to anoxia; 100% $N_2$. It is evident in the present study that; the $^{\bullet}$NO production during chronic, severe or mild hypoxia is partly NOS-dependent. However, it is difficult to explain the involvement of mt-NOS to produce $^{\bullet}$NO in the current hypoxic model. Failure of apocynin treatment to curtail DAF fluorescence during chronic, severe hypoxia indicates that intracellular $ONOO^-$ production is independent of NOX-dependent superoxide production.

The uncoupling of mitochondrial ETS and mitochondrial depolarization with FCCP did not have any effect on $^{\bullet}$NO generation during acute or chronic mild hypoxia, suggesting that $^{\bullet}$NO generation is independent from the mitochondrial uncoupling and depolarization. DAF-2-DA was developed as a $^{\bullet}$NO-detection probe (Kojima et al., 1998; Nakatsubo et al., 1998), and its specificity for $^{\bullet}$NO has since been confirmed in a variety of cell types (Leikert et al., 2001; Lebuffe et al., 2003; Tiscornia et al., 2009) by validating results with other widely used indicators of $^{\bullet}$NO production (Failli et al., 2001; Havenga et al., 2001).

However, there are other reports, which describe selectivity of DAF-2-DA for $ONOO^-$ (Jourd'heuil, 2002; Peyrot and Ducrocq, 2007). Therefore, it is hard to exclude the possibility that $ONOO^-$ contributed to changes in DAF-2-DA fluorescence in the present study, although the relative contribution of $ONOO^-$ cannot be determined under current experimental conditions. There are a number of unresolved questions regarding the performance of these probes in biological systems that affect their utility in culture systems and targets of $^{\bullet}$NO at intracellular level. The present study aimed to adapt and optimize the use of DAF-2-DA to detect and quantify $^{\bullet}$NO production in hypoxia and reperfusion systems in which H9C2 cardiomyoblasts are grown in HEPES-treated culture medium.

**(A)**

| Condition | Acute, severe hypoxia (2% $O_2$, 30min) | | | | | Acute, mild hypoxia (10% $O_2$, 30min) | | | | | Acute normoxia (21% $O_2$, 30min) | | | | |
|---|---|---|---|---|---|---|---|---|---|---|---|---|---|---|---|
| **Inhibitors** | **Ctl** | **ROT** | **FCP** | **APO** | **LNM** | **Ctl** | **ROT** | **FCP** | **APO** | **LNM** | **Ctl** | **ROT** | **FCP** | **APO** | **LNM** |
| $O_2^{\cdot-}$ | X | ↑ | ↑ | ↑ | X | X | X | ↑ | X | X | X | X | X | X | X |
| $^{\cdot}NO$ | X | - | X | X | X | X | - | X | X | X | X | - | X | X | X |

**(B)**

| Condition | Chronic, severe hypoxia (2% $O_2$, 4h) | | | | | Chronic, mild hypoxia (10% $O_2$ ,4h) | | | | | Chronic normoxia (21% $O_2$, 4h) | | | | |
|---|---|---|---|---|---|---|---|---|---|---|---|---|---|---|---|
| **Inhibitors** | **Ctl** | **ROT** | **FCP** | **APO** | **LNM** | **Ctl** | **ROT** | **FCP** | **APO** | **LNM** | **Ctl** | **ROT** | **FCP** | **APO** | **LNM** |
| $O_2^{\cdot-}$ | ↑* | ↓ | ↓ | X | X | X* | X | X | X | X | X | X | X | X | X |
| $^{\cdot}NO$ | ↑* | X | X | X | ↓ | ↑* | X | X | X | ↓ | X | X | X | X | X |

**Table 4.1 Summary of results in acute (A) and chronic (B) hypoxia.**

**Key:** Ctl - control, ROT-rotenone, FCP- FCCP, APO- apocynin and LNM- L-NAME.

↑* - Significant increase in control cells (2% $O_2$ or 10% $O_2$) vs. normoxic control cells.

↓* - Significant decrease in control cells (2% $O_2$ or 10% $O_2$) vs. normoxic control cells.

↑ - Significant increase in treated cells vs. control cells at same $O_2$ tension.

↓ - Significant decrease in treated cells vs. control cells at same $O_2$ tension.

X - In treated cells, no significant difference vs. control cells at same $O_2$ tension or if in control cells (2% $O_2$ or 10% $O_2$), no significant difference vs. normoxic cells or in normoxic cell shows the basal effect.

\- Not available.

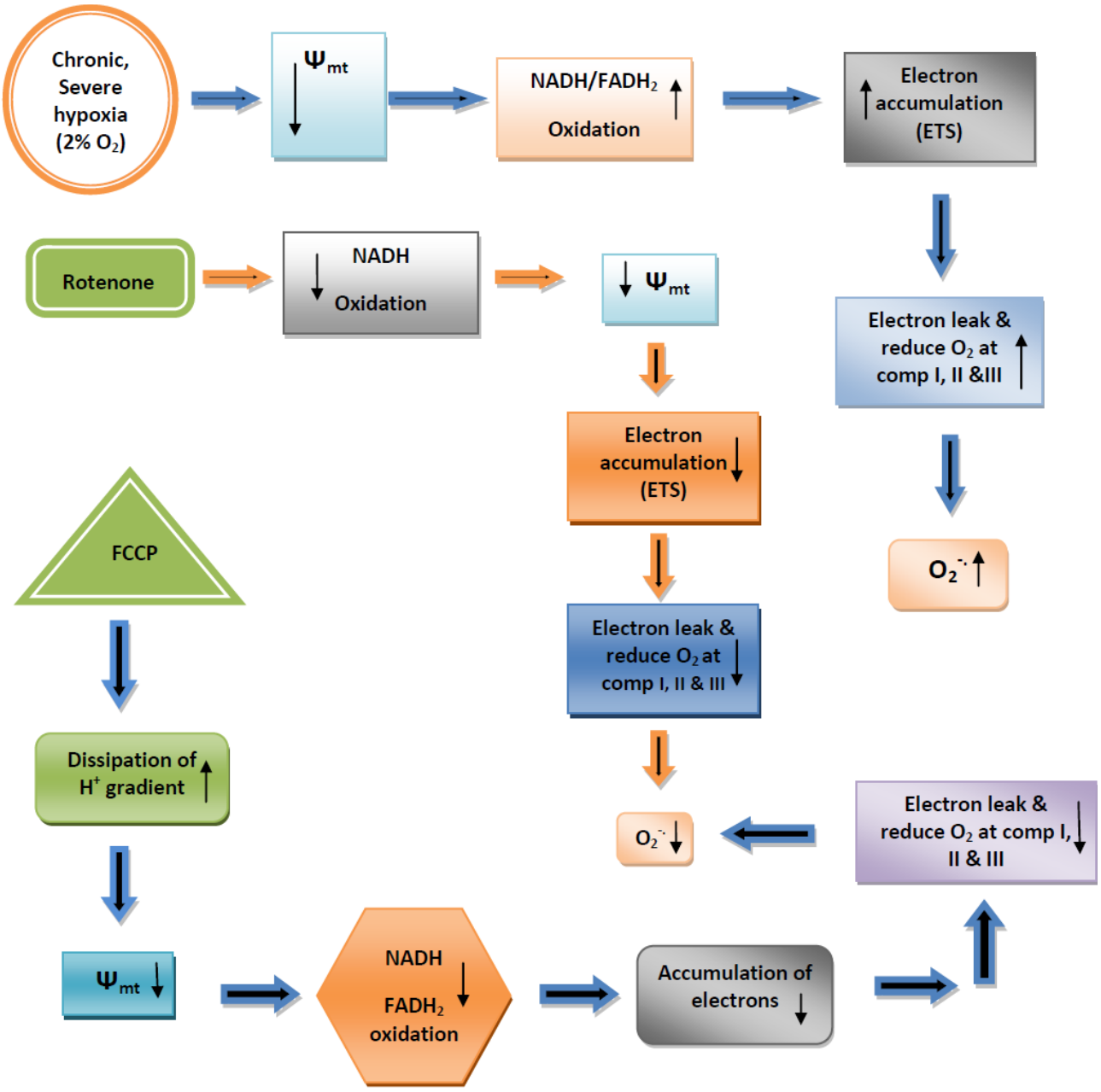


**Figure 4.7 Schematic diagram to represent effect of rotenone and FCCP on $O_2^{\cdot-}$ production during chronic, severe hypoxia. ↑ - increase or ↓ - decrease.**

# CHAPTER 5

# HYPOXIA-INDUCED CELL DEATH

## 5.1 Preface

The overproduction of $O_2^{-\bullet}$ during hypoxia may contribute to cell death via necrosis or apoptosis. This chapter examines hypoxia-induced cell death during acute and chronic, mild and severe hypoxia compared to normoxic cell viability with respect to mitochondrial metabolic activity, necrosis and apoptosis. Quantitative necrotic cell death was assessed as PI uptake by damaged cells and nuclear morphology of necrotic or late apoptotic cells was further characterised by fluorescence microscopy. Apoptosis is initiated by proteolytic cleavage of procaspase-3 during hypoxia. The quantitative measurement of procaspase-3 cleavage (the large fragment of cleaved caspase-3) was normalised to loading control; α-tubulin and assessed as the ratio between cleaved caspase-3 and procaspase-3. Mitochondrial metabolic activity during hypoxia was assessed as mitochondrial SDH activity. The contribution of ROS/RNS from mitochondria, NADPH oxidase and NOS isoforms, and $Ca^{2+}$ flux to cell death via necrosis or apoptosis and the role of NF-κB activation in these processes were investigated. The kinetics of hypoxia-induced protein carbonylation and ATP depletion and their association with cell death were analysed.

## 5.2 Introduction

### 5.2.1 Hypoxia-induced cell death

ROS and RNS generation and associated oxidative/nitrosative stress leads to irreversible cell damage during hypoxia (Murphy, 2009; Brown and Borutaite, 2007). It has been reported that exposure of hypoxic cells to reoxygenation may result in exacerbated cell death compared to that seen with than hypoxia alone in many cells (Abramov et al., 2007; Kawahara et al., 2006; Chen et al., 1998). The amount of irreversible or reversible cell damage induced by hypoxia may depend on the severity, type of tissue and duration of hypoxia. There are at least two major forms of cell death, apoptosis and necrosis that are linked to over production of ROS during hypoxia (Crompton, 1999). Cellular necrosis is associated with prolonged anoxia or severe hypoxia; however, this is dependent on the type of cells in the myocardium, their cellular metabolic rate and the intrinsic adaptive mechanism of the tissues (Adrain and Martin, 2001; Bialik et al., 1999; Bromme and Holtz, 1996; Crow et al., 2004).

Previous investigators have reported the appearance of apoptosis as caspase-3 activation at 30min and DNA fragmentation at 60min in the ischaemic myocardium after a coronary occlusion without reperfusion in rat heart (Borutaite and Brown, 2003). Levrand et al. (2006) reported an increase in apoptosis and necrosis in ventricular cardiomyocytes due to increased production of $ONOO^-$ during 2h reperfusion after 2h coronary occlusion. Cellular necrosis inevitably follows prolonged anoxia/ischaemia or chronic, severe hypoxia in which $O_2$ supply is decreased relative to metabolic demand for ATP production in many tissues including cardiomyocytes (McCord, 1985). Cells undergo necrosis instead of apoptosis in the absence of ATP that is required for the activation of proapototic factors (Zhao., 2004; Eguchi et al., 1997; Tatsumi et al., 2003; Lieberthal et al., 1998). Several studies have shown that mitochondria play an important role in apoptosis during hypoxia (Chen et al., 2002; Bonavita et al., 2003). However, the interplay between mitochondrial reactive species; $^{\bullet}NO$, ROS, $ONOO^-$, and apoptosis during hypoxia is not well understood.

Overproduction of ROS and increased [$Ca^{2+}$] is known to trigger cell death cascades in cardiomyocytes (Hajnóczky et al., 2006; Yamawaki et al., 2004; Chen et al., 2002). Moreover, both intracellular $Ca^{2+}$ overload and ROS play a role in modulation of contractility of cardiomyocytes through phosphorylation of PKC, which may then involve in ischaemic contractile dysfunction (Wang et al., 2001; Liao et al., 2002). An increase in mitochondrial $Ca^{2+}$ overload, depletion of ATP in cardiomyocytes and activation of glutamate receptors in neurons trigger cell injury during ischaemia and ischaemia/reperfusion (Crow et al., 2004; Tsujimoto and Shimizu, 2007; Eguchi et al., 1997; Crompton, 1999; Abramov et al., 2007).

It has been reported that over-production of ROS during hypoxia or ischaemia/reperfusion leads to depolarisation and loss of mitochondrial membrane potentials (Crompton, 1999; Levraut et al., 2003; Banki et al., 1999; Yamawaki et al., 2004). Also an increase in intracellular [$Ca^{2+}$] has been reported in cardiomyocytes during hypoxia (Crompton, 1999; Levraut et al., 2003; Li and Jackson, 2002). It has been reported that an imbalance exists between $Ca^{2+}$ influx by passive diffusion and $Ca^{2+}$ efflux to the cytosol from the mitochondria through the mitochondrial permeability transition pores (MPTP), which results in an increase in [$Ca^{2+}$] in the cytoplasm. $Ca^{2+}$ concentration becomes high in the mitochondrial matrix. Eventually, opening of the MPTP causes mitochondrial swelling due to water influx as a result of the imbalance between solute concentrations in the mitochondrial matrix and the cytosol (Gottleb, 2003; Crompton, 1999). Consequently, this swelling in turn causes the rupture of mitochondrial membranes and release of pro-apoptotic factors such as cytochrome *c* and apoptosis-inducing factor (AIF) (Crompton, 1999).

Activation of procaspase-3 is necessary to induce the apoptotic cascade. The inactive form of caspase-3 is known as procaspase-3 (35kDa) and consists of larger fragment (17-24kDa) and smaller (10-12kDa) fragment. The cleavage of caspase-3 requires the aspartic acid at position 175 (Nicholson et al., 1995). Then, cleaved caspase-3 cleaves the inhibitor of caspase-3-activated DNase (ICAD) into 24-and 12-kDa fragments, releasing CAD. Subsequently, CAD translocates to the nucleus and cleaves genomic DNA which is an essential evidence of apoptosis (Crow et al., 2004; Enari et al., 1998; Sakahira et al., 1998; Sabol et al., 1998).

Mechanisms involved in triggering apoptosis or necrosis during hypoxia are not known in detail, but it is generally believed that the release and/or activation of various bioactive substances such as reactive oxygen species are important. Levraut et al. (2003) showed that the use of antioxidants throughout ischaemia seemed to be more protective against reperfusion injury than if applied only at reperfusion. Pharmacological agents used to inhibit mitochondrial complexes I and II reversibly are cardiac protective (Solaini et al., 2005). Some researchers have suggested that use of uncouplers such as FCCP, dinitrophenol (DNP) (Elz and Nayler, 1988; Brennan et al., 2006a) and 3-NP (Turan et al., 2006) to inhibit complex II are cardioprotective. However, the use of antioxidants, metabolic inhibitors or mitochondrial inhibitors/ uncouplers to protect cells against hypoxia has not been studied thoroughly. Therefore, re-investigation of those inhibitory effects or uncoupler effects are important to understand the mechanism and the nature of cell damage during hypoxia.

## 5.3 Results

### 5.3.1 The effect of oxygen tension on metabolic activity and viability of cardiomyoblasts

Following mild or severe hypoxia, MTT activity was determined relative to cells maintained under normoxia as described in sections 2.3.6.1.1. As illustrated in **figure 5.1A and 5.1B**, the exposure of cells to acute (30min) or chronic (4h), mild hypoxic conditions did not result in a changed metabolic activity of cells when compared to cells grown under normoxic conditions for the same time periods. However, cells grown in severe hypoxia showed a significant loss of metabolic activity after both acute (83±0.2%; 30min) and chronic exposures (65±1%; 4h) (**Figure 5.1A and 5.1B**). PI uptake was significant during acute, severe hypoxia (127.2±6.7% vs 100.0±5.2%, $P<0.05$) and chronic, severe hypoxia (136.6±16% vs 100.00±13.6%, $P<0.05$) compared to normoxia, but not in acute or chronic, mild hypoxia (**Figure 5.1C and 5.1D**). A time-dependent reduction of cell metabolic activity was observed; 83.2±0.2% of control (100±4.2%) after 30min severe hypoxia ($P<0.001$) and 74.3±3% of control (100±1%) after 1h ($P<0.001$) with metabolic activity further reduced to 34±4% of control (100±3.7%) cells after 24h hypoxia ($P<0.0001$) **(Figure 5.2**) (see **Table 5.1** for summary of results).

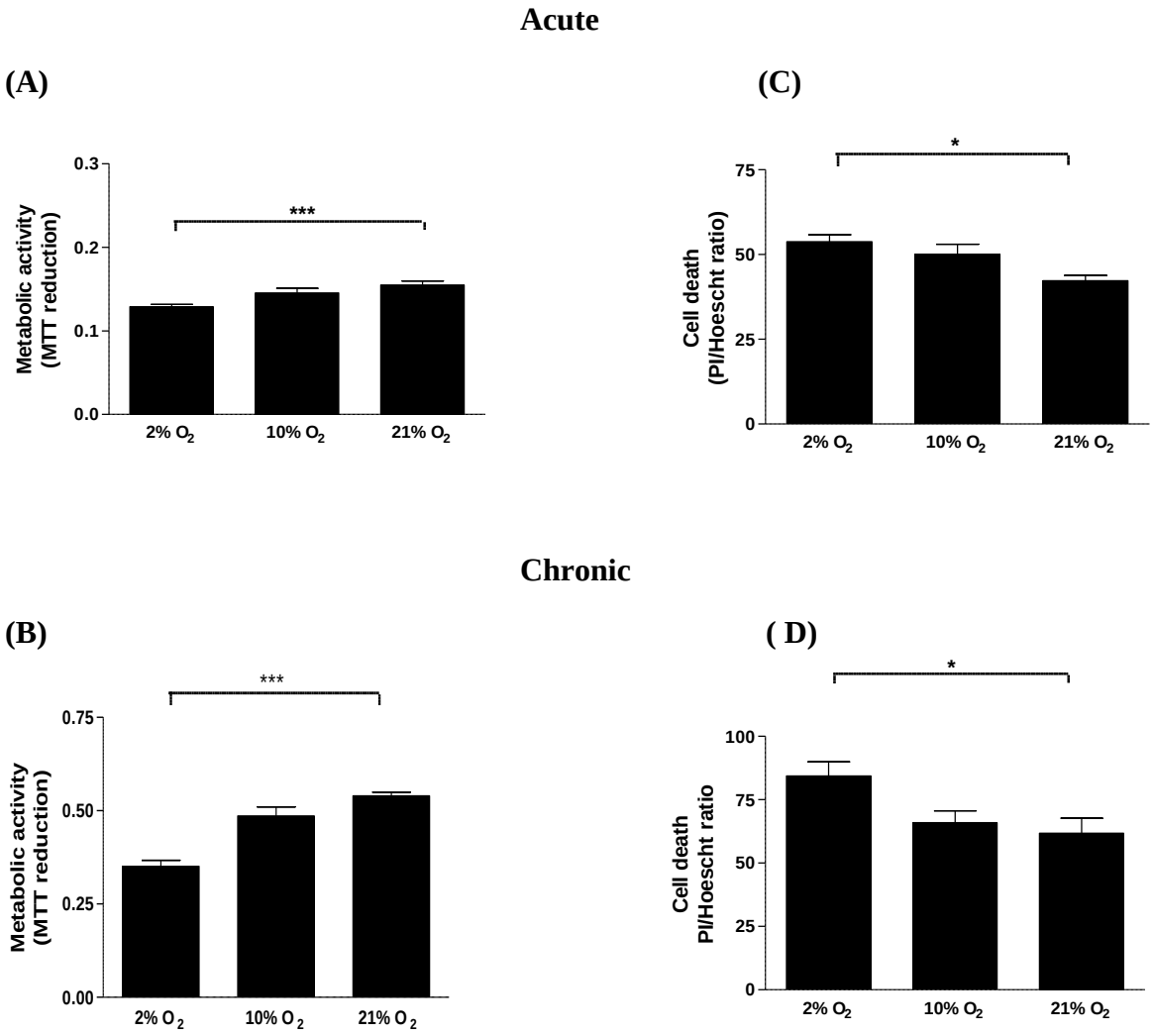


**Figure 5.1 Hypoxia reduces the metabolic activity and increases necrotic cell death of cardiomyoblasts.** At the start of each experiment, the growth media of cells (80% confluent) was changed to HEPES buffered, phenol red-free DMEM (pre-equilibrated under 2% or 10% or 21% $O_2$ for 24h). Cells were immediately transferred to incubators pre-equilibrated to the same $O_2$ tension. MTT was added 30mins (A: 30min, acute hypoxia) or 2h (B: 4h, chronic hypoxia) prior to the end of each experiment and then cells were lysed at the end of each experiment prior to analysis at 570nm. To assess necrotic cell death (C: 30min acute hypoxia and D: 4h, chronic hypoxia), following hypoxia the culture medium was removed and any detached cells were recovered by centrifugation. Attached and detached cells were suspended for 10µg/ml PI for 20min at 4ºC and after 3xPBS washes, cells were resuspended in 10µg/ml Hoechst 33342 for a further 20min at 4ºC. Finally, cells were washed in 3 x PBS and resuspended in PBS. The dual-fluorescence was measured at excitation 535nm/emission 617nm for PI and at excitation 346nm/emission and 460nm for Hoechst 33342. * represents $P < 0.05$ and *** $P<0.001$ versus 21% $O_2$ control (one-way ANOVA), Tukey's post-hoc test.

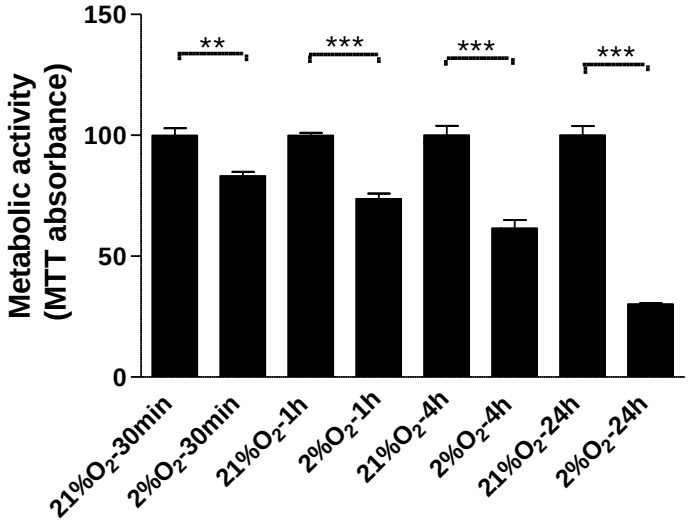


**Figure 5.2 Hypoxia induced a time-dependent decrease in metabolic activity.** H9C2 cells were seeded at $3x10^4$/well in 24-well plate and cultured until 80% confluence in DMEM, 10% FBS at 37°C in 5% $CO_2$ humidified atmosphere. At 70-80% confluence, cells were washed three times with PBS solution and 2% $O_2$ equilibrated, HEPES-buffered, phenol red-free DMEM was added and cells were exposed for hypoxia in a chamber at 2% $O_2$ for 30min, 1h, 4h and 24h. MTT was added to cells at t=0min for 30min, t=0 for 1h, t=2h for 4h and t=22h for 24 hypoxia. After completing hypoxic incubation, cells were lysed and re-incubated for further 16h at 37° C in 5% $CO_2$ humidified atmospheric conditions. An optical density was measured at 570nm. Data represents the mean±S.E.M of three independent experiments conducted in triplicates. *** represents $P < 0.001$ and ** represent $P<0.001$ (one-way ANOVA) Tukey's post-hoc test.

To further investigate whether the effect of hypoxia on MTT reduction was attributable to necrotic cell death or apoptosis, further analysis was undertaken using dual staining with Hoechst/PI. The assessment of cell death was undertaken as quantitative relative fluorescence measured by fluorescence spectrophotometer as described in methods (section 2.3.14). Microscopic analysis of apoptotic cell death was performed under Zeiss fluorescence microscopy as described in the methods (section 2.3.13.1).

**(A)** **Acute hypoxia**

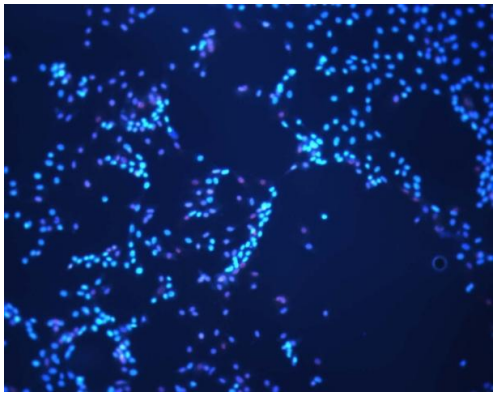

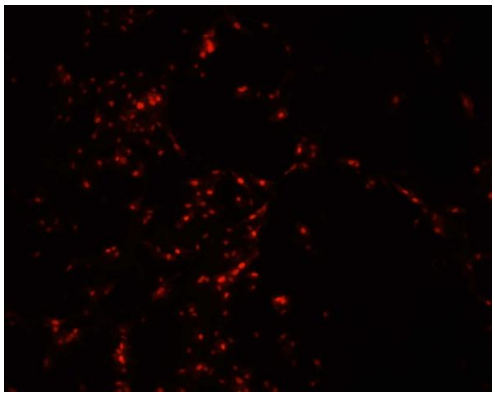

**2% $O_2$ - Hoechst** **2% $O_2$ - PI**

**(B)**

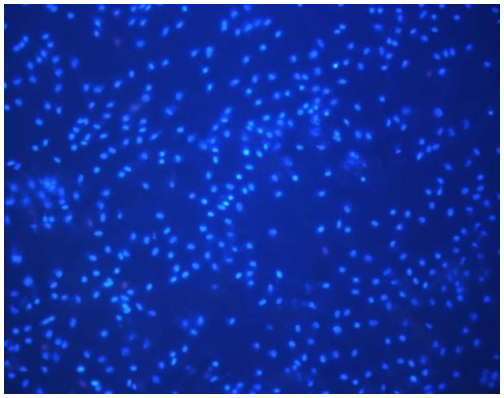

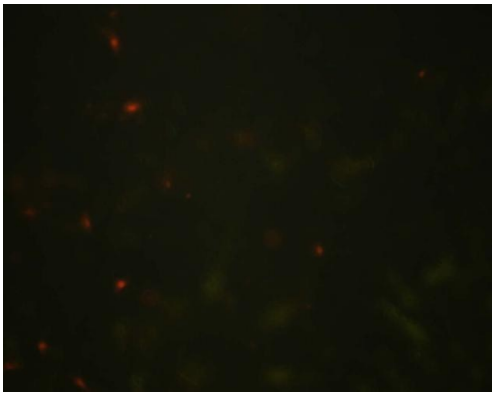

**10% $O_2$ - Hoechst** **10% $O_2$ - PI**

**(C)**

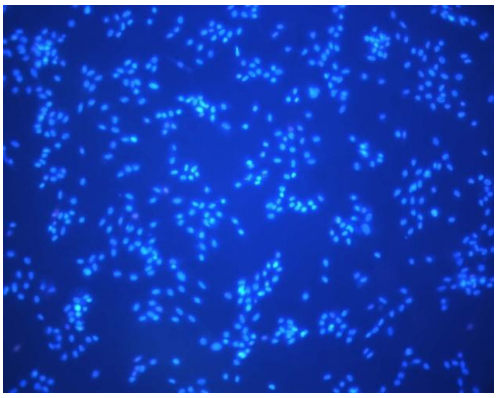

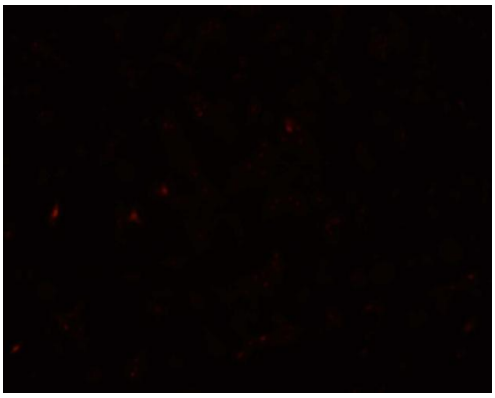

**21% $O_2$ - Hoechst** **21% $O_2$ - PI**

**(D)** **Chronic hypoxia**

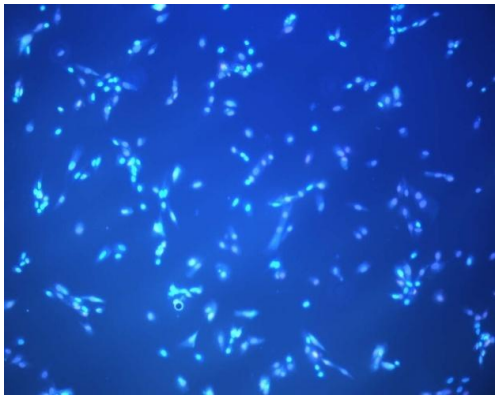

**2% $O_2$ - Hoechst**

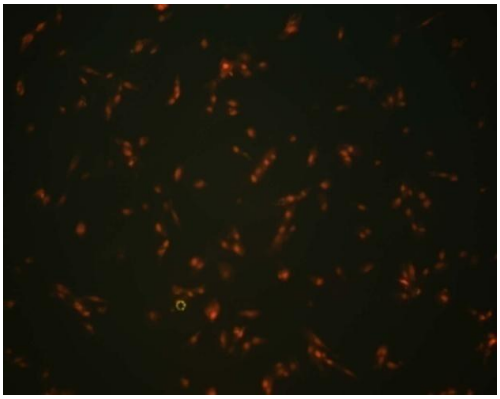

**2% $O_2$ - PI**

**(E)**

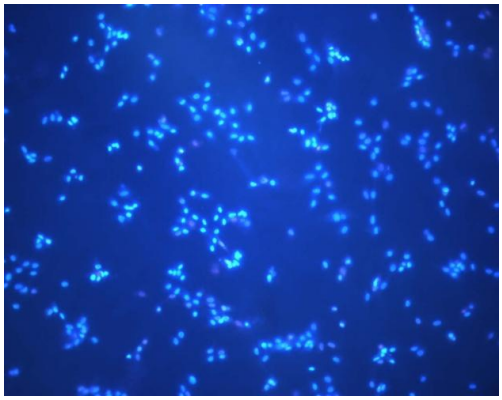

**10% $O_2$ - Hoechst**

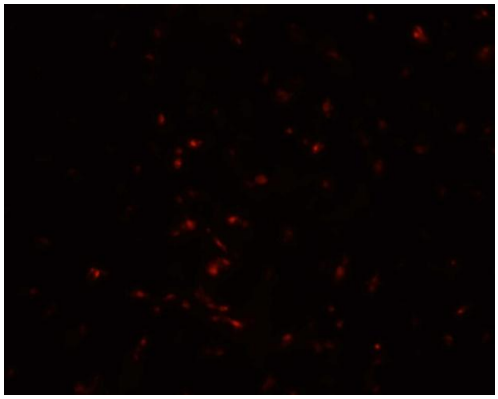

**10% $O_2$- PI**

**(F)**

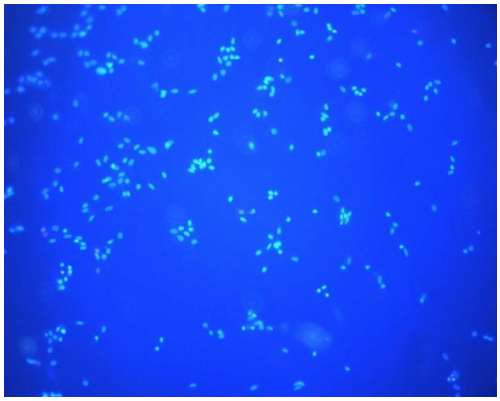

**21% $O_2$ - Hoechst**

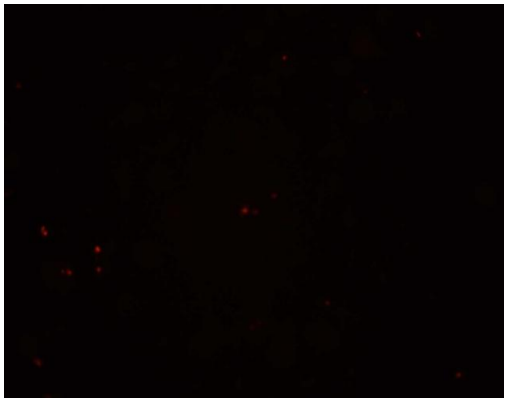

**21% $O_2$ – PI**

**Figure 5.3 Hypoxia-induced necrotic cell death as visualized by propidium iodide and Hoechst 33342 stains.** Cells were grown on cover slips in 24-well culture plates in DMEM for 30min (A, B and C) and 4h (D, E and F) at 21% $O_2$, 10% $O_2$ and 2% $O_2$. Immediately after hypoxia, cells were washed 3x with PBS and stained with PI (10µg/ml) and Hoechst 33342 (10µg/ml) on ice for 10min in the dark. Cells were washed a further 3 x in PBS and necrosis visualised as PI positive staining nuclei relative to total nuclei (Hoechst stained) under a Zeiss fluorescence microscope at the following emissions; 460nm for Hoechst 33342 and 570-590nm for PI following excitation with a 405nm UV lamp.

Necrotic cell death was increased significantly after 30min severe hypoxia and was further increased after 4h severe hypoxia compared to control cells incubated under normoxia for the same duration (**Figure 5.1C and 5.1D**). There was no significant increase in cell death under mild hypoxic conditions compared to normoxia at either time point studied. No significant effects on viability measured as PI uptake were observed in cells under normoxia after 30mins and after 4h (**Figures 5.3C and 5.3F**). **Figures 5.3A** and **5.1C** illustrate the increased uptake of PI by cells maintained under 2% $O_2$ for 30mins or 4h (**Figures 5.3D and 5.1D**) compared to cells maintained under 21% $O_2$ for the same times. In addition, fewer cells remained attached to the microscope cover slip at lower $O_2$ tension. Qualitative increases in PI uptake by cells occurred under severe hypoxia, visualised in **figure 5.3**, are confirmed by quantitative microplate fluorimetry in **figures 5**.**1**(see **Table 5.1** for summary of results).

### 5.3.2 Chronic, severe and mild hypoxia induce apoptosis

It has been reported that hypoxia can elicit apoptosis in primary cardiomyocytes (Todor et al., 2002). The proteolytic cleavage of caspases from precursor procaspase-3 is an early, sensitive indicator of caspase activation (Niquet et al., 2003; Levrand et al., 2006). In non-apoptotic cardiomyoblasts, procaspase-3 is detected as a single band (32kDa); during apoptosis caspase-3 is cleaved into large (17-24 kDa) and small (10-12kDa) fragments (Todor et al., 2002).

**(A)**

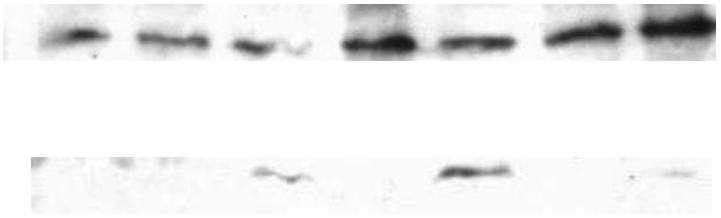


**(B)**

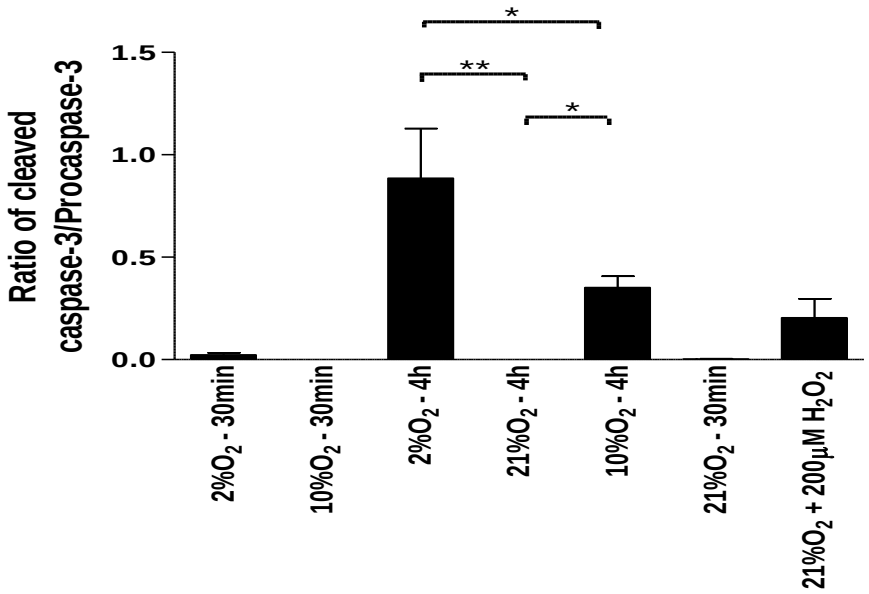


**Figure 5.4 Chronic, severe and mild hypoxia induce cleavage of procaspases-3.** Whole cell lysates from cells exposed to hypoxia (30min and 4h) or normoxia-treated controls were resolved using 15% Tricine-SDS-PAGE and transferred to PVDF membranes. Lysate from cells exposed to 200µM $H_2O_2$ for 8h was employed as a positive control. Western blot analysis was performed using; anti-cleaved caspase-3 and anti-procaspase-3 (A). Immunoreactive bands were revealed by enhanced chemiluminescence. Densitometric analysis was performed as the ratio of cleaved caspase-3 to procaspase-3 (B). Integral data are expressed as mean±SE of three independent experiments. ** and * (control vs treatment) represent $p<0.001$ and $p<0.05$ respectively (one way ANOVA), Tukey's post-hoc test.

Following treatment (2% $O_2$ severe hypoxia and 10% $O_2$ mild hypoxia for 30min and 4h or normoxia) total cell lysates (20µg) were resolved by SDS-PAGE and transferred to PVDF membranes for immunoblotting against procaspase 3 and cleaved caspase 3. The larger cleaved fragment (18kDa) of procaspase-3 was detected in cardiomyoblasts exposed to chronic, severe or mild hypoxia. However, no cleavage band was detected in cells exposed to acute, hypoxia or normoxia at any time of the investigation (**Figure 5.4**). Lysates from H9C2 cells exposed to 200µM of $H_2O_2$ (8h) were employed as a positive control as previously described (Park et al., 2003). Chronic, severe hypoxia induced activation of caspase-3 as indicated by the increased ratio of cleaved caspase-3 to procaspase-3 ($P<0.01$; **Figure 5.4B**). Similarly, chronic, mild hypoxia induced procaspase-3 cleavage as illustrated by the increase in cleaved caspase-3 to procaspase-3 ($P<0.01$, **Figure 5.4B**) (see **Table 5.1** for summary of results).

### 5.3.4 The effect of metabolic inhibitors on viability and metabolic activity during mild and severe hypoxia

To identify the contribution of different metabolic sources of $O_2^{-\bullet}$ production to the toxicity of hypoxia, the effects of incubation with mitochondrial complex I inhibitor; rotenone (20µM), the respiratory chain uncoupler; 1µM FCCP, NADPH oxidase complex inhibitor; 50µM apocynin and the non-selective NOS inhibitor; 100µM L-NAME were examined during hypoxia (see section 2.3.12).

Control cells received an equal volume of vehicle and were exposed to hypoxia or normoxia for 30min and 4h. The mitochondrial uncoupler; FCCP, and the inhibitors of the respiratory chain (rotenone) and respiratory burst (apocynin) had no effects on metabolic activity (MTT reduction) or cell viability (PI/Hoechst assay) under normoxic conditions after either 30min (**Figures 5.5C and 5.6C**) or 4h **(Figure 5.5F and 5.6F**) of treatment. The presence of FCCP enhanced metabolic activity of cells in mild and severe hypoxia at 30mins (**Figures 5.5B and 5.5A**) compared to control cells maintained under normoxia (**Figure 5.5C**).

Similarly, non-selective inhibition of NOS isoforms with L-NAME showed a significantly increased metabolic activity compared to normoxia in cells incubated under 2% $O_2$ for 4h (**Figure 5.5D**), although it did not have an effect on $O_2^{-\bullet}$ production as determined by quantitative oxidation of DHE (**Figure 4.3D**). Other inhibitors did not show any significant effects on MTT reductive capacity at 30mins. During chronic hypoxia, the presence of the mitochondrial uncoupling agent, FCCP or the NOX inhibitor apocynin significantly reduced metabolic activity in H9C2 cells during mild, but not severe hypoxia (**Figure 5.5E & 5.5D**).

In contrast, the presence of rotenone during chronic, severe hypoxia was associated with an increase in metabolic activity compared to untreated hypoxic control cells (**Figure 5.5D**), which was not significantly different from the MTT reductive activity of cells growing under normoxic conditions for 4h (**Figure 5.5F**). The inhibition of NADPH oxidase complex with apocynin and the uncoupling of the mitochondrial electron transport chain with FCCP failed to protect against severe hypoxia-induced loss of metabolic activity during chronic hypoxia (**Figures 5.5D**).

To further investigate whether the effects of metabolic inhibitors during hypoxia on MTT reduction were attributable to perturbation of the respiratory chain or cell death, further analysis was undertaken using dual staining with Hoechst/PI. In the presence of metabolic inhibitors; mitochondrial complex I inhibitor; rotenone (20µM), the uncoupler 1µM FCCP, NADPH oxidase complex inhibitor; 50mM apocynin and non-selective NOS inhibitor; 100µM L-NAME an assessment of cell death was undertaken as quantitative relative fluorescence and by fluorescence microscopic analysis as previously described in sections 2.3.12, 2.3.13 and 2.3.13.1.

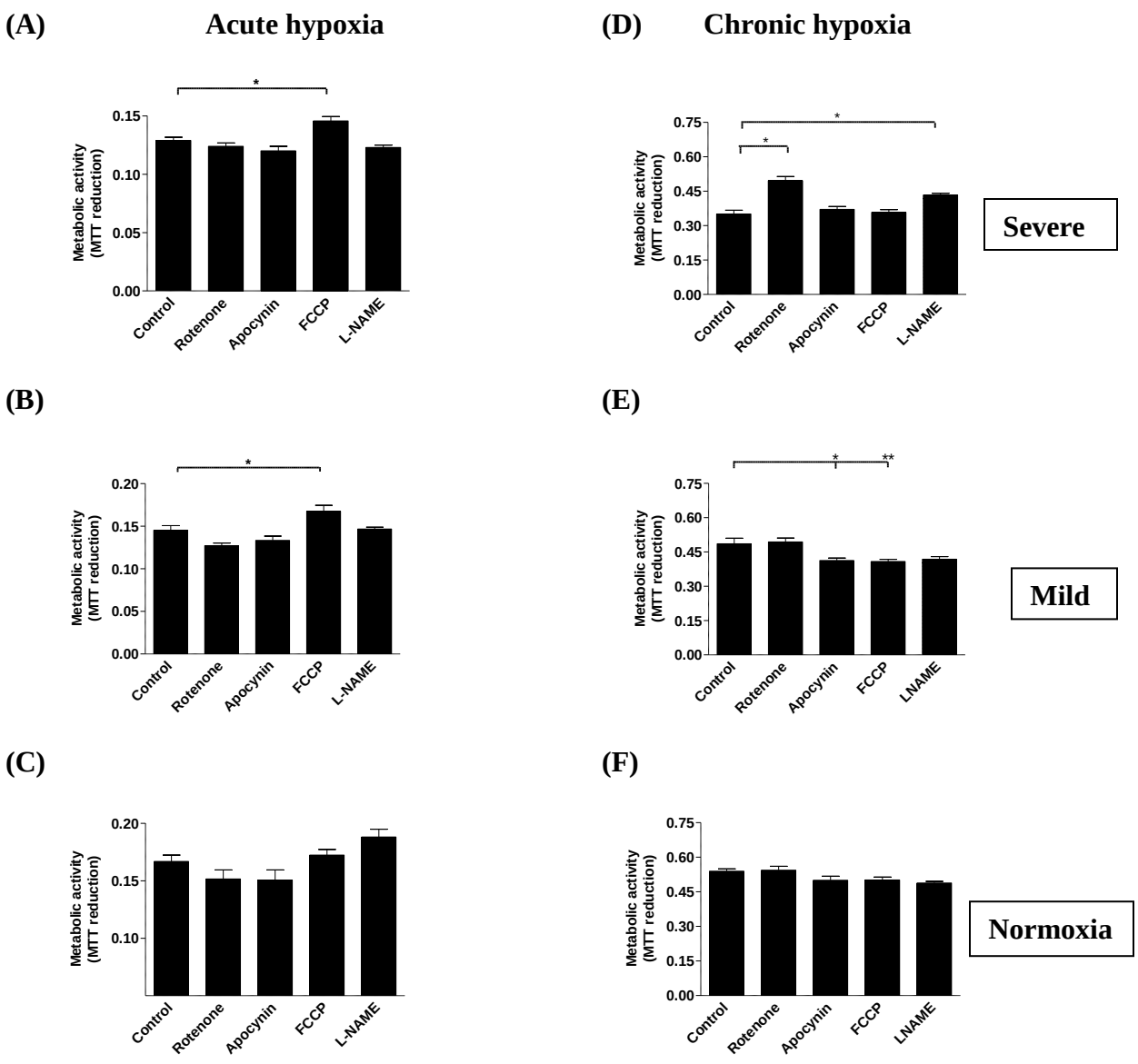


**Figure 5.5 Hypoxia-induced changes to cardiomyoblast metabolic activity are mitigated by modulators of mitochondrial metabolism.** H9C2 cells were loaded with $O_2$ equilibrated HEPES buffered-phenol red-free DMEM at 21% (C & F), 10% (B & E) or 2% (A & D) $O_2$ with and without 20µM rotenone, 100 µM apocynin, 1µM FCCP or vehicle control at t=-2min. MTT was added at t=0min (for acute hypoxia) or 2h prior to completion of 4h hypoxia. MTT reduction was determined at 570nm in a microplate reader. Cell viability was analysed with respect to control cells maintained at the same $O_2$ tension for the same time period. * represent $P < 0.05$, ** for $P<0.01$ (one-way ANOVA), Tukey's post-hoc test.

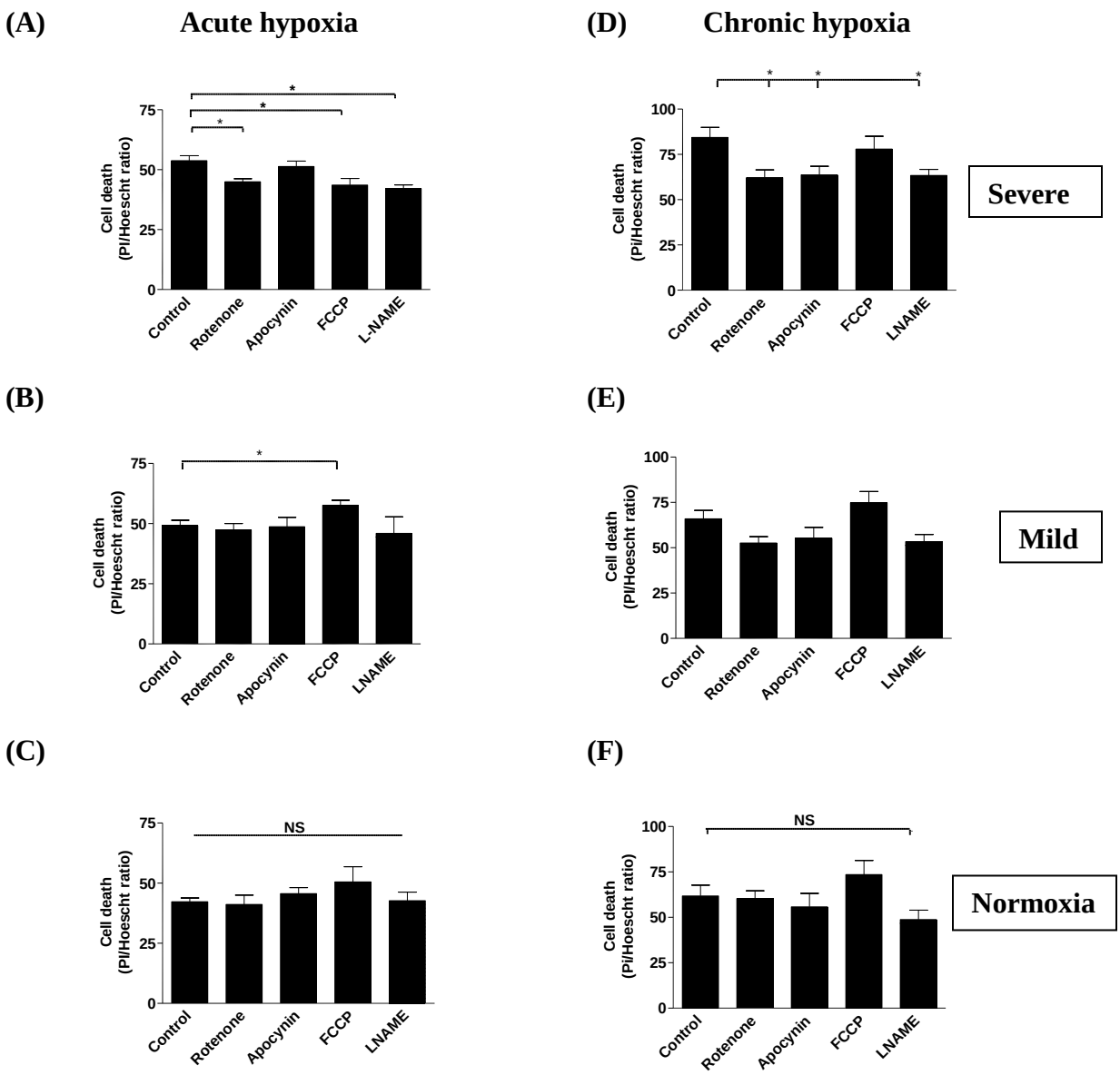


**Figure 5.6 Quantitative effects of mitochondrial uncoupling and metabolic inhibition on hypoxia-induced necrotic cell death, determined by propidium iodide (PI) and Hoechst 33342 fluorescence.** Cells were grown to 90% confluence on coverslips, washed with PBS and exposed to 2% $O_2$, 10% $O_2$ and 21% $O_2$ for 30mins (A-C) and 4h (D-F) in the presence of ROS/RNS inhibitors. Following hypoxia, cells were harvested into 10µg/ml PI for 20min at 4ºC and after 3xPBS washing, were resuspended in 10µg/ml Hoechst 33342 for further 20min at 4ºC. Finally, cells were washed in PBS and dual-fluorescence was measured by excitation at 535nm/emission at 617nm for PI and excitation at 346nm/emission at 460nm for Hoechst 33342. Data is expressed as a relative fluorescence ratio. * represent $P < 0.05$ (one-way ANOVA), Tukey's post-hoc test.

In the presence of the complex I respiratory chain inhibitor rotenone, PI uptake was reduced significantly during acute, severe hypoxia (30min, 2% $O_2$) (**Figures 5.6A)** and chronic, severe hypoxia (4h, 2% $O_2$) (**Figure 5.6D and 5.8A**) by 16% and 26% respectively ($p<0.05$) compared to hypoxia treatment alone (**Figure 5.3D**). This effect was associated with normalised MTT reductive capacity (**Figure 5.5D**) and less DHE oxidation (**Figure 4.3D**) under severe, chronic hypoxia in the presence of rotenone. The NADPH oxidase inhibitor apocynin, prevented severe hypoxia-induced PI uptake by 25% after 4h ($p<0.05$) (**Figure 5.6D and Figure 5.8B**). This associated with a small reduction in DHE oxidation (**Figure 4.3D**) but no effect on MTT reductive activity (**Figure 5.5D**).

Co-incubation of H9C2 cells with the mitochondrial uncoupler FCCP, had a profound effect on PI uptake in acute, mild hypoxia conditions, but not chronic hypoxia as visualised by fluorescence microscopy and by independent analysis using spectrofluorimetry (**Figure 5.6B**). FCCP increased cell death by 18% ($p<0.05$) over 30min at 10% $O_2$ but this effect was no longer evident after 4h (**Figure 5.6E**). Fewer cells were analysed after FCCP treatment for 4h under mild hypoxia compared to 30min mild hypoxia, possibly reflecting lysis of dead cells and analysis of resistant cells only. The effects of acute, mild hypoxia on PI uptake paralleled previous observations on MTT reductive capacity (**Figure 5.5B vs 5.6C**) of H9C2 cells, which increased significantly in the presence of FCCP under acute, mild hypoxia and acute, severe hypoxia. Severe hypoxia induced cell death was not prevented by the presence of FCCP after 30mins as observed in 4h hypoxia (**Figures 5.6D and 5.8C**) (see **Table 5.1** for summary of results).

### 5.3.5 Chronic, severe hypoxia causes ATP depletion

It has been reported that depletion of ATP during hypoxia can contribute to cell death via necrosis or/and apoptosis (Lieberthal et al., 1998).

To test whether loss of ATP associated with cell death under the time and severity of hypoxia studies, ATP production was assessed under different hypoxic conditions using an ATP luminescent assay as previously described in section: 2.3.6.1.2.

Cellular ATP was reduced significantly during chronic, severe hypoxia by 52% compared to normoxia control cells (786±15 vs 1656±29, $P<0.05$) and by 28% during mild hypoxia (1192±69) (**Figure 5.7A**). ATP production during hypoxia was also assessed in the presence of the mitochondrial complex I inhibitor; rotenone (20µM) and uncoupler; FCCP (1µM), which inhibit cell death during severe hypoxia. Under normoxic conditions (4h), ATP production was significantly reduced by 22% in the presence of rotenone ($P<0.0001$) and 12% in the presence of FCCP ($P<0.0001$) compared to untreated normoxic controls (**Figure 5.7B**) in the absence of any cytotoxicity. In the presence of FCCP, ATP production was significantly reduced by 43% during both chronic, severe (443±21 versus 786±15, $P<0.0001$) and mild hypoxia (673±28 versus 1192±69, $P<0.0001$) compared to non-inhibited, hypoxia-exposed controls (**Figure 5.7D**).

Similarly, in the presence of rotenone, ATP production was markedly reduced by 48% during chronic, mild hypoxia ($P<0.0001$) (**Figure 5.7C**) and 38% during chronic, severe hypoxia ($P<0.0001$) (**Figure 5.7D**) (see **Table 5.1** for summary of results).

### 5.3.6 Mitochondrial complex-I inhibition protects cells against chronic, severe hypoxia induced apoptosis

It has been reported that increased intracellular $O_2^{-\bullet}$ levels can activate the apoptotic cell death pathway (Lièvre et al., 2000). However, the relative contribution of $O_2^{-\bullet}$ produced from different metabolic sources during hypoxia to induction of apoptosis is unknown. Therefore, the effects of incubation with the mitochondrial complex I inhibitor; rotenone, the uncoupler; FCCP, NADPH oxidase inhibitor; apocynin and the non-selective NOS inhibitor; L-NAME were examined by western blotting for cleavage of procaspase-3 as previously described in section 2.3.12, 2.3.16 and 2.3.16.1.

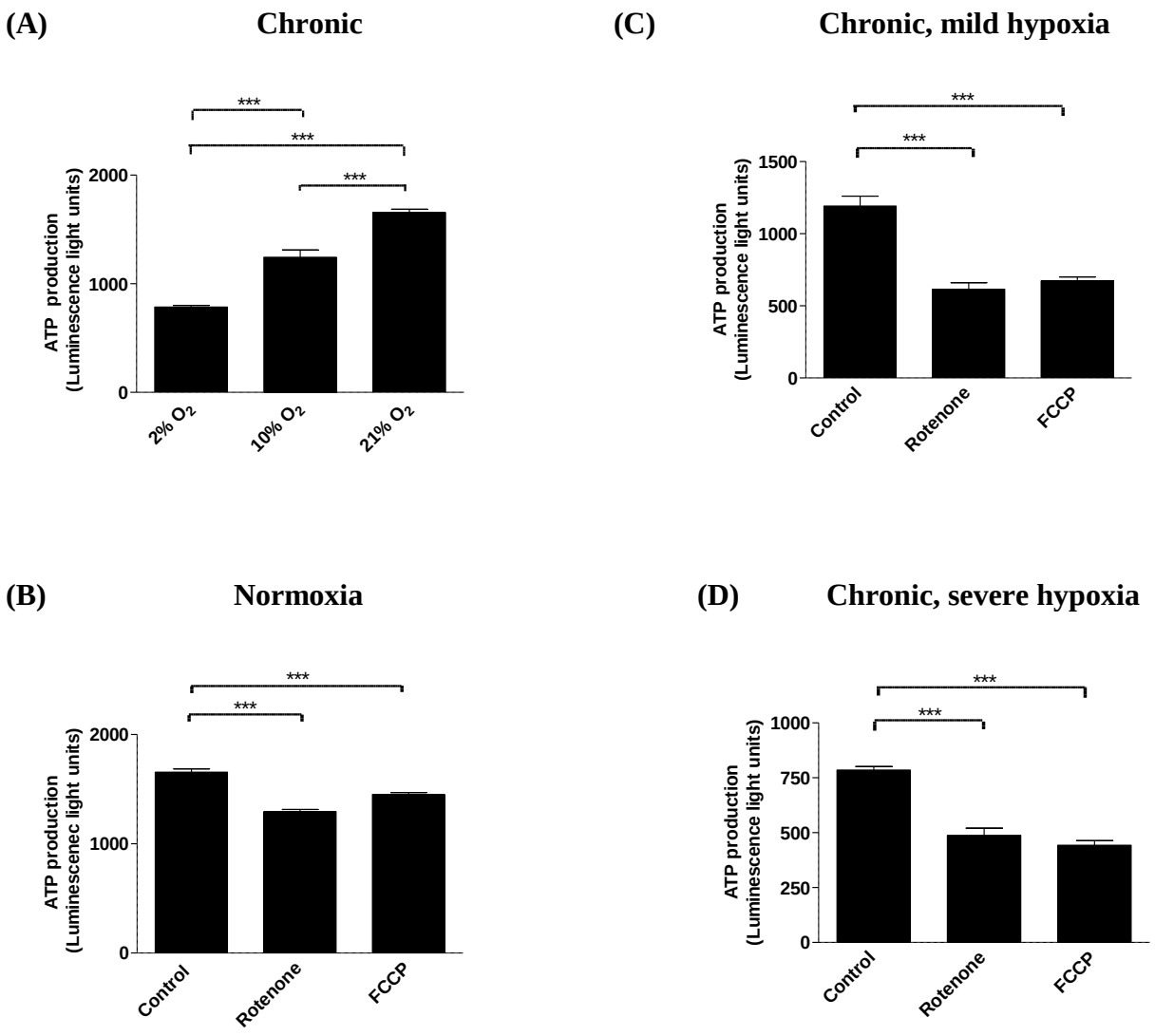


**Figure 5.7 Hypoxia and metabolic inhibition causes depletion of ATP in H9C2 cells.** Confluent (80%) H9C2 cells were pre-incubated with 20µM rotenone or 1µM FCCP for 30min prior to loading with $O_2$ equilibrated HEPES buffered-phenol red-free DMEM (21% (A, B); 10% (A, C); or 2% (A, D) $O_2$). After incubation for 4h, total ATP content was assessed in each lysate using the ATP luminescent assay. Luminescence was measured at 37°C in Spectramax GEMINI EM plate reader at 542nm. Data represent the mean ± SEM luminescence of three independent experiments conducted in triplicates. *** represents $P < 0.0001$ (one-way ANOVA), Tukey's post-hoc test.

**(A)**

| | | | | | | | |
|---|---|---|---|---|---|---|---|
| **Procaspase 3 (32kD)** | | | | | | | |
| **Cleaved caspase 3 (18kD)** | | | | | | | |
| **α-Tubulin** | | | | | | | |
| **2% $O_2$ Hypoxia** | + | + | - | + | + | + | + |
| **Rotenone** | - | + | - | - | - | - | - |
| **21% $O_2$ Normoxia** | - | - | + | - | - | - | + |
| **Apocynin** | - | - | - | + | - | - | - |
| **FCCP** | - | - | - | - | + | - | - |
| **L-NAME** | - | - | - | - | - | + | - |
| **$H_2O_2$** | - | - | - | - | - | - | + |

**(B)**

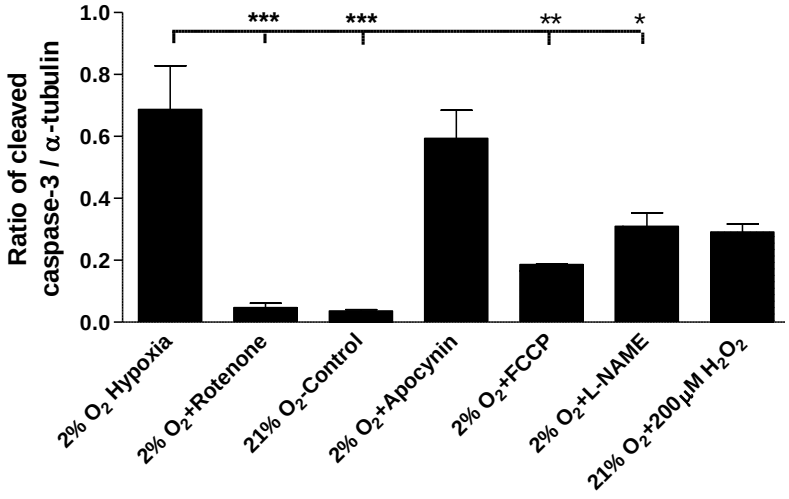

**(C)**

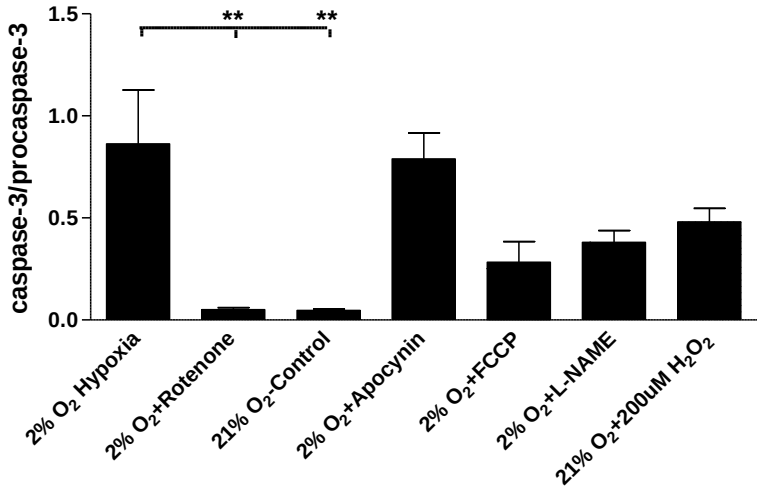


**Figure 5.8 The effect of inhibitors on cleavage of procaspase–3 during severe hypoxia** Total protein lysate (20µg) from cells exposed to severe hypoxia (4h) was resolved using 15% Tricine-SDS-PAGE and transferred to PVDF membrane. Western blot analysis was performed using the primary antibodies; anti-cleaved caspase-3, procaspase-3 and loading control; anti-α-tubulin (A). Immunoreactive bands were revealed by enhanced chemiluminescence. Densitometry analysis was performed and results are expressed as the ratio of cleaved caspase-3 to procaspase-3 (B) and the ratio between cleaved caspase-3 to α-tubulin (C). Total protein lysate from cells exposed to 200µM of $H_2O_2$ for 8h was employed as a positive control. Results are expressed as mean±SE where n=3. *, ** and *** represent $p<0.05$, $p<0.001$ and $p<0.0001$ respectively (one way ANOVA), Tukey's post-hoc test.

As illustrated in **figure 5.8A**, rotenone treatment suppressed the cleavage of procaspase-3 during chronic, severe hypoxia when compared to untreated and treated control cells. In the presence of rotenone, caspase-3 activation was suppressed as indicated by a 15-fold decrease ($P<0.0001$, 0.047±0.014 vs 0.687±0.141) in the ratio of cleaved caspase-3 to loading control to α-tubulin (**Figure 5.8B**) and a 17-fold decrease ($P<0.001$, 0.051±0.01 vs 0.863±0.263) of the ratio between cleaved caspase-3 and procaspase-3. In contrast, apocynin treatment was not able to suppress the procaspase-3 cleavage (**Figure 5.8A**) induced by severe, chronic hypoxia ($P<0.0001$, 0.594±0.091 vs hypoxia alone control). However, FCCP and L-NAME treatment afford some significant protection against procaspase 3 cleavage when analysed relative to α-tubulin expression but not caspase-3 content (FCCP; 0.186±0.002 and L-NAME; 0.309±0.044) (**Figure 5.8A**).

The positive control showed a 7-fold increase in the ratio between cleaved caspase-3 to procaspase-3 (0.258±0.047 vs 0.030±0.005) (**Figure 5.8B and 5.8C**) (see **Table 5.1** for summary of results).

**(A)**

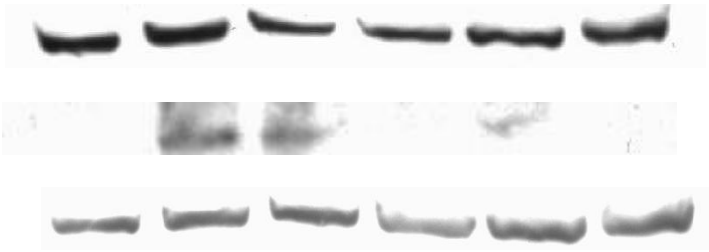


| | | | | | | |
|---|---|---|---|---|---|---|
| **21% $O_2$ Normoxia** | + | - | - | - | - | - |
| **10% $O_2$ Hypoxia** | - | + | + | + | + | + |
| **10% $O_2$ Rotenone** | - | - | + | - | - | - |
| **10% $O_2$ Apocynin** | - | - | - | + | - | - |
| **10% $O_2$ FCCP** | - | - | - | - | + | - |
| **10% $O_2$ L-NAME** | - | - | - | - | - | + |

**(B)**

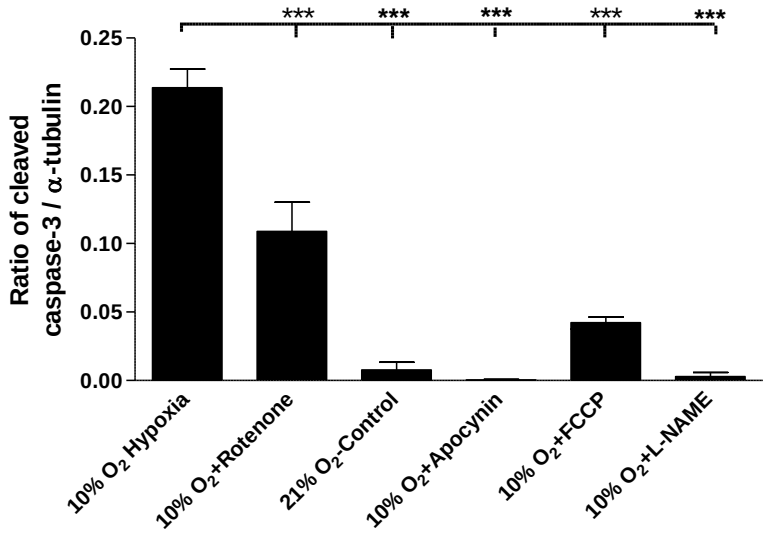

**(C)**

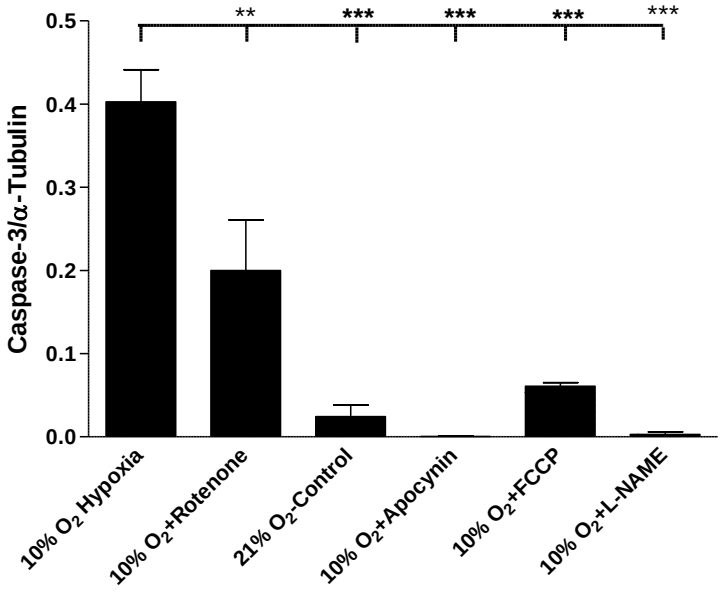


**Figure 5.9 The effect of inhibitors on cleavage of procaspase-3 during chronic, mild hypoxia.** Total protein lysate (20µg) from cells exposed to chronic, mild hypoxia in the presence of inhibitors (4h) was resolved using 15% Tricine-SDS-PAGE and transferred to PVDF membrane. Western blot analysis was performed using the primary antibodies; anti-cleaved caspase-3, anti-procaspase-3 and loading control; anti-α-tubulin (A). Immunoreactive bands were revealed by enhanced chemiluminescence. Densitometry analysis was performed as previously described (B and C). Mean±SE and n=3. ** and *** (control vs. treatment) represents $p<0.001$ and $p<0.0001$ respectively (one-way ANOVA), Tukey's post-hoc test.

Several studies indicate that cleavage of procaspase-3 in cells can be stimulated by short term exposure to $O_2^{-\bullet}$ (Madesh and Hajnoczky, 2001). In contrast, **figure 5.9** shows that chronic, mild hypoxia induced procaspase-3 cleavage even in the absence of a detectable increase in $O_2^{-\bullet}$ production. To investigate whether $O_2^{-\bullet}$ preferentially activates caspase-3 compared to reaction with DHE or whether other radical species may be important, the effects of inhibiting different metabolic sources of $O_2^{-\bullet}$ and $^{\bullet}NO$ generation were studied.

### 5.3.7 The inhibition of NADPH oxidase complex and NOS isoforms significantly protect cell against chronic, mild hypoxia-induced apoptosis

To identify any roles for ROS/RNS as inducers of apoptosis and to suppress the execution phase of apoptosis during chronic, mild hypoxia, cells were treated with rotenone (20μM), FCCP (1 μM), apocynin (100 μM) and L-NAME (100 μM) prior to exposing cells to chronic, mild hypoxia. Apoptosis was examined by western blotting for cleavage of procaspase-3.

As illustrated in **figure 5.9A**, apocynin (100μM) treatment completely suppressed the cleavage of procaspase-3 during chronic, mild hypoxia. In control cells exposed to hypoxia alone, the ratio between cleaved caspase-3 and procaspase-3 ($P<0.0001$, 0.403±0.038 vs. 0.024±0.014) (**Figure 5.9B**) and the ratio of cleaved caspase-3 to α-tubulin ($P<0.0001$, 0.214±0.014 vs. 0.002±0.002) (**Figure 5.9C**) were significantly increased compared to normoxia.

In the presence of rotenone, chronic, mild hypoxia-induced procaspase-3 cleavage was suppressed but apoptosis was not completely suppressed as indicated by a 10-fold higher ($P<0.0001$, 0.109±0.021 vs. 0.002±0.002) ratio of cleaved caspase-3 to loading control; α-tubulin and also the 8-fold higher ($P<0.001$, 0.2001±0.061 vs. 0.024±0.014) ratio between cleaved caspase-3 and procaspase-3 when compared to control cells maintained under normoxia (**Figure 5.9A, B and C**). In the presence of FCCP and L-NAME, the collapse of mitochondrial membrane potentials (Ψ) or inhibition of NOS isoforms respectively suppressed the cleavage of procaspase-3 partially during hypoxia (**Figure 5.9C**), though the rotenone treatment failed to suppress procaspase-3 cleavage during chronic, mild hypoxia (see **Table 5.1** for summary of results).

**(A)**

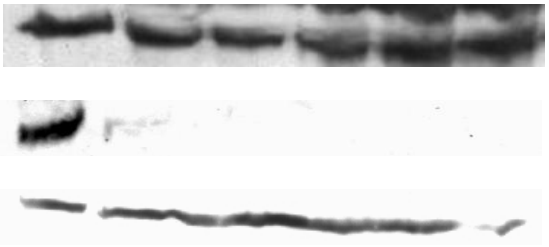


| | | | | | | |
|---|---|---|---|---|---|---|
| **21%$O_2$+200μM $H_2O_2$** | + | - | - | - | - | - |
| **21%$O_2$ +LNAME** | - | + | - | - | - | - |
| **21%$O_2$ +Rotenone** | - | - | + | - | - | - |
| **21%$O_2$+Apocynin** | - | - | - | + | - | - |
| **21%$O_2$+FCCP** | - | - | - | - | + | - |
| **21%$O_2$+L-NAME** | - | - | - | - | - | + |

**(B)**

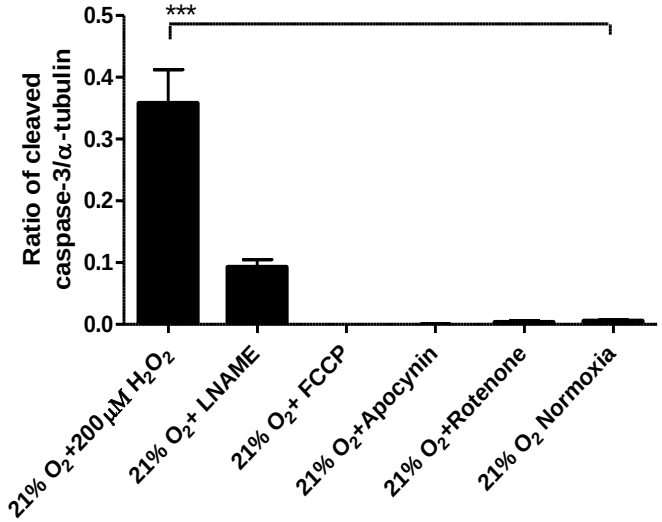

**(C)**

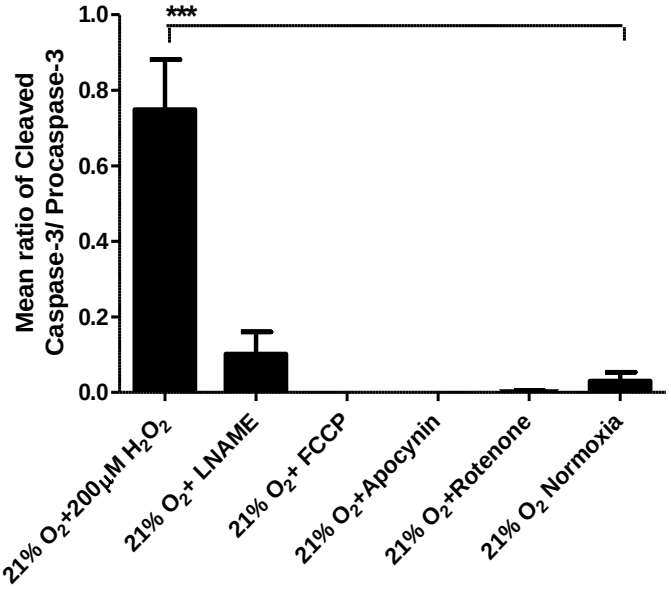


**Figure 5.10 Metabolic inhibitors do not induce procaspase-3 cleavage during normoxia** Total protein lysate (20µg) from cells exposed to normoxia in the presence of inhibitors (4h) was resolved using 15% Tricine-SDS-PAGE and transferred to PVDF membrane. Western blot analysis was performed using the primary antibodies; anti-cleaved caspase-3, anti-procaspase-3 and loading control; anti-α-tubulin (A). Immunoreactive bands were revealed by enhanced chemiluminescence. Whole cell lysate from cells exposed to 200µM of $H_2O_2$ for 8h was employed as a positive control. Densitometry analysis was performed as the ratio of cleaved caspase-3 to procaspase-3 and α-tubulin (B and C). Mean±SE and n=3. *** (control vs. treatment) represent $p<0.0001$ (one way ANOVA), Tukey's post-hoc test.

Lysates from cells exposed to 200µM $H_2O_2$ for 8h at 21% $O_2$ were employed as a positive control and showed at least 20-fold increase in procaspases-3 cleavage ((**Figure 5.10A, 5.10B and 5.10C**)). As illustrsted, all inhibitors and metabolic uncoupler did not activate significantly the cleavage of procaspase-3 during normoxia (**Figure 5.10A, 5.10B and 5.10C**).

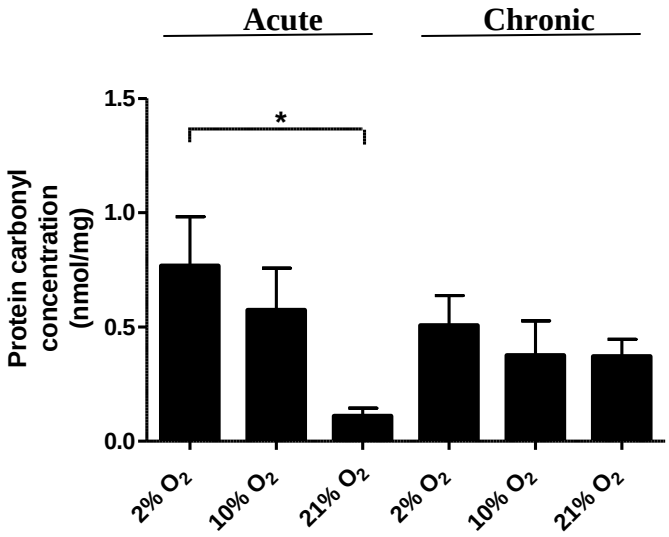


**Figure 5.11 Hypoxia-induced protein carbonylation during 30min but not 4h.** H9C2 lysate was analysed for protein carbonyl content by ELISA after hypoxia and normoxia. Data are expressed as mean±SE and n=7. * represents $p<0.05$ (one way ANOVA), Tukey's post-hoc test.

### 5.3.8 Acute, but not chronic, severe hypoxia induced protein carbonylation in H9C2 myoblasts

Increased levels of carbonylated proteins are associated with the early stages of apoptosis or necrosis (England et al., 2003). However, the effects of severity and duration of hypoxia on protein carbonyls remains unknown and therefore, carbonyl levels were examined for any relationship to cell death. Total amount of protein carbonylation (nmol/mg) was assessed using whole cell lysate extracted from H9C2 cells after exposing to hypoxia and normoxia. As shown in **figure 5.11**, there was a significant increase in protein carbonylation during acute, severe hypoxia ($P<0.05$, 0.767±0.216nmol/mg, 30min) compared to normoxic controls (0.110±0.216nmol/mg, 30min). A 40% decrease in protein carbonylation was observed during chronic, severe hypoxia (0.506±0.131nmol/mg) compared to acute hypoxia. Acute or chronic, mild hypoxia did not elicit a substantial difference in protein carbonylation compared to normoxic controls (**Figure 5.11**) (see **Table 5.1** for summary of results).

### 5.3.9 Effect of NF-κB inhibition and preventing extracellular $Ca^{2+}$ uptake during hypoxia-induced cell death

It has been reported that NF-κB activation and modulation of intracellular and/or mitochondrial $Ca^{2+}$ mediate cellular defence mechanism against hypoxia-induced cell death (Lu et al., 2009; Regula et al., 2004; Bolli,2000; Talukder et al., 2009; Persson-Rothert et al., 1994; Zhou et al., 2009). To investigate this hypothesis, cells were treated with NF-κB inhibitor; SN-50 (5 μM or 10μM) or EGTA (5mM or 10mM) which were added to culture medium in separate experiments prior to exposing cells to chronic, severe hypoxia. Cell viability was measured by the MTT assay. The inhibitors had no effect on H9C2 cells under normoxic conditions (**Figure 5.12A**).

The metabolic activity of cells was significantly reduced during chronic, severe hypoxia alone compared to that of control cells at 21% $O_2$ in the presence of NF-κB inhibitor (5 μM; 0.473±0.014, $P<0.001$ and 10 μM; 0.390±0.0104, $P<0.001$) and EGTA (5mM; 0.543±0.011, $P<0.001$ or 10mM; 0.467±0.007, $P<0.001$), suggesting that hypoxic cell injury is increased with the inhibition of NF-κB and $Ca^{2+}$ (**Figure 5.12B**) (see **Table 5.1** for summary of results).

**(A)** **Normoxia**

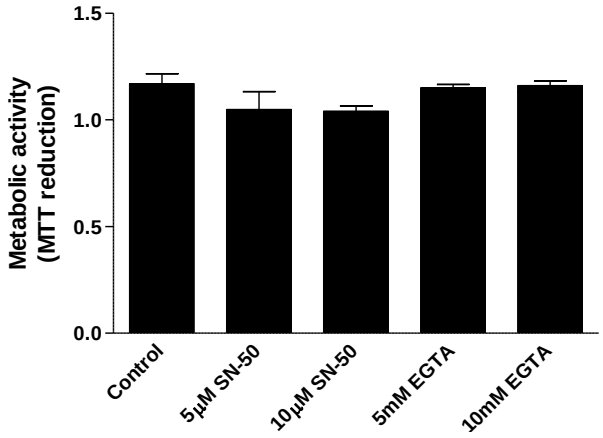


**(B)** **Chronic, severe hypoxia**

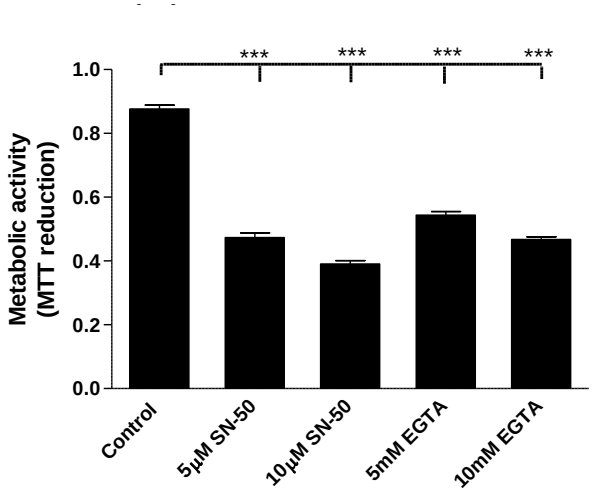


**Figure 5.12 NF-κB and intracellular $Ca^{2+}$- mediated cellular protection against cell death during chronic, severe hypoxia.** H9C2 cells at 70-80% confluence were loaded with $O_2$ equilibrated HEPES buffered-phenol red-free DMEM at 21% (A) or 2% (B) $O_2$ and then immediately cells were treated with 5μM or 10μM NF-κB inhibitor (SN-50) or 5mM or 10mM EGTA and vehicle for control cells at t= -2min and exposed for 2% $O_2$ chronic, severe hypoxia. MTT was added 2h prior to completion of 4h hypoxia and MTT reduction was determined at 570nm in a microplate reader. Cell viability was analysed with respect to control cells maintained at the same $O_2$ tension for the same time period. *** (control vs. Treatment; SN-50 or EGTA) represent $P < 0.001$ (one-way ANOVA), Tukey's post-hoc test.

## 5.4 Discussion

In summary, the present study shows that rat cardiomyoblasts under acute, severe hypoxia die by necrosis, but depletion of ATP during has not contributed to significant necrotic cell death. Mitochondrial complex I inhibition affords protection against apoptosis and necrosis, but mitochondrial uncoupling protect cells against necrosis only during acute, severe hypoxia. In contrast, apocynin treatment or inhibition of NOS isoforms protect cells against mild hypoxia induced apoptosis. Moreover, the activity of redox sensitive transcription factor, NF-κB and extracellular [$Ca^{2+}$] is required to maintain metabolism during chronic, severe hypoxia (see **Figure 5.13** and **Table 5.1**).

Cell death is a critical cellular process involved in the pathogenesis of myocardial hypoxia and hypoxia-reperfusion injury. Hypoxia-induced cell death can take place via apoptosis or necrosis. However, investigation of the significance of myocyte-initiated cell death to overall myocardial injury *in viv*o is technically difficult due to the heterogeneity of cell types in the heart, involvement of neurohormonal systems and inflammatory tissue damage. Therefore, cultures of cardiomyoblasts provide a convenient approach to overcome those complications. The data show that severe hypoxia can induce a time-dependent reduction in metabolic activity in viable cells as measured by MTT assay, and impaired mitochondrial energy production and ion homeostasis may lead to cell injury and cell death. In an MTT assay, in the presence of oxidised equivalents from the mitochondrial respiratory chain, 3-[4, 5-dimethylthiazol-2-yl] - 2, 5 diphenyltetrazolium bromide (MTT) is reduced by succinate dehydrogenase (SDH) in viable cells to insoluble violet formazan crystals (van de Loosdrecht et al., 1994). Crawford et al. (2003) reported a decrease in activity of SDH in mitochondrial complex II during hypoxia. Changes to the activity SDH affects the efficiency of MTT reduction in hypoxic cells, but this may be independent of cell death. In contrast, Hohl et al. (1987) demonstrated an increase in SDH activity during hypoxia and which was sensitive to rotenone treatment. Kinnula and Juujärvi. (1976) reported the absence of SDH activity during 3h anoxia in newborn rat heart and liver cells. An increase in PI uptake during both acute and chronic, severe hypoxia indicates necrotic cell death and probably late apoptotic cell death too.

This is further reflected in the decreased mitochondrial metabolic activity during acute, severe hypoxia. However, there was no evidence for cells with fragmented nuclei that may reflect late apoptotic conditions. Cellular necrosis is associated with tissue inflammation and cytolysis in cell cultures when they are exposed to hypoxia. Cellular ATP depletion that occurs in apoptosis may lead to necrosis; therefore mechanisms of cell death are quite likely to be overlapping via both necrosis and apoptosis (Lieberthal et al., 1998). Therefore, technically it is difficult to understand particular cell death mechanism in a cell culture system as these processes are frequently overlapped during hypoxia. It is mainly due to cells undergoing with natural apoptosis and their apoptotic bodies may not be cleared out, as there is not a phagocytic clearance system in *in vitro* cell culture system. Even though the sequence of cell death events is widely accepted, most probably with necrosis, the associated mechanisms and temporal relationship to events of apoptosis in the mitochondria during hypoxia are enigmatic to date.

Recent reports describe an elevation of intracellular [$Ca^{2+}$], which can cause depolarization of mitochondria during hypoxia (Kim et al., 2003; Crow et al., 2004; Crompton, 1999). The present study did not assess intracellular $Ca^{2+}$ level; however, the experiments reported here show that blockade of $Ca^{2+}$ uptake into cells by chelation of extracellular $Ca^{2+}$ with EGTA increased cell death in hypoxia but not normoxia, suggesting that $Ca^{2+}$ influx is important in mediating cellular defence against hypoxia-induced cell death. This is consistent with finding of Persson-Rothert et al. (1994) who demonstrated. Intracellular $Ca^{2+}$ is important to maintain mitochondrial membrane potential via $Ca^{2+}$ buffering (Crompton, 1999). However, the majority of studies report that chelating $Ca^{2+}$ may disrupt $Ca^{2+}$ influx into mitochondria and thereby reduce MPTP opening and consequently reduce apoptosis (Halestrap et al., 2004). Other sources of $Ca^{2+}$ available including endoplasmic reticulum stores (Hajnóczky et al., 2006; Gibson and Huang, 2004; Crompton, 1999), may release $Ca^{2+}$ and increase the intracellular $Ca^{2+}$concentration to induce cell death during hypoxia. There is evidence for the accumulation of oxidised DNA, protein and lipids during ischaemia (England et al., 2003; Berlett and Stadtman, 1997). Indeed, the present studies show an increase in protein carbonyls in H9C2 cell lysates after severe hypoxia for 30mins, but this does not persist at 4h.

Therefore, an increase in $O_2^{-\bullet}$ production may have contributed to form protein carbonyls whilst maintaining steady state of $O_2^{-\bullet}$ production or early accumulation of oxidised proteins in the absence of a detectable increase in ROS may arise from the absence of effective proteaosome induction or autophagy (Asa B. Gustafsson and Roberta A. Gottlieb, 2008). Early accumulation of oxidised proteins may cause severe damage to cells, and selective death may remove the cells that are heavily oxidised resulting in less protein carbonyl detection in resistant cells at later times (4h) (Yaglom et al., 2003). This is consistent with the evidence for cell death (PI: hoechst ratio) after 30 min of severe hypoxia. In conditions where severe hypoxia is prolonged for 4h, cardiac myoblasts display increased PI uptake and reduced MTT reductive activity compared to control cells or cells under acute, severe hypoxia. This was associated with a significant rise in $O_2^{-\bullet}$ levels, measured as DHE oxidation. Cleavage of procaspase-3 in cells can be stimulated by short term exposure to $O_2^{-\bullet}$ (Madesh and Hajnoczky, 2001). However, chronic, severe hypoxia-mediated apoptosis was prevented only in the presence of rotenone. The prevention of necrosis, measured as PI uptake, and MTT reductive activity was also preserved by L-NAME.

Taking these findings together, indicates that increased ROS/RNS levels detected during chronic, severe hypoxia are associated with toxicity and that inhibiting ROS/RNS affords protection. The cleavage of procaspase-3 suggest the opening of MPTP during chronic, severe hypoxia possibly as a response to increased $O_2^{-\bullet}$ production (Kim et al., 2003; Crompton, 1999). However, inhibition of NOS isoforms indicates that limited production of $^{\bullet}NO$ has contributed to reduce the cellular toxicity, probably by forming less $ONOO^-$. There are several reports which claim that cardiac cell death is induced by increased production of $ONOO^-$ (Levrand et al., 2006; Borutaite and Brown, 2005). It has been reported that a reduction of cardiac dysfunction is observed in hypoxic mice when they were pre-treated with 2mM L-NAME (Mammen et al., 2003). The suppression of procaspase-3 cleavage in the presence of rotenone and associated reduction of DHE oxidation indicate that mitochondrial-based $O_2^{-\bullet}$ is responsible for the induction of apoptosis during severe hypoxia. Indeed, others have shown the cardiac protection of ischaemic-rabbit hearts in the presence of rotenone with decreased production of ROS from mitochondrial complex I (Lesnefsky et al., 2004).

Therefore, the present study confirms cardiac protection observed during chronic, severe hypoxia in the presence of FCCP and rotenone and is consistent with previous findings (Brennan et al., 2006b; Brennan et al., 2006a; Lesnefsky et al., 2004).

**(A)**

| Condition | Acute, severe hypoxia (2% $O_2$, 30min) | | | | | Acute, mild hypoxia (10% $O_2$, 30min) | | | | | Acute normoxia (21% $O_2$, 30min) | | | | |
|---|---|---|---|---|---|---|---|---|---|---|---|---|---|---|---|
| **Inhibitors** | **Ctl** | **ROT** | **FCP** | **APO** | **LNM** | **Ctl** | **ROT** | **FCP** | **APO** | **LNM** | **Ctl** | **ROT** | **FCP** | **APO** | **LNM** |
| **Metabolic activity** | ↓* | X | ↑ | X | X | X | X | ↑ | X | X | X | X | X | X | X |
| **Necrosis** | ↑* | ↓ | ↓ | X | ↓ | X | X | ↑ | X | X | X | X | X | X | X |
| **ATP depletion** | X | - | - | - | - | X | - | - | - | - | X | - | - | - | - |
| **Apoptosis** | X | - | - | - | - | X | - | - | - | - | X | - | - | - | - |
| **Protein carbonyls** | ↑* | - | - | - | - | X | - | - | - | - | X | - | - | - | - |

**(B)**

| Condition | Chronic, severe hypoxia (2% $O_2$, 4h) | | | | | Chronic, mild hypoxia (10% $O_2$ ,4h) | | | | | Chronic normoxia (21% $O_2$, 4h) | | | | |
|---|---|---|---|---|---|---|---|---|---|---|---|---|---|---|---|
| **Inhibitors** | **Ctl** | **ROT** | **FCP** | **APO** | **LNM** | **Ctl** | **ROT** | **FCP** | **APO** | **LNM** | **Ctl** | **ROT** | **FCP** | **APO** | **LNM** |
| **Metabolic activity** | ↓* | ↑ | X | X | ↑ | X* | X | ↓ | ↓ | ↓ | X | X | X | X | X |
| **Necrosis** | ↑* | ↓ | X | ↓ | ↓ | X* | X | X | X | X | X | X | X | X | X |
| **ATP depletion** | ↑* ¤ | ↑ | ↑ | - | - | ↑* | - | - | - | - | X | ↑ | ↑ | - | - |
| **Apoptosis** | ↑* | ↓ | ↓ | ↑* | ↓ | ↑* | ↑* | ↑* | ↓ | ↓ | X | X | X | X | X |
| **Protein carbonyls** | X* | - | - | - | - | X* | - | - | - | - | X | - | - | - | - |

**Table 5.1 Summary of results in acute (A) and chronic (B) hypoxia.**

**Key:** Ctl - control, ROT-rotenone, FCP- FCCP, APO- apocynin and LNM- L-NAME.

↑* - Significant increase in control cells (2% $O_2$ or 10% $O_2$) vs. normoxic control cells.

↓* - Significant decrease in control cells (2% $O_2$ or 10% $O_2$) vs. normoxic control cells.

↑ - Significant increase in treated cells vs. control cells at same $O_2$ tension.

↓ - Significant decrease in treated cells vs. control cells at same $O_2$ tension.

X - In treated cells, no significant difference vs. control cells at same $O_2$ tension or if in control cells (2% $O_2$ or 10% $O_2$), no significant difference vs. normoxic cells or in normoxic cell shows the basal effect.

**X*** - No significant effect in control cells (2% $O_2$ or 10% $O_2$) vs. normoxic control cells.

¤ - Significant increase in control cells (2% $O_2$) vs. cells at 10%$O_2$

- Not available.

Chronic, mild hypoxia has induced procaspase-3 cleavage even in the absence of detectable increases in $O_2^{-\bullet}$ production and lack of ATP production (25% ATP depletion during chronic, mild hypoxia). This is associated with significantly increased $^{\bullet}NO$ production in the absence of increased $O_2^{-\bullet}$. Procaspase-3 cleavage was inhibited in the presence of L-NAME, reducing NOS-dependent $^{\bullet}NO$ production. In contrast, the absence of necrotic cell death or change in MTT reductive activity indicates steady state mitochondrial function. However, MPTP opening is required for the activation of procaspase-3. Crompton et al. (1999) reported procaspase-3 cleavage that associated with MPTP opening in the absence of mitochondrial $O_2^{-\bullet}$. This probably occurred via the induction of pro-apoptotic factors with available ATP, the other authors noted that apoptosis was induced during chronic, severe hypoxia, when 50% of ATP was depleted. Interestingly, the suppression of procaspase-3 cleavage in the presence of apocynin may suggest a NOX-independent effect as there is no $O_2^{-\bullet}$ produced during chronic, mild hypoxia (Heumuller et al., 2008; Touyz, 2008).

It has been reported hypoxia-induced HIF-1α activation is associated with transcription of cellular antioxidant genes. The NF-κB transcription factor is known as both a death factor and a survival factor during oxidative stress. The present study indicates that inhibition of NF-κB exacerbates the hypoxia induced cell death, suggesting that NF-κB mediates a hypoxia-induced antioxidant defence mechanism as previously reported ischaemia in rat cerebral endothelial cells (Lee, 2003)**.** Therefore, NF-κB may play a vital role in hypoxic defence mechanism, probably by expression of antioxidant genes including MnSOD.

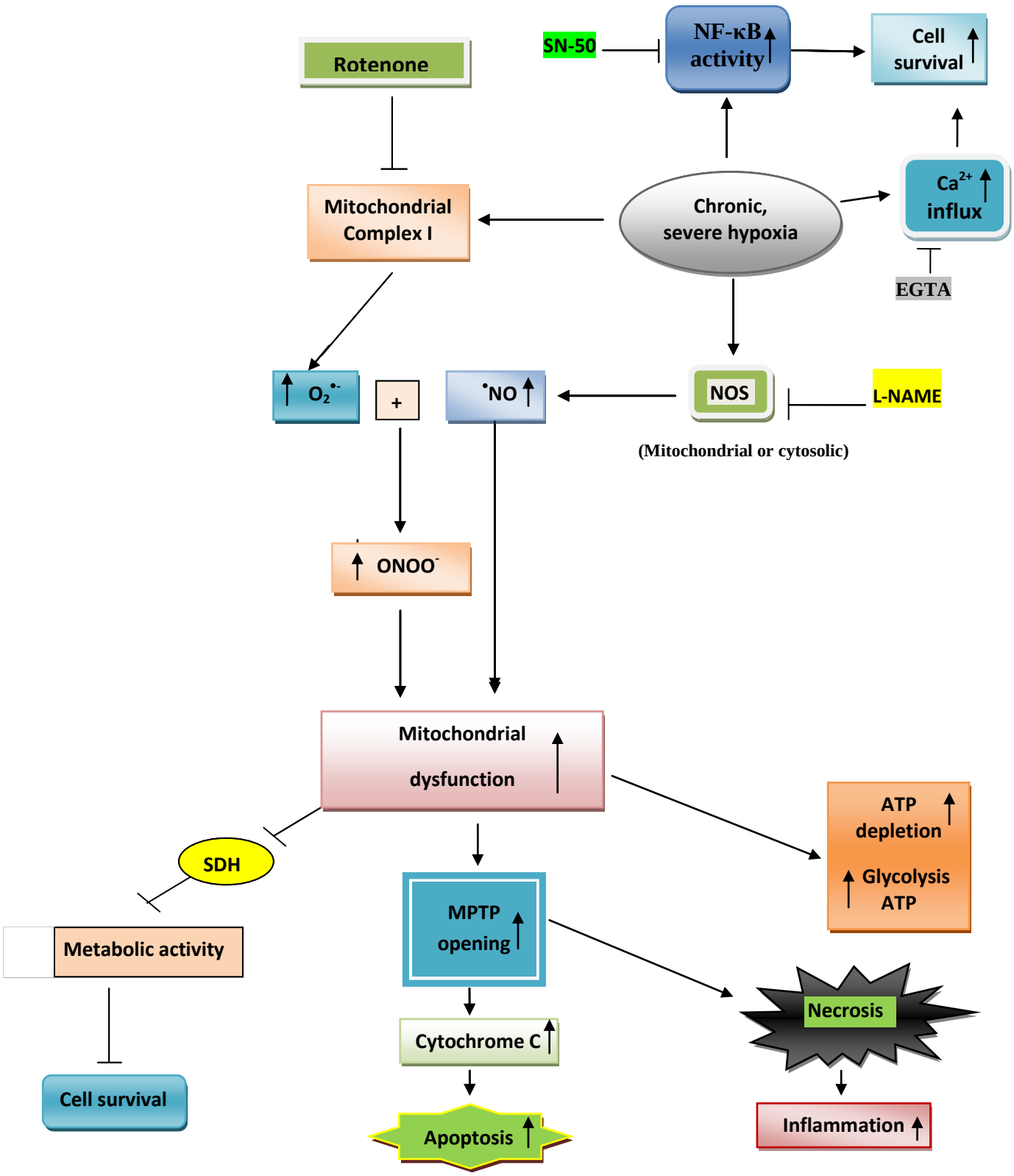


**Figure 5.13 Hypoxia or hypoxia/reperfusion-induced ROS/RNS generation and cell death. ↑- increase or ↓ - decrease.**

# CHAPTER 6

# HYPOXIA/REPERFUSION-INDUCED ROS/RNS GENERATION AND ASSOCIATED CELL DEATH

## 6.1 Preface

This chapter describes the generation of $O_2^{-\bullet}$ and $^{\bullet}NO$ during acute, severe hypoxia/reperfusion and chronic, severe hypoxia/reperfusion and their association with mitochondrial metabolic dysfunction. $O_2^{-\bullet}$ and $^{\bullet}NO$ combine at diffusion controlled rates to produce $ONOO^-$ and may affect cell function. The independent contribution of different radical sources was investigated using inhibitors of mitochondrial uncoupling, the superoxide scavenger MnTBAP, and a $^{\bullet}NO$ donor. The goal of this chapter was to identify whether ROS/RNS generation was more significant during reperfusion than hypoxia alone and to understand the sources of ROS/RNS.

## 6.2 Introduction

### 6.2.1 Hypoxia/reperfusion-induced ROS/RNS generation

Reperfusion of hypoxic tissue is an important mechanism of cell and tissue injury. Hypoxia/reperfusion (H/R) increases ROS/RNS and attenuation of these radical species can protect cardiomyocytes from the irreversible damage of hypoxia/reperfusion (Li and Jackson, 2002). While the rapid restoration of blood supply to hypoxic tissue is imperative to minimise injury, paradoxically, reperfusion itself can lead to excessive injury in the form of cardiac dysfunction, reperfusion arrhythmias and irreversible myocardial infarction. The severity of hypoxia influences the outcome for cell damage during reperfusion. Hypoxic tolerance for various tissues differs and depends on their metabolic rate and intrinsic adaptive potential (Li et al., 2002). Acute, sublethal hypoxia has no reported deleterious effects and can enhance resistance to reperfusion injury (preconditioning). The extent of cellular injury after hypoxia/reperfusion is due to a balance of energy availability, mitochondrial ROS/RNS generation and adaptation. Other sources of ROS in cardiovascular tissue include the NADPH oxidase complex (Lopez-Barneo et al., 2001) and xanthine oxidase (Lee et al., 2009). ROS production during hypoxia/reperfusion may be due to other sources than mitochondria.

The membrane associated NADPH oxidase complex that generates $O_2^{-\bullet}$ under normoxic conditions has been implicated in ROS generation during ischaemia/reperfusion (Walder et al., 1997). NADPH oxidase is a major source of ROS generation in the intact heart, whose activity appears to be increased by several stimuli such as PKC, angiotensin II, and TNFα in vascular diseases (Murdoch et al., 2006). Moreover, the membrane oxidase complex is an important source of ROS in ischaemic mouse lungs and other oxygenated tissues (Li and Jackson, 2002). $^{\bullet}$NO has favourable and unfavourable activities in cardiac ischaemia/reperfusion injury (Brown and Borutaite, 2007); many of the deleterious effects in cardiomyocytes can be attributed to the overproduction of $^{\bullet}$NO by NOS isoforms, most probably due to activation of iNOS and/or eNOS during hypoxia (Zenebe et al., 2007). During the early stage of reperfusion, the myocardium produces a large concentrated burst of $^{\bullet}$NO.

At the same time that $^{\bullet}NO$ is being produced, large amounts of $O_2^{-\bullet}$ are also generated and these molecules combine at diffusion controlled rates to produce $ONOO^-$. $^{\bullet}NO$ outcompetes SOD for $O_2^{-\bullet}$ (Beckman and Koppenol, 1996), so under normoxia the dismutation of $O_2^{-\bullet}$ by SOD is likely to predominate over $ONOO^-$ genesis due to the low concentration of $^{\bullet}NO$ available. However, when both $^{\bullet}NO$ and $O_2^{-\bullet}$ increase during reperfusion, $^{\bullet}NO$ can outcompete intracellular SOD for the reaction with $O_2^{-\bullet}$.

It is worthwhile to consider that in a physiological $CO_2/HCO_3^-$ environment, $^{\bullet}NO$ reacts with $CO_2$ to form nitrosoperoxycarbonate anion ($ONOOCO_2^-$). The protonation and homolytic cleavage of this molecule results in $NO_2$, $^{\bullet}OH$ and $CO_2$ and ultimate cellular injury is associated with highly reactive $NO_2$ and $^{\bullet}OH$ in addition to peroxynitrite (Zweier et al., 1999; Lepore, 2000). The accumulation of $ONOO^-$ is associated with cell injury or cell death, possibly due to lipid peroxidation and nitration of tyrosine residues. It has been reported that $ONOO^-$ can irreversibly inhibit mitochondrial complexes I, II, IV and V. Further, $ONOO^-$ can react with NADH present in complex I and change the mitochondrial redox state. Jiao et al. (2009) and Lalu et al. (2002) showed an increase in tissue injury with $^{\bullet}NO/ONOO^-$, where cardiac cell death was attenuated by inhibiting $ONOO^-$ formation. $^{\bullet}NO$ from mtNOS can combine with $O_2^{-\bullet}$ to form $ONOO^-$ within the mitochondrial compartments (Ghafourifar and Cadenas, 2005).

This $ONOO^-$ derived from mtNOS can cause oxidation of mitochondrial components and result in release of key mitochondrial pro-apoptotic factors such as cytochrome *c* (Ghafourifar et al., 1999) and thereby activate caspase-3 cleavage in apoptotic cell death. In contrast to the cytotoxic effects of $^{\bullet}NO$, $^{\bullet}NO$ generation during ischaemia-reperfusion may act as an antioxidant in mitochondria to attenuate hypoxia/reperfusion injury. $^{\bullet}NO$ can inhibit lipid peroxidation and exert protective effects in many *in vitro* and *in vivo* hypoxia/reperfusion models (Li and Jackson, 2002). The pre-exposure of cardiomyocytes to hypoxia increases iNOS mRNA and protects against subsequent chronic ischaemia (Rakhit et al., 2000). $ONOO^-$ can also act as a signalling molecule in cardiac protection during reperfusion-injury (Ottenheijm et al., 2006).

The non-selective NOS inhibitor; LNAME, blocked cardiac preconditioning, but addition of the $^{\bullet}$NO donor; S-nitroso-N-acetyl-L-penicillamine (SNAP), protected cells during reoxygenation (Gonon et al., 2004; Li et al., 1999b)**.** Therefore, the protective effects of $^{\bullet}$NO depend critically on the severity of hypoxia ($pO_2$), its duration and the balance of $^{\bullet}$NO and $O_2^{-\bullet}$ production at intracellular level (Huang et al., 1997).

### 6.2.2 ROS generation from NADPH oxidase

Structurally, NADPH oxidase is a multimeric enzyme that is constructed of core membrane-bound flavocytochrome comprising a catalytic NOX subunit and smallest p22phox subunit. Currently, there are five NOX isoforms (NOX1–5) which have been identified in different tissues **(**Bedard and Krause, 2007). Among them, NOX2 and NOX4 are the main isoforms of NADPH oxidase complex that are expressed in cardiac cells (Bendall et al., 2002). In order to activate, NOX4 or NOX2 (or gp91phox), the complex association of cytosolic regulatory subunits (p47phox, p67phox, p40phox and Rac1) are required (Bedard and Krause, 2007). The GTPase binding protein Rac1 regulates membrane NADPH oxidase activity, NF-κB activation and mouse liver necrosis during liver ischaemia-reperfusion (Ozaki et al., 2000). The increase in subunit expression and/or the translocation of regulatory subunits (in particular p47phox) from cytosol to the membrane are necessary to stimulate NOX2 activation and ROS production (Bedard and Krause, 2007).

Recently, it has been reported that NADPH oxidase activity is increased in the left and right ventricle of myocardium of patients with end-stage of heart failure (Elisabetta et al., 2008). In summary, there are many possible sources of ROS/RNS that may contribute to hypoxia/reperfusion injury and their respective roles in affecting cardiac myocyte metabolism are investigated in the following chapter.

## 6.3 Results

### 6.3.1 Hypoxia/reoxygenation decreased metabolic activity and viability of cardiac myoblasts

The overproduction of ROS/RNS during hypoxia/reperfusion may lead to mitochondrial dysfunction with associated cell death (Petrosillo et al., 2005; Abramov et al., 2007)**.** To test this hypothesis, the following experiments were performed to determine acute or chronic hypoxia/reperfusion-induced metabolic change and cell death. As illustrated in **figure 6.1A**, hypoxia (30min)/reoxygenation (2h) did not induce a significant reduction in cell viability or mitochondrial metabolic activity compared to normoxia or hypoxia-maintained control cells (91.78±4.81% vs. 100.00±6.13%, $P>0.05$). However, the hypoxia control at 2% $O_2$ for 2.5h showed a significant reduction in metabolic activity and cell viability compared to the normoxia control (78.05±4.26 vs. 100.00±6.13%, $P<0.0001$). Moreover, hypoxia (30min)/reoxygenation (2h) promoted mitochondrial metabolism by 14% compared to the hypoxia-maintained control during the reoxygenation period (91.78±4.81% vs. 78.05±4.26%; $P<0.05$).

When cells were exposed to reoxygenation (2h) after chronic, severe hypoxia (2% $O_2$, 4h), and mitochondrial metabolic activity was measured by MTT assay, **figure 6.1B**, shows a significant reduction in metabolic activity compared to normoxia controls (85.21±1.41% vs. 100.00±1.77%, $P<0.001$). Chronic, severe hypoxic controls showed a greater loss of mitochondrial metabolic activity compared to normoxia controls (77.78±1.51% vs. 100.00±1.77%, $P<0.0001$). However, total protein concentration after chronic, severe hypoxia/reoxygenation showed the greatest trend for loss (**Figure 6.1C**) (see **Table 6.1** for summary of results).

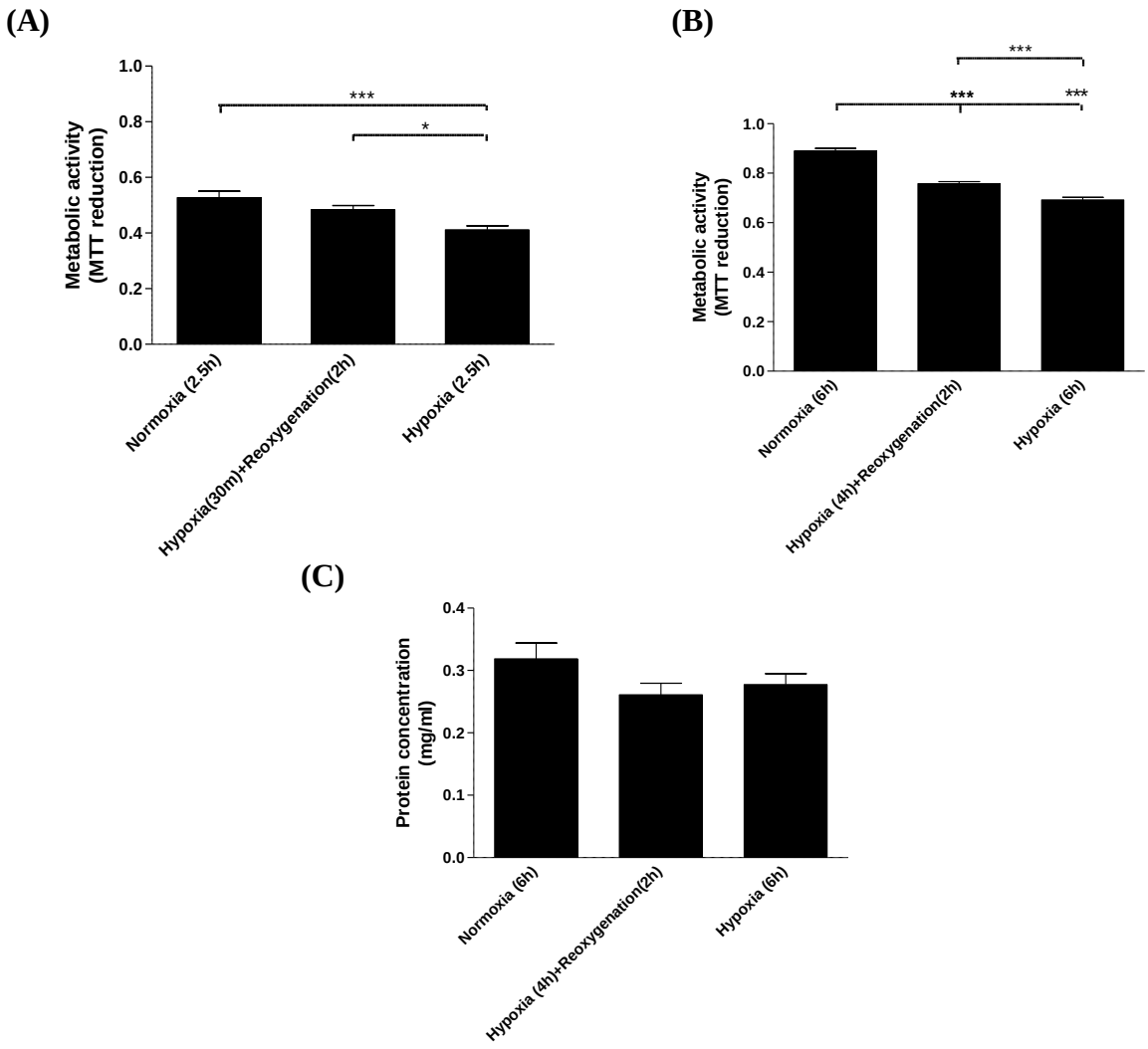


**Figure 6.1 Hypoxia/reoxygenation effects on metabolic activity and protein concentration of cells.** H9C2 cells were seeded at $3x10^4$/well in 24-well plate and cultured until 70-80% confluence in DMEM, 10% FBS at 37°C in 5% $CO_2$ humidified atmosphere. At 70-80% confluence, cells were washed three times with PBS solution and 2% $O_2$ equilibrated, HEPES-buffered, phenol red-free DMEM was added and cells were exposed for hypoxia in a chamber at 2% $O_2$ for 30min (acute hypoxia, A) or 4h (chronic hypoxia, B) and protein concentration (C). After hypoxia, the medium was replaced with reoxygenated (21% $O_2$+79% $N_2$) medium for experimental cells (hypoxia/reoxygenation) and normoxic controls, and fresh $O_2$ pre-equilibrated (2% $O_2$ + 98% $N_2$) medium in hypoxic control cells (sustained hypoxia). Then, experimental and control cells were treated with MTT reagent and incubated for 2h in either severe hypoxia or normoxia in the chamber. After 2h incubation, cells were lysed and re-incubated for further 16h at 37°C in 5% $CO_2$ in humidified atmospheric conditions. The optical density was measured at 570nm. Data represents the mean±S.E.M of three independent experiments conducted in triplicates. * represents $P < 0.05$ and *** represents $P < 0.001$ (one-way ANOVA), Tukey's post-hoc test.

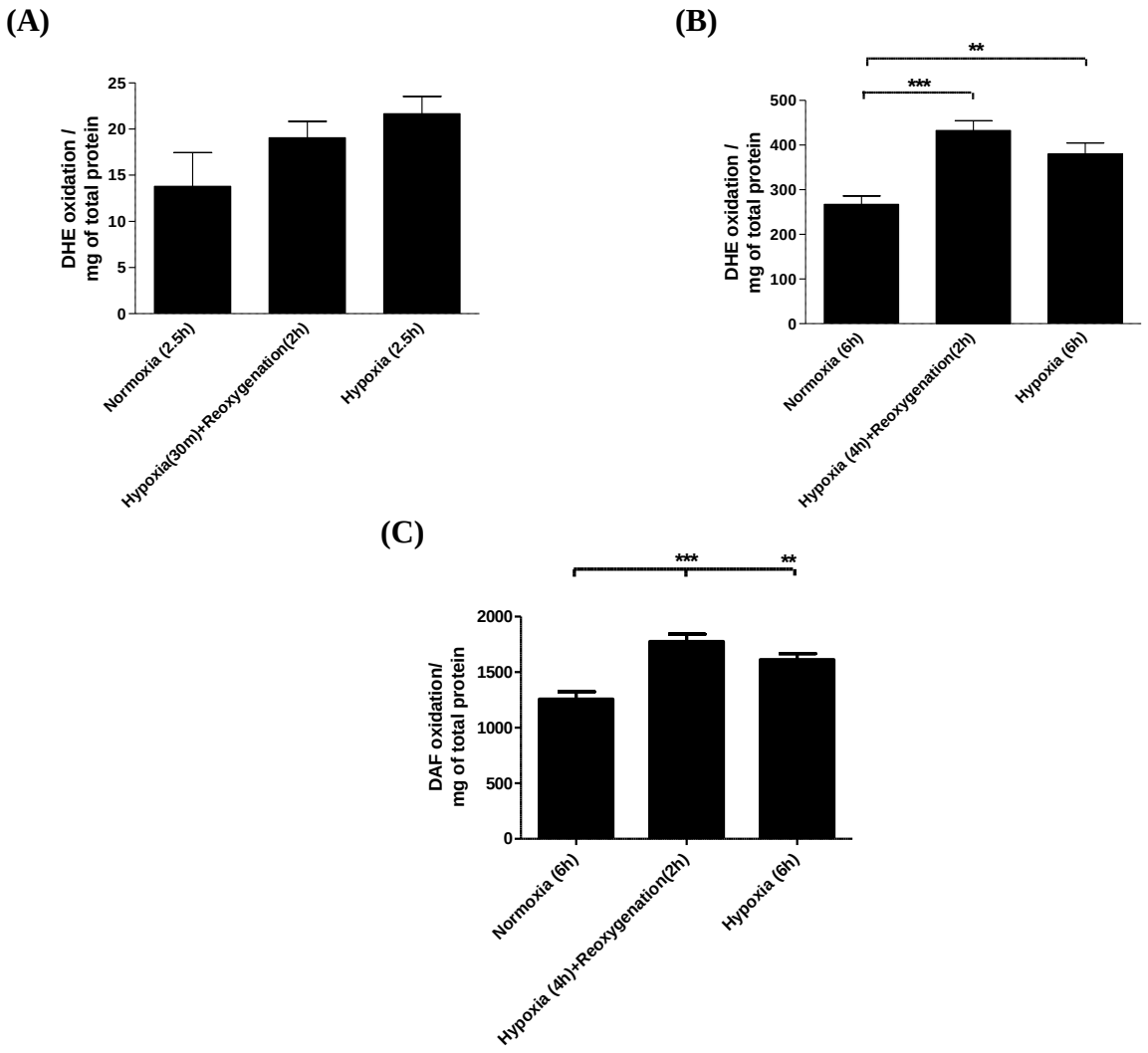


**Figure 6.2 Hypoxia/reoxygenation-induced $O_2^{-\bullet}$ and $^{\bullet}NO$ generation.** H9C2 cells were seeded at $3x10^4$/well in 24-well plate and cultured in DMEM, 10% FBS at 37°C in 5% $CO_2$ humidified atmosphere. At 70-80% confluence, cells were washed three times with PBS solution and 2% $O_2$ equilibrated, HEPES-buffered, phenol red-free DMEM was added and cells were exposed for hypoxia in a chamber at 2% $O_2$ for 30min or 4h. After hypoxia, the medium was replaced with reoxygenated (21% $O_2$+79% $N_2$) medium for experimental cells and normoxic controls, and fresh $O_2$ pre-equilibrated (2% $O_2$+98% $N_2$) medium for hypoxic control cells and then exposed for 2h reoxygenation or normoxia. Then, cells in acute hypoxia were treated at t=1h and 45min with 20µM DHE for acute hypoxia/reoxygenation (A) whereas, cells in chronic, severe hypoxia were treated at t=5h and 15minMTT with 20µM DHE (B) or at t=5h and 30min with 10µM DAF (C) and further incubated until completion of 2h reoxygenation. Then, cells were lysed and fluorescence was measured at 37°C in Spectramax GEMINI EM fluorescence reader at Excitation: 488nm, Emission; 570nm, cut off filter; 550nm. The optical density was measured at 570nm. Data represents the mean±S.E.M of three independent experiments conducted in triplicates. ** represents $P < 0.01$ and *** represents $P < 0.001$ (one-way ANOVA), Tukey's post-hoc test.

### 6.3.2 Hypoxia/reoxygenation induced $O_2^{-\bullet}$ generation

A greater, significant increase in $O_2^{-\bullet}$ production during hypoxia/reperfusion than hypoxia alone was previously reported to result in mitochondrial dysfunction and triggered cell death during reperfusion (Li and Jackson, 2002). To investigate whether hypoxia/reoxygenation may increase $O_2^{-\bullet}$ production more than hypoxia alone in rat myoblasts, $O_2^{-\bullet}$ production was measured as described in section 2.3.9.2.

As shown in **figure 6.2B** but not **figure 6.2A**, DHE fluorescence was significantly increased after 2h but not 30min reoxygenation compared to hypoxic and normoxic controls, suggesting a significant increase in $O_2^{-\bullet}$ production during the reoxygenation period alone after chronic, severe hypoxia (161.96±14.00% of normoxic control, P<0.0001). The DHE fluorescence in cells after reoxygenation increased by ~14% compared to that of cells maintained in chronic, severe normoxia (100%), but was not significantly different under the conditions employed in this study. Hypoxic controls alone significantly increased DHE fluorescence compared to normoxia (142.25±13.69%, P<0.001)**.** In contrast, acute, severe hypoxia/reoxygenation did not significantly increase DHE fluorescence, however acute hypoxia alone showed an increasing trend of DHE fluorescence compared to normoxia (**Figure 6.2A**).

### 6.3.3 Hypoxia/reoxygenation increases $^{\bullet}$NO generation

It has been reported that an increase in myocardial $^{\bullet}$NO production occurs during hypoxia/reperfusion. To test this hypothesis, $^{\bullet}$NO generation during chronic, severe hypoxia/reoxygenation was measured by quantitative oxidation of DAF-2-DA (a fluorescent probe for $^{\bullet}NO/ONOO^-$) following the method described in section 2.3.9.2. As illustrated in **figure 6.2C**, chronic, severe hypoxia/reoxygenation significantly increased DAF fluorescence compared to normoxia (141.26±21.83% vs. 100.00±15.92, P<0.001). In control hypoxic cells, the increase in DAF fluorescence was also significant compared to normoxia (128.35±19.71% of control, P<0.01).

Chronic, severe hypoxia/reoxygenation showed a trend towards an increase in DAF fluorescence compared to the hypoxic control, but was not statistically significant (**Figure 6.2C**).

### 6.3.4 Respiratory chain inhibition or uncoupling, or inhibition of NADPH oxidase complex decrease DHE oxidation during chronic, severe hypoxia/reoxygenation

To identify whether mitochondria and NADPH oxidase-dependent production of $O_2^{-\bullet}$ are implicated in the toxicity of hypoxia/reperfusion, the effect of H9C2 incubation with mitochondrial complex 1 inhibitor rotenone (20μM), the uncoupler FCCP (1μM) or the NADPH oxidase (NOX) inhibitor apocynin (100μM) were examined during chronic severe hypoxia (4h) and reoxygenation (2h). Control cells received an equal volume of vehicle and were exposed to hypoxia or normoxia for 6h. MnTBAP was employed as a $O_2^{-\bullet}$ scavenger.

As illustrated in **figure 6.3C**, the mitochondrial uncoupler FCCP, and the inhibitor of respiratory chain rotenone, had no effect on DHE oxidation during the last 2h of normoxia. However, the presence of rotenone or FCCP reduced DHE oxidation significantly during chronic, severe hypoxia/reoxygenation and chronic, severe hypoxia alone (FCCP; 62.42±2.21% or rotenone; 62.42±7.05% of control, $P<0.0001$) (**Figure 6.3A and 6.3B**).

In contrast, apocynin treatment significantly reduced DHE oxidation by 19% during chronic, severe hypoxia/reoxygenation (81.00±2.47% compared to untreated H/R cells $P< 0.05$) (**Figure 6.3A**). In control hypoxic or normoxic cells, apocynin failed to protect against DHE oxidation as shown in **figures 6.3B and 6.3C**. In the presence of MnTBAP, DHE oxidation was significantly decreased during chronic, severe hypoxia/reoxygenation, or hypoxia and normoxia (**Figures 6.3A, 6.3B and 6.3C**) (see **Table 6.1** for summary of results).

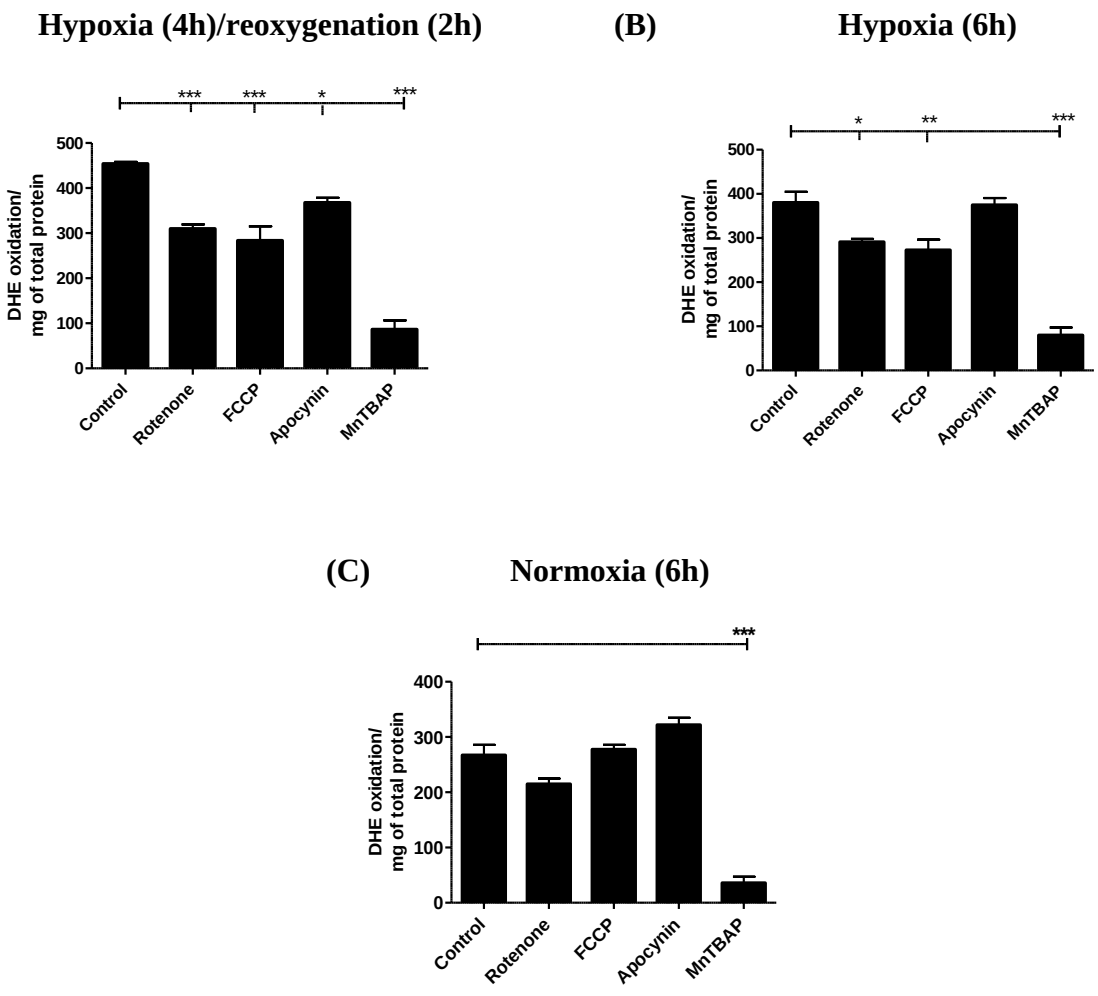


**Figure 6.3 Effects of mitochondrial uncouplers and inhibitors of the respiratory chain and respiratory burst on $O_2^{-\bullet}$ generation during chronic, severe hypoxia/reoxygenation.** H9C2 cells were seeded at $3x10^4$/well in 24-well plate and cultured for 48h in DMEM, 10%FBS at 37°C in 5% $CO_2$ in humidified atmosphere. At 70-80% confluence, cells were washed three times with PBS solution and 2% $O_2$ equilibrated, HEPES-buffered, phenol red-free DMEM was added. Control cells were maintained in 21% $O_2$**.** After 4h hypoxia, old culture medium was replaced with reoxygenated (21% $O_2$+79% $N_2$, A) medium in experimental cells and fresh $O_2$ pre-equilibrated (2% $O_2$ + 98% $N_2$, B or 21% $O_2$ +79% $O_2$, C) medium in control cells. Experimental cells were independently treated with 1µM FCCP or 20µM rotenone or 100µM apocynin or 50µM MnTBAP. Control cells received an equal volume of vehicle. Then, cells were exposed to reoxygenation for 2h at 21% $O_2$ in the chamber and at t=5h and 15min, cells were treated with 20µM DHE and further incubated for 45min.The fluorescence was measured at 37°C in Spectramax GEMINI EM fluorescence reader at Excitation: 488nm, Emission: 570nm, cut off filter: 550nm. Data represent the mean±SEM fluorescence of three independent experiments conducted in triplicates. * represents $P < 0.05$ or ** for $P<0.001$ or *** for $P<0.0001$ (one-way ANOVA), Tukey's post-hoc test.

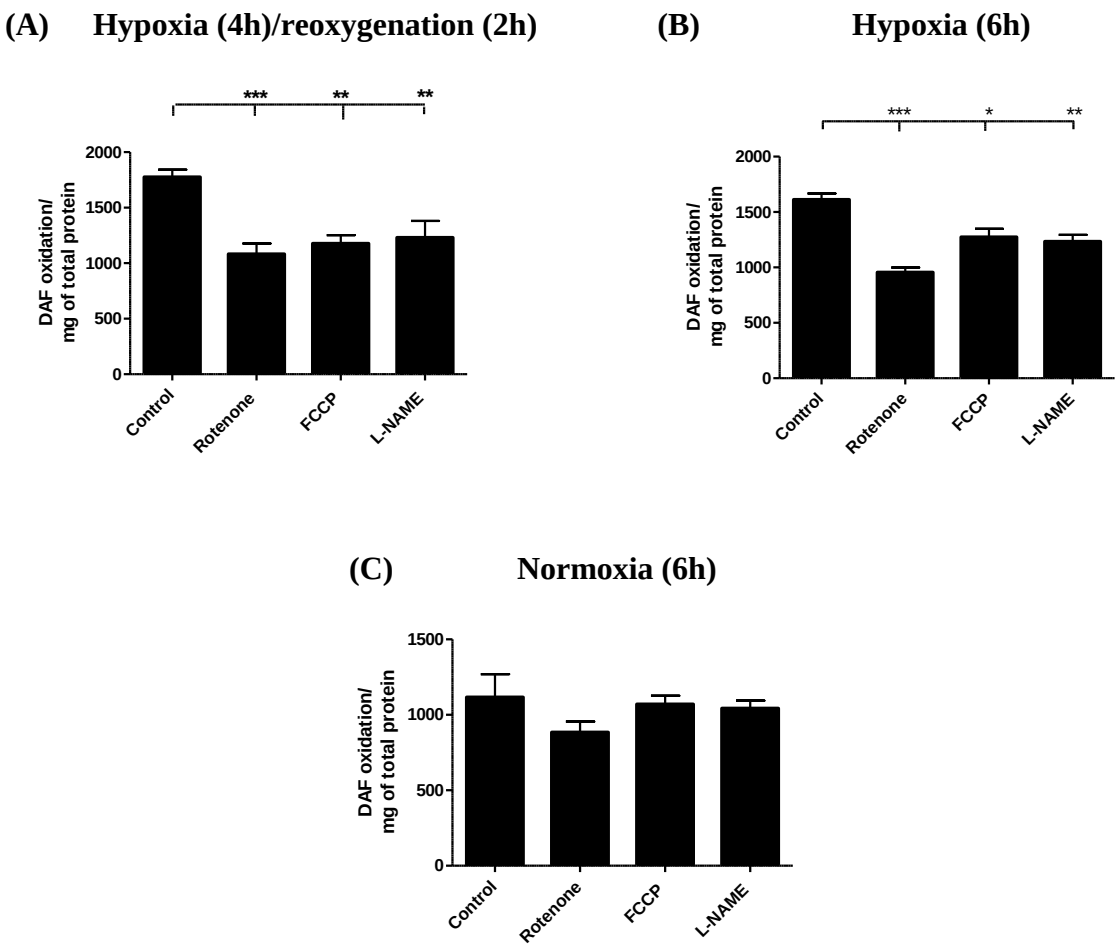


**Figure 6.4 Effects of mitochondrial uncouplers, inhibitors of the respiratory chain and NOS isoforms on RNS generation during chronic, severe hypoxia/reoxygenation.** H9C2 cells were seeded at $3x10^4$/well in 24-well plate and cultured for 48h in DMEM, 10%FBS at 37°C in 5% $CO_2$ in humidified atmosphere. At 70-80% confluence, cells were washed three times with PBS solution and 2% $O_2$ or 21% $O_2$ equilibrated, HEPES-buffered, phenol red-free DMEM was added. After 4h hypoxia, culture medium was replaced with reoxygenated (21% $O_2$+79% $N_2$, A) medium in experimental cells and fresh $O_2$ pre-equilibrated (2% $O_2$ + 98% $N_2$, B or 21% $O_2$ +79% $O_2$, C) medium in control cells. Cells were independently treated with 1µM FCCP or 40µM rotenone or 100µM L-NAME. Control cells received an equal volume of vehicle. Then, cells were exposed to reoxygenation for 2h at 21% $O_2$ in the chamber and at t=5h and 15min, cells were treated with 10µM DAF-2-DA and further incubated for 30min.The fluorescence was measured at 37°C in Spectramax GEMINI EM fluorescence reader at Excitation: 491nm, Emission; 513nm, cut off filter; 495nm. Data represent the mean±SEM fluorescence of three independent experiments conducted in triplicates. * represents $P < 0.05$ or ** for $P<0.001$ or *** for $P<0.0001$ (one-way ANOVA), Tukey's post-hoc test.

### 6.3.5 Respiratory chain inhibition, uncoupling and inhibition of NOS isoforms decrease DAF-2-DA oxidation during chronic, severe hypoxia/reoxygenation

It has been reported that up-regulation of NOS isoforms increases $^{\bullet}$NO during hypoxia/reperfusion (Lacza et al., 2001). In contrast, Lacza et al. (2006) reported that the heart mitochondrion is capable of significant RNS production via the respiratory chain which is independent of the mitochondrial NOS and arginine pathway. To investigate this hypothesis, hypoxia/reperfusion induced $^{\bullet}$NO production was assessed during reoxygenation period, in the presence of mitochondrial complex I inhibitor rotenone (40µM), uncoupler; FCCP (1 µM) and non-selective NOS inhibitor; L-NAME (100 µM). Hypoxic and normoxic controls received an equal volume of vehicle and were exposed to hypoxia (6h) or normoxia (6h).

As illustrated in **figure 6.4C**, the mitochondrial uncoupler FCCP had no significant effect on DAF oxidation during last 2h of normoxia (6h). The presence of rotenone, FCCP and non-selective NOS inhibitor reduced DAF oxidation significantly compared to untreated normoxic cells during last 2h of hypoxia (rotenone; 70.32±6.83%, $P<0.0001$, L-NAME; 80.85±6.02%, $P< 0.05$ of control DAF fluorescence) (**Figure 6.4B**). The effect of the inhibitors; rotenone or L-NAME and the mitochondrial uncoupler FCCP had a similar effect on DAF oxidation during hypoxia/reoxygenation too (**Figure 6.4A**).

The presence of rotenone, FCCP or L-NAME reduced DAF oxidation significantly during chronic, severe hypoxia/reoxygenation (rotenone; 61.00±11.74% FCCP; 66.32±12.15% and 69.30±14.62% as % of controls in the absence of inhibitors) or chronic, severe hypoxia (rotenone; 59.29±3.27% FCCP; 78.95±5.39% and L-NAME; 76.44±4.52 as % of control in the absence of inhibitors) (see **Table 6.1** for summary of results).

### 6.3.6 The effect of MnTBAP and L-NAME on metabolic activity during hypoxia /reoxygenation

To identify whether $O_2^{-\bullet}$, $^{\bullet}NO$ and/or $ONOO^-$ production are implicated in the toxicity of hypoxia/reoxygenation, the effects of MnTBAP and L-NAME were studied during chronic, severe hypoxia/reoxygenation. As illustrated in **figure 6.5A**, treatment of hypoxic cells with MnTBAP during the reperfusion period resulted in a significantly increased mitochondrial metabolic activity compared to untreated cells. In contrast, inhibition of NOS isoforms with L-NAME showed an exacerbation of hypoxia/reoxygenation-induced impairment of mitochondrial metabolic activity by ~17% compared to untreated cells (83.17±1.23% of control $P<0.05$) (**Figure 6.5A**).

In cells maintained in hypoxia in the presence of L-NAME during the last 2h of sustained 6h hypoxia, the mitochondrial metabolic activity was also increased (~12%) significantly compared to untreated cells (111.66±3.42% of control $P<0.001$), suggesting that $^{\bullet}NO$ production may contribute to impaired metabolic activity (**Figure 6.4B**). MnTBAP treated cells also showed a significantly enhanced metabolic activity during hypoxia.

Treatment with the $^{\bullet}NO$ donor, spermine nonoate, did not significantly affect hypoxia/reoxygenation induced mitochondrial metabolic activity compared to untreated, and L-NAME treated cells (spermine nonoate, 99.94±9.4% vs. L-NAME; 83.17±1.23% , $P<0.001$), Spermine nonoate, L-NAME and MnTBAP had no effect on metabolic activity during normoxia for 6h (**Figure 6.5C**) (see **Table 6.1** for summary of results).

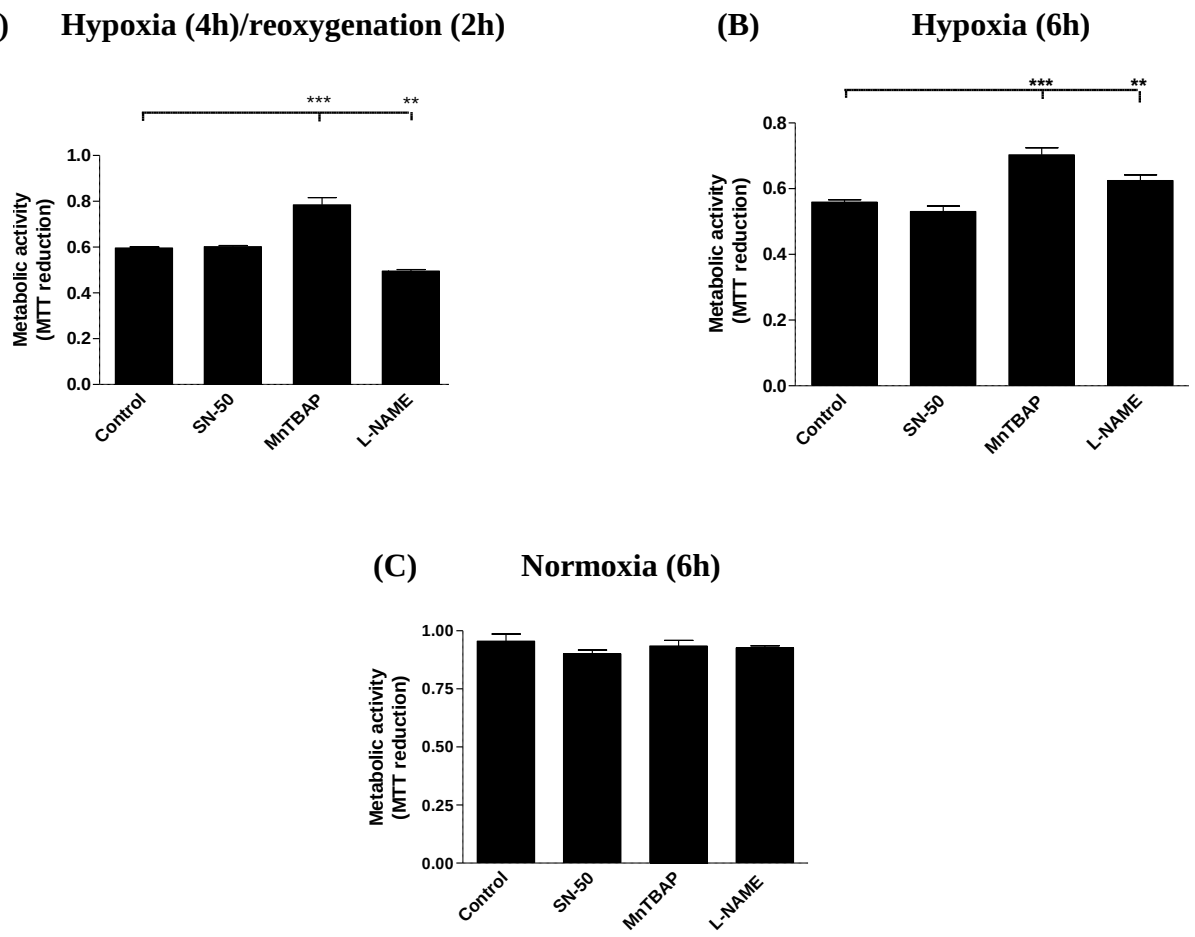


**Figure 6.5 Effect of MnTBAP, L-NAME and spermine nonoate on hypoxia/reoxygenation induced cell death in rat cardiomyoblasts.** H9C2 cells were seeded at $3x10^4$/well in 24-well plate and cultured for 48h in DMEM, 10% FBS at 37°C in 5% $CO_2$ and humidified atmosphere. At 70-80% confluence, cells were washed three times with PBS solution and 2% or 21% $O_2$ equilibrated, HEPES-buffered, phenol red-free DMEM was added. After 4h hypoxia, culture medium was replaced with reoxygenated (21% $O_2$+79% $N_2$, A) medium in experimental cells and fresh $O_2$ pre-equilibrated (2% $O_2$ + 98% $N_2$, B or 21% $O_2$ +79% $O_2$, C) medium in control cells. Cells were independently administered with 10µM SN-50 or 50µM MnTBAP or 100µM L-NAME or 100µM spermine nonoate. Untreated cells received an equal volume of vehicle. Then, cells were treated with the MTT reagent and experimental cells were reoxygenated for 2h at 21% $O_2$ in the chamber whereas control cells at hypoxia and normoxia. After completing hypoxic or normoxic incubations, cells were lysed at t= 6h and reincubated for further 16h at 37°C in 5% $CO_2$ in humidified atmospheric conditions. The optical density was measured at 570nm. Data represents the mean±S.E.M of three independent experiments conducted in triplicates. *** represents $P < 0.0001$ and ** for $P<0.001$ (one-way ANOVA), Tukey's post-hoc test.

### 6.3.7 Inhibition of NF-κB did not exacerbate or inhibit changes to metabolic activity during hypoxia/reoxygenation.

As shown in **figure 6.5A**, the inhibition of NF-κB activation with SN-50 during reoxygenation period did not affect the cellular metabolic activity compared to untreated cells. Treatment with SN-50 in control hypoxic cells during the last 2h of hypoxia did not cause a significant change in metabolic activity (**Figure 6.5B**), unlike the inhibition of NF-κB activation with SN-50 during chronic, severe hypoxia (**Figure 5.12B**).

## 6.4 Discussion

### 6.4.1 Hypoxia/reoxygenation-induced ROS/RNS generation and cell death

Reperfusion refers to the restoration of an oxygenated blood supply to a tissue after a period of ischaemia, which has the potential to save tissue from hypoxic/anoxic cell death, but, paradoxically, oxygenation may result in permanent damage. Growing evidence from animal studies and clinical observations indicates that reperfusion itself can cause cellular or tissue injury by increasing free radicals and/or other inflammatory factors as reported by many authors (Li and Jackson, 2002; Penna et al., 2009; Jiao et al., 2009; Dhalla and Duhamel, 2007). However, the specific mechanism(s) of reperfusion injury, the nature and extent of free radicals produced and the effects of severity and duration of previous hypoxia within the cardiac cells have not been well documented.

It is clear from the present work that chronic, severe hypoxia (4h) and reperfusion (2h) cause overproduction of $O_2^{-\bullet}$ / $^{\bullet}NO$ in rat cardiomyoblasts, probably thereby reducing metabolic activity. However, during the present conditions, acute, severe hypoxia (30min)/reoxygenation (2h) does not cause any increase in $O_2^{-\bullet}$.

Two important sources of $O_2^{-\bullet}$/$^{\bullet}NO$ generation; mitochondria and NOX have been identified in neurones during 2h reoxygenation after 30min ischaemia (Abramov et al., 2007) and mitochondria during 15min reoxygenation after 30min ischaemia in cardiomyocytes (Petrosillo et al., 2005). In contrast, the present work has shown that acute, severe hypoxia/reoxygenation did not elicit increased production of $O_2^{-\bullet}$. This was actually a reduction in $O_2^{-\bullet}$ production from mitochondria, probably due to restoration of the membrane potentials during reoxygenation. Chapter 5 showed that during 30min severe hypoxia alone, cell death and the decrease in metabolic activity was manifest in the absence of a detectable change in $O_2^{-\bullet}$ production **(Figure 4.1)**. Metabolic recovery of cells during reoxygenation after a brief period of severe hypoxia (30min) compared to sustained hypoxia that restores metabolism to normoxic controls is consistent with the cardiac protection during reperfusion as previously reported by Serviddio et al. (2005).

Sirviddio et al. (2005) showed the recovery of mitochondrial function in rat hearts during 40min reperfusion period after 45min ischaemia in respect of mitochondrial glutathione and protein oxidation levels. However, the Sirviddio et al. (2005), reperfusion strategy followed hypoxia with 3min reperfusion with 150mmHg $O_2$ and 47min reperfusion with 600mmHg $O_2$.

Reperfusion after chronic, severe hypoxia also elicited a significant recovery of mitochondrial metabolism compared to hypoxia alone as measured by the MTT assay, but cells did not recover to the extent seen in normoxia. It may suggest that reperfusion after chronic, severe hypoxia is the turning point between irreversible cell damage or hypoxic recovery. Jiao et al. (2009) recently reported significant apoptotic and necrotic cell death during 3h reperfusion after 30min ischaemia induced by coronary occlusion in mouse heart. Potential sources of free radicals during hypoxia/reperfusion include mitochondria, NADPH oxidase, NOS isoforms and xanthine oxidase as previously reported (Abramov et al., 2007; Meneshian and Bulkley, 2002; Giordano, 2005; Asimakis et al., 2002; Frantseva et al., 2001).

The relative contribution of these systems to cellular outcome during reperfusion after different severities of hypoxia has not yet been elucidated. The evidence for the presence of xanthine oxidase is lacking in H9C2 cardiomyoblasts and cardiomyocytes. Moreover, Elisabetta et al. (2008) showed the failure of xanthine oxidase inhibitor; oxypurinol to inhibit ROS production during hypoxia/reperfusion in H9C2 myoblasts. Initial studies in this thesis were not able to demonstrate any effect of oxypurinol and therefore, its application was not considered further. In the present study, cardiomyoblasts exposed to chronic, severe hypoxia/reoxygenation showed an increase in intracellular $O_2^{-\bullet}$ and $^{\bullet}NO$ production as measured by DHE and DAF-2-DA fluorescent probes respectively. $O_2^{-\bullet}$ generation during the reoxygenation phase after hypoxia was remarkably suppressed by the superoxide scavenger MnTBAP and this scavenger exerted significant protection against chronic, severe hypoxia-induced metabolic inhibition, measured by MTT assay.

In the presence of FCCP (mitochondrial uncoupler) and rotenone (complex 1 inhibitor), the increase in $O_2^{-\bullet}$ and $^{\bullet}NO$ production during chronic, severe hypoxia/reoxygenation and chronic, severe sustained hypoxia was abolished, suggesting the contribution of mitochondria as a major source of ROS/RNS production during sustained hypoxia and hypoxia/reperfusion. The $O_2^{-\bullet}$-inhibitory effect of FCCP suggests that the loss of mitochondrial membrane potential in sustained hypoxia and reoxygenation was the crucial effect. In contrast, Abramov et al. (2007) reported a lack of protective effect of FCCP on $O_2^{-\bullet}$ generation in neurons during ischaemia/reperfusion, which may indicate the contribution of alternative sources of $O_2^{-\bullet}$ production including NADPH oxidase and/or xanthine oxidase or metabolic differences between the cell types. Harrison et al. (2003) reported differences in ATP synthase activity in compensating ATP demand in neurones and cardiomyocytes.

In the present study, a significant reduction in $O_2^{-\bullet}$ production was obtained during hypoxia/reoxygenation but not sustained hypoxia, with apocynin. This indicates the activation of NADPH oxidase was responsible for some of the global $O_2^{-\bullet}$ production in chronic, severe hypoxia/reoxygenation in addition to mitochondrial $O_2^{-\bullet}$.

The failure of apocynin treatment to inhibit $O_2^{-\bullet}$ production in control hypoxic cells (6h) indicates the absence of NADPH oxidase activity in these cells. Therefore, these findings suggest that activation of NADPH oxidase complex occurs during reoxygenation to produce $O_2^{-\bullet}$ and is in agreement with other investigators (Elisabetta et al., 2008). Others have used different hypoxia/reoxygenation conditions and systems than employed in the present study.

Elisabetta et al. (2008) made H9C2 cells anoxic in an anaerobic medium (serum, glucose and pyruvate free, 95%$N_2$ and 5%$CO_2$) for 24h and then followed up for 60min during reperfusion in normoxic culture medium. Abramov et al. (2007) made neurones chemically anoxic for 30min in culture medium (serum and glucose free, 100% $N_2$ or argon) and then exposing cells for 1h normoxia. Both investigators reported the sole contribution of NADPH oxidase complex to $O_2^{-\bullet}$ production during the reperfusion phase. Use of 2% $O_2$ tension in the presence of glucose is more pathophysiologically likely and has been used here to study free radical generation under oxidative stress. Cellular $O_2$ depletion occurs at a faster rate than glucose depletion during hypoxia, and inhibition of glucose metabolism in the absence of $O_2$ accelerates consumption of the reductant, glutathione, which depends on cellular NADPH for regeneration from the oxidised glutathione disulphide form, and poses an additional stress before reperfusion occurs. The current strategy has supported the assessment of individual contributions and balance between mitochondria and NADPH oxidase to produce $O_2^{-\bullet}$ during reperfusion. Therefore, activation of different complexes to produce $O_2^{-\bullet}$ mainly depends on the severity and duration of hypoxia and/or reperfusion and the cell type.

The present data also confirm $^{\bullet}NO$ production during hypoxia/reoxygenation; the inhibition of mitochondrial complex I with rotenone blocks electron flux from mitochondrial complex I and has a significant impact on $^{\bullet}NO$ generation during sustained hypoxia or reoxygenation. DAF fluorescence increases following intracellular oxidation by $^{\bullet}NO$ and/or $ONOO^-$. Increased production of both $O_2^{-\bullet}$ and $^{\bullet}NO$ during hypoxia/reoxygenation may increase $ONOO^-$ formation.

During reperfusion, at high concentrations, $^{\bullet}NO$ can outcompete intracellular SOD for reaction with $O_2^{-\bullet}$. $ONOO^-$ is formed at a ratio of 1:1, $^{\bullet}NO$ and $O_2^{-\bullet}$ (Jiao et al., 2009). In addition, SOD activity may be diminished during reperfusion by $O_2^{-\bullet}$ (Maulik et al., 1995). As a result, there may be sustained $ONOO^-$ production. Therefore, the significant reduction of DAF fluorescence in the presence of FCCP or rotenone may indicate the absence of $O_2^{-\bullet}$ to form $ONOO^-$ with modest available $^{\bullet}NO$. Moreover, the disruption of the mitochondrial respiratory chain either reduces NOS (mtNOS) activity or the $^{\bullet}NO$ that can be generated by either direct disproportionation or reduction of nitrite to $^{\bullet}NO$ under the acidic and highly reduced conditions of hypoxia is eliminated (Zweier et al, 1999). Zenebe et al. (2007) and Lacza et al. (2001) reported activation of mtNOS in rat hearts by increasing $Ca^{2+}$ during hypoxia/reperfusion, thereby enhancing $ONOO^-$ and triggering apoptosis.

The reduction in DAF fluorescence in rotenone or FCCP-treated cells during severe hypoxia/reoxygenation support the hypothesis of greater contribution of mitochondria to generate $^{\bullet}NO$ or $ONOO^-$ under these conditions. In the presence of L-NAME, decreased DAF nitrosation was observed during sustained hypoxia and hypoxia/reoxygenation and that significant reduction may reflect the NOS-dependent $^{\bullet}NO$ production. However, ~30% decrease in DAF fluorescence in the presence of L-NAME during reoxygenation and ~20% decrease in DAF fluorescence during sustained hypoxia suggests ineffective inhibition or significant non-enzymatic production of $^{\bullet}NO$/related species. Lacza et al. (2006) reported the heart mitochondrion is capable of significant $^{\bullet}NO$ production via the respiratory chain which is independent from mitochondrial NOS and cellular arginine pathway. Lacza et al. (2006) further suggested pre-accumulated mitochondrial nitrosothiols could act as $^{\bullet}NO$ donors to produce RNS after reaction with $O_2^{-\bullet}$. However, functional up-regulation of $^{\bullet}NO$ production from nitrosothiols during mild hypoxia is not demonstrated by the current study; therefore further work is warranted to clarify the issue.

Overproduction of $ONOO^-$ can induce lipid, protein and DNA oxidation and ultimately lead to cellular dysfunction, induce necrosis and/or apoptosis. Therefore, attempts at blocking either $^{\bullet}NO$ and $O_2^{-\bullet}$ overproduction during hypoxia/reperfusion may attenuate tissue injury. The current study has demonstrated the inhibition of cells with non-specific NOS inhibitor, L-NAME can attenuate $^{\bullet}NO$ production via NOS isoforms and reduce DAF fluorescence during hypoxia/reoxygenation whilst the SOD mimetic and $ONOO^-$ scavenger, MnTBAP can block the formation $ONOO^-$ and $O_2^{-\bullet}$ (Levrand et al., 2006; Levrand et al., 2005). In contrast to the effects of L-NAME, dismutation of $O_2^{-\bullet}$ with MnTBAP elicited significant protection against hypoxia/reoxygenation-induced loss of metabolic activity, providing evidence for mitochondrial metabolic recovery. In the presence of L-NAME during the last 2h of sustained severe hypoxia (6h), cells were protected against hypoxia (6h)-induced metabolic loss. The effect of L-NAME during sustained hypoxia (6h) alone underlines the efficacy of blocking one arm of $ONOO^-$ formation and the resulted protection against irreversible cell damage induced by hypoxia. This data is consistent the protective role of L-NAME against chronic, severe hypoxia-induced necrotic and apoptotic cell death as previously described in sections 5.4.4 and 5.4.7. To support this, increased $^{\bullet}NO$ production by mitochondria may have deleterious effects for mitochondrial regulation (Li et al., 2002). During the late stage of severe hypoxia (2% $O_2$; 4h or 2% $O_2$, 6h), $^{\bullet}NO$ production was significantly increased.

Recent reports suggest the functional activation of the NOS system to produce more $^{\bullet}NO$ during hypoxia in cardiomyocytes and coronary microvessels under lower $O_2$ tension (Strijdom et al., 2006). In contrast, in the presence of L-NAME, the complete inhibition of $^{\bullet}NO$ production via NOS isoforms worsens the hypoxia/reperfusion injury. The addition of the $^{\bullet}NO$ donor, spermine nonoate (200µM) did not affect the loss of cell viability compared to the viability of control hypoxic cells. However, the release of $^{\bullet}NO$ from spermine nonoate was not confirmed by the Griess assay, nor was a dose response curve established – it is known that the effects of $^{\bullet}NO$ to protect or damage biological systems are highly dose dependent.

Therefore, the cardiac protective role of $^{\bullet}NO$ during reperfusion period requires further investigation. In support of this hypothesis, Li et al. (2002) reported significantly worsened effects of lung injury during air ventilation when cells were pre-treated with L-NAME. These authors showed an accumulation of NOS substrates in lungs that were exposed to ischaemia/reperfusion. Moreover, Li et al. (2004) suggested an antioxidant effect of $^{\bullet}NO$ that protected against ischaemia/reperfusion in lung injury. Kawahara et al. (2006) reported the enhanced production of $^{\bullet}NO$ in cardiomyocytes that was critical in compromising cellular ATP supply, but conferred a protective role against ischaemia-reperfusion injury. Taken together, the current study suggests that the decrease in cell viability or metabolic loss during hypoxia/reoxygenation can been attributed to overproduction of $ONOO^-$ in the face of significantly increased $O_2^{-\bullet}$ with partially or increasingly available $^{\bullet}NO$ (Lalu et al., 2002, Yasmin et al., 1997). In support of this, Radi at al. (2002) reported a 100-fold increase in $ONOO^-$ production with 10-fold increase in $^{\bullet}NO$ and $O_2^{-\bullet}$.

### 6.4.2 NF-κB activation during hypoxia/reoxygenation

Inhibition of NF-κB with SN-50 did not exacerbate hypoxia/reoxygenation-induced or hypoxia-induced metabolic change during the last 2h of normoxia (reoxygenated cells) or hypoxia (control cells). In contrast, when SN-50 was added to cells for 4h during severe hypoxia, loss of metabolic activity was significantly increased as measured by MTT reduction (**Figure: 5.12**). These data suggest that NF-κB is activated during hypoxia, probably to induce antioxidants or/and protective genes but that further exposure to hypoxia (+2h) or reoxygenation (+2h) cause a reduction in metabolic activity that is NF-κB independent.

In summary, the present study has confirmed the dual contribution of mitochondria and NADPH oxidase to produce $O_2^{-\bullet}$ during the early phase of reoxygenation (2h) after chronic, severe hypoxia (4h). Chronic, severe hypoxia (4h)/reoxygenation (2h) and sustained hypoxia (6h) decrease metabolic activity, but reperfusion only partially restores the metabolic activity.

Acute, severe hypoxia (30min)/reoxygenation (2h) did not significantly increase $O_2^{-\bullet}$ production, and cells recovered from metabolic loss during the reoxygenation period. The $^{\bullet}NO$ production during chronic, severe hypoxia/reoxygenation is partly NOS-dependent. The NOS-dependent $^{\bullet}NO$ generation during reoxygenation after hypoxia is cardiac protective against hypoxia/reoxygenation-induced cell dysfunction.

| **Condition** | **Chronic, severe hypoxia/reperfusion** | | | | | **Sustained, severe hypoxia Control (2% $O_2$, 6h)** | | | | | **Normoxia Control (21% $O_2$, 6h)** | | | | |
|---|---|---|---|---|---|---|---|---|---|---|---|---|---|---|---|
| **Inhibitors** | **Ctl** | **ROT** | **FCP** | **APO** | **LNM** | **Ctl** | **ROT** | **FCP** | **APO** | **LNM** | **Ctl** | **ROT** | **FCP** | **APO** | **LNM** |
| **$O_2^{-\bullet}$** | ↑* | ↓ | ↓ | ↓ | **X** | ↑* | ↓ | ↓ | **X** | **X** | **X** | **X** | **X** | **X** | **X** |
| **$^{\bullet}NO$** | ↑* | ↓ | ↓ | - | ↓ | ↑* | ↓ | ↓ | - | ↓ | **X** | **X** | **X** | - | **X** |
| **Inhbitors** | **Ctl** | **MnBP** | **SPN** | **APO** | **LNM** | **Ctl** | **MnBP** | **SPN** | **APO** | **LNM** | **Ctl** | **MnBP** | **SPN** | **APO** | **LNM** |
| **Metabolic activity** | ↓* | ↑ | **X** | - | ↓ | ↓* | ↑ | **X** | - | ↑ | **X** | **X** | **X** | - | **X** |

**Table 6.1 Summary of results of chronic, severe hypoxia/reperfusion induced-ROS/RNS generation and metabolic inhibition.**

**Key:** Ctl - control, ROT-rotenone, FCP- FCCP, APO- apocynin, LNM- L-NAME, MnBP- MnTBAP and SPN- spermine Nonoate.

↑* - Significant increase in control cells (2% $O_2$ or 10% $O_2$) vs. normoxic control cells.

↓* - Significant decrease in control cells (2% $O_2$ or 10% $O_2$) vs. normoxic control cells.

↑ - Significant increase in treated cells vs. control cells at same $O_2$ tension.

↓ - Significant decrease in treated cells vs. control cells at same $O_2$ tension.

X - In treated cells, no significant difference vs. control cells at same $O_2$ tension or if in control cells (2% $O_2$ or 10% $O_2$), no significant difference vs. normoxic cells or in normoxic cell shows the basal effect.

**X***- No significant effect in control cells (2% $O_2$ or 10% $O_2$) vs. normoxic control cells.

¤ - Significant increase in control cells (2% $O_2$) vs. cells at 10%$O_2$

- Not available.

# CHAPTER 7

# ANALYSIS OF REDOX-SENSITIVE TRANSCRIPTION FACTORS; NF-κB AND Nrf2 DURING HYPOXIA AND REOXYGENATION

## 7.1 Preface

This chapter describes the optimisation of transfection conditions including DNA to Lipofectamine ratio to achieve the highest transfection efficiency and determine the activity of nuclear factor kappa B (NF-κB) and nuclear factor erythroid-2 related factor 2 (Nrf2) after exposing cells to hypoxia alone and hypoxia/reoxygenation. Activation of redox sensitive transcription factors; NF-κB and Nrf2 was studied during chronic, severe hypoxia and chronic, severe hypoxia/reoxygenation. To find out any cytoprotective role of NF-κB expression, cell viability of H9C2 cardiomyoblasts was assessed with inhibition of NF-κB during chronic, severe hypoxia. The activation of redox sensitive transcription factor Nrf2 was studied during hypoxia and hypoxia/reoxygenation. Nrf2 activation was further assessed in the presence of the SOD mimetic; MnTBAP, NOS inhibitor; L-NAME and the nitric oxide donor; spermine nonoate to determine the contribution of $O_2^{-\bullet}$, $^{\bullet}NO$ and related species such as $ONOO^-$ to activate Nrf2 during chronic, hypoxia and hypoxia/reoxygenation. A possible mechanism for Nrf2 activation during hypoxia and hypoxia/reperfusion is discussed.

## 7.2 Introduction

### 7.2.1 NF-κB activation during hypoxia

Hypoxia is a stress condition of low $O_2$ concentration. It has clinical significance in cardiovascular disease-related conditions such as myocardial infarction, ischaemia reperfusion and heart failure. However, cells have their own natural defence mechanisms to protect against hypoxia-induced deleterious effects by expressing a number of genes as a result of transcription factor activation during hypoxia. The regulated genes/transcription factors include erythropoietin and vascular endothelial growth factor by hypoxia inducible factor (Hif-1α), heat shock proteins by heat shock factors. However, the cellular signals that mediate the activation of transcription factors by hypoxia alone have not been clearly elucidated. It has been reported that growing numbers of stress-related genes are involved in the activation of transcription factor, NF-κB (Kukreja, 2002). It is evident that activation of NF-κB occurs rapidly upon ischaemic insult in many tissues such as renal epithelial cells (Lee and Han, 2005), brain, liver and myocardium (Kukreja, 2002). Li et al. (1999a) reported a 2-fold increase of NF-kB DNA binding activity in rat heart following a brief period of ischaemia.

The NF-κB-dependent activation of gene transcription does not require *de novo* protein synthesis and this is a characteristic feature of early response gene inducers. This feature allows activated NF-κB to bind to a promoter site where it can initiate the rapid synthesis of protective and signaling proteins after exposure to various stress conditions including hypoxia. The activation of NF-κB during hypoxia or ischaemia or reperfusion is complex as the family of transcription factors autoregulate themselves. There are three distinct subunits of NF-κB found in a cells; p50, p65 and IkBα. The major isoforms of NF-κB is inactive in the cytoplasm with the inhibitory subunit, IkBα, bound to the p50-65 heterodimer. Upon activation, phosphorylation of the IkBα subunit takes place and results in the cleavage of IkBα. Then, the p50-p65 heterodimer complex is translocated from the cytoplasm to the nucleus where it binds with high affinity kB binding motifs.

*In vitro* studies have shown that c-AMP-dependent kinases, membrane-associated kinases and heme-regulated kinases are responsible for the activation of NF-κB (Lee, 2003; Kukreja, 2002; Guro et al., 2001). It has been reported that ROS, TNF-α , PMA and LPS cause activation of membrane associated kinases (src, ras and raf) which lead to dissociation of IkBα and the activation of NF-κB (Kukreja, 2002). NF-κB has been reported to regulate iNOS gene expression in rat glioma cells stimulated by TNF-α and LPS (Lee et al., 2003) and increases the production of $^{\bullet}$NO in LPS treated cells (Lee et al., 2003). Moreover, NF-κB activation induces anti-apoptotic genes and proteins such as cellular inhibitors of apoptosis (cIAP-2), Bcl-2, haem oxygenase-1 (HO-1) and MnSOD (Koong et al., 1994; Lee, 2003). It has been documented that activation of NF-κB may reflect an early response for the transcription of redox-sensitive genes whose products may have a vital role during defence mechanism against hypoxia. Indeed, the activation of the NF-κB signaling pathway is sufficient to suppress cell death of ventricular myocytes during chronic, severe hypoxia for 24h (Regula et al., 2004).

In contrast, it has been reported that reduction of infarct size occurred in rat hearts when NF-κB activation was inhibited by specific peptide inhibitors; PR11 and PR39 (Adrienn et al., 2003). Moreover, Zingarelli et al. (2002) have reported that the sesquiterpene lactone parthenolide; the inhibitor of Ikk and NF-κB activation, reduced reperfusion injury in rat hearts. Xuan et al. (1999) reported that activation of NF-κB is essential to achieve ischaemia preconditioning after 24h. However, prolonged activation of NF-κB may contribute to cardiac dysfunction and ischaemia/reperfusion injury through over expression of myocardial cytokines (Kukreja, 2002). Therefore, various explanations about the role of NF-κB during hypoxia or ischaemia with regard to cell death and cardiac protection must be investigated.

### 7.2.2 Nrf2 activation during hypoxia and hypoxia/reperfusion

It has been widely accepted that exposure to ischaemia or hypoxia or reperfusion leads to induction of protective genes, however, the mechanism of their induction remains unclear. Transcriptional up-regulation of cytoprotective genes is responsible for buffering the cell's "antioxidant capacity". These genes are responsible for maintenance of cellular glutathione content and conjugational activity. Moreover, they play a vital role in detoxification of damaging radical products of oxidative stress which include glutathione S-tranferase, aldehyde dehydrogenases, haem oxygenase-1, ferritin and quinine oxidoreductases such as NADPH quinone oxidoreductase (Nioi et al., 2003).

Nrf2 activation during hypoxia or ischaemia/reperfusion occurs due to an alteration in the redox state of cells by increased amounts of ROS/RNS which can activate an antioxidant response to protect themselves from future oxidant damage (Nioi et al., 2003). Nrf2 is a flavoprotein which catalyses the two electron reduction of quinones, thereby inhibiting redox cycling of xenobiotics. Recent studies indicate that Nrf2 is essential for transcriptional activation of mouse NQO1 and other cytoprotective genes following treatment with electrophiles (Itoh et al., 1997). Therefore, Nrf2 transcription factor is reported as a master regulator of this specific antioxidant phenotype (Mathers, 2004).

The promoter regions of the Nrf2 dependent genes are *cis*-acting sequences and antioxidant response elements (AREs). AREs have been identified in variety of genes including NQO1. The consensus sequence of ARE is important in transcriptional activation of NQO1 upon oxidative stress. During oxidative stress, Nrf2 can bind with the ARE sequence and thereby increased antioxidant-gene expression occurs (Itoh et al., 1997). During normoxia, this transcription factor is held in the cytoplasm by a cytoskeletal-associated inhibitory protein; Kelch-like ECH-associated protein 1(KEAP1), however, Nrf2 is constantly targeted for proteasomal degradation.

During oxidative stress, thiol oxidation occurs in cysteine residues of the hinge region of KEAP1, resulting in a conformational change in KEAP1 with the loss of Nrf2 binding and proteosomal targeting of KEAP 1 (Li et al., 2004). Then, Nrf2 accumulates and localizes to the nucleus and with its cofactors, up-regulates cytoprotective genes through the transcriptional activation of ARE. A reduction in infarcted volume is observed following focal cerebral ischaemia in the presence of the Nrf2 inducer; sulforaphane (Shah et al., 2007).

Moreover, Lee and Johnson, (2004 ) showed that neural cells that lacked Nrf2 (Nrf2-/- mice) were more susceptible to oxidative stress than control neurons from control animals (Nrf2 +/+ wild mice), however, when the cells (Nrf2-/- mice) were transfected with a functional Nrf2 construct, they became resistant to oxidative stress. Dhakshinamoorthy and Porter, (2004) reported that dominant negative-Nrf2 stable neuroblastoma cells were more prone to apoptosis induced by nitric oxide when they were silenced with siRNA.

The contribution of $^{\bullet}NO$ and/or $O_2^{-\bullet}$ or related species including $ONOO^-$ to modulate Nrf2 activity and thereby affect cell death has not yet been studied in detail during hypoxia or hypoxia/reperfusion. Excessive production of $O_2^{-\bullet}$ and $^{\bullet}NO$ may result overproduction of $ONOO^-$ which is known to cause cell death and has been implicated in the pathophysiology of ischaemia/reperfusion and inflammation. However, $ONOO^-$ produced in low amounts may serve as an intracellular signal molecule inducing the adaptive survival response to cellular stress. In this context, it has been reported that expression of several phase II detoxifying or antioxidant enzymes such as glutathione *S*-transferase and Mn superoxide dismutase (MnSOD) occurs in the presence of $ONOO^-$ (Kang et al., 2002; Li et al., 2006). Moreover, $ONOO^-$ has also been reported to induce HO-1 in rat liver in vivo (Motterlini et al., 1996). The underlying mechanisms of $ONOO^-$ or other ROS/RNS including $O_2^{-\bullet}$ and $^{\bullet}NO$ to protect cardiomyoblasts via modulation of NF-κB and/or Nrf2 during hypoxia/reperfusion remains to be clarified.

## 7.3 Results

### 7.3.1 DNA: Lipofectamine 2000 ratio

In order to achieve higher transfection efficiency, the ratio of total DNA and Lipofectamine 2000 was optimised for each transfection with pGL 3 [*nqo1*/luc] plasmid for Nrf2 activation and pGL3 [*3enh*/conA/luc] for NF-κB activation and pGL 4.4 [*hRluc*/TK] for TKRL activation in control cells as described in section 2.3.21.1 and 2.3.21.2.

Lipofectamine 2000 is supplied as a 1mg/ml solution. According to the manufacturer's instructions, generally the mass ratio of DNA to Lipofectamine 2000 is 1:2 to 1:3; however a greater ratio can be employed in transfection. As shown in **Figure 7.1**, the amount of plasmid DNA is held constant at 1.2µg (experimental plasmid DNA to control plasmid at 1:10 ratio) and a significant increase in *Con A* promoter mediated luciferase gene expression was observed at 1:4 ratio (DNA to Lipofectamine 2000), whereas a significant increase in ARE/NQO1 mediated luciferase gene expression was observed at both 1:3 and 1:4 ratio. Therefore, all subsequent experiments were conducted using 1:4, plasmid DNA to Lipofectamine 2000 ratio.

### 7.3.2 NF-κB and Nrf2 activation during chronic, severe hypoxia

It has been reported that a marked increase in NF-κB activation occurs during hypoxia (Koong et al., 1994). To test the hypothesis that NF-κB mediates a cellular defence mechanism during chronic, severe hypoxia, H9C2 cells at 90-95% confluence were co-transfected with pGL3 [*3enh*/conA/luc]/ pGL 4.4 [*hRluc*/TK] : Lipofectamine at 1:4 ratio and incubated for 24h at 37ºC in a humidified atmosphere of 5% $CO_2$ and 95% air. After 24h, cells were washed with PBS and loaded with 2% $O_2$ equilibrated, HEPES buffered phenol red-free DMEM and incubated at 2% $O_2$ for 4h and then firefly to renila luciferase luminescence was measured as previously described in Section 2.3.21.2.

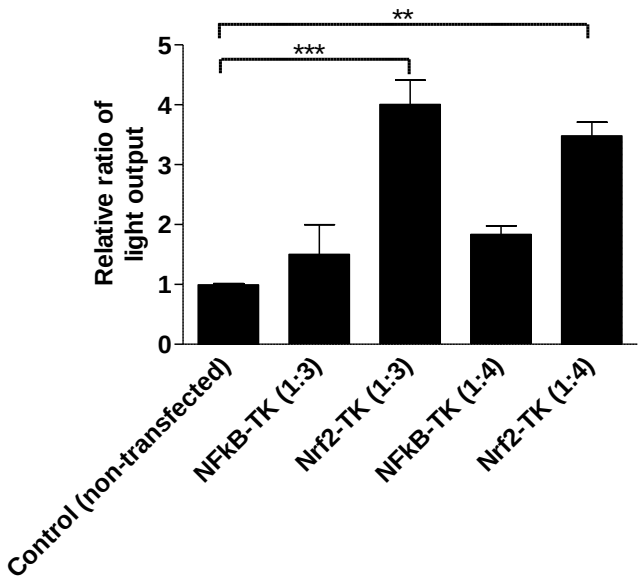


**Figure 7.1 Effect of plasmid DNA: Lipofectamine 2000 ratio on reporter transfection efficiency.** H9C2 cells grown at 90-95% confluence in 24-well plates were washed with PBS and Opti-MEM and transfected with NF-κB plasmid; pGL 3 [*3enh/conA/luc*]) DNA with control plasmid; pGL 4.4 [*hRluc*/TK] DNA in total of 1.2µg/ml DNA to Lipofectamine 2000 at 1:3 and 1:4 ratios. Same procedure was applied to Nrf2 plasmid; pGL3 [*nqo*1*/luc*]/TKRL plasmid with pGL 4.4 [*hRluc*/TK]. Following transfection, cells were incubated for 24h. Then, cells were washed gently, loaded with phenol red-free medium containing 1µg/ml LPS and incubated for 4h at 37ºC in a humidified atmosphere of 5% $CO_2$ and 95% air. Plates were centrifuged and medium was replaced with 100µl of phenol red-free DMEM. Then, firefly to renila luciferase luminescence was measured at 542nm in a Spectramax luminometer at room temperature. Data were normalised as described in section 2.3.21.2. Data represents the mean±S.E.M of three independent experiments conducted in triplicates. *** represents $P < 0.0001$ and ** represents $P<0.001$ (one-way ANOVA), Tukey's post-hoc test.

As illustrated in **Figure 7.2** and **7.3**, an increase in luciferase gene expression suggest that chronic, severe hypoxia significantly increased the NF-κB /DNA and Nrf2/DNA binding activity compared to control cells maintained at 21% $O_2$ normoxia ($P<0.001$). Cells treated with the NF-κB inhibitor; SN-50 showed suppression of NF-κB - activation as indicated by a lower value ratio of firefly/renila luminescence. The suppression of NF-κB /DNA binding was significant in the presence of the NF-κB inhibitor; SN-50 in positive LPS-treated controls, whereas LPS treatment-induced significant NF-κB (**Figure. 7.2**) and Nrf2 activity (**Figure. 7.3**) compared to untreated control cells as indicated by luciferase gene expression and luminescence ($P<0.001$,control vs. treatment).

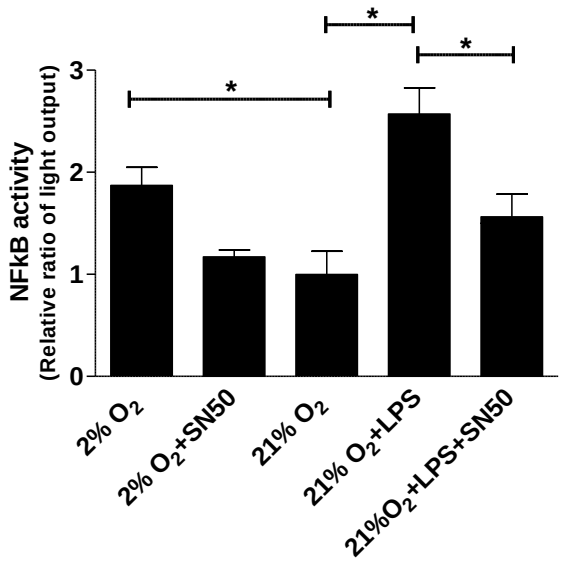


**Figure 7.2 Effect of hypoxia on NF-κB /DNA binding activity in H9C2 cells subjected to chronic, severe hypoxia.** H9C2 cells grown at 90-95% confluence in 24-well plates were washed with PBS and Opti-MEM and transfected with pGL 3 [*3enh/conA/luc*]/ pGL 4.4 [*hRluc*/TK] plasmids (1.2µg/ml): Lipofectamine 2000 complexes at 1:4 ratio for NF-κB expression and cells were then incubated for further 24h. Then, cells were washed gently, loaded with 2% $O_2$ equilibrated, HEPES buffered phenol red-free DMEM and incubated at 2% $O_2$ for 4h. Positive control cells were loaded with phenol red-free DMEM, containing 1µg/ml LPS and incubated for 4h at 37ºC in a humidified atmosphere of 5% $CO_2$ and 95% air. After 4h, plates were centrifuged and medium was replaced with 100µl of phenol red-free DMEM and firefly to renila luciferase luminescence was measured at 542nm in a Spectramax luminometer at room temperature. Data were normalised as described in section 2.2.8.9.2. Data represents the mean±S.E.M of three independent experiments conducted in triplicates. * represents $P < 0.05$ (one-way ANOVA), Tukey's post-hoc test.

### 7.3.3 Nrf2 activation during hypoxia and hypoxia/reoxygenation

A marked increase in the activation of antioxidant transcription factor Nrf2 during ischaemia-reperfusion has been reported (Leonard et al., 2006). To ascertain whether this occurs in H9C2 cells during chronic, severe hypoxia or hypoxia/reperfusion, cells at 90-95% confluence were co-transfected with pGL 3 [*nqo1*/luc] plasmid harbouring the NQO1 promoter / pGL 4.4 [*hRluc*/TK] control plasmid : Lipofectamine at 1:4 ratio and incubated for 24h at 37ºC in a humidified atmosphere of 5% $CO_2$ and 95% air.

After 24h, cells were washed with PBS and loaded with 2% $O_2$ equilibrated, HEPES buffered phenol red-free DMEM and incubated at 2% $O_2$ for 4h. For reperfusion, the medium was replaced with pre-equilibrated oxygenated medium and incubated for a further 2h at 21% $O_2$. The firefly to renila luciferase luminescence ratio was measured as described in section 2.3.21.2.

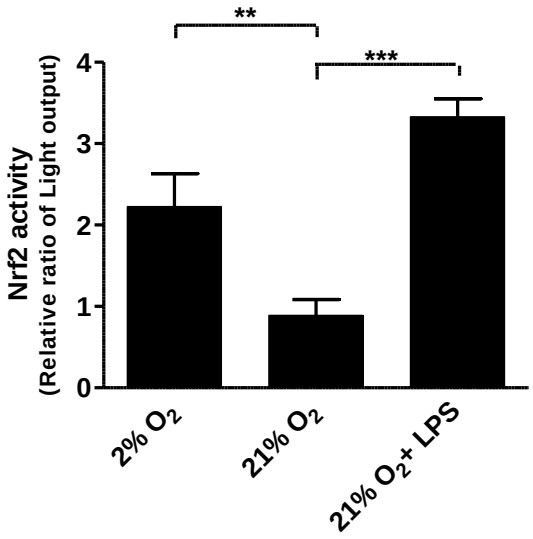


**Figure 7.3 Effect of hypoxia on Nrf2/DNA binding activity in H9C2 cells subjected to chronic, severe hypoxia.** H9C2 cells grown at 90-95% confluence in 24-well plates were washed with PBS and Opti-MEM and transfected with pGL3[*nqo1*/*luc*]/pGL 4.4 [*hRluc*/TK] plasmids (1.2µg/ml): Lipofectamine 2000 complexes at 1:4 ratio for NF-κB expression and cells were then incubated for a further 24h. Then, cells were washed gently, loaded with 2% $O_2$ equilibrated, HEPES buffered phenol red-free DMEM and incubated at 2% $O_2$ for 4h. Positive control cells were loaded with phenol red-free DMEM, containing 1µg/ml LPS and incubated for 4h at 37ºC in a humidified atmosphere of 5% $CO_2$ and 95% air. After 4h, plates were centrifuged and medium was replaced with 100µl of phenol red-free DMEM and firefly to renila luciferase luminescence was measured at 542nm in a Spectramax luminometer at room temperature. Data were normalised as described in section 2.3.21.2. Data represents the mean±S.E.M of three independent experiments conducted in triplicates. *** represents $P < 0.0001$ and ** represent $P<0.001$ (one-way ANOVA), Tukey's post-hoc test.

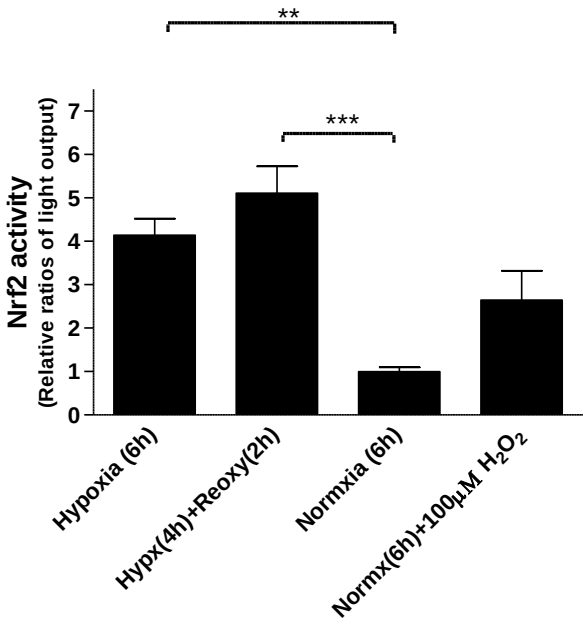


**Figure 7.4 Effect of severe hypoxia and hypoxia/reoxygenation on Nrf2/DNA binding activity in H9C2 cells.** H9C2 cells grown at 90-95% confluence in 24-well plates were washed with PBS and Opti-MEM and transfected with pGL3 [*3enh*/conA/luc]/pGL 4.4 [*hRluc*/TK] (1.2μg/ml): Lipofectamine 2000 complexes at 1:4 ratio for NF-κB to TKRL expression and cells were then incubated for a further 24h. Then, cells were washed gently, loaded with 2% $O_2$ equilibrated, HEPES buffered phenol red-free DMEM and incubated at 2% $O_2$ for 4h. Control normoxic cells were incubated at 21% $O_2$ for 4h and positive control cells were loaded with phenol red-free DMEM, containing 100μM $H_2O_2$ and incubated for 6h at 37ºC in a humidified atmosphere of 5% $CO_2$ and 95% air. After 4h, experimental cells were centrifuged and medium was replaced with pre-equilibrated (21% $O_2$) medium and further incubated for 2h at 21% $O_2$. Control pates were centrifuged and medium was replaced with preequilibrated medium (2% $O_2$ or 21% $O_2$) accordingly and further incubated for 2h. After 6h (hypoxia/reoxygenation or sustained hypoxia or normoxia), plates were gently centrifuged and medium was replaced with 100μl of phenol red-free DMEM and firefly to renila luciferase luminescence was measured at 542nm in a Spectramax luminometer at room temperature. Data were normalised as described in section 2.3.21.2. Data represents the mean±S.E.M of three independent experiments conducted in triplicates. *** represents $P < 0.0001$ and ** represents $P<0.001$ (one-way ANOVA), Tukey's post-hoc test.

The transfection of H9C2 cells with pGL 3 [*nqo1*/luc] plasmid leads to ARE-mediated luciferase gene expression (Nioi et al., 2003). **Figure 7.3** confirms that chronic,severe hypoxia promotes Nrf2 activity.

As illustrated in **figure 7.4**, Nrf2 DNA/binding activity was significantly increased during chronic, severe hypoxia/reoxygenation and sustained hypoxia alone when compared to normoxia alone ($P<0.001$, hypoxia vs. hypoxia/reoxygenation). However, Nrf2, DNA/binding activity after during hypoxia/reoxygenation was not significantly different to chronic, severe hypoxia (6h) alone. The positive control, LPS-treated cells showed a significant increase in Nrf2/DNA binding activity after 4h compared to control normoxic cells (**Figure 7.3**), whereas the positive control, $H_2O_2$ (6h) cells showed a trend for increased Nrf2/DNA binding response, but it was not significant compared to control normoxic cells (**Figure 7.4**) (see **Table 7.1** for summary of results).

### 7.3.4 Nrf2 activation during severe hypoxia/reoxygenation in the presence of SOD mimetic; MnTBAP, non-selective NOS inhibitor; L-NAME and $^{\bullet}$NO donor; spermine nonoate.

In order to find out the effect of $O_2^{-\bullet}$ and $^{\bullet}$NO on Nrf2 activation during severe hypoxia/reperfusion, cells were initially exposed to chronic, severe hypoxia for 4h and then subjected to reoxygenation (2h) in the presence of a SOD mimetic; 50µM MnTBAP, or a non-selective NOS inhibitor; L-NAME or the $^{\bullet}$NO donor; spermine nonoate.

In the presence of MnTBAP, ARE-mediated luciferase gene expression in sustained hypoxia and hypoxia/reoxygenation was significantly reduced, suggesting the suppression of Nrf2/DNA binding activity in ARE/NQO1 promoter region compared to normoxia alone. It further showed that $O_2^{-\bullet}$ is important in activation of Nrf2 gene transcription during both hypoxia and hypoxia/reoxygenation. The non-selective inhibition of NOS isforms in the presence of L-NAME, resulted in a decrease in ARE/NQO1 mediated luciferase gene expression during sustained hypoxia (6h), but it was not significant compared to normoxic controls (**Figure 7.5A**).

In contrast, in the presence of L-NAME, ARE/NQO1 mediated luciferase gene expression was significantly reduced during hypoxia/reoxygenation compared to normoxic controls, suggesting that $^{\bullet}$NO generation is important for Nrf2 activation during reoxygenation period.

In the present study, there is no significant increase in Nrf2 activity in the presence of the $^{\bullet}$NO donor; spermine nonoate as measured by luciferase gene expression during hypoxia/reoxygenation and normoxia. Perhaps, Nrf2 activation is $^{\bullet}$NO concentration-dependent or may require alternative species to induce activation (**Figure 7.5B and 7.5C**).

In the presence of MnTBAP, ARE/NQO1 mediated luciferase gene expression was not significantly changed during normoxia, suggesting that $O_2^{-\bullet}$ generation during normoxia does not contribute to Nrf2 activation. Moreover, the addition of the $^{\bullet}$NO donor; spermine nonoate during normoxia did not increase the activation of Nrf2/DNA binding significantly with ARE/NQO1 promoter gene (**Figure 7.5C**), suggesting that $^{\bullet}$NO alone is not responsible for Nrf2 activation (see **Table 7.1** for summary of results).

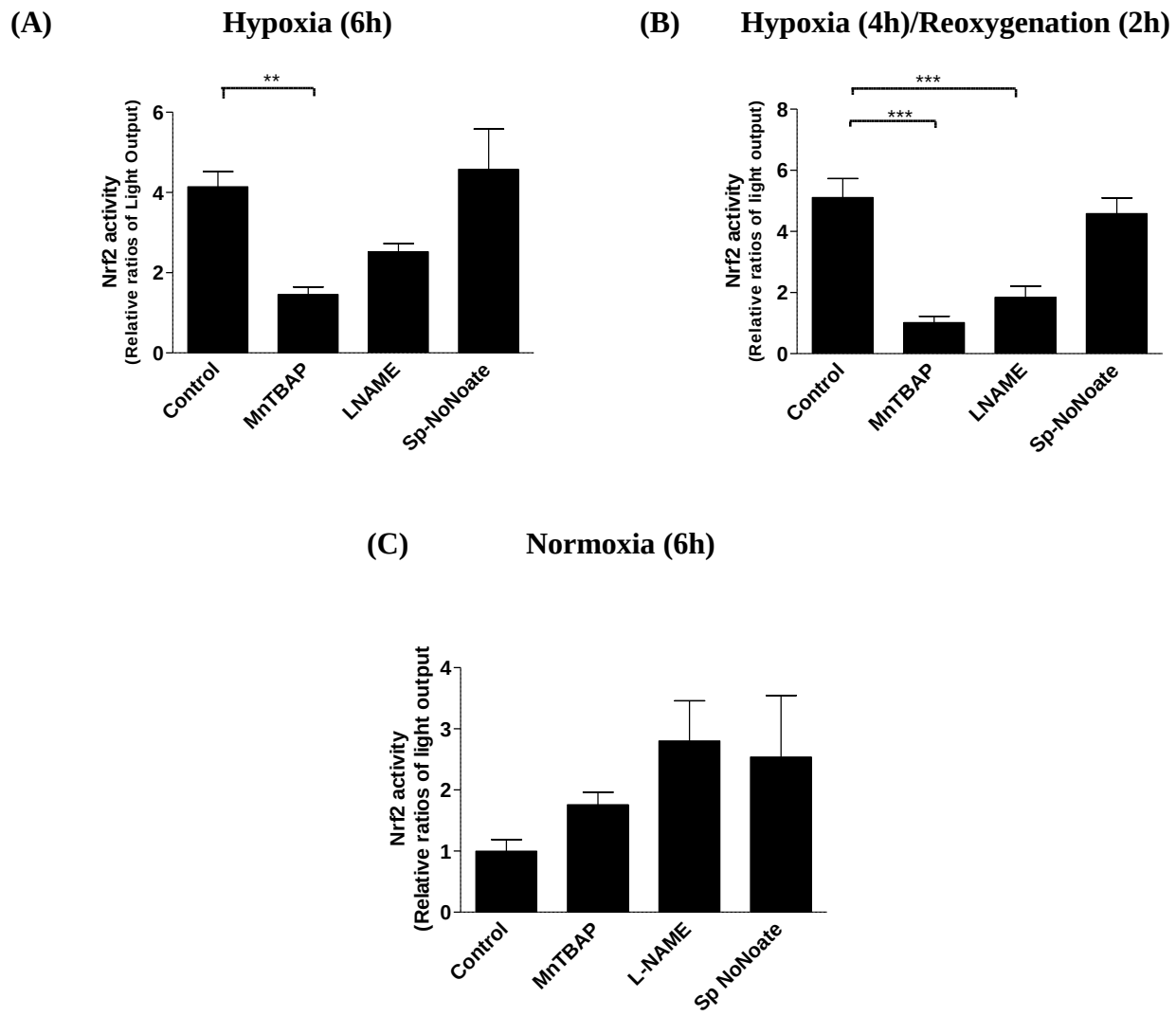


**Figure 7.5 ROS or RNS-dependent activation of Nrf2 gene expression during hypoxia/reoxygenation.** H9C2 cells grown at 90-95% confluence in 24-well plates were washed with PBS and Opti-MEM and co-transfected with pGL 3 [*nqo1*/luc] plasmid / pGL 4.4 [*hRluc*/TK] plasmid (1.2µg/ml): Lipofectamine 2000 complexes at 1:4 ratio and cells were then incubated for a further 24h. After that, cells were washed gently and loaded with 2% $O_2$ equilibrated, HEPES buffered phenol red-free DMEM and incubated at 2% $O_2$ for 4h. After hypoxia, existing culture medium was replaced with pre-equilibrated reoxygenated medium containing 50µM MnTBAP or 100µM L-NAME or 100µM spermine (Sp) nonoate and further incubated for 2h at 21% $O_2$. Hypoxic and normoxic controls were also treated as appropriate. After hypoxia (A) or reoxygenation (B) alone or normoxia (C), firefly to renila luciferase luminescence was measured at 542nm in a Spectramax luminometer at room temperature. Data were normalised as described in section 2.3.21.2. Data represents the mean±S.E.M of three independent experiments conducted in triplicate. ** represents $P<0.001$ and *** represents $P < 0.0001$ (one-way ANOVA), Tukey's post-hoc test.

## 7.4 Discussion

### 7.4.1 NF-κB activation during hypoxia

The present study indicates that the transcription factor, NF-κB may play a role in cardiac protection against hypoxic injury. This is supportive of previous data, that NF-κB activation may play a vital role in ischaemic preconditioning (Kukreja, 2002). Others have shown that the NF-κB pathway is involved in the activation of apoptosis through suppression of bcl-2 as previously reported in aortic endothelial cells during hypoxia (Matsushita et al., 2000). In the present study, a significant increase in c*on-A* promoter mediated luciferase gene expression suggests an increase in the activation of NF-κB /DNA binding during chronic, severe hypoxia compared to normoxia treated controls. The observed increase in NF-κB activation associates with $O_2^{-\bullet}$ production during chronic, severe hypoxia (section 4.4.1). The inhibition of NF-κB activation in the presence of the NF-κB inhibitor, SN-50 was associated with an increase in cell death by 40% and the presence of SN-50 reduced NF-κB activation to the same as observed in normoxia controls in the current reporter assay.

A statistically significant increase in LPS-induced NF-κB activation was observed, and was inhibited by SN-50 according to the conditions employed in present system. A significant increase in NF-κB activity occurred at 4h during glucose-oxygen deprivation in cerebral endothelial cells with a 10% reduction in cell viability after 8h of oxygen-glucose deprivation (Lee, 2003). In contrast, H9C2 cells showed higher sensitivity in the current cell-system of 2% $O_2$ hypoxic medium containing 4.5g/L glucose and significant cell death was induced at 4h. Koong et al. (1994) showed the activation of NF-κB during 0.02% hypoxia for 4h in Jurkat-T cells grown in culture medium containing 10% FBS and 4.5g/L glucose. However, hypoxia-induced cell death was not measured. Regula et al. (2004) reported a significant decrease in apoptotic cell death during hypoxia ($pO_2$ <5mmHg, 24h) in ventricular myocytes transfected with luciferase reporter plasmid after activation of IkB-wt mediated NF-κB gene transcription compared to normoxic cells.

To test the role of hypoxia alone, measurement of cell metabolic activity during chronic, severe hypoxia in cardiomyoblasts transfected with the luciferase reporter plasmid containing NF-κB promoter site has been studied. Therefore, the present system investigates the balance between hypoxia-induced cell death and NF-κB activation-induced cell protection.

It is presumed that redox imbalance during hypoxia may have led to IkBα phosphorylation and ubiquitination (4h), during chronic, severe hypoxia leading to NF-κB release. Subsequent nuclear translocation of the activated p65 subunit (containing transactivation domain) then activates the *con*-A promoter of the plasmid and thereby, induces luciferase gene expression in transiently transfected H9C2 cells (Gao et al., 2005). Ischaemic preconditioning is an important area for potential treatment of ischaemic reperfusion injury. Myocardial protection by NF-κB activation leads to a reduction of inflammation or upregulation of protective enzymes such as MnSOD and iNOS (Adrienn et al., 2003; Nguyen et al., 2009; Rushworth et al., 2008). In summary, the present study suggests NF-κB activation as a therapeutic target to protect cells against myocardial hypoxic injury. It has been reported that activation of NF-κB occurs during myocardial reperfusion (Regula et al., 2004). Therefore, further work should investigate the effect of hypoxia/reperfusion on NF-κB activation and its association with hypoxia/reperfusion-induced cell death using this reporter cell line.

### 7.4.2 Nrf2 activation during chronic, severe hypoxia and hypoxia/reoxygenation

ROS/RNS generated during hypoxia, hypoxia/reperfusion have been proposed to act as signalling intermediates for cellular defence, or preconditioning, however downstream targets have not been fully elucidated. Nrf2 activation occurs due to an alteration in the redox state of cell in the presence of increased amounts of ROS/RNS. Therefore, the present study examined the pattern of Nrf2 mediated reporter gene expression during chronic, severe hypoxia and hypoxia/reperfusion (severe hypoxia for 4h+reoxygenation for 2h) and also has investigated the role of $O_2^{-\bullet}$ and $^{\bullet}NO$ production in Nrf2 activation.

According to recent reports, Nrf2-mediated antioxidant gene expression affords a highly specific and co-ordinated response to protect the cells against hypoxia or hypoxia reperfusion-induced oxidative stress (Nguyen et al., 2009; Dreger et al., 2009; He et al., 2009).

Moreover, the activation of Nrf2 has been identified as an inducer of antioxidant genes; NQO1, MnSOD, iNOS and the GST pathway (Rushworth et al., 2008; Nioi et al., 2003; Nguyen et al., 2009). Evidence to support this has been gained by increased activation of ARE/NQO1 mediated Nrf2 reporter gene expression during chronic, severe hypoxia and hypoxia/reoxygenation compared to normoxic controls.

The current study presents evidence that supports the concept that hypoxia and hypoxia/reoxygenation-dependent activation of Nrf2 is mediated through ROS/RNS production. This was evidenced through the use of superoxide dismutase mimetic; MnTBAP, which resulted in an inhibition of activation of Nrf2 during hypoxia and hypoxia/reperfusion. Previous work (chapter 4) confirmed the significant reduction of $O_2^{-\bullet}$ production in the presence of MnTBAP, during chronic, severe hypoxia. Similarly, in the presence of the non-selective NOS inhibitor; L-NAME, Nrf2 activation was significantly decreased during hypoxia reoxygenation, suggesting that $^{\bullet}NO$ generation may have contributed to Nrf2 activation, but not $O_2^{-\bullet}$ generation alone.

During hypoxia alone, the presence of L-NAME showed a trend to protect against Nrf2 activation, but was not statistically significant. In contrast, in the presence of MnTBAP, $^{\bullet}NO$ generation from NOS would induce Nrf2, but no activation of Nrf2 was observed, suggesting that $^{\bullet}NO$ alone is not responsible for Nrf2 activation. This is further evident as there is no significant increase in Nrf2 activation upon addition of $^{\bullet}NO$ donor, spermine nonoate in hypoxia, hypoxia/reperfusion and normoxia.Supporting this, Li et al. (2006) reported that $ONOO^-$ activates Nrf2 via PI3K/Akt signalling and enhances Nrf2–ARE binding, which leads to upregulation of HO-1 expression in nitrosative stress in PC12 cells.

During hypoxia/reoxygenation in the presence of L-NAME, the significant inhibition of Nrf2 activation suggests a requirement for $^{\bullet}NO$ production possibly to make $ONOO^{-}$, as an Nrf2 inducer. In contrast, Nrf2 activation during normoxia was not affected by the presence of MnTBAP, L-NAME and spermine nonoate. In summary, the present study concludes that Nrf2 activation depends on $O_2^{\bullet-}$ and $^{\bullet}NO$, probably to generate $ONOO^{-}$ during hypoxia and hypoxia/reperfusion.

**(A)**

| Condition | Chronic, severe hypoxia (2% $O_2$, 4h) | | | | | Chronic, mild hypoxia (10% $O_2$ ,4h) | | | | | Chronic normoxia (21% $O_2$, 4h) | | | | |
|---|---|---|---|---|---|---|---|---|---|---|---|---|---|---|---|
| **Inhibitors** | **Ctl** | **ROT** | **FCP** | **APO** | **LNM** | **Ctl** | **ROT** | **FCP** | **APO** | **LNM** | **Ctl** | **ROT** | **FCP** | **APO** | **LNM** |
| **NFkB activity** | ↑* | - | - | - | - | - | - | - | - | - | X | X | X | X | X |
| **Nrf2 activity** | ↑* | - | - | - | - | - | - | - | - | - | X | X | X | X | X |

**(B)**

| Condition | Chronic, severe hypoxia/reperfusion | | | | | Sustained, severe hypoxia Control (2% $O_2$, 6h) | | | | | Normoxia Control (21% $O_2$, 6h) | | | | |
|---|---|---|---|---|---|---|---|---|---|---|---|---|---|---|---|
| **Inhbitors** | **Ctl** | **MnBP** | **SPN** | **APO** | **LNM** | **Ctl** | **MnBP** | **SPN** | **APO** | **LNM** | **Ctl** | **MnBP** | **SPN** | **APO** | **LNM** |
| **Nrf2 activation** | ↑* | ↓ | X | - | ↓ | ↑* | ↓ | X | - | ↓ | X | X | X | - | X |

**Table 7.1 Summary of results of chronic, severe hypoxia and hypoxia/reperfusion induced - NFkB and Nrf2 activation.**

**Key:** Ctl - control, ROT-rotenone, FCP- FCCP, APO- apocynin, LNM- L-NAME, MnBP- MnTBAP and SPN- spermine Nonoate.

↑* - Significant increase in control cells (2% $O_2$ or 10% $O_2$) vs. normoxic control cells.

↓ - Significant decrease in treated cells vs. control cells at same $O_2$ tension.

X - In treated cells, no significant difference vs. control cells at same $O_2$ tension or if in control cells (2% $O_2$ or 10% $O_2$), no significant difference vs. normoxic cells or in normoxic cell shows the basal effect.

\- Not available.

# CHAPTER 8

# DISCUSSION, CONCLUSION AND FUTURE WORKS

## 8.1 Discussion

Pathobiology of ischaemia-reperfusion injury in the myocardium has long been established in *in vivo* and *in vitro* vascular research. Antioxidants in cardiomyocytes maintain redox homeostasis and any perturbation of its status has distinctive deleterious effects. It appears that while excessive generation of reactive species (Chapter 4 and Chapter 6) leads to cellular injury (Chapter 5 and Chapter 6), their regulated generation may cause transient and reversible modifications leading to signal transduction for induction of adaptive responses (Chapter 7). Taken together, the present study demonstrated that generation of reactive oxygen-nitrogen species in cardiomyocytes plays a central role in mediating both cardiac injury and cardioprotection.

It has been suggested that increased levels of ROS are produced during hypoxia although others have disputed this (Waypa and Schumacker, 2005; Toescu, 2004; Duranteau et al., 1998). Others propose that ROS production during hypoxia is an artifact of analytical methods, where hydroethidine may be acting as a mitochondrial membrane potential sensor detecting depolarisation that occurs during hypoxia (Budd et al., 1997). However, these arguments can be discounted if the fluorescence of superoxide-dependent oxidation product, 2-OH-$E^+$ is analysed rather than oxidised ethidine and if changes observed after hypoxia are maintained in lysates; after lysis, all oxidised hydroethidine is released from organelles and effects on fluorescence due to different pH between subcellular compartmentalization are eliminated (Luetjens et al., 2000; Zhao et al., 2003).

In this study, analysis of H9C2 cell fluorescence attributable to 2-OH-$E^+$ was not different between lysates and intact cells supporting the hypothesis of present study that an increase in fluorescence during hypoxia is attributable to mitochondrial superoxide anion radical production (Chapter 4). Moreover, to minimize the contribution of artefactual oxidation due to photooxidation, all experiments were conducted in the dark and old culture medium was replaced with fresh pre-equilibrated medium to minimize background fluorescence prior to analysis (Chapter 3).

Fluorescence of DHE or DAF was measured or visualized according to optimum incubation times in respect to stability of oxidized probe, minimal fluorescent decay and low light excitation in order to minimise photo-activation (Chapter 4) (Abramov et al., 2007; McArdle et al., 2005; Murrant et al., 1999).

The present study describes a systematic, time and dose-dependent study of the kinetics and effects of ROS/RNS formation during hypoxia in H9C2 rat cardiac myoblasts which show morphological, biochemical and electrophysiological properties of cardiac cells but with the advantage of being derived from a single clonal population (Hescheler et al., 1991). The present study has established a culture system which mimics a physiological ischaemic period. Cells were maintained in DMEM as $O_2$ depletion occurs at a faster rate than glucose depletion during hypoxia, and inhibition of glucose metabolism accelerates consumption of the reductants, glutathione, as cellular NADPH is depleted, posing hypoxic cells under additional oxidative stress.

Cardiac myoblasts exposed to 0.23mg/L $O_2$ (severe hypoxia) showed a reduction in metabolic activity associated with oxidative phosphorylation and a reduction in membrane integrity (PI uptake) during acute and chronic, severe hypoxia. During acute, severe hypoxia, cell death was manifest in the absence of a detectable change in $O_2^{-\bullet}$ or $^{\bullet}NO$ production (**Table 8.1A**), whereas others have reported induction of ROS/RNS in different hypoxic models (Abramov et al., 2007; Becker et al., 1999). Together these data suggest that either; (1) the steady state $O_2^{-\bullet}$ or $^{\bullet}NO$ level is unchanged during an acute hypoxic event; or (2) the steady state of $O_2^{-\bullet}$ in the cell is maintained although its rate of production may be increased as it is rapidly removed through dismutation by SOD and subsequent degradation by catalase or by reaction with other molecules e.g. proteins, lipids and DNA or production of $ONOO^-$ (Aulak et al., 2004). In the present study, there was ample evidence for an accumulation of protein carbonyls during acute severe hypoxia which fits with this hypothesis (Kowaltowski and Vercesi, 1999; Levraut et al., 2003) (**Table 8.1A**).

Intracellular $^{\bullet}$NO production during acute, severe hypoxia may trigger tyrosine nitration which is a biomarker for $^{\bullet}$NO generation in cells (Aulak et al., 2004). Present study has not described the investigation of tyrosine nitration, although it is warranted as a future direction. Cell death during chronic, severe hypoxia; metabolic loss, necrosis and apoptosis was associated with significantly increased $O_2^{-\bullet}$ and $^{\bullet}$NO levels, measured by DHE and DAF respectively. There is a high chance of $ONOO^-$ formation with the increased production of both $O_2^{-\bullet}$ and $^{\bullet}$NO. $^{\bullet}$NO production during chronic, severe or mild hypoxia is partly NOS-dependent as evident by the decrease in DAF fluorescence in the presence of L-NAME (**Table 8.1A**).

It is presumed that mtNOS contributes to $^{\bullet}$NO production during hypoxia and hypoxia reperfusion (Zenebe et al., 2007; Lacza et al., 2001; Kojima et al., 1998; Brown and Borutaite, 2007), although eNOS or iNOS in the cytosol may also be important. The study of isolated mitochondria during chronic, severe hypoxia is warranted to measure $^{\bullet}$NO generation in the presence of L-NAME. $ONOO^-$ can cause irreversible damage to all mitochondrial compartments, leading to mitochondrial dysfunction (Brown and Borutaite, 2007; Brown, 1999; Borutaite and Brown, 2005). Therefore, cell death during hypoxia may reflect both ROS/RNS effects. The reported increase of NF-κB and Nrf2 activity during chronic, severe hypoxia suggests the activation of gene expression at a point of balance between protection and cell death (**Table 8.1A**). However, $ONOO^-$ is reported as an inhibitor of NF-κB/DNA binding (Levrand et al., 2006; Levrand et al., 2005; Liaudet et al., 2009). In contrast, Matata and Galiñanes, (2002) reported the activation of NF-κB using micro molar concentrations of $ONOO^-$. It is likely that NF-κB activation or inhibition by $ONOO^-$ is dose, time and cell type-dependent. The increase in PI uptake during acute, severe hypoxia suggests necrotic cell death during acute or chronic, severe hypoxia and is associated with accumulation of protein carbonyls (Shimizu et al., 1996; England et al., 2003). Closer examination by fluorescence microscopy confirmed the presence of both necrotic and "late" apoptotic cells, during chronic, severe hypoxia, but not in acute, severe hypoxia. Necrosis can be initiated by quantitative ATP depletion (Gasbarrini et al., 1992; Nicotera et al., 1986) and elevation of intracellular $Ca^{2+}$ which may disrupt the cytoskeleton and membrane integrity by activating $Ca^{2+}$-dependent proteases (Shimizu et al., 1996).

However, the present study does not support this hypothesis as ATP depletion does not change during acute, severe hypoxia. Early accumulation of oxidized proteins in the absence of detectable increase in ROS/RNS may reflect rapid oxidation of protein carbonyls in the absence of effective proteasome induction or autophagy (Asa B. Gustafsson and Roberta A. Gottlieb, 2008). The most severely damaged cells that are heavily oxidised may undergo selective death with the more adapted, viable cells exhibiting lower levels of protein carbonyls at 4h (Asa B. Gustafsson and Roberta A. Gottlieb, 2008) (**Table 8.1A**).

However, the effects of significant ATP depletion during chronic, severe hypoxia, the likely elevation of intracellular $Ca^{2+}$ and the activation of $Ca^{2+}$- dependent proteases (Nicotera et al., 1986; Gasbarrini et al., 1992) were excluded. Incorporation of 5 or 10mM EGTA into the medium exacerbated cell death during chronic, severe hypoxia. Instead dysfunctional mitochondria or other organelles due to increased protein carbonyl formation by overproduction of $O_2^{-\bullet}$ or protein/tyrosine nitration induced by overproduction of $^{\bullet}NO/ONOO^-$ may account for toxicity of hypoxia.

The increase in protein oxidation is likely to occur at the mitochondrion, thereby stimulating autophagy and may contribute to further organelle dysfunction under prolonged hypoxia (Zorov et al.,2006; Kowaltowski and Vercesi, 1999). In addition, triggering of the mitochondrial permeability transition (Crompton, 1999) may occur leading to apoptosis. Increased production of $^{\bullet}NO$ during chronic, mild hypoxia did not trigger loss of mitochondrial metabolism, necrosis or ATP depletion, but did trigger apoptosis (Brown and Borutaite, 2007; Brown, 1999; Davidson and Duchen, 2006). Therefore, the study of mitochondrial permeability transition, cytochrome *c* release or other apoptogenic factors in the cytoplasm is warranted after chronic, mild hypoxia. Activation of apoptosis observed under these conditions involved $^{\bullet}NO$, as the presence of L-NAME was associated with suppression of procaspase-3 cleavage. In contrast, a decrease in MTT activity in the presence of L-NAME indicates $^{\bullet}NO$ generation and its association to maintain balance of ETS, probably by contributing mitochondrial $^{\bullet}NO$ production from mt-NOS (**Table 8.1A**).

However, further works might be warranted to investigate this hypothesis to determine if $^{\bullet}NO$ is produced by cytosolic NOS or mt-NOS (Nagendran and Michelakis, 2009; Nisoli and Carruba, 2006). Rotenone or FCCP treatment did not protect against chronic, mild hypoxia-induced apoptosis. The availability of ATP is important for cytoplasmic cytochrome *c* mediated oligomerisation of Apaf-1 and thereby formation of the apoptosome complex, after permeability transition has taken place and with the rupture of mitochondrial outer membrane. During hypoxia, the ATP requirement of apoptosis was met via the TCA with accumulated $NAD^{+}/FAD^{2+}$ or glycolysis with abundantly available glucose in the culture medium (Kim et al., 2003; Tsujimoto and Shimizu, 2007; Eguchi et al., 1997; Enari et al., 1998; Tatsumi et al., 2003; Crompton, 1999). Indeed, apoptosis has been reported to occur in cardiomyocytes with exclusive supply of ATP through glycolysis (Tatsumi et al., 2003). ATP production from glycolysis and intracellular high energy stores can contribute 50% of total ATP production under anaerobic conditions (Kim et al., 2003).

The effect of rotenone in mitigating the toxicity associated with severe, chronic hypoxia implies a different mechanism of toxicity at 4h compared to that toxicity at 30minutes that may be principally driven by accumulation of protein damage, but not ATP depletion at 30 mins (Becker et al., 1999), whereas at 4h, the ability of rotenone to prevent ROS formation is of greater significance (**Table 8.1A**). This hypothesis is supported by the observations that ATP levels drop by 50% during chronic (4h) hypoxia and are reduced by a further 50% in the presence of rotenone, however the additional depletion of ATP caused by rotenone is not associated with any further loss in viability, rather it protects cells against necrosis and apoptosis. It is interesting that suppression of apoptosis in the presence of rotenone during chronic, severe hypoxia associates with reduction of $O_2^{-\bullet}$ production despite further ATP depletion. To support this hypothesis further, FCCP treatment during chronic, severe hypoxia elicited inhibition of a cleavage of procaspase-3, with further depletion of ATP, similar to rotenone treatment (**Table 8.1A**). In the presence of FCCP, uncoupling of mitochondria during severe hypoxia allows the dissipation of reducing equivalents more readily thereby allowing the TCA cycle to continue unhindered for removal of lactate in a situation when the cell is dependent on anaerobic glycolysis for ATP

production (Abramov et al., 2007). In the presence of L-NAME, chronic, severe hypoxia-induced cell death via necrosis and apoptosis was significantly reduced, suggesting that $^{\bullet}NO$ is responsible for associated cytoxicity (Strijdom et al., 2006; Zweier et al., 1995). NOS isoforms are responsible in production of $^{\bullet}NO$ during chronic, mild hypoxia, and the induction of apoptosis where L-NAME treatment showed a significant protection against cell death. During chronic, severe hypoxia, fragmented cell structure/nuclei were observed in Hoescht 33342 stained (blue) cells for early apoptotic cells and fragmented nuclei as stained with PI (red) for late apoptotic cells (Tsujimoto and Shimizu, 2007; Shimizu et al., 1996) in the absence of necrotic nuclei.

Cellular "acidosis" during chronic, severe hypoxia due to lactic acid accumulation inhibits pore opening and may act as a protective mechanism against apoptosis (Kim et al., 2003; Crompton, 1999). However, in the present model, hypoxia induced ROS/RNS-mediated mitochondrial dysfunction is suggested to have overcome those inhibitory processes to induce apoptosis by cleaving procaspase-3. During chronic, severe hypoxia, when electron transport has ceased, it is reported that the membrane potentials are developed at the expense of ATP depletion by the mitochondrial ATP synthase (Kim et al., 2003). In the present model, ATP availability is assumed to be sufficient to promote apoptosis events. The decrease in metabolic activity during acute, severe hypoxia parallels the decrease activity of succinate dehydrogenase in mitochondrial complex II during hypoxia (Crawford et al., 2003). During acute or chronic, severe hypoxia, the mitochondrial membrane potential decreases lost owing to reversal of electron flow through ETS in the presence of a limiting $O_2$ supply. Therefore, the loss of membrane potential would decrease oxidation of NADH in complex I and $FADH_2$ in complex II, thereby decreasing the activity of both dehydrogenase enzymes present in complex I and II. Supporting this, increased production of $O_2^{-\bullet}$ inactivates complex I; NADH dehydrogenase and complex II; succinate dehydrogenase (Powell and Jackson, 2003). However, the absence of ATP depletion during acute, severe hypoxia confirms the closely matched balance between ATP production and ATP demand when cells are metabolically compromised (Vogt et al., 2002).

$^{\bullet}$NO alone can cause reversible inhibition of cytochrome *c* oxidase and complex I, and may therefore contribute to mitochondrial $O_2^{-\bullet}$ production and irreversible damage caused by $ONOO^-$ (Arciello et al., 2010). Metabolic activity was retained during chronic, severe hypoxia in the presence of L-NAME, MnTBAP and rotenone independently, suggesting involvement of $O_2^{-\bullet}$ and $^{\bullet}$NO, possibly via $ONOO^-$ production to inhibit the ETS (Powell and Jackson, 2003; Hassouna et al., 2006; Levrand et al., 2006). Complex I generated $O_2^{-\bullet}$ has also been implicated in altered neuronal cell metabolism during hypoxia (Guglielmotto et al., 2009). In contrast, mitochondrial complex II or III has been proposed as a $O_2^{-\bullet}$ generation site in the rat heart (Chandel et al., 2000), but this has not been investigated in this thesis. Rotenone inhibits irreversibly the dehydrogenase enzyme present in mitochondrial complex I, and this probably results in a decrease in NADH oxidation which leads to greater loss of membrane potential in the absence of electron flux through ETS, thereby reducing $O_2^{-\bullet}$ production. In support of this hypothesis, the irreversible inhibition of mitochondrial complex I in rabbit hearts showed protection against ischaemic damage by preserving of cardiolipin and cytochrome *c* content (Lesnefsky et al., 2004).

Complex 1 is reported as the major ROS generation centre with complex III (Chandel and Schumacker, 1999; Chandel et al., 1998; Chandel et al., 2000; Duranteau et al., 1998; Chandel and Budinger, 2007). The electron leakage from complex I leads to formation of $O_2^{-\bullet}$ via two mechanisms; forward and reverse electron transfer (Tahara et al., 2009). Forward transfer is due to electron leakage from NADH oxidation which may then generate $O_2^{-\bullet}$ at different sites; the FMN group, low-potential Fe-S centres and Q binding sites within complex I. Rotenone blocks Q binding and maximizes FMN and Fe-S centre reduction (Tahara et al., 2009) in addition to inhibiting electron flux from NADH oxidation. Therefore, reduction of $O_2^{-\bullet}$ production from complex I, in the presence of rotenone reduces the mitochondrial dysfunction due to $O_2^{-\bullet}$ and $ONOO^-$ mediated oxidation and inhibition, thereby promoting $FADH_2$ oxidation via increased succinate dehydrogenase activity. Therefore, rotenone decreases production of $O_2^{-\bullet}$ during hypoxia and reduces PI uptake; necrosis and apoptosis probably by reducing protein carbonyl and nitrotyrosine formation.

The suppression of procaspase-3 cleavage indicates the inhibition of one or more upstream processes; release of cytochrome *c* and Apaf-1 after opening of the MPTP and ATP- dependent oligomerisation of Apaf-1 to induce apoptosome complex. ROS production during hypoxia has been attributed to NADPH oxidase activity by several authors (Abramov et al., 2007; Zulueta et al., 1997). Apocynin-inhibitable NADPH oxidase activity did not contribute to increased ROS production as neither DHE oxidation nor caspase 3 activity were altered in H9C2 cells maintained in chronic severe hypoxia. Apocynin did afford protection against necrosis induced by chronic severe hypoxia and apoptosis induced by chronic, mild hypoxia (Heumuller et al., 2008; Touyz, 2008). Consistent with previous works, the present study did not show any protective effects of the xanthine oxidase inhibitor, allopurinol, neither on viability or detectable ROS production (Becker et al., 1999).

The foregoing discussion has focused on the effects of 2% $O_2$ hypoxia on $O_2^{-\bullet}$ steady state levels, metabolic activity and viability of cardiacmyoblasts. For the purposes of current experiments, 21% $O_2$ conditions is referred as normoxia, although this is unphysiological (Zuurbier et al., 1999). Instead, estimates of $O_2$ tension in tissue vary between 10-14% $O_2$ and will fluctuate during physiological stress and pathophysiological conditions which reduce $O_2$ delivery to tissues (Zuurbier et al., 1999).

In this regard, present studies of the effects of 10% $O_2$ and on cardiac myoblasts and referred to this as mild hypoxia. The H9C2 cultured cells used in this investigation were maintained and adapted to 21% $O_2$ during routine culture over many passages (cells between 14-18 passages were used) and are therefore expected to have adapted to living under high $O_2$ tension. This may have some impact on the levels of "antioxidant" enzymes present and therefore the cells ability to withstand ROS/RNS. Cells under 10% $O_2$ did not exhibit any significant change in metabolic activity, propidium iodide uptake or DHE oxidation compared to 21% $O_2$, except, $^{\bullet}NO$ generation during chronic, mild hypoxia. However, $^{\bullet}NO$ generation and apoptosis were increased in cells maintained at 10% $O_2$ for 4h (**Table 8.1A**).

**(A)**

| Condition | Chronic, severe hypoxia (2% $O_2$, 4h) | | | | | Chronic, mild hypoxia (10% $O_2$, 4h) | | | | | Chronic normoxia (21% $O_2$, 4h) | | | | |
|---|---|---|---|---|---|---|---|---|---|---|---|---|---|---|---|
| Inhibitors | Ctrl | ROT | FCCP | APO | LNAM | Ctrl | ROT | FCCP | APO | LNAM | Ctrl | ROT | FCCP | APO | LNAM |
| ROS ($O_2^-$) | ↑* | ↓ | ↓ | X | X | X* | X | X | X | X | X | X | X | X | X |
| RNS | ↑* | X | X | X | ↓ | ↑* | X | X | X | ↓ | X | X | X | X | X |
| Metabolic activity | ↓* | ↑ | X | X | ↑ | X* | X | ↓ | ↓ | ↓ | X | X | X | X | X |
| Necrosis | ↑* | ↓ | X | ↓ | ↓ | X* | X | X | X | X | X | X | X | X | X |
| ATP depletion | ↑* ♀ | ↑ | ↑ | - | - | ↑* | - | - | - | - | X | ↑ | ↑ | - | - |
| Apoptosis | ↑* | ↓ | ↓ | ↑* | ↓ | ↑* | ↑* | ↑* | ↓ | ↓ | X | X | X | X | X |
| Protein carbonyls | X* | - | - | - | - | X* | - | - | - | - | X | - | - | - | - |
| NFkB activity | ↑* | - | - | - | - | - | - | - | - | - | X | X | X | X | X |
| Nrf2 activity | ↑* | - | - | - | - | - | - | - | - | - | X | X | X | X | X |

| Condition | Acute, severe hypoxia (2% $O_2$, 30min) | | | | | Acute, mild hypoxia (10% $O_2$, 30min) | | | | | Acute normoxia (21% $O_2$, 30min) | | | | |
|---|---|---|---|---|---|---|---|---|---|---|---|---|---|---|---|
| Inhibitors | Ctrl | ROT | FCCP | APO | LNAM | Ctrl | ROT | FCCP | APO | LNAM | Ctrl | ROT | FCCP | APO | LNAM |
| ROS ($O_2^-$) | X | ↑ | ↑ | ↑ | X | X | X | ↑ | X | X | X | X | X | X | X |
| RNS | X | - | X | X | X | X | - | X | X | X | X | - | X | X | X |
| Metabolic activity | ↓* | X | ↑ | X | X | X | X | ↑ | X | X | X | X | X | X | X |
| Necrosis | ↑* | ↓ | ↓ | X | ↓ | X | X | ↑ | X | X | X | X | X | X | X |
| ATP depletion | X | - | - | - | - | X | - | - | - | - | X | - | - | - | - |
| Apoptosis | X | - | - | - | - | X | - | - | - | - | X | - | - | - | - |
| Protein carbonyls | ↑* | - | - | - | - | X | - | - | - | - | X | - | - | - | - |

**(B)**

| Condition | Chronic, severe hypoxia/reperfusion | | | | | Chronic, severe hypoxia Control (2% $O_2$, 6h) | | | | | Chronic normoxia Control (21% $O_2$, 6h) | | | | |
|---|---|---|---|---|---|---|---|---|---|---|---|---|---|---|---|
| Inhibitors | Ctrl | ROT | FCCP | APO | LNAM | Ctrl | ROT | FCCP | APO | LNAM | Ctrl | ROT | FCCP | APO | LNAM |
| ROS ($O_2^{\cdot-}$) | ↑* | ↓ | ↓ | ↓ | X | ↑* | ↓ | ↓ | X | X | X | X | X | X | X |
| RNS | ↑* | ↓ | ↓ | - | ↓ | ↑* | ↓ | ↓ | - | ↓ | X | X | X | - | X |
| Inhbitors2 | Ctrl | MnTBP | SP-N | APO | LNAM | Ctrl | MnTBP | SP-N | APO | LNAM | Ctrl | MnTBP | SP-N | APO | LNAM |
| Metabolic activity | ↓* | ↑ | X | - | ↓ | ↓* [2] | ↑ | X | - | ↑ | X | X | X | - | X |
| Nrf2 activation | ↑* | ↓ | X | - | ↓ | ↑* | ↓ | X | - | ↓ | X | X | X | - | X |

Key:

↑* - Significant increase in control cells (2% $O_2$ or 10% $O_2$) vs. normoxic control cells

↓* - Significant decrease in control cells (2% $O_2$ or 10% $O_2$) vs. normoxic control cells

↑ - Significant increase in treated cells vs. control cells at same $O_2$ tension

↓ - Significant decrease in treated cells vs. control cells at same $O_2$ tension

X* - No significant effect in control cells (2% $O_2$ or 10% $O_2$) vs. normoxic control cells

X - In treated cells, no significant difference vs. control cells at same $O_2$ tension or if in control cells (2% $O_2$ or 10% $O_2$), no significant difference, vs. normoxic control cells or in normoxic cell shows the basal effect

↓ - Decrease (non-significant) in treated cells vs. control cells at same $O_2$ tension

\- N/A

**Table 8.1 Summary of results.** (A) Summary of results of acute and chronic hypoxia (severe and mild) and normoxia (B) Summary of results of chronic hypoxia/reoxygenation, sustained hypoxia and normoxia.

In the presence of FCCP, the increase in steady state metabolic activity and the significantly increased PI uptake, during acute, mild hypoxia suggest FCCP toxicity, although this effect did not persist under conditions of chronic, mild hypoxia. However, FCCP did not protect against changes to $O_2^{-\bullet}$ steady state levels and increased $^{\bullet}NO$ levels, nor against PI uptake induced by chronic hypoxia alone despite FCCP being effective in ROS inhibition during severe hypoxia (**Table 8.1A**). This suggests that the respiratory chain is exquisitely sensitive to small fluxes in $O_2$ tensions. The effects of uncoupling and inhibition of mitochondrial complex may have significantly reduced ATP production, although there is no observed necrotic cell death or decreased metabolic activity in the presence of rotenone and FCCP during mild, severe hypoxia which concurs with previous work (Brennan et al., 2006b; Brennan et al., 2006a).

As reperfusion has been considered a major inducer of ROS/RNS after hypoxia and cause of death, the kinetics and nature of their production was investigated in cardiomyocytes. The recovery of metabolic activity during acute, hypoxia/reperfusion compared to hypoxia indicates the capacity to restore membrane potential (Serviddio et al., 2005). However, an increase in irreversible necrotic cell death was expected, reflecting the increased PI uptake during acute, severe hypoxia alone, associated with protein carbonyl formation (Chapter 5) (**Table 8.1A**). In fact, 30min hypoxia followed by reoxygenation or sustained hypoxia had little effect on ROS/RNS or viability. During chronic, severe hypoxia/reoxygenation, the decrease in metabolic activity of H9C2 cells compared to cells grown under normoxia and measured by MTT reduction was associated with the increase in $O_2^{-\bullet}$ and $^{\bullet}NO$ production (**Table 8.1B**).

However, restoration of metabolic activity during chronic, severe hypoxia indicates repolarisation the mitochondrial membrane precluding the irreversible damage to mitochondrial complexes. It is interesting to speculate that sustained reperfusion (2h) after chronic, severe hypoxia is the turning point between irreversible cell damage and hypoxic recovery, as evident by significant viability loss after long periods of reperfusion (Jiao et al., 2009).

The irreversible damage reported during chronic, severe hypoxia in the present study resulted in necrotic and apoptotic cell death during chronic, severe hypoxia/reoxygenation. In the presence of rotenone or FCCP, the reduction in $O_2^{-\bullet}$ and $^{\bullet}NO$ levels during sustained hypoxia or reperfusion indicated the contribution of mitochondria as a major ROS/RNS producer. Inhibition of enhanced $O_2^{-\bullet}$ production during reperfusion in the presence of apocynin, but not during hypoxia alone indicates the induction of NADPH oxidase complex activation during reperfusion as a major contributor to $O_2^{-\bullet}$ (**Table 8.1B**). However, its activation is evasive as there is a trend to increasing $O_2^{-\bullet}$ during normoxia in the presence of apocynin. Apocynin may function as antioxidant rather than impairing NADPH oxidase complex in H9C2 cells which are non-phagocytes (Heumuller et al., 2008).

Other investigators reported the contribution of NADPH oxidase activity in H9C2 cells to generate ROS under different ischaemia/reperfusion periods in anoxic culture medium (Elisabetta et al., 2008). It appears that activation of different sources to produce $O_2^{-\bullet}$ depends on severity and duration of hypoxia and/or reperfusion.

Decreased $^{\bullet}NO$ production in the presence of L-NAME suggest $^{\bullet}NO$ generation is partly NOS-dependent during chronic, severe hypoxia/reperfusion. There may be alternative non-enzymatic sources that are activated to generate $^{\bullet}NO$ (Lacza et al., 2006; Lepore, 2000; Brown and Borutaite, 2007; Zweier et al., 1999) or related species as evident by ~ 25% decrease in NOS-dependent $^{\bullet}NO$ production when normoxic cells were co-incubated with L-NAME. Having elucidated the temporal relationship between ROS/RNS generation, cell dysfunction and death during hypoxia and hypoxia/reperfusion, the possible effects of ROS/RNS in inducing gene expression were investigated using reporter assay for NF-κB and Nrf2.

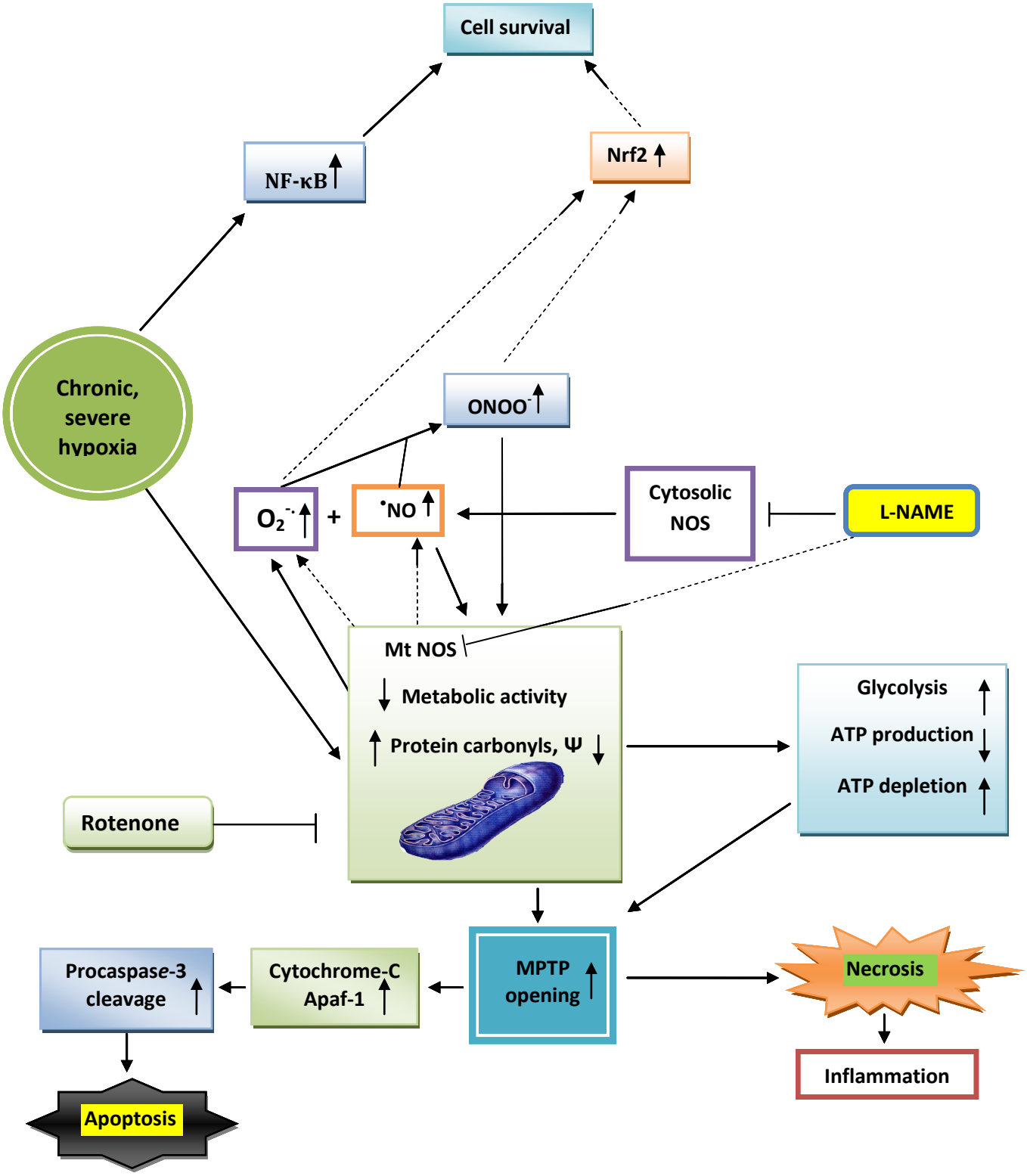


**Figure 8.1 Summary of chronic, severe hypoxia-induced $O_2^{-\bullet}$/$^{\bullet}NO$ generation and cell death. ↑ - increase or ↓ - decrease.**

The significant increase in NF-κB/DNA binding suggests the increased activation of NF-κB during chronic, severe hypoxia and probably may be associated with the increased production of ROS/RNS (Baeuerle and Baltimore, 1996, Baldwin, 1996) (**Table 8.1A**). Therefore, use of ROS/RNS specific inhibitors or scavengers could be used to test this hypothesis. However, understanding of the mechanism of hypoxia-dependent activation of NF-κB remains limited (Taylor and Cummins, 2009). Cell death reported in the presence of NF-κB inhibitor, SN-50 may describe the importance of NF-κB activation as an adaptive response during chronic, severe hypoxia. Several authors have reported the increased activity of NF-κB and associated cardiac protection during ischaemia and ischaemia/reperfusion (Li et al., 1999; Regula et al., 2004; Adrienn et al., 2003; Nguyen et al., 2009; Lee, 2003). In contrast, other authors reported that NF-κB co-ordinates cell homeostasis during stress and control the balance between cell survival and cell death (Perkins, 1997). Therefore, therapeutic interventions should be carefully weighed given its potential dual role (Adrienn et al., 2003). **Figure 8.1** illustrate the summary of key events in respect to ROS/RNS generation and cell death during chronic, severe hypoxia in the present study.

A study by Lee and Johnson. (2004) showed that neural cells from Nrf2-/- mice were more sensitive to oxidative stress than were neurons from control animals, but, they became less prone to oxidative stress when the cells were transfected with a functional Nrf2 construct (Lee and Johnson, 2004 ). Similarly, transient ischaemia followed by reperfusion induced more extensive brain damage in Nrf2-/- mice than in WT mice (Shah et al., 2007). Moreover, Nrf2-KO diabetic mice showed increased apoptosis by increasing ROS compared to Nrf2-WT diabetic mice and the authors suggested that Nrf2 induced expression of antioxidant defence genes to scavenge the overproduced ROS (He et al., 2009). In the present study, Nrf2 activation during sustained hypoxia may mediate Nrf2-mediated antioxidant defence, probably by increasing expression of SOD1, NQO1 and/or GST when ROS/RNS are overproduced. In other words, when ROS/RNS are overproduced, Nrf2 is activated to scavenge ROS/RNS by increasing the expression of antioxidant genes or detoxifying genes (**Figure 8.2**). However, further work is required to resolve the importance of Nrf2 activation using Nrf2-KO/WT cell line under hypoxia and reperfusion.

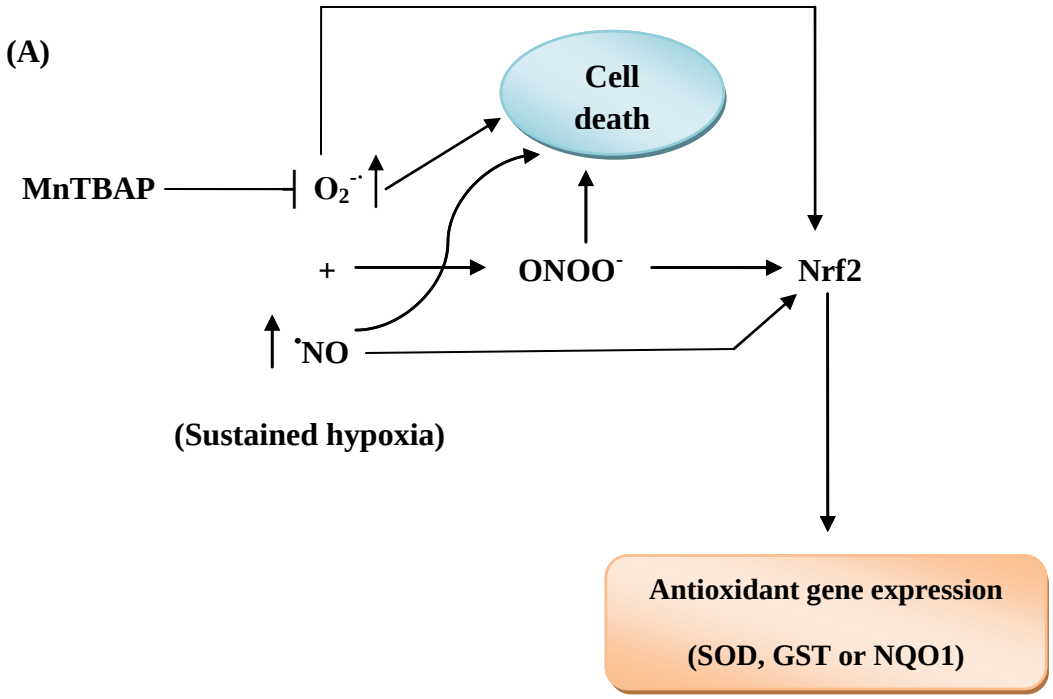


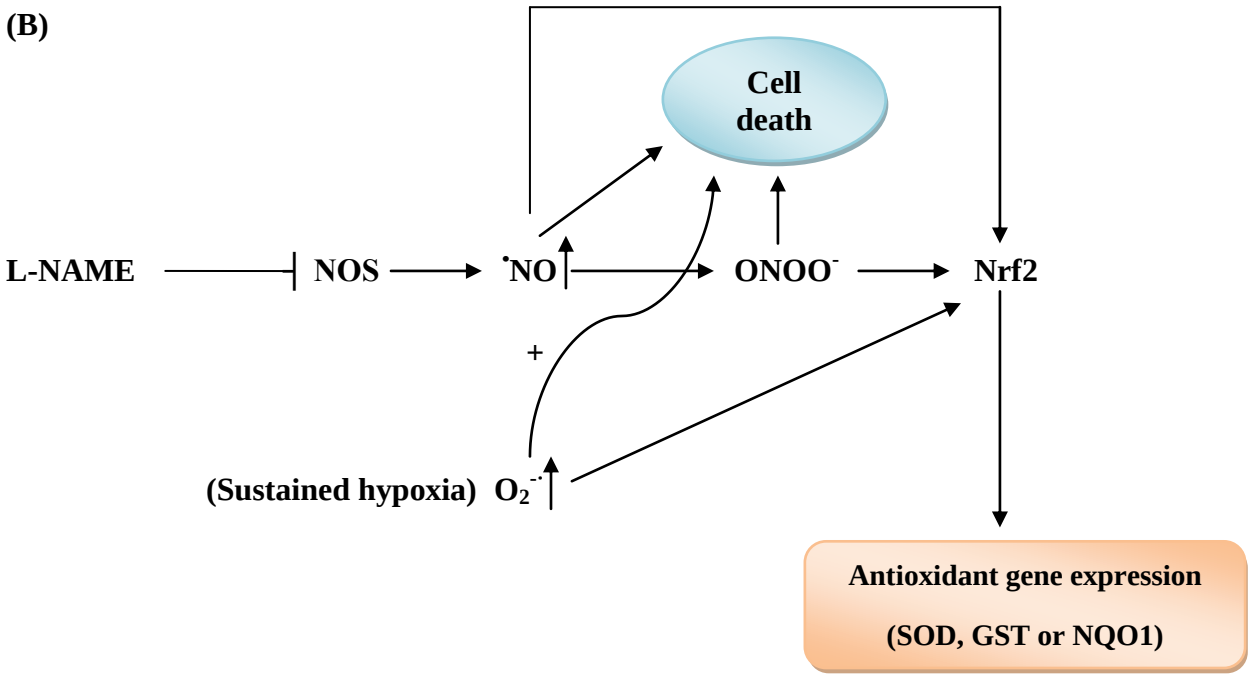


**Figure 8.2 Schematic illustration of Nrf2 activation during sustained hypoxia in the presence of MnTBAP or L-NAME. ↑ - increase or ↓ - decrease.**

In the presence of MnTBAP, cellular protection during reoxygenation was achieved in the absence of $O_2^{-\bullet}$ and/or $ONOO^-$, though $^{\bullet}NO$ is abundant. Due to unavailability of $ONOO^-$ in the presence of MnTBAP, there is no Nrf2 activation, nor $ONOO^-$ induced cytotoxicity. However, exacerbation of cell death in the presence of L-NAME during reoxygenation may be associated with the lack of $^{\bullet}NO$-mediated protective mechanism against excessive generation of $O_2^{-\bullet}$ during reoxygenation (**Table 8.1B**) (**Figure 8.3**). It has been reported that overproduction of $O_2^{-\bullet}$ occurs during hypoxia/reperfusion more than hypoxia alone in many redox models (Abramov et al., 2007; Li and Jackson, 2002).

But, the present system did not show an excessive generation of $O_2^{-\bullet}$ during hypoxia/reoxygenation compared to sustained hypoxia, though the protective role of $^{\bullet}NO$ broadly agreed with other investigators (Beckman and Koppenol, 1996; Gonon et al., 2004; Dhakshinamoorthy and Porter, 2004; Jones et al., 1999) (**Table 8.1B**). A study by Kanno et al. (2000) showed that attenuation of myocardial ischaemia/reperfusion injury in eNOS-KO mice by super-induction of iNOS to produce $^{\bullet}NO$ during early ischaemia was an adaptive mechanism (Kanno et al., 2000), but, it occurred prior to reperfusion, probably to induced preconditioning pathway. However, $^{\bullet}NO$ mediated protection during reperfusion in the present system remains to be resolved.

Similar to the effects observed in sustained hypoxia, the presence of MnTBAP (**Figure 8.3B**) and L-NAME (**Figure 8.3A**), the decreases in Nrf2 activation during reoxygenation possibly due to inhibition of $O_2^{-\bullet}$- dependent formation of $ONOO^-$ (**Figure 8.3**) (**Table 8.1B**). Supporting this idea, previous workers have shown that $ONOO^-$ produced from NOS-dependent $^{\bullet}NO$ or exogenous $ONOO^-$ donors, but not $^{\bullet}NO$ donors alone, caused an induction of GST gene expression in hepatoma cells via activation of Nrf2/ARE (Kang et al., 2002). In PC12 cells, $ONOO^-$ activates Nrf2 via PI3K/Akt signalling and enhances Nrf2–ARE binding to upregulate HO-1 expression in nitrosative stress (Li et al., 2006).

(A)

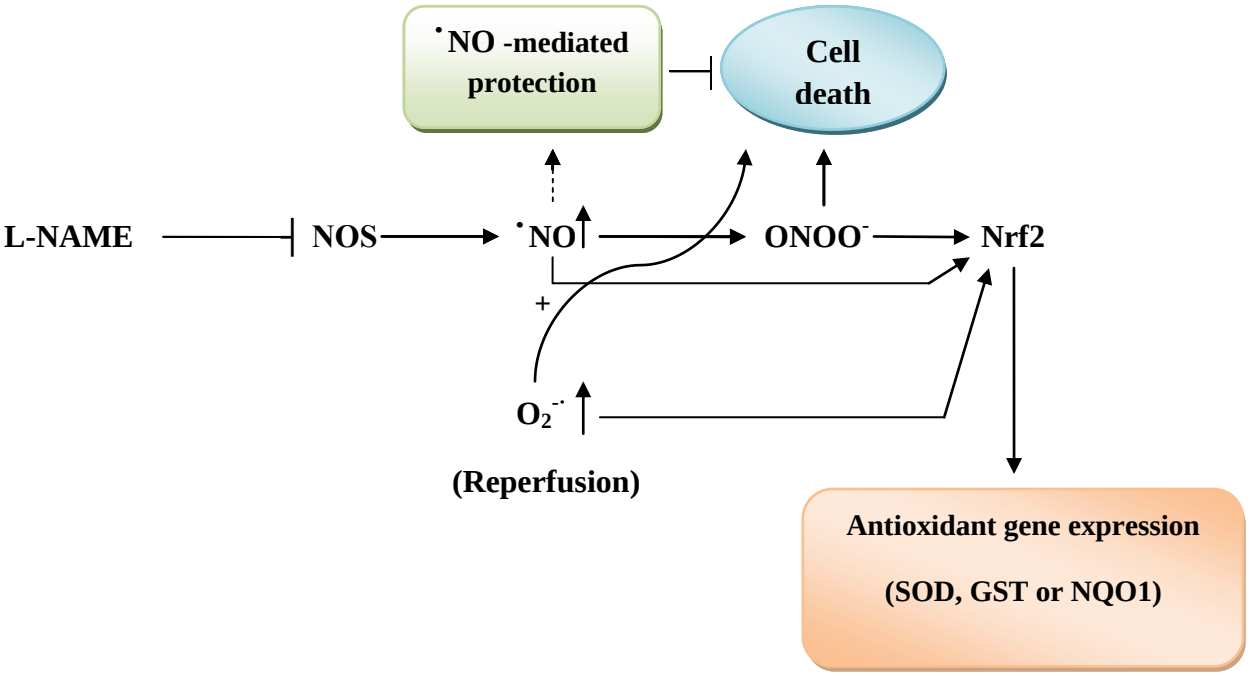


(B)

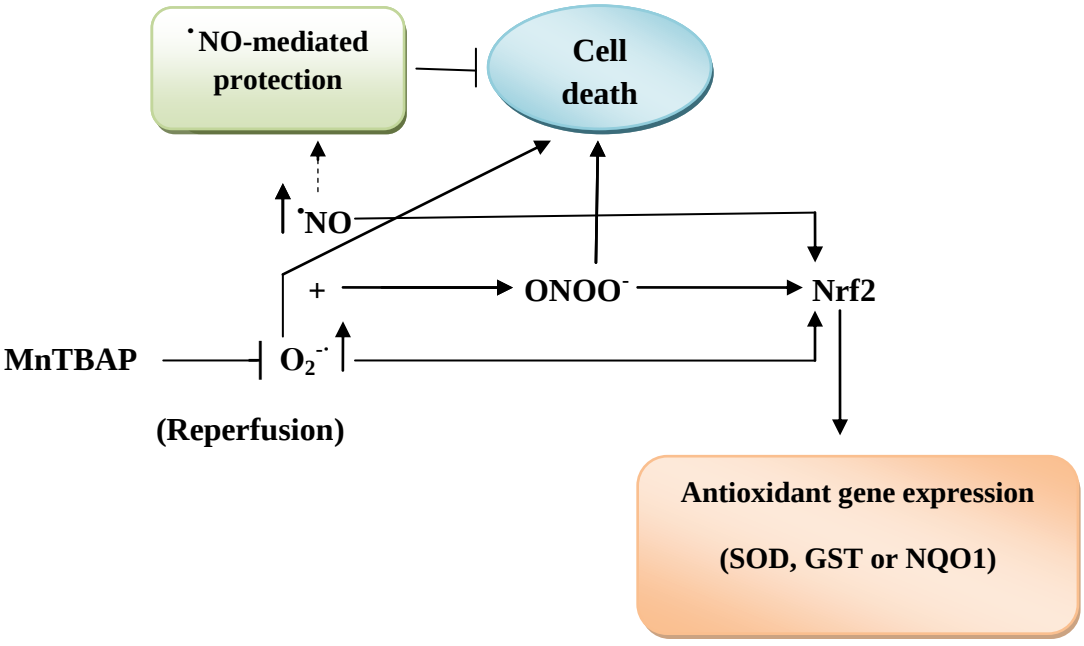


**Figure 8.3 Schematic illustration of Nrf2 activation during reperfusion and the effects of MnTBAP or L-NAME. ↑ increase or ↓ decrease.**

The exacerbation of cell death was observed in the presence of L-NAME during reoxygenation, suggesting that NO-mediates protective mechanisms during reperfusion which is broadly in agreement with other investigators (Beckman and Koppenol, 1996, Gonon et al., 2004, Dhakshinamoorthy and Porter, 2004, Jones et al., 1999) (**Figure 8.3A**). Overproduction of $O_2^{-\bullet}$ during hypoxia/reperfusion compared to hypoxia alone has been reported redox models by many authors (Abramov et al., 2007, Li and Jackson, 2002), although, the present system did not show an excessive generation of $O_2^{-\bullet}$ compared to sustained hypoxia (**Table 8.1B**). Kanno et al., 2000 showed the attenuation of myocardial ischemia/reperfusion injury in eNOS-KO mice by superinduction of iNOS, with production of $^{\bullet}NO$ during early ischemia as an adaptive mechanism (Kanno et al., 2000), probably inducing a preconditioning pathway.

Moreover, the absence of eNOS in mouse heart exacerbated the ischaemia/reperfusion injury in eNOS-KO mice (Jones et al., 1999). Similarly, the administration of $^{\bullet}NO$ donors prevents ischaemia/reperfusion injury (Mizuno et al., 1998). In contrast, other studies using pharmacological inhibition of NOS and eNOS-KO mice showed protective effects against ischaemia/reperfusion injury in the heart. Comparisons between these studies are difficult because of differences in agents and experimental design (Parrino et al., 1998). The mechanism involved in $^{\bullet}NO$-mediated cellular protection and $^{\bullet}NO/O_2^{-\bullet}$ mediated activation during hypoxia/reperfusion is unknown. In the present study, targeting ROS/RNS formation has been proposed as a promising therapeutic strategy. Several approaches that have successfully reduced tissue damage in animal or cell culture models by scavenging ROS/RNS, but, have failed to be beneficial in clinical trials (Fang et al., 2009).

Also, the present study reflects the clinical importance of $^{\bullet}NO$ donors or the therapeutic activation of NOS isoforms to induce $^{\bullet}NO$ during reperfusion after ischaemia in heart patients. Nevertheless, the beneficial effects in treating ischaemia/reperfusion injury by therapeutic NOS-gene transfer has been reported very recently (Szelid et al., 2009). Improved understanding of $^{\bullet}NO$ dose and time-dependent effects on reperfusion injury is needed.

In contrast, cell metabolic activity was increased in conditions where Nrf2 activity was decreased in the presence of MnTBAP during both sustained, severe hypoxia and severe hypoxia/reoxygenation. Similarly, cell metabolic activity was increased in the presence of L-NAME during sustained hypoxia, but not during reoxygenation (**Table 8.1B**). Therefore, Nrf2 activation and cell survival in the present system may be independent during sustained hypoxia and reoxygenation. The association of cell survival and Nrf2 activation during sustained hypoxia and reoxygenation does not imply causality, although the given outcome in the presence of inhibitors. However, the effect of inhibitors depends on three factors; (1) specificity of inhibitor; (2) length of pre-incubation required to have an effect; and (3) concentration of inhibitor required to have an effect under conditions in the present study.

According to hypotheses in the present study; (1) hypoxia increases ROS and RNS, and their effects may be cytotoxic and/or required for survival, with both pathways probably being activated during severe hypoxia (NF-kB being protective in first instance and Nrf-2 being protective), however the effects of ROS and RNS depends on their relative concentration and duration; and (2) that chronic, severe hypoxia/reoxygenation further increases ROS/RNS and in this instance, the balance of outcome is a greater drive towards cell death, probably NF-κB mediated if apoptosis is occurring or independent of transcription factor activity during necrosis with death being $O_2^{-\bullet}$ dependent and protected by $^{\bullet}NO$. However, further increase in $^{\bullet}NO$ may be cytoprotective by scavenging a more damaging $O_2^{-\bullet}$ anion and this effect may be gene expression dependent or independent. In addressing these hypotheses, the present study supports hypothesis 1, but not hypothesis 2 as there is no significant increase in ROS/RNS or cell death during chronic, severe hypoxia/reoxygenation compared control cells in sustained, severe hypoxia (**Table 8.1B**). This is possibly due to presence of glucose in culture medium throughout hypoxia. Therefore, present model validates the current paradigm in which $O_2$ depletion precedes glucose depletion in *in vivo* models.

## 8.2 Conclusion

### 8.2.1 Hypoxia

In the present work, both mitochondria and NOS are shown to contribute to overproduction of $O_2^{-\bullet}$ and $^{\bullet}NO$ during chronic hypoxia. Rat cardiomyoblasts during chronic, severe hypoxia elicit a significant increase in $O_2^{-\bullet}$/$^{\bullet}NO$ production and ATP depletion with decreased metabolic activity. Cell death during chronic, severe hypoxia is via necrosis and apoptosis. Chronic, mild hypoxia induces apoptosis, with increased production of $^{\bullet}NO$, ATP depletion and decreased metabolic activity. Significant production of $O_2^{-\bullet}$, but not depletion of ATP during chronic, severe hypoxia (2% $O_2$; 4h) has contributed to significant necrotic cell death and induction of apoptosis. Treatment with rotenone afforded protection against apoptosis and necrosis, and this associated with a reduction of $O_2^{-\bullet}$ production and enhanced metabolism during chronic hypoxia. L-NAME afforded protection against necrosis, but not apoptosis during chronic, severe hypoxia and this associated with the reduction of NOS-dependent $^{\bullet}NO$ production and enhanced metabolic activity.

Significant $O_2^{-\bullet}$ production during chronic, severe hypoxia did not change in the presence of apocynin, but apocynin afforded protection against necrosis, probably via its antioxidant property as previously reported (Heumuller et al., 2008). Induction of apoptosis during chronic, mild hypoxia associates with a significant production of NOS-dependent $^{\bullet}NO$ and reduction in $^{\bullet}NO$ levels by L-NAME treatment affords a protection against apoptosis. Rat cardiomyoblasts do not show any significant change in $O_2^{-\bullet}$ steady state or ATP levels in acute, severe hypoxia despite being metabolically compromised, exhibiting elevated levels of protein carbonyls and showing evidence of necrosis. Autophagy may contribute to the observed loss of viability (Asa B. Gustafsson and Roberta A. Gottlieb, 2008), however, if mitochondrial respiration is uncoupled (i.e.: FCCP treatment) cell survival and metabolism under acute, severe hypoxia conditions are enhanced in the absence of necrosis. The inhibition of mitochondria at complex I during acute and chronic, severe hypoxia prevents necrosis.

Both mitochondrial uncoupling and complex I inhibition afforded protection during acute, severe hypoxia, via a $O_2^{-\bullet}$-dependent pathway. These data suggest that it is the management of mitochondrial ROS and NOS-dependent $^{\bullet}NO$ levels rather than ATP that is required for improved survival during hypoxia. Chronic, severe hypoxia activates both NF-κB and Nrf2. Nrf2 activation during severe, hypoxia is $O_2^{-\bullet}$ and $^{\bullet}NO$ -dependant, probably via $ONOO^-$. NF-κB activation during chronic, severe hypoxia mediates the cellular defence mechanism against hypoxia-induced metabolic inhibition via an unknown mechanism. Taken together, the data suggest delicate balance exists between cell survival (promoted by NF-κB mediated antioxidant system) and cell death (induced by $O_2^{-\bullet}$ and $^{\bullet}NO$ produced during hypoxia).

### 8.2.2 Hypoxia/reoxygenation

Mitochondria, NOX and NOS contribute to significant ROS/RNS production during hypoxia/reoxygenation thereby, inducing metabolic inhibition in mitochondria. Chronic, severe hypoxia/reoxygenation partially restores the metabolic activity lost under hypoxia in the conditions employed in this study. The mitochondria and NOX jointly produce $O_2^{-\bullet}$ during reperfusion after chronic, severe hypoxia in rat cardiomyoblasts. Mitochondrial inhibition or uncoupling during the reoxygenation period or the last 2h of sustained hypoxia significantly reduces $O_2^{-\bullet}$ production. NOX appears to elicit $O_2^{-\bullet}$ production during reoxygenation, but not during sustained hypoxia as evident by inhibition of DHE oxidation with apocynin treatment, although this remains to be confirmed with more specific NOX inhibitors.

Both mitochondria and NOS contribute to $^{\bullet}NO$ production during reoxygenation and sustained hypoxia. $^{\bullet}NO$ generation during reoxygenation or sustained hypoxia partly depends on NOS and $^{\bullet}NO$ released from non-enzymatic sources. Also, mitochondrial inhibition and uncoupling reduced $^{\bullet}NO$ production during reoxygenation and sustained hypoxia. Significant production of $O_2^{-\bullet}$ during reoxygenation or sustained hypoxia is cardiotoxic and causes metabolic inhibition. In contrast, $^{\bullet}NO$ generation during reoxygenation is cardiacprotective, but, it is cardiotoxic during sustained hypoxia. Cardiotoxicity of $^{\bullet}NO$ may associate with increased production of $O_2^{-\bullet}$,

probably to make $ONOO^-$ during sustained hypoxia. Therefore, cardiacprotection of $^{\bullet}NO$ during reoxygenation may associate with the activation of antioxidant defence in rat cardiomyoblasts, independent to Nrf2 activation. Cardio-protection or cardio-toxicity may depend on $^{\bullet}NO$ concentration, severity and duration of hypoxia or reoxygenation. Both sustained severe hypoxia and chronic, severe hypoxia/reoxygenation activates Nrf2 gene expression and depends on $O_2^{-\bullet}$ and $^{\bullet}NO$, probably to make $ONOO^-$. Cell survival mechanism and activation of Nrf2 may be independent in the situation of hypoxia/reoxygenation or sustained hypoxia. But, Nrf2 activation probably associate with antioxidant gene expression during hypoxia alone or hypoxia/reoxygenation if both $O_2^{-\bullet}$ and $^{\bullet}NO$ are sufficiently available.

### 8.3 Future directions

In the present study, the molecular mechanisms underlying $O_2^{-\bullet}$ and $^{\bullet}NO$-mediated cell death via apoptosis remain unknown and warrant further investigation. Apoptosis is an ATP-dependent cell death programme in the myocardium; inhibition of this process may have cardioprotective effects under many pathological conditions and represents a potential target for therapeutic intervention to prevent ischemia/reperfusion damage. This work has demonstrated the suppression of apoptosis despite the depletion of ATP, by curtailing mitochondrial $O_2^{-\bullet}$ production in the presence of rotenone. Expressing of upstream targets of apoptosis; ATP dependent-pro-apoptotic proteins: Puma, Noxa, Bax and Bak, and anti-apoptotic proteins: Bcl-2, Bcl-$x_L$ may further clarify their roles during apoptosis via cytochrome *c* release during chronic, severe hypoxia. In order to further investigate the mitochondria as a source of $^{\bullet}NO$ that scavenges $O_2^{-\bullet}$ during chronic, severe hypoxia, the assessment of 3-nitrotyrosine (3-NT) formation as a biomarker of $ONOO^-$ formation is proposed. Peptide sequencing of those nitrated proteins may identify specific proteins undergoing nitration during chronic hypoxia and thereby, locate their organelle of origin. This information may assist understanding of ROS/RNS-mediated cell death mechanism during chronic, severe hypoxia. Cells operate a delicate balance between the protective oxidants/antioxidant signalling versus deleterious effect of ROS/RNS.

It is now known that low concentrations of ROS/RNS play a vital role in induction of cardioprotective mechanism (Penna et al., 2009). In this thesis, the excessive generation of ROS/RNS in hypoxia/reoxygenation, their cytotoxic role, and finally their signalling effects to activate redox transcription factors; Nrf2 and NF-κB probably as a defence mechanism during hypoxia has been demonstrated. However, the site and specific ROS/RNS-mediated NF-κB activation and the effects of activation during chronic hypoxia still remain unknown. Therefore, $O_2^{-\bullet}$ and $^{\bullet}NO$ effects on NF-κB activation and their targeted gene expression during chronic severe hypoxia warrants further investigation.

The present study demonstrates that Nrf2 activation is $O_2^{-\bullet}$/$^{\bullet}NO$ dependent and there a high chance of making $ONOO^-$ to induce Nrf2 activation. Therefore, finding the specific radical species required for activation of redox transcription factors; including Nrf2 and NF-κB may point to new avenues of therapeutic interventions. It is well established that the master regulator of antioxidant response element is Nrf2. The specific downstream targeted gene expression involved in antioxidant/detoxifying mechanisms and apoptosis during hypoxia/reperfusion remains to be elucidated. Therefore, future works are warranted to investigate Nrf2 mediated defence mechanism during hypoxia or hypoxia/reoxygenation using methods such as silencing Nrf2 activity with siRNA and gene expression systems for antioxidants (i.e.; MnSOD, GST and NOS) (Nguyen et al., 2009; Heiss et al., 2009; Jaiswal, 2004; Nioi et al., 2003).

The present data suggest that NOS activation and probably, non-enzymatic $^{\bullet}NO$ production during reoxygenation is cardiacprotective.In contrast, the spermine nonoate $^{\bullet}NO$ donor (100μM) did not show any affordable protection during hypoxia/reoxygenation. Recent reports have shown dose-dependency of protection by an exogenous $^{\bullet}NO$ donor during ischemia/reperfusion injury in rat and guinea pig hearts (Schulz et al., 2004). Therefore, future works are warranted to investigate the dose dependency of exogenous $^{\bullet}NO$ donors in cardiacprotection of H9C2 cells during hypoxia/reoxygenation. Under the present conditions, the magnitude of enzyme-independent $^{\bullet}NO$ generation exceeds the NOS-dependent $^{\bullet}NO$ generation during hypoxia and hypoxia/reoxygenation. Therefore, future works are warranted to understand its role in protection during hypoxia and hypoxia/reoxygenation.

# CHAPTER 9

# REFERENCES

ABRAMOV, A. Y., SCORZIELLO, A. & DUCHEN, M. R. 2007. Three distinct mechanisms generate oxygen free radicals in neurons and contribute to cell death during anoxia and reoxygenation. *J Neurosci,* 27**,** 1129-38.

ADAMS, J. M. & CORY, S. 2001. Life-or-death decisions by the Bcl-2 protein family. *Trends in Biochemical Sciences,* 26**,** 61-66.

ADRAIN, C. & MARTIN, S. J. 2001. The mitochondrial apoptosome: a killer unleashed by the cytochrome seas. *Trends Biochem Sci,* 26**,** 390-7.

ADRIENN, K., DEREK, M. Y. & GARY, F. B. 2003. Role of nuclear factor-kB activation in acute ischaemia-reperfusion injury in myocardium. *British Journal of Pharmacology,* 138**,** 894-900.

ALBERTS, B., ALEXANDER, .J, JULIAN, L., MARTIN, R., ROBERTS, K and WALTER, P., 2008. Molecular Biology of THE CELL, 5th edition, Garland Science, Taylor & Francis Group, New York, USA and Oxford, UK.

ARCHER, S. 1993. Measurement of nitric oxide in biological models. *FASEB J.,* 7**,** 349-360.

ARCIELLO, M., CAPO, C. R., COZZOLINO, M., FERRI, A., NENCINI, M., CARRÌ, M. T. & ROSSI, L. 2010. Inactivation of cytochrome c oxidase by mutant SOD1s in mouse motoneuronal NSC-34 cells is independent from copper availability but is because of nitric oxide. *Journal of Neurochemistry,* 112**,** 183-192.

ARDEHALI, H. 2006. Signaling Mechanisms in Ischemic Preconditioning: Interaction of PKC and MitoKATP in the Inner Membrane of Mitochondria. *Circ Res,* 99**,** 798-800.

ASA B. GUSTAFSSON & ROBERTA A. GOTTLIEB 2008. Eat your heart out: Role of autophagy in myocardial ischemia/reperfusion *Autophagy* 4**,** 416 - 421

ASIMAKIS, G. K., LICK, S. & PATTERSON, C. 2002. Postischemic recovery of contractile function is impaired in SOD2(+/-) but not SOD1(+/-) mouse hearts. *Circulation,* 105**,** 981-6.

AULAK, K. S., KOECK, T., CRABB, J. W. & STUEHR, D. J. 2004. Dynamics of protein nitration in cells and mitochondria. *Am J Physiol Heart Circ Physiol,* 286**,** H30-38.

BAEUERLE, P. A. & BALTIMORE, D. 1996. NF-[kappa]B: Ten Years After. *Cell,* 87**,** 13-20.

BALDWIN, A. S. 1996. THE NF-κB AND IκB PROTEINS: New Discoveries and Insights. *Annual Review of Immunology,* 14**,** 649-681.

BALAKUMAR, P., SINGH, H., SINGH, M. & ANAND-SRIVASTAVA, M. B. 2009. The impairment of preconditioning-mediated cardioprotection in pathological conditions. *Pharmacological Research,* 60**,** 18-23.

BALCERCZYK, A., SOSZYNSKI, M., RYBACZEK, D., PRZYGODZKI, T., KAROWICZ-BILINSKA, A., MASZEWSKI, J. & BARTOSZ, G. 2005. Induction of apoptosis and modulation of production of reactive oxygen species in human endothelial cells by diphenyleneiodonium. *Biochem Pharmacol,* 69**,** 1263-73.

BANKI, K., HUTTER, E., GONCHOROFF, N. J. & PERL, A. 1999. Elevation of mitochondrial transmembrane potential and reactive oxygen intermediate levels are early events and occur independently from activation of caspases in Fas signaling. *J Immunol,* 162**,** 1466-79.

BEARDSLEY, A., FANG, K., MERTZ, H., CASTRANOVA, V., FRIEND, S. & LIU, J. 2005. Loss of caveolin-1 polarity impedes endothelial cell polarization and directional movement. *J Biol Chem,* 280**,** 3541-7.

BECKER, L. B. 2004a. New concepts in reactive oxygen species and cardiovascular reperfusion physiology. *Cardiovasc Res,* 61**,** 461-70.

BECKER, L. B. 2004b. New concepts in reactive oxygen species and cardiovascular reperfusion physiology. *Cardiovasc Res,* 61**,** 461-470.

BECKER, L. B., VANDEN HOEK, T. L., SHAO, Z. H., LI, C. Q. & SCHUMACKER, P. T. 1999. Generation of superoxide in cardiomyocytes during ischemia before reperfusion. *Am J Physiol,* 277**,** H2240-6.

BECKMAN, J. S. & KOPPENOL, W. H. 1996. Nitric oxide, superoxide, and peroxynitrite: the good, the bad, and ugly. *Am J Physiol Cell Physiol,* 271**,** C1424-1437.

BEDARD, K. & KRAUSE, K.-H. 2007. The NOX Family of ROS-Generating NADPH Oxidases: Physiology and Pathophysiology. *Physiol. Rev.,* 87**,** 245-313.

BEINKE, S. & LEY, S. C. 2004. Functions of NF-kappaB1 and NF-kappaB2 in immune cell biology. *Biochem. J.,* 382**,** 393-409.

BELKIN, S., SMULSKI, D., VOLLMER, A., VAN DYK, T. & LAROSSA, R. 1996. Oxidative stress detection with Escherichia coli harboring a katG'::lux fusion. *Appl. Environ. Microbiol.,* 62**,** 2252-2256.

BELL, R. M., CAVE, A. C., JOHAR, S., HEARSE, D. J., SHAH, A. M. & SHATTOCK, M. J. 2005. Pivotal role of NOX-2-containing NADPH oxidase in early ischemic preconditioning. *FASEB J.***,** 04-2774fje.

BENDALL, J. K., CAVE, A. C., HEYMES, C., GALL, N. & SHAH, A. M. 2002. Pivotal Role of a gp91phox-Containing NADPH Oxidase in Angiotensin II-Induced Cardiac Hypertrophy in Mice. *Circulation,* 105**,** 293-296.

BENOV, L., SZTEJNBERG, L. & FRIDOVICH, I. 1998. Critical evaluation of the use of hydroethidine as a measure of superoxide anion radical. *Free Radic Biol Med,* 25**,** 826.

BEREESEWICZ, A., KARWATOWSKA-PROKOPCZUK, E., LEWARTOWSKI, B. & CEDRO-CEREMUZYNSKA, K. 1995. A protective role of nitric oxide in isolated ischaemic/reperfused rat heart. *Cardiovasc Res,* 30**,** 1001-1008.

BERLETT, B. S. & STADTMAN, E. R. 1997. Protein Oxidation in Aging, Disease, and Oxidative Stress. *Journal of Biological Chemistry,* 272**,** 20313-20316.

BERLINER, L. J., KHRAMTSOV, V., FUJII, H. & CLANTON, T. L. 2001. Unique in vivo applications of spin traps. *Free Radical Biology and Medicine,* 30**,** 489-499.

BIALIK, S., CRYNS, V. L., DRINCIC, A., MIYATA, S., WOLLOWICK, A. L., SRINIVASAN, A. & KITSIS, R. N. 1999. The Mitochondrial Apoptotic Pathway Is Activated by Serum and Glucose Deprivation in Cardiac Myocytes. *Circ Res,* 85**,** 403-414.

BISHOPRIC, N. H., DISCHER, D. J., KAISER, S., HERNANDEZ, O., SATO, B., ZANG, J. & WEBSTER, K. A. 1999. Hypoxia-activated apoptosis of cardiac myocytes requires reoxygenation or a pH shift and is independent of p53. *The Journal of Clinical Investigation,* 104**,** 239-252.

BJÖRK, J., HEDQVIST, P. & ARFORS, K.-E. 1982. Increase in vascular permeability induced by leukotriene b4 and the role of polymorphonuclear leukocytes. *Inflammation,* 6**,** 189-200.

BOLLI, R. 2000. The Late Phase of Preconditioning. *Circ Res,* 87**,** 972-983.

BONAVITA, F., STEFANELLI, C., GIORDANO, E., COLUMBARO, M., FACCHINI, A., BONAFE, F., CALDARERA, C. M. & GUARNIERI, C. 2003. H9c2 cardiac myoblasts undergo apoptosis in a model of ischemia consisting of serum deprivation and hypoxia: inhibition by PMA. *FEBS Lett,* 536**,** 85-91.

BORNER, C. 2003. The Bcl-2 protein family: sensors and checkpoints for life-or-death decisions. *Molecular Immunology,* 39**,** 615-647.

BORUTAITE, V. & BROWN, G. 2005. What else has to happen for nitric oxide to induce cell death? *Biochem. Soc. Trans.,* 33**,** 1394-1396.

BORUTAITE, V. & BROWN, G. C. 2003. Mitochondria in apoptosis of ischemic heart. *FEBS letters,* 541**,** 1-5.

BOVERIS, A. & CHANCE, B. 1973. The mitochondrial generation of hydrogen peroxide. General properties and effect of hyperbaric oxygen. *Biochem J,* 134**,** 707-16.

BOVERIS, A., OSHINO, N. & CHANCE, B. 1972. The cellular production of hydrogen peroxide. *Biochem J,* 128**,** 617-30.

BRENNAN, J. P., BERRY, R. G., BAGHAI, M., DUCHEN, M. R. & SHATTOCK, M. J. 2006a. FCCP is cardioprotective at concentrations that cause mitochondrial oxidation without detectable depolarisation. *Cardiovasc Res,* 72**,** 322-30.

BRENNAN, J. P., SOUTHWORTH, R., MEDINA, R. A., DAVIDSON, S. M., DUCHEN, M. R. & SHATTOCK, M. J. 2006b. Mitochondrial uncoupling, with low concentration FCCP, induces ROS-dependent cardioprotection independent of KATP channel activation. *Cardiovasc Res,* 72**,** 313-21.

BRISTOW, R. G. & HILL, R. P. 2008. Hypoxia and metabolism: Hypoxia, DNA repair and genetic instability. *Nat Rev Cancer,* 8**,** 180-192.

BROMME, H. J. & HOLTZ, J. 1996. Apoptosis in the heart: when and why? *Mol Cell Biochem,* 163-164**,** 261-75.

BROWN, G. C. 1999. Nitric oxide and mitochondrial respiration. *Biochim Biophys Acta,* 1411**,** 351-69.

BROWN, G. C. & BORUTAITE, V. 2007. Nitric oxide and mitochondrial respiration in the heart. *Cardiovasc Res,* 75**,** 283-290.

BUDD, S. L., CASTILHO, R. F. & NICHOLLS, D. G. 1997. Mitochondrial membrane potential and hydroethidine-monitored superoxide generation in cultured cerebellar granule cells. *FEBS letters,* 415**,** 21-24.

CARTY, J. L., BEVAN, R., WALLER, H., MISTRY, N., COOKE, M., LUNEC, J. & GRIFFITHS, H. R. 2000. The Effects of Vitamin C Supplementation on Protein Oxidation in Healthy Volunteers. *Biochemical and Biophysical Research Communications,* 273**,** 729-735.

CHACHAMI, G., SIMOS, G., HATZIEFTHIMIOU, A., BONANOU, S., MOLYVDAS, P. A. & PARASKEVA, E. 2004. Cobalt induces hypoxia-inducible factor-1alpha expression in airway smooth muscle cells by a reactive oxygen species- and PI3K-dependent mechanism. *Am J Respir Cell Mol Biol,* 31**,** 544-51.

CHANDEL, N., BUDINGER, G. R., KEMP, R. A. & SCHUMACKER, P. T. 1995. Inhibition of cytochrome-c oxidase activity during prolonged hypoxia. *Am J Physiol Lung Cell Mol Physiol,* 268**,** L918-925.

CHANDEL, N. S. & BUDINGER, G. R. 2007. The cellular basis for diverse responses to oxygen. *Free Radic Biol Med,* 42**,** 165-74.

CHANDEL, N. S., MALTEPE, E., GOLDWASSER, E., MATHIEU, C. E., SIMON, M. C. & SCHUMACKER, P. T. 1998. Mitochondrial reactive oxygen species trigger hypoxia-induced transcription. *Proc Natl Acad Sci U S A,* 95**,** 11715-20.

CHANDEL, N. S., MCCLINTOCK, D. S., FELICIANO, C. E., WOOD, T. M., MELENDEZ, J. A., RODRIGUEZ, A. M. & SCHUMACKER, P. T. 2000. Reactive oxygen species generated at mitochondrial complex III stabilize hypoxia-inducible factor-1alpha during hypoxia: a mechanism of O2 sensing. *J Biol Chem,* 275**,** 25130-8.

CHANDEL, N. S. & SCHUMACKER, P. T. 1999. Cells depleted of mitochondrial DNA (rho0) yield insight into physiological mechanisms. *FEBS Lett,* 454**,** 173-6.

CHANDEL, N. S. & SCHUMACKER, P. T. 2000. Cellular oxygen sensing by mitochondria: old questions, new insight. *J Appl Physiol,* 88**,** 1880-9.

CHEN, H.-W., CHIEN, C.-T., YU, S.-L., LEE, Y.-T. & CHEN, W.-J. 2002. Cyclosporine A regulate oxidative stress-induced apoptosis in cardiomyocytes: mechanisms via ROS generation, iNOS and Hsp70. *British Journal of Pharmacology,* 137**,** 771-781.

CHEN, Z., SIU, B., HO, Y. S., VINCENT, R., CHUA, C. C., HAMDY, R. C. & CHUA, B. H. 1998. Overexpression of MnSOD protects against myocardial ischemia/reperfusion injury in transgenic mice. *J Mol Cell Cardiol,* 30**,** 2281-9.

CHENG, G., RITSICK, D. & LAMBETH, J. D. 2004. Nox3 regulation by NOXO1, p47phox, and p67phox. *J Biol Chem,* 279**,** 34250-5.

CLEMPUS, R. E. & GRIENDLING, K. K. 2006. Reactive oxygen species signaling in vascular smooth muscle cells. *Cardiovasc Res,* 71**,** 216-25.

CLERK, A., COLE, S. M., CULLINGFORD, T. E., HARRISON, J. G., JORMAKKA, M. & VALKS, D. M. 2003. Regulation of cardiac myocyte cell death. *Pharmacol Ther,* 97**,** 223-61.

CORAL, L. M. & MICHAEL, B. R. 2001. Detection of reactive oxygen and reactive nitrogen species in skeletal muscle. *Microscopy Research and Technique,* 55**,** 236-248.

COSTA, A. D. T., GARLID, K. D., WEST, I. C., LINCOLN, T. M., DOWNEY, J. M., COHEN, M. V. & CRITZ, S. D. 2005. Protein Kinase G Transmits the Cardioprotective Signal From Cytosol to Mitochondria. *Circ Res,* 97**,** 329-336.

CRAIG, R., LARKIN, A., MINGO, A. M., THUERAUF, D. J., ANDREWS, C., MCDONOUGH, P. M. & GLEMBOTSKI, C. C. 2000. p38 MAPK and NF-ÎºB Collaborate to Induce Interleukin-6 Gene Expression and Release. *Journal of Biological Chemistry,* 275**,** 23814-23824.

CRAWFORD, R. M., JOVANOVIÄ‡, S., BUDAS, G. R., DAVIES, A. M., LAD, H., WENGER, R. H., ROBERTSON, K. A., ROY, D. J., RANKI, H. J. & JOVANOVIÄ‡, A. 2003. Chronic Mild Hypoxia Protects Heart-derived H9c2 Cells against Acute Hypoxia/Reoxygenation by Regulating Expression of the SUR2A Subunit of the ATP-sensitive K+ Channel. *Journal of Biological Chemistry,* 278**,** 31444-31455.

CROMPTON, M. 1999. The mitochondrial permeability transition pore and its role in cell death. *Biochem. J.,* 341**,** 233-249.

CROW, J. P. 1997. Dichlorodihydrofluorescein and dihydrorhodamine 123 are sensitive indicators of peroxynitrite in vitro: implications for intracellular measurement of reactive nitrogen and oxygen species. *Nitric Oxide,* 1**,** 145-57.

CROW, M. T., MANI, K., NAM, Y.-J. & KITSIS, R. N. 2004. The Mitochondrial Death Pathway and Cardiac Myocyte Apoptosis. *Circ Res,* 95**,** 957-970.

CRUCHTEN, S. V. & BROECK, W. V. D. 2002. Morphological and Biochemical Aspects of Apoptosis, Oncosis and Necrosis. *Anatomia, Histologia, Embryologia,* 31**,** 214-223.

DALBY, B., CATES, S., HARRIS, A., OHKI, E. C., TILKINS, M. L., PRICE, P. J. & CICCARONE, V. C. 2004. Advanced transfection with Lipofectamine 2000 reagent: primary neurons, siRNA, and high-throughput applications. *Methods,* 33**,** 95-103.

DAVE, K. R., DEFAZIO, R. A., RAVAL, A. P., TORRACO, A., SAUL, I., BARRIENTOS, A. & PEREZ-PINZON, M. A. 2008. Ischemic Preconditioning Targets the Respiration of Synaptic Mitochondria via Protein Kinase C. *J. Neurosci.,* 28**,** 4172-4182.

DAVIDSON, C., GOW, A. J., LEE, T. H. & ELLINWOOD, E. H. 2001. Methamphetamine neurotoxicity: necrotic and apoptotic mechanisms and relevance to human abuse and treatment. *Brain Research Reviews,* 36**,** 1-22.

DAVIDSON, S. M. & DUCHEN, M. R. 2006. Effects of NO on mitochondrial function in cardiomyocytes: Pathophysiological relevance. *Cardiovasc Res,* 71**,** 10-21.

DAWN, B. & BOLLI, R. 2002. Role of Nitric Oxide in Myocardial Preconditioning. *Annals of the New York Academy of Sciences,* 962**,** 18-41.

DAWSON, R.M.C., ELLIOTT, D.C., ELLIOTT, W.H., JONES, K.M. (1986) Metal binding properties of compounds used in biochemistry. In: Data for Biochemical Research, Third Edition. Oxford Science Publication, Oxford.

DE GROOT, H. & RAUEN, U. 2007. Ischemia-Reperfusion Injury: Processes in Pathogenetic Networks: A Review. *Transplantation Proceedings,* 39**,** 481-484.

DE SOUZA DURAO, M., JR., RAZVICKAS, C. V., GONCALVES, E. A., OKANO, I. R., CAMARGO, S. M., MONTE, J. C. & DOS SANTOS, O. F. 2003. The role of growth factors on renal tubular cells submitted to hypoxia and deprived of glucose. *Ren Fail,* 25**,** 341-53.

DHAKSHINAMOORTHY, S. & PORTER, A. G. 2004. Nitric Oxide-induced Transcriptional Up-regulation of Protective Genes by Nrf2 via the Antioxidant Response Element Counteracts Apoptosis of Neuroblastoma Cells. *Journal of Biological Chemistry,* 279**,** 20096-20107.

DHALLA, N. S. & DUHAMEL, T. A. 2007. The paradoxes of reperfusion in the ischemic heart. *Heart Metabolism,* 37**,** 31-34.

DIZDAROGLU, M., JARUGA, P., BIRINCIOGLU, M. & RODRIGUEZ, H. 2002. Free radical-induced damage to DNA: mechanisms and measurement. *Free Radical Biology and Medicine,* 32**,** 1102-1115.

DODD-O, J. M. & PEARSE, D. B. 2000. Effect of the NADPH oxidase inhibitor apocynin on ischemia-reperfusion lung injury. *Am J Physiol Heart Circ Physiol,* 279**,** H303-312.

DOWNEY, J. M. & COHEN, M. V. 2006. Reducing Infarct Size in The Setting of Acute Myocardial Infarction. *Progress in Cardiovascular Diseases,* 48**,** 363-371.

DREGER, H., WESTPHAL, K., WELLER, A., BAUMANN, G., STANGL, V., MEINERS, S. & STANGL, K. 2009. Nrf2-dependent upregulation of antioxidative enzymes: a novel pathway for proteasome inhibitor-mediated cardioprotection. *Cardiovasc Res,* 83**,** 354-361.

DURANTEAU, J., CHANDEL, N. S., KULISZ, A., SHAO, Z. & SCHUMACKER, P. T. 1998. Intracellular signaling by reactive oxygen species during hypoxia in cardiomyocytes. *J Biol Chem,* 273**,** 11619-24.

EGUCHI, Y., SHIMIZU, S. & TSUJIMOTO, Y. 1997. Intracellular ATP Levels Determine Cell Death Fate by Apoptosis or Necrosis. *Cancer Res,* 57**,** 1835-1840.

ELISABETTA, B., MATTEO, P., LAURA, P., MATTEO, B., NICCOLÒ, N., PAOLO, N. & CHIARA, N. 2008. Role of NADPH oxidase in H9c2 cardiac muscle cells exposed to simulated ischemia-reperfusion. *Journal of Cellular and Molecular Medicine,* 9999.

ELSÄSSER, A., SUZUKI, K., LORENZ-MEYER, S., BODE, C. & SCHAPER, J. 2001. The role of apoptosis in myocardial ischemia: a critical appraisal. *Basic Research in Cardiology,* 96**,** 219-226.

ELZ, J. S. & NAYLER, W. G. 1988. Calcium gain during postischemic reperfusion. The effect of 2,4-dinitrophenol. *Am J Pathol,* 131**,** 137-45.

EMAUS, R. K., GRUNWALD, R. & LEMASTERS, J. J. 1986. Rhodamine 123 as a probe of transmembrane potential in isolated rat-liver mitochondria: spectral and metabolic properties. *Biochim Biophys Acta,* 850**,** 436-48.

ENARI, M., SAKAHIRA, H., YOKOYAMA, H., OKAWA, K., IWAMATSU, A. & NAGATA, S. 1998. A caspase-activated DNase that degrades DNA during apoptosis, and its inhibitor ICAD. *Nature,* 391**,** 43.

ENGLAND, K., ODRISCOLL, C. & COTTER, T. G. 2003. Carbonylation of glycolytic proteins is a key response to drug-induced oxidative stress and apoptosis. *Cell Death Differ,* 11**,** 252.

FANG, J., SEKI, T. & MAEDA, H. 2009. Therapeutic strategies by modulating oxygen stress in cancer and inflammation. *Advanced Drug Delivery Reviews,* 61**,** 290-302.

FAILLI, P., NISTRI, S., QUATTRONE, S., MAZZETTI, L., BIGAZZI, M., SACCHI, T. B. & BANI, D. 2001. Relaxin up-regulates inducible nitric oxide synthase expression and nitric oxide generation in rat coronary endothelial cells. *FASEB J.***,** 01-0569fje.

FENNELL, J.P & BAKER, A.H. 2005. Hypertension: Methods & Protocols. *Methods in Mol Medicine*,108,Humana Press Inc,Totowa,NJ.

FERNANDES, D. C., WOSNIAK, J., JR., PESCATORE, L. A., BERTOLINE, M. A., LIBERMAN, M., LAURINDO, F. R. M. & SANTOS, C. X. C. 2007. Analysis of DHE-derived oxidation products by HPLC in the assessment of superoxide production and NADPH oxidase activity in vascular systems. *Am J Physiol Cell Physiol,* 292**,** C413-422.

FERRARI, R. 1996. The Role of Mitochondria in Ischemic Heart Disease. *Journal of Cardiovascular Pharmacology,* 28**,** 1-10.

FLORES-SANCHEZ, I. & VERPOORTE, R. 2008. Secondary metabolism in cannabis. *Phytochemistry Reviews,* 7**,** 615-639.

FRANTSEVA, M. V., CARLEN, P. L. & PEREZ VELAZQUEZ, J. L. 2001. Dynamics of intracellular calcium and free radical production during ischemia in pyramidal neurons. *Free Radic Biol Med,* 31**,** 1216-27.

GAO, Z., CHIAO, P., ZHANG, X., ZHANG, X., LAZAR, M. A., SETO, E., YOUNG, H. A. & YE, J. 2005. Coactivators and Corepressors of NF-κB in IκBα Gene Promoter. *Journal of Biological Chemistry,* 280**,** 21091-21098.

GALONEK, H. L. & HARDWICK, J. M. 2006. Upgrading the BCL-2 Network. *Nat Cell Biol,* 8**,** 1317-1319.

GASBARRINI, A., BORLE, A. B., FARGHALI, H., BENDER, C., FRANCAVILLA, A. & VAN THIEL, D. 1992. Effect of anoxia on intracellular ATP, Na+i, Ca2+i, Mg2+i, and cytotoxicity in rat hepatocytes. *Journal of Biological Chemistry,* 267**,** 6654-6663.

GHAFOURIFAR, P. & CADENAS, E. 2005. Mitochondrial nitric oxide synthase. *Trends in Pharmacological Sciences,* 26**,** 190-195.

GHAFOURIFAR, P., SCHENK, U., KLEIN, S. D. & RICHTER, C. 1999. Mitochondrial Nitric-oxide Synthase Stimulation Causes Cytochromec Release from Isolated Mitochondria. *Journal of Biological Chemistry,* 274**,** 31185-31188.

GIBSON, G. E. & HUANG, H.-M. 2004. Mitochondrial Enzymes and Endoplasmic Reticulum Calcium Stores as Targets of Oxidative Stress in Neurodegenerative Diseases. *Journal of Bioenergetics and Biomembranes,* 36**,** 335-340.

GIORDANO, F. J. 2005. Oxygen, oxidative stress, hypoxia, and heart failure. *The Journal of Clinical Investigation,* 115**,** 500-508.

GLEBSKA, J. & KOPPENOL, W. H. 2003. Peroxynitrite-mediated oxidation of dichlorodihydrofluorescein and dihydrorhodamine. *Free Radical Biology and Medicine,* 35**,** 676-682.

GOMES, A., FERNANDES, E. & LIMA, J. L. F. C. 2005. Fluorescence probes used for detection of reactive oxygen species. *Journal of Biochemical and Biophysical Methods,* 65**,** 45.

GONON, A. T., ERBAS, D., BROIJERSEN, A., VALEN, G. & PERNOW, J. 2004. Nitric oxide mediates protective effect of endothelin receptor antagonism during myocardial ischemia and reperfusion. *Am J Physiol Heart Circ Physiol,* 286**,** H1767-1774.

GOTTLIEB, R. A. 2003. Debatable contribution of mitochondrial swelling to cell swelling in ischemia. *Journal of Molecular and Cellular Cardiology,* 35**,** 735-737.

GRANT, M. M., SCHEEL-TOELLNER, D. & GRIFFITHS, H. R. 2007. Contributions to our understanding of T cell physiology through unveiling the T cell proteome. *Clin Exp Immunol,* 149**,** 9-15.

GRANT, M. M. & GRIFFITHS, H. R. 2007. Cell passage-associated transient high oxygenation causes a transient decrease in cellular glutathione and affects T cell responses to apoptotic and mitogenic stimuli. *Environmental Toxicology and Pharmacology,* 23**,** 335-339.

GRIENDLING, K. K., SORESCU, D., LASSEGUE, B. & USHIO-FUKAI, M. 2000. Modulation of protein kinase activity and gene expression by reactive oxygen species and their role in vascular physiology and pathophysiology. *Arterioscler Thromb Vasc Biol,* 20**,** 2175-83.

GRIFFITHS, H. R. 2005. ROS as signalling molecules in T cells--evidence for abnormal redox signalling in the autoimmune disease, rheumatoid arthritis. *Redox Rep,* 10**,** 273-80.

GRIFFITHS, H. R., MØLLER, L., BARTOSZ, G., BAST, A., BERTONI-FREDDARI, C., COLLINS, A., COOKE, M., COOLEN, S., HAENEN, G., HOBERG, A.-M., LOFT, S., LUNEC, J., OLINSKI, R., PARRY, J., POMPELLA, A., POULSEN, H., VERHAGEN, H. & ASTLEY, S. B. 2002. Biomarkers. *Molecular Aspects of Medicine,* 23**,** 101-208.

GUGLIELMOTTO, M., ARAGNO, M., AUTELLI, R., GILIBERTO, L., NOVO, E., COLOMBATTO, S., DANNI, O., PAROLA, M., SMITH, M. A., PERRY, G., TAMAGNO, E. & TABATON, M. 2009. The up-regulation of BACE1 mediated by hypoxia and ischemic injury: role of oxidative stress and HIF1&#x03B1. *Journal of Neurochemistry,* 108**,** 1045-1056.

GUO, Y., LI, Q., WU, W.-J., TAN, W., ZHU, X., MU, J. & BOLLI, R. 2008. Endothelial nitric oxide synthase is not necessary for the early phase of ischemic preconditioning in the mouse. *Journal of Molecular and Cellular Cardiology,* 44**,** 496-501.

GURO, V., ZHONG-QUN, Y. & GÃRAN, K. H. 2001. Nuclear factor kappa-B and the heart. *Journal of the American College of Cardiology,* 38**,** 307.

GUZY, R. D., HOYOS, B., ROBIN, E., CHEN, H., LIU, L., MANSFIELD, K. D., SIMON, M. C., HAMMERLING, U. & SCHUMACKER, P. T. 2005. Mitochondrial complex III is required for hypoxia-induced ROS production and cellular oxygen sensing. *Cell Metab,* 1**,** 401-8.

HAJNÓCZKY, G., CSORDÁS, G., DAS, S., GARCIA-PEREZ, C., SAOTOME, M., SINHA ROY, S. & YI, M. 2006. Mitochondrial calcium signalling and cell death: Approaches for assessing the role of mitochondrial $Ca^{2+}$ uptake in apoptosis. *Cell Calcium,* 40**,** 553-560.

HALESTRAP, A. P., CLARKE, S. J. & JAVADOV, S. A. 2004. Mitochondrial permeability transition pore opening during myocardial reperfusion—a target for cardioprotection. *Cardiovascular Research,* 61**,** 372-385.

HALLIWELL, B. 1999. Oxygen and nitrogen are pro-carcinogens. Damage to DNA by reactive oxygen, chlorine and nitrogen species: measurement, mechanism and the effects of nutrition. *Mutation Research/Genetic Toxicology and Environmental Mutagenesis,* 443**,** 37-52.

HARRISON, D., GRIENDLING, K. K., LANDMESSER, U., HORNIG, B. & DREXLER, H. 2003. Role of oxidative stress in atherosclerosis. *The American Journal of Cardiology,* 91**,** 7-11.

HASBAK, P., ESKESEN, K., SCHIFTER, S. & EDVINSSON, L. 2005. Increased alphaCGRP potency and CGRP-receptor antagonist affinity in isolated hypoxic porcine intramyocardial arteries. *Br J Pharmacol,* 145**,** 646-55.

HASSOUNA, A., LOUBANI, M., MATATA, B. M., FOWLER, A., STANDEN, N. B. & GALINANES, M. 2006. Mitochondrial dysfunction as the cause of the failure to precondition the diabetic human myocardium. *Cardiovasc Res,* 69**,** 450-458.

HAVENGA, M. J. E., VAN DAM, B., GROOT, B. S., GRIMBERGEN, J. M., VALERIO, D., BOUT, A. & QUAX, P. H. A. 2001. Simultaneous Detection of NOS-3 Protein Expression and Nitric Oxide Production Using a Flow Cytometer. *Analytical Biochemistry,* 290**,** 283-291.

HE, X., KAN, H., CAI, L. & MA, Q. 2009. Nrf2 is critical in defense against high glucose-induced oxidative damage in cardiomyocytes. *Journal of Molecular and Cellular Cardiology,* 46**,** 47-58.

HEISS, E. H., SCHACHNER, D., WERNER, E. R. & DIRSCH, V. M. 2009. Active NF-E2-related Factor (Nrf2) Contributes to Keep Endothelial NO Synthase (eNOS) in the Coupled State. *Journal of Biological Chemistry,* 284**,** 31579-31586.

HELM, I., JALUKSE, L., VILBASTE, M. & LEITO, I. 2009. Micro-Winkler titration method for dissolved oxygen concentration measurement. *Analytica Chimica Acta,* 648**,** 167-173.

HEMPEL, S. L., BUETTNER, G. R., O'MALLEY, Y. Q., WESSELS, D. A. & FLAHERTY, D. M. 1999. Dihydrofluorescein diacetate is superior for detecting intracellular oxidants: comparison with 2',7'-dichlorodihydrofluorescein diacetate, 5(and 6)-carboxy-2',7'-dichlorodihydrofluorescein diacetate, and dihydrorhodamine 123. *Free Radic Biol Med,* 27**,** 146-59.

HENDERSON, L. M. & CHAPPELL, J. B. 1993. Dihydrorhodamine 123: a fluorescent probe for superoxide generation? *Eur J Biochem,* 217**,** 973-80.

HESCHELER, J., MEYER, R., PLANT, S., KRAUTWURST, D., ROSENTHAL, W. & SCHULTZ, G. 1991. Morphological, biochemical, and electrophysiological characterization of a clonal cell (H9c2) line from rat heart. *Circ Res,* 69**,** 1476-86.

HEUMULLER, S., WIND, S., BARBOSA-SICARD, E., SCHMIDT, H. H. H. W., BUSSE, R., SCHRODER, K. & BRANDES, R. P. 2008. Apocynin Is Not an Inhibitor of Vascular NADPH Oxidases but an Antioxidant. *Hypertension,* 51**,** 211-217.

HOHL, C., OESTREICH, R., RÖSEN, P., WIESNER, R. & GRIESHABER, M. 1987. Evidence for succinate production by reduction of fumarate during hypoxia in isolated adult rat heart cells. *Archives of Biochemistry and Biophysics,* 259**,** 527-535.

HONDA, H. M., KORGE, P. & WEISS, J. N. 2005. Mitochondria and Ischemia/Reperfusion Injury. *Annals of the New York Academy of Sciences,* 1047**,** 248-258.

HOOL, L. C. & ARTHUR, P. G. 2002. Decreasing cellular hydrogen peroxide with catalase mimics the effects of hypoxia on the sensitivity of the L-type Ca2+ channel to beta-adrenergic receptor stimulation in cardiac myocytes. *Circ Res,* 91**,** 601-9.

HOOL, L. C., DI MARIA, C. A., VIOLA, H. M. & ARTHUR, P. G. 2005. Role of NAD(P)H oxidase in the regulation of cardiac L-type Ca2+ channel function during acute hypoxia. *Cardiovasc Res,* 67**,** 624-635.

HUANG, Y. C., FISHER, P. W., NOZIK-GRAYCK, E. & PIANTADOSI, C. A. 1997. Hypoxia compared with normoxia alters the effects of nitric oxide in ischemia-reperfusion lung injury. *Am J Physiol Lung Cell Mol Physiol,* 273**,** L504-512.

HUANG, D. C. S. & STRASSER, A. 2000. BH3-Only Proteins--Essential Initiators of Apoptotic Cell Death. *Cell,* 103, 839-842.

IWATA, S., LEE, J. W., OKADA, K., LEE, J. K., IWATA, M., RASMUSSEN, B., LINK, T. A., RAMASWAMY, S. & JAP, B. K. 1998. Complete Structure of the 11-Subunit Bovine Mitochondrial Cytochrome bc1 Complex. *Science,* 281**,** 64-71

ISCHIROPOULOS, H. & BECKMAN, J. S. 2003. Oxidative stress and nitration in neurodegeneration: Cause, effect, or association? *The Journal of Clinical Investigation,* 111**,** 163-169.

ITOH, K., CHIBA, T., TAKAHASHI, S., ISHII, T., IGARASHI, K., KATOH, Y., OYAKE, T., HAYASHI, N., SATOH, K., HATAYAMA, I., YAMAMOTO, M. & NABESHIMA, Y.-I. 1997. An Nrf2/Small Maf Heterodimer Mediates the Induction of Phase II Detoxifying Enzyme Genes through Antioxidant Response Elements. *Biochemical and Biophysical Research Communications,* 236**,** 313-322.

JACOBSON, M. D., WEIL, M. & RAFF, M. C. 1997. Programmed cell death in animal development. *Cell,* 88**,** 347-54.

JACKSON, M. J., PAPA, S., BOLANOS, J., BRUCKDORFER, R., CARLSEN, H., ELLIOTT, R. M., FLIER, J., GRIFFITHS, H. R., HEALES, S., HOLST, B., LORUSSO, M., LUND, E., OIVIND MOSKAUG, J., MOSER, U., DI PAOLA, M., POLIDORI, M. C., SIGNORILE, A., STAHL, W., VINA-RIBES, J. & ASTLEY, S. B. 2002. Antioxidants, reactive oxygen and nitrogen species, gene induction and mitochondrial function. *Mol Aspects Med,* 23**,** 209-85.

JIANG, X. & WANG, X. 2004. CYTOCHROME C-MEDIATED APOPTOSIS. *Annual Review of Biochemistry,* 73**,** 87-106.

JAISWAL, A. K. 2004. Nrf2 signaling in coordinated activation of antioxidant gene expression. *Free Radical Biology and Medicine,* 36**,** 1199-1207.

JENNINGS, R., GANOTE, C. & REIMER, K. 1975. Ischemic tissue injury. *Am J Pathol,* 81**,** 179-198.

JENNINGS, R. B. & REIMER, K. A. 1991. The Cell Biology of Acute Myocardial Ischemia. *Annual Review of Medicine,* 42**,** 225-246.

JIAO, X.-Y., GAO, E., YUAN, Y., WANG, Y., LAU, W. B., KOCH, W., MA, X.-L. & TAO, L. 2009. INO-4885 [5,10,15,20-Tetra[N-(benzyl-4′-carboxylate)-2-pyridinium]-21H,23H-porphine Iron(III) Chloride], a Peroxynitrite Decomposition Catalyst, Protects the Heart against Reperfusion Injury in Mice. *Journal of Pharmacology and Experimental Therapeutics,* 328**,** 777-784.

JONES, S. P. & BOLLI, R. 2006. The ubiquitous role of nitric oxide in cardioprotection. *J Mol Cell Cardiol,* 40**,** 16-23.

JONES, S. P., GIROD, W. G., PALAZZO, A. J., GRANGER, D. N., GRISHAM, M. B., JOURD'HEUIL, D., HUANG, P. L. & LEFER, D. J. 1999. Myocardial ischemia-reperfusion injury is exacerbated in absence of endothelial cell nitric oxide synthase. *Am J Physiol Heart Circ Physiol,* 276**,** H1567-1573.

JOURD'HEUIL, D. 2002. Increased nitric oxide-dependent nitrosylation of 4,5-diaminofluorescein by oxidants: implications for the measurement of intracellular nitric oxide. *Free Radical Biology and Medicine,* 33**,** 676-684.

KANG, K. W., CHOI, S. H. & KIM, S. G. 2002. Peroxynitrite activates NF-E2-related factor 2/antioxidant response element through the pathway of phosphatidylinositol 3-kinase: The role of nitric oxide synthase in rat glutathione S-transferase A2 induction. *Nitric Oxide,* 7**,** 244-253.

KANNO, S., LEE, P. C., ZHANG, Y., HO, C., GRIFFITH, B. P., SHEARS, L. L., II & BILLIAR, T. R. 2000. Attenuation of Myocardial Ischemia/Reperfusion Injury by Superinduction of Inducible Nitric Oxide Synthase. *Circulation,* 101**,** 2742-2748.

KAWAHARA, K., HACHIRO, T., YOKOKAWA, T., NAKAJIMA, T., YAMAUCHI, Y. & NAKAYAMA, Y. 2006. Ischemia/reperfusion-induced death of cardiac myocytes: possible involvement of nitric oxide in the coordination of ATP supply and demand during ischemia. *J Mol Cell Cardiol,* 40**,** 35-46.

KEHRER, J. P. 2000. The Haber-Weiss reaction and mechanisms of toxicity. *Toxicology,* 149**,** 43-50.

KETTLE, A. J., GEDYE, C. A. & WINTERBOURN, C. C. 1993. Superoxide is an antagonist of anti-inflammatory drugs that inhibit hypochlorous acid production by myeloperoxidase. *Biochemical Pharmacology,* 45**,** 2003-2010.

KEVIN, L. G., CAMARA, A. K. S., RIESS, M. L., NOVALIJA, E. & STOWE, D. F. 2003. Ischemic preconditioning alters real-time measure of O2 radicals in intact hearts with ischemia and reperfusion. *Am J Physiol Heart Circ Physiol,* 284**,** H566-574.

KILLILEA, D. W., HESTER, R., BALCZON, R., BABAL, P. & GILLESPIE, M. N. 2000. Free radical production in hypoxic pulmonary artery smooth muscle cells. *Am J Physiol Lung Cell Mol Physiol,* 279**,** L408-12.

KIM, H., RAFIUDDIN-SHAH, M., TU, H.-C., JEFFERS, J. R., ZAMBETTI, G. P., HSIEH, J. J. D. & CHENG, E. H. Y. 2006. Hierarchical regulation of mitochondrion-dependent apoptosis by BCL-2 subfamilies. *Nat Cell Biol,* 8**,** 1348-1358.

KIM, B. C., YOUN, C. H., AHN, J.-M. & GU, M. B. 2005. Screening of Target-Specific Stress-Responsive Genes for the Development of Cell-Based Biosensors Using a DNA Microarray. *Analytical Chemistry,* 77**,** 8020-8026.

KIM, J.-S., HE, L. & LEMASTERS, J. J. 2003. Mitochondrial permeability transition: a common pathway to necrosis and apoptosis. *Biochemical and Biophysical Research Communications,* 304**,** 463-470.

KIMES, B. W. & BRANDT, B. L. 1976. Properties of a clonal muscle cell line from rat heart. *Exp Cell Res,* 98**,** 367-81.

KINNULA, V. L. & JUUJÄRVI, K. 1976. Liver and Heart Mitochondrial Succinate Dehydrogenase Activity of Newborn Rats in Anoxic Hypoxia and Starvation. *Acta Physiologica Scandinavica,* 97**,** 357-361.

KLESCHYOV, A. L., WENZEL, P. & MUNZEL, T. 2007. Electron paramagnetic resonance (EPR) spin trapping of biological nitric oxide. *Journal of Chromatography B,* 851**,** 12-20.

KOBAYASHI, S. D., VOYICH, J. M. & DELEO, F. R. 2003. Regulation of the neutrophil-mediated inflammatory response to infection. *Microbes and Infection,* 5**,** 1337-1344.

KOJIMA, H., NAKATSUBO, N., KIKUCHI, K., KAWAHARA, S., KIRINO, Y., NAGOSHI, H., HIRATA, Y. & NAGANO, T. 1998. Detection and imaging of nitric oxide with novel fluorescent indicators: diaminofluoresceins. *Anal Chem,* 70**,** 2446-53.

KOO, M.-S., LEE, J.-H., RAH, S.-Y., YEO, W.-S., LEE, J.-W., LEE, K.-L., KOH, Y.-S., KANG, S.-O. & ROE, J.-H. 2003. A reducing system of the superoxide sensor SoxR in Escherichia coli. *EMBO J,* 22**,** 2614-2622.

KOONG, A. C., CHEN, E. Y. & GIACCIA, A. J. 1994. Hypoxia Causes the Activation of Nuclear Factor {kappa} B through the Phosphorylation of I{kappa}B{alpha} on Tyrosine Residues. *Cancer Res,* 54**,** 1425-1430.

KOOY, N. W., ROYALL, J. A., ISCHIROPOULOS, H. & BECKMAN, J. S. 1994. Peroxynitrite-mediated oxidation of dihydrorhodamine 123. *Free Radic Biol Med,* 16**,** 149-56.

KOWALTOWSKI, A. J. & VERCESI, A. E. 1999. Mitochondrial damage induced by conditions of oxidative stress. *Free Radic Biol Med,* 26**,** 463-71.

KROEMER, G., DALLAPORTA, B. & RESCHE-RIGON, M. 1998. THE MITOCHONDRIAL DEATH/LIFE REGULATOR IN APOPTOSIS AND NECROSIS. *Annual Review of Physiology,* 60**,** 619-642.

KUDIN, A. P., DEBSKA-VIELHABER, G. & KUNZ, W. S. 2005. Characterization of superoxide production sites in isolated rat brain and skeletal muscle mitochondria. *Biomed Pharmacother,* 59**,** 163-8.

KUKREJA, R. C. 2002. NF[kappa]B Activation During Ischemia/Reperfusion in Heart: Friend or Foe? *Journal of Molecular and Cellular Cardiology,* 34**,** 1301.

KUMAR, D. & JUGDUTT, B. I. 2003. Apoptosis and oxidants in the heart. *Journal of Laboratory and Clinical Medicine,* 142**,** 288-297.

KUPATT, C., WEBER, C., WOLF, D. A., BECKER, B. F., SMITH, T. W. & KELLY, R. A. 1997. Nitric Oxide Attenuates Reoxygenation-induced ICAM-1 Expression in Coronary Microvascular Endothelium: Role of NF[kappa]B. *Journal of Molecular and Cellular Cardiology,* 29**,** 2599-2609.

KUPPUSAMY, P. & ZWEIER, J. L. 2004. Cardiac applications of EPR imaging. *NMR in Biomedicine,* 17**,** 226-239.

KWAK, M.-K., WAKABAYASHI, N., GREENLAW, J. L., YAMAMOTO, M. & KENSLER, T. W. 2003. Antioxidants Enhance Mammalian Proteasome Expression through the Keap1-Nrf2 Signaling Pathway. *Mol. Cell. Biol.,* 23**,** 8786-8794.

LACZA, Z., KOZLOV, A. V., PANKOTAI, E., CSORDAS, A., WOLF, G., REDL, H., KOLLAI, M., SZABO, C., BUSIJA, D. W. & HORN, T. F. 2006. Mitochondria produce reactive nitrogen species via an arginine-independent pathway. *Free Radic Res,* 40**,** 369-78.

LACZA, Z., PUSKAR, M., FIGUEROA, J. P., ZHANG, J., RAJAPAKSE, N. & BUSIJA, D. W. 2001. Mitochondrial nitric oxide synthase is constitutively active and is functionally upregulated in hypoxia. *Free Radic Biol Med,* 31**,** 1609-15.

LALU, M. M., WANG, W. & SCHULZ, R. 2002. Peroxynitrite in Myocardial Ischemia-Reperfusion Injury. *Heart Failure Reviews,* 7**,** 359-369.

LEBUFFE, G., SCHUMACKER, P. T., SHAO, Z.-H., ANDERSON, T., IWASE, H. & VANDEN HOEK, T. L. 2003. ROS and NO trigger early preconditioning: relationship to mitochondrial KATP channel. *Am J Physiol Heart Circ Physiol,* 284**,** H299-308.

LEE, B. E., TOLEDO, A. H., ANAYA-PRADO, R., ROACH, R. R. & TOLEDO-PEREYRA, L. H. 2009. Allopurinol, Xanthine Oxidase, and Cardiac Ischemia. *Journal of Investigative Medicine,* 57**,** 902-909 10.231/JIM.0b013e3181bca50c.

LEE, J.-K., CHOI, S.-S., WON, J.-S. & SUH, H.-W. 2003. The regulation of inducible nitric oxide synthase gene expression induced by lipopolysaccharide and tumor necrosis factor-[alpha] in C6 cells: involvement of AP-1 and NF[kappa]B. *Life Sciences,* 73**,** 595-609.

LEE, J. & JOHNSON, J. A. 2004 An Important Role of Nrf2-ARE Pathway in the Cellular Defense Mechanism. *Journal of Biochemistry and Molecular Biology,* 37(2)**,** 139~143.

LEE, J., KIM C.H,SHIM,K.D,AHN,Y.S 2003. Inhbition of NF-κB Activation Oxygen-Glucose Deprivation-Induced Cerebral Endothelial Cell Death. *Korean J Physiol Pharmacol,* 7**,** 65-71.

LEE, S., IBEY, B. L., COTÉ, G. L. & PISHKO, M. V. 2008. Measurement of pH and dissolved oxygen within cell culture media using a hydrogel microarray sensor. *Sensors and Actuators B: Chemical,* 128**,** 388.

LEE, Y. J. & HAN, H. J. 2005. Effect of adenosine triphosphate in renal ischemic injury: Involvement of NF-kappaB. *Journal of Cellular Physiology,* 204**,** 792-799.

LEIKERT, J. F., RÄTHEL, T. R., MÜLLER, C., VOLLMAR, A. M. & DIRSCH, V. M. 2001. Reliable in vitro measurement of nitric oxide released from endothelial cells using low concentrations of the fluorescent probe 4,5-diaminofluorescein. *FEBS letters,* 506**,** 131-134.

LEMASTERS, J. J., THERUVATH, T. P., ZHONG, Z. & NIEMINEN, A.-L. 2009. Mitochondrial calcium and the permeability transition in cell death. *Biochimica et Biophysica Acta (BBA) - Bioenergetics,* 1787**,** 1395-1401.

LEONARD, M. O., KIERAN, N. E., HOWELL, K., BURNE, M. J., VARADARAJAN, R., DHAKSHINAMOORTHY, S., PORTER, A. G., O'FARRELLY, C., RABB, H. & TAYLOR, C. T. 2006. Reoxygenation-specific activation of the antioxidant transcription factor Nrf2 mediates cytoprotective gene expression in ischemia-reperfusion injury. *FASEB J.,* 20**,** 2624-2626.

LEPORE, D. A. 2000. Nitric Oxide Synthase-Independent Generation of Nitric Oxide in Muscle Ischemia-Reperfusion Injury. *Nitric Oxide,* 4**,** 541-545.

LERI, A., CLAUDIO, P. P., LI, Q., WANG, X., REISS, K., WANG, S., MALHOTRA, A., KAJSTURA, J. & ANVERSA, P. 1998. Stretch-mediated release of angiotensin II induces myocyte apoptosis by activating p53 that enhances the local renin-angiotensin system and decreases the Bcl-2-to-Bax protein ratio in the cell. *J Clin Invest,* 101**,** 1326-42.

LESNEFSKY, E. J., CHEN, Q., MOGHADDAS, S., HASSAN, M. O., TANDLER, B. & HOPPEL, C. L. 2004. Blockade of Electron Transport during Ischemia Protects Cardiac Mitochondria. *Journal of Biological Chemistry,* 279**,** 47961-47967.

LEVONEN, A.-L., PATEL, R. P., BROOKES, P., GO, Y.-M., JO, H., PARTHASARATHY, S., ANDERSON, P. G. & DARLEY-USMAR, V. M. 2001. Mechanisms of Cell Signaling by Nitric Oxide and Peroxynitrite: From Mitochondria to MAP Kinases. *Antioxidants & Redox Signaling,* 3**,** 215-229.

LEVRAND, S., PESSE, B., FEIHL, F., WAEBER, B., PACHER, P., ROLLI, J., SCHALLER, M.-D. & LIAUDET, L. 2005. Peroxynitrite Is a Potent Inhibitor of NF-κB Activation Triggered by Inflammatory Stimuli in Cardiac and Endothelial Cell Lines. *Journal of Biological Chemistry,* 280**,** 34878-34887.

LEVRAND, S., VANNAY-BOUCHICHE, C., PESSE, B., PACHER, P., FEIHL, F., WAEBER, B. & LIAUDET, L. 2006. Peroxynitrite is a major trigger of cardiomyocyte apoptosis in vitro and in vivo. *Free Radical Biology and Medicine,* 41**,** 886.

LEVRAUT, J., IWASE, H., SHAO, Z. H., VANDEN HOEK, T. L. & SCHUMACKER, P. T. 2003. Cell death during ischemia: relationship to mitochondrial depolarization and ROS generation. *Am J Physiol Heart Circ Physiol,* 284**,** H549-58.

LI, P.-F., DIETZ, R. & VON HARSDORF, R. 1997. Differential Effect of Hydrogen Peroxide and Superoxide Anion on Apoptosis and Proliferation of Vascular Smooth Muscle Cells. *Circulation,* 96**,** 3602-3609.

LI, C., BROWDER, W. & KAO, R. L. 1999a. Early activation of transcription factor NF-kappa B during ischemia in perfused rat heart. *Am J Physiol Heart Circ Physiol,* 276**,** H543-552.

LI, D., TOMSON, K., YANG, B., MEHTA, P., CROKER, B. P. & MEHTA, J. L. 1999b. Modulation of constitutive nitric oxide synthase, bcl-2 and Fas expression in cultured human coronary endothelial cells exposed to anoxia-reoxygenation and angiotensin II: role of AT1 receptor activation. *Cardiovasc Res,* 41**,** 109-115.

LI, C. & JACKSON, R. M. 2002. Reactive species mechanisms of cellular hypoxia-reoxygenation injury. *Am J Physiol Cell Physiol,* 282**,** C227-241.

LI, N., ALAM, J., VENKATESAN, M. I., EIGUREN-FERNANDEZ, A., SCHMITZ, D., DI STEFANO, E., SLAUGHTER, N., KILLEEN, E., WANG, X., HUANG, A., WANG, M., MIGUEL, A. H., CHO, A., SIOUTAS, C. & NEL, A. E. 2004. Nrf2 Is a Key Transcription Factor That Regulates Antioxidant Defense in Macrophages and Epithelial Cells: Protecting against the Proinflammatory and Oxidizing Effects of Diesel Exhaust Chemicals. *J Immunol,* 173**,** 3467-3481.

LI, M.-H., CHA, Y.-N. & SURH, Y.-J. 2006. Peroxynitrite induces HO-1 expression via PI3K/Akt-dependent activation of NF-E2-related factor 2 in PC12 cells. *Free Radical Biology and Medicine,* 41**,** 1079-1091.

LI, W., KHOR, T. O., XU, C., SHEN, G., JEONG, W.-S., YU, S. & KONG, A.-N. 2008. Activation of Nrf2-antioxidant signaling attenuates NF[kappa]B-inflammatory response and elicits apoptosis. *Biochemical Pharmacology,* 76**,** 1485-1489.

LIAO, P., WANG, S.-Q., WANG, S., ZHENG, M., ZHENG, M., ZHANG, S.-J., CHENG, H., WANG, Y. & XIAO, R.-P. 2002. p38 Mitogen-Activated Protein Kinase Mediates a Negative Inotropic Effect in Cardiac Myocytes. *Circ Res,* 90**,** 190-196.

LIAUDET, L., VASSALLI, G. & PACHER, P. 2009. Role of peroxynitrite in the redox regulation of cell signal transduction pathways. *Front Biosci,* 14**,** 4809-14.

LIEBERTHAL, W., MENZA, S. A. & LEVINE, J. S. 1998. Graded ATP depletion can cause necrosis or apoptosis of cultured mouse proximal tubular cells. *Am J Physiol Renal Physiol,* 274**,** F315-327.

LIEM, D. A., HONDA, H. M., ZHANG, J., WOO, D. & PING, P. 2007. Past and present course of cardioprotection against ischemia- reperfusion injury. *J Appl Physiol,* 103**,** 2129-2136.

LIÈVRE, V., BECUWE, P., BIANCHI, A., KOZIEL, V., FRANCK, P., SCHROEDER, H., NABET, P., DAUÇA, M. & DAVAL, J.-L. 2000. Free radical production and changes in superoxide dismutases associated with hypoxia/reoxygenation-induced apoptosis of embryonic rat forebrain neurons in culture. *Free Radical Biology and Medicine,* 29**,** 1291.

LIU, Y., YANG, X.-M., ILIODROMITIS, E., KREMASTINOS, D., DOST, T., COHEN, M. & DOWNEY, J. 2008. Redox signaling at reperfusion is required for protection from ischemic preconditioning but not from a direct PKC activator. *Basic Research in Cardiology,* 103**,** 54-59.

LONGMORE, M., WILKINSON, I. & TOROK, E. 2001. Oxford Handbook of Clinical Medicine. 178-179.

LOPEZ-BARNEO, J., PARDAL, R. & ORTEGA-SAENZ, P. 2001. Cellular mechanism of oxygen sensing. *Annu Rev Physiol,* 63**,** 259-87.

LOOR, G. & SCHUMACKER, P. T. 2008. Role of hypoxia-inducible factor in cell survival during myocardial ischemia-reperfusion. *Cell Death Differ,* 15**,** 686-690.

LOWRY, O. H., ROSEBROUGH, N. J., FARR, A. L. & RANDALL, R. J. 1951. PROTEIN MEASUREMENT WITH THE FOLIN PHENOL REAGENT. *Journal of Biological Chemistry,* 193**,** 265-275.

LU, X., LIU, H., WANG, L. & SCHAEFER, S. 2009. Activation of NF-{kappa}B is a critical element in the antiapoptotic effect of anesthetic preconditioning. *Am J Physiol Heart Circ Physiol,* 296**,** H1296-1304.

LUETJENS, C. M., BUI, N. T., SENGPIEL, B., MUNSTERMANN, G., POPPE, M., KROHN, A. J., BAUERBACH, E., KRIEGLSTEIN, J. & PREHN, J. H. M. 2000. Delayed Mitochondrial Dysfunction in Excitotoxic Neuron Death: Cytochrome c Release and a Secondary Increase in Superoxide Production. *J. Neurosci.*, 20**,** 5715-5723.

LYNN, E. G., LU, Z., MINERBI, D. & SACK, M. N. 2007. The Regulation, Control, and Consequences of Mitochondrial Oxygen Utilization and Disposition in the Heart and Skeletal Muscle During Hypoxia. *Antioxidants & Redox Signaling,* 9**,** 1353-1362.

MADESH, M. & HAJNOCZKY, G. 2001. VDAC-dependent permeabilization of the outer mitochondrial membrane by superoxide induces rapid and massive cytochrome c release. *J. Cell Biol.*, 155**,** 1003-1016.

MALHOTRA, R. & BROSIUS, F. C., 3RD 1999. Glucose uptake and glycolysis reduce hypoxia-induced apoptosis in cultured neonatal rat cardiac myocytes. *J Biol Chem,* 274**,** 12567-75.

MAMMEN, P. P. A., KANATOUS, S. B., YUHANNA, I. S., SHAUL, P. W., GARRY, M. G., BALABAN, R. S. & GARRY, D. J. 2003. Hypoxia-induced left ventricular dysfunction in myoglobin-deficient mice. *Am J Physiol Heart Circ Physiol,* 285**,** H2132-2141.

MARK, P. M., CARSTEN, C., ZAIFANG, Y. & SIMONETTA, C. 2000. Roles of Nuclear Factor κB in Neuronal Survival and Plasticity. *Journal of Neurochemistry,* 74**,** 443-456.

MARUMO, T., SCHINI-KERTH, V. B., FISSLTHALER, B. & BUSSE, R. 1997. Platelet-derived growth factor-stimulated superoxide anion production modulates activation of transcription factor NF-kappaB and expression of monocyte chemoattractant protein 1 in human aortic smooth muscle cells. *Circulation,* 96**,** 2361-7.

MASON, P. 1995. Antioxidant Supplements: Should they be recommended ? *The Pharmaceutical Journal,* 254**,** 264-266.

MATATA, B. M. & GALIÑANES, M. 2002. Peroxynitrite Is an Essential Component of Cytokines Production Mechanism in Human Monocytes through Modulation of Nuclear Factor-κB DNA Binding Activity. *Journal of Biological Chemistry,* 277**,** 2330-2335.

MATHERS, J., FRASER,J.A.,MCMAHON,M., SAUNDERS,R.D., HAYES,J.D., AND MCLELLAN., L.I.(2004) . . 2004. Antioxidant and cytoprotective responses to redox stress. *Biochem.Soc.Symp,* 71**,** 157-176.

MATSUSHITA, H., MORISHITA, R., NATA, T., AOKI, M., NAKAGAMI, H., TANIYAMA, Y., YAMAMOTO, K., HIGAKI, J., YASUFUMI, K. & OGIHARA, T. 2000. Hypoxia-induced endothelial apoptosis through nuclear factor-kB (NF-κB)-mediated bcl-2 suppression: In vivo evidence of the importance of NF-κB in endothelial cell regulation. *Circulation research* 86, no9, pp. **,** 974-981.

MAULIK, N., ENGELMAN, D. T., WATANABE, M., ENGELMAN, R. M., MAULIK, G., CORDIS, G. A. & DAS, D. K. 1995. Nitric oxide signaling in ischemic heart. *Cardiovasc Res,* 30**,** 593-601.

MAULIK, N., SASAKI, H., ADDYA, S. & DAS, D. K. 2000. Regulation of cardiomyocyte apoptosis by redox-sensitive transcription factors. *FEBS Lett,* 485**,** 7-12.

MCARDLE, F., PATTWELL, D. M., VASILAKI, A., MCARDLE, A. & JACKSON, M. J. 2005. Intracellular generation of reactive oxygen species by contracting skeletal muscle cells. *Free Radical Biology and Medicine,* 39**,** 651.

MCCORD, J. 1985. Oxygen-derived free radicals in postischemic tissue injury. *N Engl J Med,* 312**,** 159-163.

MCCULLY, J. D., WAKIYAMA, H., HSIEH, Y.-J., JONES, M. & LEVITSKY, S. 2004. Differential contribution of necrosis and apoptosis in myocardial ischemia-reperfusion injury. *Am J Physiol Heart Circ Physiol,* 286**,** H1923-1935.

MCQUADE, L. E. & LIPPARD, S. J. 2010. Fluorescent probes to investigate nitric oxide and other reactive nitrogen species in biology (truncated form: fluorescent probes of reactive nitrogen species). *Current Opinion in Chemical Biology,* 14**,** 43-49.

MENESHIAN, A. & BULKLEY, G. B. 2002. The Physiology of Endothelial Xanthine Oxidase: From Urate Catabolism to Reperfusion Injury to Inflammatory Signal Transduction. *Microcirculation,* 9**,** 161 - 175.

MILLAR, T. M., PHAN, V. & TIBBLES, L. A. 2007. ROS generation in endothelial hypoxia and reoxygenation stimulates MAP kinase signaling and kinase-dependent neutrophil recruitment. *Free Radical Biology and Medicine,* 42**,** 1165.

MIZUNO, T., WATANABE, M., SAKAMOTO, T. & SUNAMORI, M. 1998. L-Arginine, a nitric oxide precursor, attenuates ischemia-reperfusion injury by inhibiting inositol-1,4,5-triphosphate. *J Thorac Cardiovasc Surg,* 115**,** 931-936.

MOHAZZAB, K. M. & WOLIN, M. S. 1994. Properties of a superoxide anion-generating microsomal NADH oxidoreductase, a potential pulmonary artery PO2 sensor. *Am J Physiol Lung Cell Mol Physiol,* 267**,** L823-831.

MORTIMER, C. H. 1956. The oxygen content of air-saturated fresh waters, and aids in calculating percentage saturation. *Intern. Assoc.Theoret. Appl. Commun,* 6.

MOTTERLINI, R., HIDALGO, A., SAMMUT, I., SHAH, K. A., MOHAMMED, S., SRAI, K. & GREEN, C. J. 1996. A Precursor of the Nitric Oxide Donor SIN-1 Modulates the Stress Protein Heme Oxygenase-1 in Rat Liver. *Biochemical and Biophysical Research Communications,* 225**,** 167-172.

MUELLER, A. R., PLATZ, K. P., SCHUMACHER, G., RIGER, J., GEBAUER, B., NEUMANN, U. & NEUHAUS, P. 1997. Mechanisms of preservation and reperfusion injury in human liver transplantation. *Transplantation Proceedings,* 29**,** 3455-3457.

MUKHOPADHYAY, P., RAJESH, M., YOSHIHIRO, K., HASKÓ, G. & PACHER, P. 2007. Simple quantitative detection of mitochondrial superoxide production in live cells. *Biochemical and Biophysical Research Communications,* 358**,** 203.

MURDOCH, C. E., ZHANG, M., CAVE, A. C. & SHAH, A. M. 2006. NADPH oxidase-dependent redox signalling in cardiac hypertrophy, remodelling and failure. *Cardiovasc Res,* 71**,** 208-215.

MURPHY, M. P. 2009. How mitochondria produce reactive oxygen species. *Biochem J,* 417**,** 1-13.

MURRANT, ANDRADE & REID 1999. Exogenous reactive oxygen and nitric oxide alter intracellular oxidant status of skeletal muscle fibres. *Acta Physiologica Scandinavica,* 166**,** 111-121.

MURRAY, C. J. L. & LOPEZ, A. D. 1997. Alternative projections of mortality and disability by cause 1990-2020: Global Burden of Disease Study. *The Lancet,* 349**,** 1498-1504.

MURRY, C., JENNINGS, R. & REIMER, K. 1986. Preconditioning with ischemia: a delay of lethal cell injury in ischemic myocardium. *Circulation,* 74**,** 1124-1136.

MUSCHEL, R. J., BERNHARD, E. J., GARZA, L., GILLIES MCKENNA, W. & KOCH, C. J. 1995. Induction of Apoptosis at Different Oxygen Tensions: Evidence That Oxygen Radicals Do Not Mediate Apoptotic Signaling. *Cancer Res,* 55**,** 995-998.

NAGENDRAN, J. & MICHELAKIS, E. D. 2009. Mitochondrial NOS is upregulated in the hypoxic heart: implications for the function of the hypertrophied right ventricle. *Am J Physiol Heart Circ Physiol,* 296**,** H1723-1726.

NAKANO, M., KAWANISHI, Y., KAMOHARA, S., UCHIDA, Y., SHIOTA, M., INATOMI, Y., KOMORI, T., MIYAZAWA, K., GONDO, K. & YAMASAWA, I. 2003. Oxidative DNA damage (8-hydroxydeoxyguanosine) and body iron status: a study on 2507 healthy people. *Free Radical Biology and Medicine,* 35**,** 826-832.

NAKATSUBO, N., KOJIMA, H., KIKUCHI, K., NAGOSHI, H., HIRATA, Y., MAEDA, D., IMAI, Y., IRIMURA, T. & NAGANO, T. 1998. Direct evidence of nitric oxide production from bovine aortic endothelial cells using new fluorescence indicators: diaminofluoresceins. *FEBS Lett,* 427**,** 263-6.

NAOI, M., MARUYAMA, W., AKAO, Y., ZHANG, J. & PARVEZ, H. 2000. Apoptosis induced by an endogenous neurotoxin, N-methyl(R)salsolinol, in dopamine neurons. *Toxicology,* 153**,** 123-141.

NARULA, J., HAIDER, N., VIRMANI, R., DISALVO, T. G., KOLODGIE, F. D., HAJJAR, R. J., SCHMIDT, U., SEMIGRAN, M. J., DEC, G. W. & KHAW, B.-A. 1996. Apoptosis in Myocytes in End-Stage Heart Failure. *N Engl J Med,* 335**,** 1182-1189.

NGUYEN, T., NIOI, P. & PICKETT, C. B. 2009. The Nrf2-Antioxidant Response Element Signaling Pathway and Its Activation by Oxidative Stress. *Journal of Biological Chemistry,* 284**,** 13291-13295.

NIAZI, J., KIM, B. & GU, M. 2007. Characterization of superoxide-stress sensing recombinant Escherichia coli constructed using promoters for genes zwf and fpr fused to lux operon. *Applied Microbiology and Biotechnology,* 74**,** 1276-1283.

NICHOLSON, D. W., ALI, A., THORNBERRY, N. A., VAILLANCOURT, J. P., DING, C. K., GALLANT, M., GAREAU, Y., GRIFFIN, P. R., LABELLE, M., LAZEBNIK, Y. A., MUNDAY, N. A., RAJU, S. M., SMULSON, M. E., YAMIN, T.-T., YU, V. L. & MILLER, D. K. 1995. Identification and inhibition of the ICE/CED-3 protease necessary for mammalian apoptosis. *Nature,* 376**,** 37.

NICOTERA, P., HARTZELL, P., DAVIS, G. & ORRENIUS, S. 1986. The formation of plasma membrane blebs in hepatocytes exposed to agents that increase cytosolic Ca2+ is mediated by the activation of a non-lysosomal proteolytic system. *FEBS letters,* 209**,** 139-144.

NIOI, P., MCMAHON, M., ITOH, K., YAMAMOTO, M. & HAYES, J. D. 2003. Identification of a novel Nrf2-regulated antioxidant response element (ARE) in the mouse NAD(P)H:quinone oxidoreductase 1 gene: reassessment of the ARE consensus sequence. *Biochem. J.,* 374**,** 337-348.

NIQUET, J., BALDWIN, R. A., ALLEN, S. G., FUJIKAWA, D. G. & WASTERLAIN, C. G. 2003. Hypoxic neuronal necrosis: Protein synthesis-independent activation of a cell death program. *Proceedings of the National Academy of Sciences of the United States of America,* 100**,** 2825-2830.

NISOLI, E. & CARRUBA, M. O. 2006. Nitric oxide and mitochondrial biogenesis. *J Cell Sci,* 119**,** 2855-2862.

NORDBERG, J. & ARNÉR, E. S. J. 2001. Reactive oxygen species, antioxidants, and the mammalian thioredoxin system. *Free Radical Biology and Medicine,* 31**,** 1287-1312.

OBROSOVA, I. G. 2006. Peroxynitrite and cardiomyocyte cell death: an evolving story: A commentary on "Peroxynitrite is a major trigger of cardiomyocyte apoptosis in vitro and in vivo". *Free Radical Biology and Medicine,* 41**,** 866-868.

OKADO-MATSUMOTO, A. & FRIDOVICH, I. 2001. Subcellular Distribution of Superoxide Dismutases (SOD) in Rat Liver. *Journal of Biological Chemistry,* 276**,** 38388-38393.

OLIVETTI, G., QUAINI, F., SALA, R., LAGRASTA, C., CORRADI, D., BONACINA, E., GAMBERT, S. R., CIGOLA, E. & ANVERSA, P. 1996. Acute Myocardial Infarction in Humans is Associated with Activation of Programmed Myocyte Cell Death in the Surviving Portion of the Heart. *Journal of Molecular and Cellular Cardiology,* 28**,** 2005-2016.

OTTENHEIJM, C. A., HEUNKS, L. M., GERAEDTS, M. C. & DEKHUIJZEN, P. N. 2006. Hypoxia-induced skeletal muscle fiber dysfunction: role for reactive nitrogen species. *Am J Physiol Lung Cell Mol Physiol,* 290**,** L127-35.

OZAKI, M., DESHPANDE, S. S., ANGKEOW, P., BELLAN, J., LOWENSTEIN, C. J., DINAUER, M. C., GOLDSCHMIDT-CLERMONT, P. J. & IRANI, K. 2000. Inhibition of the Rac1 GTPase protects against nonlethal ischemia/reperfusion-induced necrosis and apoptosis in vivo. *FASEB J.,* 14**,** 418-429.

PABLA, R. & CURTIS, M. J. 1996. Endogenous Protection Against Reperfusion-induced Ventricular Fibrillation: Role of Neuronal versus Non-neuronal Sources of Nitric Oxide and Species Dependence in the Rat versus Rabbit Isolated Heart. *Journal of Molecular and Cellular Cardiology,* 28**,** 2097-2110.

PACHER, P., SCHULZ, R., LIAUDET, L. & SZABÓ, C. 2005. Nitrosative stress and pharmacological modulation of heart failure. *Trends in Pharmacological Sciences,* 26**,** 302-310.

PACHER, P., BECKMAN, J. S. & LIAUDET, L. 2007. Nitric Oxide and Peroxynitrite in Health and Disease. *Physiol. Rev.,* 87**,** 315-424.

PAGANO, P. J., CHANOCK, S. J., SIWIK, D. A., COLUCCI, W. S. & CLARK, J. K. 1998. Angiotensin II induces p67phox mRNA expression and NADPH oxidase superoxide generation in rabbit aortic adventitial fibroblasts. *Hypertension,* 32**,** 331-7.

PAGLIARO, P. 2003. Differential biological effects of products of nitric oxide (NO) synthase: it is not enough to say NO. *Life Sciences,* 73**,** 2137-2149.

PAKY, A., MICHAEL, J. R., BURKE-WOLIN, T. M., WOLIN, M. S. & GURTNER, G. H. 1993. Endogenous production of superoxide by rabbit lungs: effects of hypoxia or metabolic inhibitors. *J Appl Physiol,* 74**,** 2868-2874.

PALACIOS-CALLENDER, M., HOLLIS, V., FRAKICH, N., MATEO, J. & MONCADA, S. 2007. Cytochrome c oxidase maintains mitochondrial respiration during partial inhibition by nitric oxide. *J Cell Sci,* 120**,** 160-5.

PARK, C., SO, H.-S., SHIN, C.-H., BAEK, S.-H., MOON, B.-S., SHIN, S.-H., LEE, H.-S., LEE, D.-W. & PARK, R. 2003. Quercetin protects the hydrogen peroxide-induced apoptosis via inhibition of mitochondrial dysfuntion in H9C2 cardiomyoblast cells. *Biochemical Pharmacology,* 66**,** 1287.

PARRINO, P. E., LAUBACH, V. E., GAUGHEN, J. R., JR, SHOCKEY, K. S., WATTSMAN, T.-A., KING, R. C., TRIBBLE, C. G. & KRON, I. L. 1998. Inhibition of inducible nitric oxide synthase after myocardial ischemia increases coronary flow. *Ann Thorac Surg,* 66**,** 733-739.

PATEL, R. P., MCANDREW, J., SELLAK, H., WHITE, C. R., JO, H., FREEMAN, B. A. & DARLEY-USMAR, V. M. 1999. Biological aspects of reactive nitrogen species. *Biochim Biophys Acta,* 1411**,** 385-400.

PATEL, R. P., MOELLERING, D., MURPHY-ULLRICH, J., JO, H., BECKMAN, J. S. & DARLEY-USMAR, V. M. 2000. Cell signaling by reactive nitrogen and oxygen species in atherosclerosis. *Free Radical Biology and Medicine,* 28**,** 1780-1794.

PEARLSTEIN, D. P., ALI, M. H., MUNGAI, P. T., HYNES, K. L., GEWERTZ, B. L. & SCHUMACKER, P. T. 2002. Role of mitochondrial oxidant generation in endothelial cell responses to hypoxia. *Arterioscler Thromb Vasc Biol,* 22**,** 566-73.

PENNA, C., CAPPELLO, S., MANCARDI, D., RAIMONDO, S., RASTALDO, R., GATTULLO, D., LOSANO, G. & PAGLIARO, P. 2006. Post–conditioning reduces infarct size in the isolated rat heart: Role of coronary flow and pressure and the nitric oxide/cGMP pathway. *Basic Research in Cardiology,* 101**,** 168-179.

PENNA, C., MANCARDI, D., RASTALDO, R. & PAGLIARO, P. 2009. Cardioprotection: A radical view: Free radicals in pre and postconditioning. *Biochimica et Biophysica Acta (BBA) - Bioenergetics,* 1787**,** 781-793.

PERKINS, N. D. 1997. Achieving transcriptional specificity with nf-[kappa]b. *The International Journal of Biochemistry & Cell Biology,* 29**,** 1433-1448.

PERSSON-ROTHERT, M., EGAS-KENNIPHAAS, J. M., VALK-KOKSHOORN, E. J. M., BUYS, J. P. & LAARSE, A. 1994. Oxidative stress-induced perturbations of calcium homeostasis and cell death in cultured myocytes: Role of extracellular calcium. *Molecular and Cellular Biochemistry,* 136**,** 1-9.

PESSE, B., LEVRAND, S., FEIHL, F., WAEBER, B., GAVILLET, B., PACHER, P. & LIAUDET, L. 2005. Peroxynitrite activates ERK via Raf-1 and MEK, independently from EGF receptor and p21Ras in H9C2 cardiomyocytes. *Journal of Molecular and Cellular Cardiology,* 38**,** 765-775.

PETERS, B., WALKA, M. M., FRIEDMANN, W., STOLTENBURG-DIDINGER, G. & OBLADEN, M. 2000. Hypoxic-ischemic encephalopathy with cystic brain stem necroses and thalamic calcifications in a preterm twin. *Brain and Development,* 22**,** 265-271.

PETROSILLO, G., DI VENOSA, N., RUGGIERO, F. M., PISTOLESE, M., D'AGOSTINO, D., TIRAVANTI, E., FIORE, T. & PARADIES, G. 2005. Mitochondrial dysfunction associated with cardiac ischemia/reperfusion can be attenuated by oxygen tension control. Role of oxygen-free radicals and cardiolipin. *Biochimica et Biophysica Acta (BBA) - Bioenergetics,* 1710**,** 78-86.

PEYROT, F. & DUCROCQ, C. 2007. Nitrosation of <I>N</I>-Terminally Blocked Tryptophan and Tryptophan-Containing Peptides by Peroxynitrite. *ChemBioChem,* 8**,** 217-223.

PIGNATTI, C. & STEFANELLI, C. 2003. Ischemia/reperfusion-induced apoptosis: connecting nitric oxide and cell cycle regulators. *Cardiovasc Res,* 59**,** 268-270.

PORASUPHATANA, S., TSAI, P. & ROSEN, G. M. 2003. The generation of free radicals by nitric oxide synthase. *Comparative Biochemistry and Physiology Part C: Toxicology & Pharmacology,* 134**,** 281.

POU, S., KEATON, L., SURICHAMORN, W. & ROSEN, G. M. 1999. Mechanism of superoxide generation by neuronal nitric-oxide synthase. *J Biol Chem,* 274**,** 9573-80.

POWELL, C. S. & JACKSON, R. M. 2003. Mitochondrial complex I, aconitase, and succinate dehydrogenase during hypoxia-reoxygenation: modulation of enzyme activities by MnSOD. *Am J Physiol Lung Cell Mol Physiol,* 285**,** L189-198.

RAAT, N. J. H., SHIVA, S. & GLADWIN, M. T. 2009. Effects of nitrite on modulating ROS generation following ischemia and reperfusion. *Advanced Drug Delivery Reviews,* 61**,** 339-350.

RAKHIT, R. D., EDWARDS, R. J., MOCKRIDGE, J. W., BAYDOUN, A. R., WYATT, A. W., MANN, G. E. & MARBER, M. S. 2000. Nitric oxide-induced cardioprotection in cultured rat ventricular myocytes. *Am J Physiol Heart Circ Physiol,* 278**,** H1211-7.

RAMACHANDRAN, A., LEVONEN, A. L., BROOKES, P. S., CEASER, E., SHIVA, S., BARONE, M. C. & DARLEY-USMAR, V. 2002. Mitochondria, nitric oxide, and cardiovascular dysfunction. *Free Radic Biol Med,* 33**,** 1465-74.

REED, J. C., ZHA, H., AIME-SEMPE, C., TAKAYAMA, S. & WANG, H. G. 1996. Structure-function analysis of Bcl-2 family proteins. Regulators of programmed cell death. *Adv Exp Med Biol,* 406**,** 99-112.

REGULA, K. M., BAETZ, D. & KIRSHENBAUM, L. A. 2004. Nuclear Factor-{kappa}B Represses Hypoxia-Induced Mitochondrial Defects and Cell Death of Ventricular Myocytes. *Circulation,* 110**,** 3795-3802.

RENZING, J., HANSEN, S. & LANE, D. 1996. Oxidative stress is involved in the UV activation of p53. *J Cell Sci,* 109**,** 1105-1112.

ROBINSON, K. M., JANES, M. S., PEHAR, M., MONETTE, J. S., ROSS, M. F., HAGEN, T. M., MURPHY, M. P. & BECKMAN, J. S. 2006. Selective fluorescent imaging of superoxide in vivo using ethidium-based probes. *Proc Natl Acad Sci U S A,* 103**,** 15038-43.

ROYALL, J. A. & ISCHIROPOULOS, H. 1993a. Evaluation of 2',7'-dichlorofluorescin and dihydrorhodamine 123 as fluorescent probes for intracellular H2O2 in cultured endothelial cells. *Arch Biochem Biophys,* 302**,** 348-55.

ROYALL, J. A. & ISCHIROPOULOS, H. 1993b. Evaluation of 2[prime], 7[prime]-dichlororfluorescin and dihydrorhodamine 123 as fluorescent probes for intracellular H2O2 in cultured endothelial cells. *Arch Biochem Biophys,* 302**,** 348.

RUSHWORTH, S. A., MACEWAN, D. J. & O'CONNELL, M. A. 2008. Lipopolysaccharide-Induced Expression of NAD(P)H:Quinone Oxidoreductase 1 and Heme Oxygenase-1 Protects against Excessive Inflammatory Responses in Human Monocytes. *J Immunol,* 181**,** 6730-6737.

SABOL, S. L., LI, R., LEE, T. Y. & ABDUL-KHALEK, R. 1998. Inhibition of Apoptosis-Associated DNA Fragmentation Activity in Nonapoptotic Cells: The Role of DNA Fragmentation Factor-45 (DFF45/ICAD). *Biochemical and Biophysical Research Communications,* 253**,** 151.

SAKAHIRA, H., ENARI, M. & NAGATA, S. 1998. Cleavage of CAD inhibitor in CAD activation and DNA degradation during apoptosis. *Nature,* 391**,** 96.

SALLY, E. P.-D., YAN, L., MATT, D., STEVE, M., JEFFERY, J. & QIN, M. C. 2007. Induction of antioxidant and detoxification response by oxidants in cardiomyocytes: Evidence from gene expression profiling and activation of Nrf2 transcription factor. *Journal of Molecular and Cellular Cardiology,* 42**,** 159-176.

SATO, H., ZHAO, Z.-Q., MCGEE, D. S., WILLIAMS, M. W., HAMMON, J. J. W. & VINTEN-JOHANSEN, J. 1995. Supplemental l-arginine during cardioplegic arrest and reperfusion avoids regional postischemic injury. *The Journal of Thoracic and Cardiovascular Surgery,* 110**,** 302-314.

SATRIANO, J. & SCHLONDORFF, D. 1994. Activation and attenuation of transcription factor NF-kB in mouse glomerular mesangial cells in response to tumor necrosis factor-alpha, immunoglobulin G, and adenosine 3':5'-cyclic monophosphate. Evidence for involvement of reactive oxygen species. *The Journal of Clinical Investigation,* 94**,** 1629-1636.

SAUER, H., WARTENBERG, M. & HESCHELER, J. 2001. Reactive Oxygen Species as Intracellular Messengers During Cell Growth and Differentiation. *Cellular Physiology and Biochemistry,* 11**,** 173-186.

SCHAFER, M., SCHAFER, C., EWALD, N., PIPER, H. M. & NOLL, T. 2003. Role of Redox Signaling in the Autonomous Proliferative Response of Endothelial Cells to Hypoxia. *Circ Res***,** 01.RES.0000070882.81508.FC.

SCHULZ, R., KELM, M. & HEUSCH, G. 2004. Nitric oxide in myocardial ischemia/reperfusion injury. *Cardiovasc Res,* 61**,** 402-413.

SCHUMACKER, P. T. 2002. Hypoxia, anoxia, and O2 sensing: the search continues. *Am J Physiol Lung Cell Mol Physiol,* 283**,** L918-21.

SCHUMACKER, P. T. 2003. Current paradigms in cellular oxygen sensing. *Adv Exp Med Biol,* 543**,** 57-71.

SCHUMACKER, P. T., CHANDEL, N. & AGUSTI, A. G. 1993. Oxygen conformance of cellular respiration in hepatocytes. *Am J Physiol Lung Cell Mol Physiol,* 265**,** L395-402.

SERVIDDIO, G., DI VENOSA, N., FEDERICI, A., D'AGOSTINO, D., ROLLO, T., PRIGIGALLO, F., ALTOMARE, E., FIORE, T. & VENDEMIALE, G. 2005. Brief hypoxia before normoxic reperfusion (postconditioning) protects the heart against ischemia-reperfusion injury by preventing mitochondria peroxyde production and glutathione depletion. *FASEB J.,* 19**,** 354-361.

SHACKELFORD, R. E., KAUFMANN, W. K. & PAULES, R. S. 2000. Oxidative stress and cell cycle checkpoint function. *Free Radical Biology and Medicine,* 28**,** 1387-1404.

SHAH, Z. A., LI, R. C., THIMMULAPPA, R. K., KENSLER, T. W., YAMAMOTO, M., BISWAL, S. & DORÉ, S. 2007. Role of reactive oxygen species in modulation of Nrf2 following ischemic reperfusion injury. *Neuroscience,* 147**,** 53-59.

SHAO, N., KRIEGER-LISZKAY, A., SCHRODA, M. & BECK, C. F. 2007. A reporter system for the individual detection of hydrogen peroxide and singlet oxygen: its use for the assay of reactive oxygen species produced in vivo. *The Plant Journal,* 50**,** 475-487.

SHIBUYA, A., TSUKAGOSHI, N., OHTSU, I., DOKYU, N. & AONO, R. 2004. Convenient and Sensitive Evaluation of a Superoxide Anion-Generating Reagent Methyl Viologen by Escherichia coli Harboring a soxS’::gfp Reporter Plasmid. *Bioscience, Biotechnology, and Biochemistry,* 68**,** 2637-2639.

SHIMIZU, S., EGUCHI, Y., KAMIIKE, W., ITOH, Y., HASEGAWA, J.-I., YAMABE, K., OTSUKI, Y., MATSUDA, H. & TSUJIMOTO, Y. 1996. Induction of Apoptosis as well as Necrosis by Hypoxia and Predominant Prevention of Apoptosis by Bcl-2 and Bcl-XL. *Cancer Res,* 56**,** 2161-2166.

SOLAINI, G. & HARRIS, D. A. 2005. Biochemical dysfunction in heart mitochondria exposed to ischaemia and reperfusion. *Biochem. J.,* 390**,** 377-394.

SOUZA, H. P., LIU, X., SAMOUILOV, A., KUPPUSAMY, P., LAURINDO, F. R. & ZWEIER, J. L. 2002. Quantitation of superoxide generation and substrate utilization by vascular NAD(P)H oxidase. *Am J Physiol Heart Circ Physiol,* 282**,** H466-74.

ŠTAJNER, D., POPOVIĆ, M. & ŠTAJNER, M. 2003. Herbicide Induced Oxidative Stress in Lettuce, Beans, Pea Seeds and Leaves. *Biologia Plantarum,* 47**,** 575-579.

STOLK, J., HILTERMANN, T. J., DIJKMAN, J. H. & VERHOEVEN, A. J. 1994a. Characteristics of the inhibition of NADPH oxidase activation in neutrophils by apocynin, a methoxy-substituted catechol. *Am J Respir Cell Mol Biol,* 11**,** 95-102.

STOLK, J., HILTERMANN, T. J., DIJKMAN, J. H. & VERHOEVEN, A. J. 1994b. Characteristics of the inhibition of NADPH oxidase activation in neutrophils by apocynin, a methoxy-substituted catechol. *Am. J. Respir. Cell Mol. Biol.,* 11**,** 95-102.

STRIJDOM, H., JACOBS, S., HATTINGH, S., PAGE, C. & LOCHNER, A. 2006. Nitric oxide production is higher in rat cardiac microvessel endothelial cells than ventricular cardiomyocytes in baseline and hypoxic conditions: a comparative study. *Faseb J,* 20**,** 314-6.

STRIJDOM, H., FRIEDRICH, S., HATTINGH, S., CHAMANE, N. & LOCHNER, A. 2009. Hypoxia-induced regulation of nitric oxide synthase in cardiac endothelial cells and myocytes and the role of the PI3-K/PKB pathway. *Molecular and Cellular Biochemistry,* 321**,** 23-35.

SULEIMAN, M. S., HALESTRAP, A. P. & GRIFFITHS, E. J. 2001. Mitochondria: a target for myocardial protection. *Pharmacol Ther,* 89**,** 29-46.

SUMERAY, M. S., REES, D. D. & YELLON, D. M. 2000. Infarct Size and Nitric Oxide Synthase in Murine Myocardium. *Journal of Molecular and Cellular Cardiology,* 32**,** 35-42.

SUN, Y. & OBERLEY, L. W. 1996. Redox regulation of transcriptional activators. *Free Radical Biology and Medicine,* 21**,** 335-348.

SZELID, Z., POKREISZ, P., LIU, X., VERMEERSCH, P., MARSBOOM, G., GILLIJNS, H., PELLENS, M., VERBEKEN, E., VAN DE WERF, F., COLLEN, D. & JANSSENS, S. 2009. Cardioselective nitric oxide synthase 3 gene transfer protects against myocardial reperfusion injury. *Basic Research in Cardiology*.

TAHARA, E. B., NAVARETE, F. D. T. & KOWALTOWSKI, A. J. 2009. Tissue-, substrate-, and site-specific characteristics of mitochondrial reactive oxygen species generation. *Free Radical Biology and Medicine,* 46**,** 1283-1297.

TAKANO, H., MANCHIKALAPUDI, S., TANG, X.-L., QIU, Y., RIZVI, A., JADOON, A. K., ZHANG, Q. & BOLLI, R. 1998. Nitric Oxide Synthase Is the Mediator of Late Preconditioning Against Myocardial Infarction in Conscious Rabbits. *Circulation,* 98**,** 441-449.

TALMAN, W. T. 2006. NO and Central Cardiovascular Control: A Simple Molecule With a Complex Story. *Hypertension,* 48**,** 552-554.

TALUKDER, M. A. H., ZWEIER, J. L. & PERIASAMY, M. 2009. Targeting calcium transport in ischaemic heart disease. *Cardiovascular Research,* 84**,** 345-352.

TANAKA, M., ITO, H., ADACHI, S., AKIMOTO, H., NISHIKAWA, T., KASAJIMA, T., MARUMO, F. & HIROE, M. 1994. Hypoxia induces apoptosis with enhanced expression of Fas antigen messenger RNA in cultured neonatal rat cardiomyocytes. *Circ Res,* 75**,** 426-33.

TANIYAMA, Y. & GRIENDLING, K. K. 2003. Reactive Oxygen Species in the Vasculature: Molecular and Cellular Mechanisms. *Hypertension,* 42**,** 1075-1081.

TARPEY, M. M. & FRIDOVICH, I. 2001. Methods of detection of vascular reactive species: nitric oxide, superoxide, hydrogen peroxide, and peroxynitrite. *Circ Res,* 89**,** 224-36.

TARPEY, M. M., WINK, D. A. & GRISHAM, M. B. 2004. Methods for detection of reactive metabolites of oxygen and nitrogen: in vitro and in vivo considerations. *Am J Physiol Regul Integr Comp Physiol,* 286**,** R431-44.

TATSUMI, T., SHIRAISHI, J., KEIRA, N., AKASHI, K., MANO, A., YAMANAKA, S., MATOBA, S., FUSHIKI, S., FLISS, H. & NAKAGAWA, M. 2003. Intracellular ATP is required for mitochondrial apoptotic pathways in isolated hypoxic rat cardiac myocytes. *Cardiovasc Res,* 59**,** 428-440.

TAYLOR, C. T. & CUMMINS, E. P. 2009. The Role of NF-B in Hypoxia-Induced Gene Expression. *Annals of the New York Academy of Sciences,* 1177**,** 178-184.

THANNICKAL, V. J. & FANBURG, B. L. 2000. Reactive oxygen species in cell signaling. *Am J Physiol Lung Cell Mol Physiol,* 279**,** L1005-28.

THIMMULAPPA, R. K., MAI, K. H., SRISUMA, S., KENSLER, T. W., YAMAMOTO, M. & BISWAL, S. 2002. Identification of Nrf2-regulated Genes Induced by the Chemopreventive Agent Sulforaphane by Oligonucleotide Microarray. *Cancer Res,* 62**,** 5196-5203.

THOMADAKI, H., KARALIOTA, A., LITOS, C. & SCORILAS, A. 2007. Enhanced Antileukemic Activity of the Novel Complex 2,5-Dihydroxybenzoate Molybdenum(VI) against 2,5-Dihydroxybenzoate, Polyoxometalate of Mo(VI), and Tetraphenylphosphonium in the Human HL-60 and K562 Leukemic Cell Lines. *Journal of Medicinal Chemistry,* 50**,** 1316-1321.

THORNBERRY, N. A. & LAZEBNIK, Y. 1998. Caspases: Enemies Within. *Science,* 281**,** 1312-1316.

TIRAVANTI, E., SAMOUILOV, A. & ZWEIER, J. L. 2004. Nitrosyl-Heme Complexes Are Formed in the Ischemic Heart. *Journal of Biological Chemistry,* 279**,** 11065-11073.

TISCORNIA, A., CAIROLI, E., MARQUEZ, M., DENICOLA, A., PRITSCH, O. & CAYOTA, A. 2009. Use of diaminofluoresceins to detect and measure nitric oxide in low level generating human immune cells. *Journal of Immunological Methods,* 342**,** 49-57.

TODOR, A., SHAROV, V. G., TANHEHCO, E. J., SILVERMAN, N., BERNABEI, A. & SABBAH, H. N. 2002. Hypoxia-induced cleavage of caspase-3 and DFF45/ICAD in human failed cardiomyocytes. *Am J Physiol Heart Circ Physiol,* 283**,** H990-995.

TOESCU, E. C. 2004. Hypoxia sensing and pathways of cytosolic Ca2+ increases. *Cell Calcium,* 36**,** 187-99.

TOUYZ, R. M. 2008. Apocynin, NADPH Oxidase, and Vascular Cells: A Complex Matter. *Hypertension,* 51**,** 172-174.

TRITTO, I., D'ANDREA, D., ERAMO, N., SCOGNAMIGLIO, A., DE SIMONE, C., VIOLANTE, A., ESPOSITO, A., CHIARIELLO, M. & AMBROSIO, G. 1997. Oxygen Radicals Can Induce Preconditioning in Rabbit Hearts. *Circ Res,* 80**,** 743-748.

TSAO, P. S., BUITRAGO, R., CHAN, J. R. & COOKE, J. P. 1996. Fluid flow inhibits endothelial adhesiveness. Nitric oxide and transcriptional regulation of VCAM-1. *Circulation,* 94**,** 1682-9.

TSUCHIYA, K., TAKASUGI, M., MINAKUCHI, K. & FUKUZAWA, K. 1996. Sensitive quantitation of nitric oxide by EPR spectroscopy. *Free Radical Biology and Medicine,* 21**,** 733-737.

TSUJIMOTO, Y. & SHIMIZU, S. 2007. Role of the mitochondrial membrane permeability transition in cell death. *Apoptosis,* 12**,** 835-840.

TURAN, N., CSONKA, C., CSONT, T., GIRICZ, Z., FODOR, G., BENCSIK, P., GYONGYOSI, M., CAKICI, I. & FERDINANDY, P. 2006. The role of peroxynitrite in chemical preconditioning with 3-nitropropionic acid in rat hearts. *Cardiovasc Res,* 70**,** 384-90.

TURRENS, J. F. 1997. Superoxide production by the mitochondrial respiratory chain. *Biosci Rep,* 17**,** 3-8.

USHIO-FUKAI, M., TANG, Y., FUKAI, T., DIKALOV, S. I., MA, Y., FUJIMOTO, M., QUINN, M. T., PAGANO, P. J., JOHNSON, C. & ALEXANDER, R. W. 2002. Novel role of gp91(phox)-containing NAD(P)H oxidase in vascular endothelial growth factor-induced signaling and angiogenesis. *Circ Res,* 91**,** 1160-7.

VAN DE LOOSDRECHT, A. A., BEELEN, R. H., OSSENKOPPELE, G. J., BROEKHOVEN, M. G. & LANGENHUIJSEN, M. M. 1994. A tetrazolium-based colorimetric MTT assay to quantitate human monocyte mediated cytotoxicity against leukemic cells from cell lines and patients with acute myeloid leukemia. *J Immunol Methods,* 174**,** 311-20.

VANDEN HOEK, T. L., BECKER, L. B., SHAO, Z., LI, C. & SCHUMACKER, P. T. 1998. Reactive oxygen species released from mitochondria during brief hypoxia induce preconditioning in cardiomyocytes. *J Biol Chem,* 273**,** 18092-8.

VANDEN HOEK, T. L., LI, C., SHAO, Z., SCHUMACKER, P. T. & BECKER, L. B. 1997. Significant Levels of Oxidants are Generated by Isolated Cardiomyocytes During Ischemia Prior to Reperfusion. *Journal of Molecular and Cellular Cardiology,* 29**,** 2571.

VASSILOPOULOS, A. & PAPAZAFIRI, P. 2005. Attenuation of oxidative stress in HL-1 cardiomyocytes improves mitochondrial function and stabilizes Hif-1alpha. *Free Radic Res,* 39**,** 1273-84.

VEJRAZKA, M., MÍCEK, R. & STÍPEK, S. 2005. Apocynin inhibits NADPH oxidase in phagocytes but stimulates ROS production in non-phagocytic cells. *Biochimica et Biophysica Acta (BBA) - General Subjects,* 1722**,** 143-147.

VERHAGEN, A., COULSON, E. & VAUX, D. 2001. Inhibitor of apoptosis proteins and their relatives: IAPs and other BIRPs. *Genome Biology,* 2**,** reviews3009.1 - reviews3009.10.

VIVANCOS, A. P., CASTILLO, E. A., BITEAU, B., NICOT, C., AYTE, J., TOLEDANO, M. B. & HIDALGO, E. 2005. A cysteine-sulfinic acid in peroxiredoxin regulates H2O2-sensing by the antioxidant Pap1 pathway. *Proc Natl Acad Sci U S A,* 102**,** 8875-80.

VOGT, A. M., ACKERMANN, C., YILDIZ, M., SCHOELS, W. & KÜBLER, W. 2002. Lactate accumulation rather than ATP depletion predicts ischemic myocardial necrosis: Implications for the development of lethal myocardial injury. *Biochimica et Biophysica Acta (BBA) - Molecular Basis of Disease,* 1586**,** 219-226.

VON BOHLEN UND HALBACH, O. 2003. Nitric oxide imaging in living neuronal tissues using fluorescent probes. *Nitric Oxide,* 9**,** 217-228.

VOUSDEN, K. H. 2005. APOPTOSIS: p53 and PUMA: A Deadly Duo. *Science,* 309**,** 1685-1686.

WAINWRIGHT, C. L. & MARTORANA, P. A. 1993. Pirsidomine, A Novel Nitric Oxide Donor, Suppresses Ischemic Arrhythmias in Anesthetized Pigs. *Journal of Cardiovascular Pharmacology,* 22**,** S44-50.

WALDER, C. E., GREEN, S. P., DARBONNE, W. C., MATHIAS, J., RAE, J., DINAUER, M. C., CURNUTTE, J. T. & THOMAS, G. R. 1997. Ischemic Stroke Injury Is Reduced in Mice Lacking a Functional NADPH Oxidase. *Stroke,* 28**,** 2252-2258.

WANG, G., HAZRA, T. K., MITRA, S., LEE, H. M. & ENGLANDER, E. W. 2000. Mitochondrial DNA damage and a hypoxic response are induced by CoCl(2) in rat neuronal PC12 cells. *Nucleic Acids Res,* 28**,** 2135-40.

WANG, W., SAWICKI, G. & SCHULZ, R. 2002. Peroxynitrite-induced myocardial injury is mediated through matrix metalloproteinase-2. *Cardiovasc Res,* 53**,** 165-174.

WANG, Y. G., BENEDICT, W. J., HUSER, J., SAMAREL, A. M., BLATTER, L. A. & LIPSIUS, S. L. 2001. Brief rapid pacing depresses contractile function via Ca2+/PKC-dependent signaling in cat ventricular myocytes. *Am J Physiol Heart Circ Physiol,* 280**,** H90-98.

WARDMAN, P. 2007. Fluorescent and luminescent probes for measurement of oxidative and nitrosative species in cells and tissues: Progress, pitfalls, and prospects. *Free Radical Biology and Medicine,* 43**,** 995-1022.

WASSERMAN, W. W. & FAHL, W. E. 1997. Functional antioxidant responsive elements. *Proceedings of the National Academy of Sciences of the United States of America,* 94**,** 5361-5366.

WATKINS, M. T., HAUDENSCHILD, C. C., AL-BADAWI, H., VELAZQUEZ, F. R. & LARSON, D. M. 1995. Immediate responses of endothelial cells to hypoxia and reoxygenation: an in vitro model of cellular dysfunction. *Am J Physiol Heart Circ Physiol,* 268**,** H749-758.

WAYPA, G. B. & SCHUMACKER, P. T. 2005. Hypoxic pulmonary vasoconstriction: redox events in oxygen sensing. *J Appl Physiol,* 98**,** 404-14.

WEBSTER, K. A. 2007. Hypoxia: Life on the Edge. *Antioxidants & Redox Signaling,* 9**,** 1303-1308.

WEISS, S. 1989. Tissue destruction by neutrophils. *N Engl J Med,* 320**,** 365-376.

WILLIS, S. N. & ADAMS, J. M. 2005. Life in the balance: how BH3-only proteins induce apoptosis. *Current Opinion in Cell Biology,* 17**,** 617-625.

WINKLER, L. W. 1888. Die Bestimmung des im Wasser gelösten Sauerstoffes. *Berichte der deutschen chemischen Gesellschaft,* 21**,** 2843-2854.

XI-MING, Y., PROCTOR, J. B., LIN, C., THOMAS, K., JAMES, M. D. & MICHAEL, V. C. 2004. Multiple, brief coronary occlusions during early reperfusion protect rabbit hearts by targeting cell signaling pathways. *Journal of the American College of Cardiology,* 44**,** 1103-1110.

XUAN, Y.-T., TANG, X.-L., BANERJEE, S., TAKANO, H., LI, R. C. X., HAN, H., QIU, Y., LI, J.-J. & BOLLI, R. 1999. Nuclear Factor-{kappa}B Plays an Essential Role in the Late Phase of Ischemic Preconditioning in Conscious Rabbits. *Circ Res,* 84**,** 1095-1109.

YAGLOM, J. A., EKHTERAE, D., GABAI, V. L. & SHERMAN, M. Y. 2003. Regulation of Necrosis of H9c2 Myogenic Cells upon Transient Energy Deprivation. *Journal of Biological Chemistry,* 278**,** 50483-50496.

YAMAWAKI, M., SASAKI, N., SHIMOYAMA, M., MIAKE, J., OGINO, K., IGAWA, O., TAJIMA, F., SHIGEMASA, C. & HISATOME, I. 2004. Protective effect of edaravone against hypoxia–reoxygenation injury in rabbit cardiomyocytes. *British Journal of Pharmacology,* 142**,** 618-626.

YAOITA, H., OGAWA, K., MAEHARA, K. & MARUYAMA, Y. 1998. Attenuation of ischemia/reperfusion injury in rats by a caspase inhibitor. *Circulation,* 97**,** 276-81.

YASMIN, W., STRYNADKA, K. D. & SCHULZ, R. 1997. Generation of peroxynitrite contributes to ischemia-reperfusion injury in isolated rat hearts. *Cardiovasc Res,* 33**,** 422-432.

YELLON, D. M. & DOWNEY, J. M. 2003. Preconditioning the Myocardium: From Cellular Physiology to Clinical Cardiology. *Physiol. Rev.,* 83**,** 1113-1151.

YOSHIMOTO, T., FUKAI, N., SATO, R., SUGIYAMA, T., OZAWA, N., SHICHIRI, M. & HIRATA, Y. 2004. Antioxidant effect of adrenomedullin on angiotensin II-induced reactive oxygen species generation in vascular smooth muscle cells. *Endocrinology,* 145**,** 3331-7.

YOUNG, I. S. & MCENENY, J. 2001. Lipoprotein oxidation and atherosclerosis. *Biochem Soc Trans,* 29**,** 358-62.

YU, J. & ZHANG, L. 2008. PUMA, a potent killer with or without p53. *Oncogene,* 27, S71-S83.

ZANELLA, B., CALONGHI, N., PAGNOTTA, E., MASOTTI, L. & GUARNIERI, C. 2002. Mitochondrial nitric oxide localization in H9c2 cells revealed by confocal microscopy. *Biochem Biophys Res Commun,* 290**,** 1010-4.

ZASTAWNY, T. H., DABROWSKA, M., JASKOLSKI, T., KLIMARCZYK, M., KULINSKI, L., KOSZELA, A., SZCZESNIEWICZ, M., SLIWINSKA, M., WITKOWSKI, P. & OLINSKI, R. 1998. Comparison of Oxidative Base Damage in Mitochondrial and Nuclear DNA. *Free Radical Biology and Medicine,* 24**,** 722-725.

ZENEBE, W. J., NAZAREWICZ, R. R., PARIHAR, M. S. & GHAFOURIFAR, P. 2007. Hypoxia/Reoxygenation of isolated rat heart mitochondria causes cytochrome c release and oxidative stress; evidence for involvement of mitochondrial nitric oxide synthase. *Journal of Molecular and Cellular Cardiology,* 43**,** 411-419.

ZHANG, J., LIU, A., HOU, R., ZHANG, J., JIA, X., JIANG, W. & CHEN, J. 2009. Salidroside protects cardiomyocyte against hypoxia-induced death: A HIF-1[alpha]-activated and VEGF-mediated pathway. *European Journal of Pharmacology,* 607**,** 6-14.

ZHAO, H., JOSEPH, J., FALES, H. M., SOKOLOSKI, E. A., LEVINE, R. L., VASQUEZ-VIVAR, J. & KALYANARAMAN, B. 2005. Detection and characterization of the product of hydroethidine and intracellular superoxide by HPLC and limitations of fluorescence. *Proceedings of the National Academy of Sciences of the United States of America,* 102**,** 5727-5732.

ZHAO, H., KALIVENDI, S., ZHANG, H., JOSEPH, J., NITHIPATIKOM, K., VASQUEZ-VIVAR, J. & KALYANARAMAN, B. 2003. Superoxide reacts with hydroethidine but forms a fluorescent product that is distinctly different from ethidium: potential implications in intracellular fluorescence detection of superoxide. *Free Radic Biol Med,* 34**,** 1359-68.

ZHAO, Z.-Q. 2004. Oxidative stress-elicited myocardial apoptosis during reperfusion. *Current Opinion in Pharmacology,* 4**,** 159-165.

ZHOU, Z. H., PENG, J., YE, F., LI, N. S., DENG, H. W. & LI, Y. J. 2002. Delayed cardioprotection induced by nitroglycerin is mediated by alpha-calcitonin gene-related peptide. *Naunyn Schmiedebergs Arch Pharmacol,* 365**,** 253-9.

ZHOU, Q., LAM, P. Y., HAN, D. & CADENAS, E. 2009. Activation of c-Jun-N-terminal kinase and decline of mitochondrial pyruvate dehydrogenase activity during brain aging. *FEBS letters,* 583**,** 1132-1140.

ZINGARELLI, B., HAKE, P. W., DENENBERG, A. & WONG, H. R. 2002. Sesquiterpene Lactone Parthenolide, an Inhibitor of I[kappa]B Kinase Complex and Nuclear Factor-[kappa]B, Exerts Beneficial Effects in Myocardial Reperfusion Injury. *Shock,* 17**,** 127-134.

ZMIJEWSKI, J. W., MOELLERING, D. R., GOFFE, C. L., LANDAR, A., RAMACHANDRAN, A. & DARLEY-USMAR, V. M. 2005. Oxidized LDL induces mitochondrially associated reactive oxygen/nitrogen species formation in endothelial cells. *Am J Physiol Heart Circ Physiol,* 289**,** H852-861.

ZOROV, D. B., JUHASZOVA, M. & SOLLOTT, S. J. 2006. Mitochondrial ROS-induced ROS release: An update and review. *Biochimica et Biophysica Acta (BBA) - Bioenergetics,* 1757**,** 509-517.

ZULUETA, J. J., SAWHNEY, R., YU, F. S., COTE, C. C. & HASSOUN, P. M. 1997. Intracellular generation of reactive oxygen species in endothelial cells exposed to anoxia-reoxygenation. *Am J Physiol,* 272**,** L897.

ZUURBIER, C. J., VAN ITERSON, M. & INCE, C. 1999. Functional heterogeneity of oxygen supply-consumption ratio in the heart. *Cardiovasc Res,* 44**,** 488-497.

ZWEIER, J. L., SAMOUILOV, A. & KUPPUSAMY, P. 1999. Non-enzymatic nitric oxide synthesis in biological systems. *Biochimica et Biophysica Acta (BBA) - Bioenergetics,* 1411**,** 250-262.

ZWEIER, J. L., WANG, P. & KUPPUSAMY, P. 1995. Direct Measurement of Nitric Oxide Generation in the Ischemic Heart Using Electron Paramagnetic Resonance Spectroscopy. *Journal of Biological Chemistry,* 270**,** 304-307.

# Appendix I Vector plasmid maps and DNA sequence information


**pGL3-Basic Vector**

This vector can be obtained from Promega Corporation, Madison, WI.

**pGL3-Basic Vector sequence reference points:**

| | |
|---|---|
| Base pairs | 4818 bases |
| Promoter | (none) |
| Enhancer | (none) |
| Multiple cloning region | 1-58 |
| Luciferase gene (luc+) | 88-1740 |
| GLprimer2 binding site | 89-111 |
| SV40 late poly(A) signal | 1772-1993 |
| RVprimer4 binding site | 2061-2080 |
| ColE1-derived plasmid replication origin | 2318 |
| beta-lactamase gene (Ampr) | 3080-3940 |
| f1 origin | 4072-4527 |
| Synthetic (upstream) poly(A) signal | 4658-4811 |
| RVprimer3 binding site | 4760-4779 |

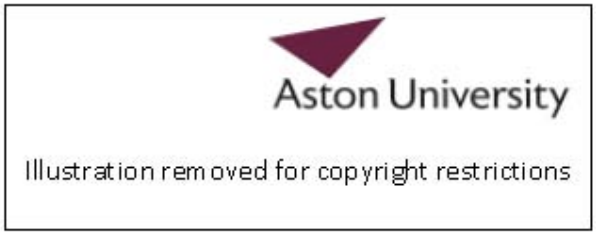


**pGL4.74 [hRluc/TK] Vector**

This vector can be obtained from Promega Corporation, Madison, WI.

**pGL4.74 [hRluc/TK] Vector sequence reference points:**

| | |
|---|---|
| Base pairs | 4237 |
| HSV-TK promoter | 27-779 |
| hRluc reporter gene | 815-1750 |
| SV40 late poly(A) region | 1784-2005 |
| Reporter Vector primer 4 (RVprimer4) binding region | 2071-2090 |
| ColE1-derived plasmid replication origin | 2330 |
| Synthetic beta-lactamase (Ampr) coding region | 3119-3979 |
| Synthetic poly(A) signal/transcriptional pause region | 4084-4237 |
| Reporter Vector primer 3 (RVprimer3) binding region | 4186-4205 |

Restriction enzyme that cut pGL4.74 [hRluc/TK] Vector;

**Enzyme**: Hind III **No of Sites**: 1 **Location** : 781

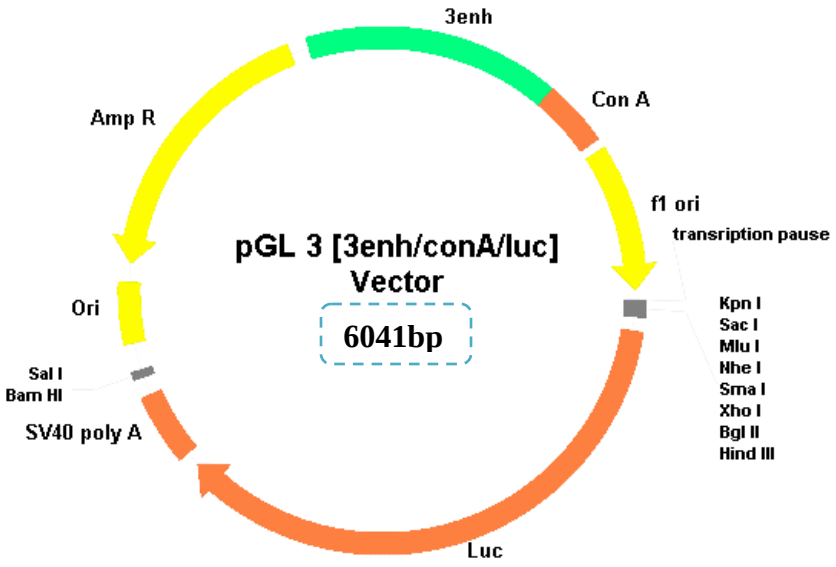


**DNA sequence of chicken conalbumin (Con A) promoter and enhancer (3enh) region (1223bp).**

**pGL 3 [*3enh/conA/luc*] plasmid sequence analysis**


Aston University
Illustration removed for copyright restrictions

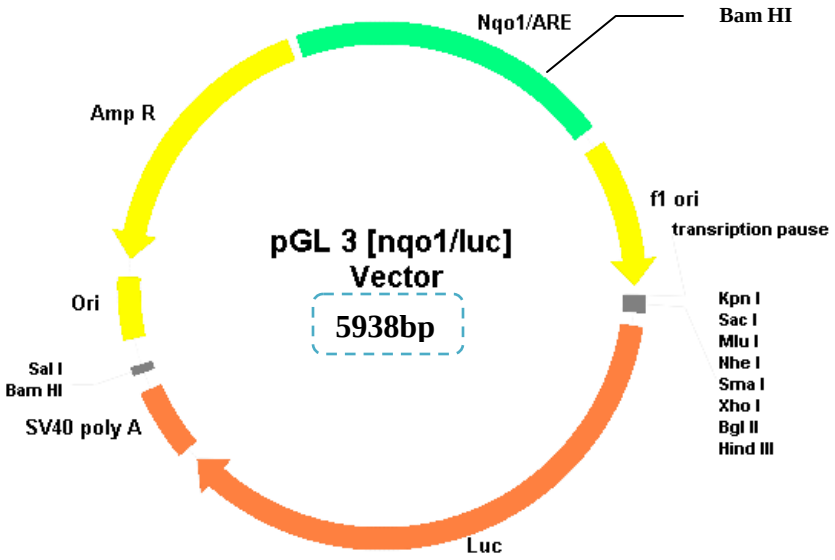


**DNA sequence of mouse Nqo1/ARE region (1120bp)**

**pGL 3 [*nqo1/luc*] plasmid sequence analysis**


Aston University
Illustration removed for copyright restrictions

# Appendix II Publications

1. M.M. GRANT[1], R.T. KOLAMUNNE[2], I.L. CHAPPLE[3], and H.R. GRIFFITHS[2] (July 2008) Oxygen tension modulates oral epithelial cytokine response to bacterial stimuli", [1]University of Birmingham, United Kingdom, [2]Aston University, Birmingham, United Kingdom, [3]Periodontal Research Group, The University of Birmingham, United Kingdom (Abstract) Annual Meeting International Association of Dental Research, Toronto, Canada.

2. RAJITHA KOLAMUNNE, HELEN GRIFFITHS (Dec 2007) An investigation into the kinetics and effects of reactive oxygen and nitrogen species (ROS/RNS) released during hypoxia/reoxygenation-induced cell death in rat cardiomyoblasts (Abstract) Winter Meeting, British Pharmacology Society, Brighton, UK.

3. RAJITHA KOLAMUNNE, DAVID POYNER, HELEN GRIFFITHS (Oct 2006) An investigation of kinetics of ROS/RNS generation in cardiomyoblasts in hypoxia-reperfusion (Abstract) International Free Radical Summer School, Spetses Island, Greece.